A HYDROMETRIC DATA-BASED FLOOD FORECASTING MODEL USING A SIMPLIFIED ROUTING TECHNIQUE

A THESIS

Submitted in partial fulfilment of the requirements for the award of the degree

of

DOCTOR OF PHILOSOPHY

in

HYDROLOGY

by

CHINTALACHERUVU MADHUSUDANA RAO

DEPARTMENT OF HYDROLOGY
INDIAN INSTITUTE OF TECHNOLOGY ROORKEE
ROORKEE-247 667 (INDIA)

SEPTEMBER, 2011

INDIAN INSTIUTE OF TECHNOLOGY ROORKEE
ROORKEE

CANDIDATE'S DECLARATION

I hereby certify that the work which is being presented in the thesis entitled **A HYDROMETRIC DATA-BASED FLOOD FORECASTING MODEL USING A SIMPLIFIED ROUTING TECHNIQUE** in partial fulfilment of the requirements for the award of the degree of Doctor of Philosophy and submitted in the Department of Hydrology, Indian Institute of Technology Roorkee, Roorkee is an authentic record of my own work carried out during the period from July 2007 to September 2011 under the supervision of Dr. M. Perumal, Professor, and Dr. D. K Srivastava, Professor, Department of Hydrology, Indian institute of Technology Roorkee, Roorkee.

The matter presented in this thesis has not been submitted by me for the award of any other degree of this or any other Institute.

(CHINTALACHERUVU MADHUSUDANA RAO)

This is to certify that the above statement made by the candidate is correct to the best of our knowledge.

(D. K Srivastava)
Supervisor

(M. Perumal)
Supervisor

Date: September 19, 2011

The Ph. D. Viva-Voce Examination of **Mr. Chintalacheruvu Madhusudana Rao**, Research Scholar, has been held on 4th Jan., 2012.

Supervisor (s)

Chairman SRC

External Examiner

Head of the Department & Chairman ODC

ABSTRACT

Adverse effects are experienced when high river flows occur in the form of floods causing loss of life and damage to property which have to be mitigated by employing economically feasible structural measures such as levees, flood walls and channel improvement. However, these types of measures cannot eliminate completely the hydraulic risk, given the impossibility of building larger and larger structures to cope with extremely low probability events. Therefore, an important role remains for non-structural measures to be compared, evaluated and implemented in real-time. Flood forecasting is an important non-structural measure for flood damage reduction and for minimizing flood-related deaths and, hence, its implementation as an effective tool requires accurate forecasting with sufficient lead-time. Therefore, it is essential that flood forecasting methods should be physically based, less data intensive and, over and above, should be easily understood by the field engineers for troubleshooting of the problems related to these methods during real-time operation. Typically, the flood forecasting models have two components: The deterministic flow component and the stochastic flow component. While the former is determined by the hydrologic/hydraulic model, the latter is determined based on the error series of the difference between the forecasted flow for a specified lead-time and the corresponding observed one. The residual series reflects both the model error, due to the inability of the deterministic model to correctly reproduce the flow process, and the observational error while measuring the flow. It is imperative, therefore, to use an appropriate model to reduce the model error. The hydrometric data-based flood forecasting model studied herein is employed for forecasting flood for a given lead-time at a gauging station knowing the evolving flood hydrograph at an upstream gauging station without involving rainfall, the causative factor for runoff

generation. Accordingly, the deterministic model employed herein is the river routing method.

The emphasis of this study is on the development of a routing procedure for the application of a Variable Parameter Muskingum method, known as the Variable Parameter McCarthy-Muskingum Discharge–routing (VPMMD) method which has been directly derived from the Saint-Venant equations by *Price and Perumal*, [2011], for the purpose of real-time flood forecasting in natural rivers under data deficient conditions, especially the morphometric data. It is considered that the morphometric data of the river reach required for the study is available only at the river gauging stations, where also the rating curves are available. The proposed routing procedure using the VPMMD method envisages the development of a reach-averaged rating curve for the river reach using the rating curves available at the upstream and downstream ends of the study reach and the development of the reach averaged cross-sectional geometrical elements information using the cross-sections data available at both the reach ends. The parameters of the VPMMD method required for channel routing are estimated based on these reach-averaged rating curve and channel cross-section information. The routing parameters of the VPMMD method are linked to the channel and flow characteristics which enable the variation of these parameters at every routing time step. The routing procedure of the VPMMD method employs the aforesaid reach averaged rating curve and channel cross-section data supplied in the form of look-up tables for linking uniquely the normal flow depth with the flow characteristics such as the normal discharge, the normal velocity and the normal celerity, and with the geometrical elements such as the area and top width of the reach-averaged flow section for determining the variable parameters of the routing method. This routing procedure enables the routing of floods in hypothetical channels as well as in natural rivers, covering the main channels as well as the floodplains. This

method is studied herein for its strengths and weaknesses by routing hypothetical inflow hydrographs in two synthetic channels: 1) a natural river section look alike artificial uniform channel as employed by Price [2009], and 2) a uniform compound channel section reach consisting of main and floodplain trapezoidal section. While ten channel types based on the former artificial sections were used for conducting numerical experiments of the proposed routing approach, it was tested in 72 artificial channels of the latter type. A number of hypothetical inflow hydrographs were routed through these artificial channels using the VPMMD method based routing procedure described herein and the solutions obtained were compared with the corresponding benchmark solutions of the Saint-Venant equations. Successful simulations of the benchmark solutions using the routing procedure formulated herein based on the VPMMD method demonstrate the theoretical correctness of the VPMMD method as well as that of the suggested routing procedure. These simulations also verified the ability of the VPMMD method to estimate the stage hydrographs by closely reproducing the corresponding benchmark stage hydrographs obtained from the solutions of the Saint-Venant equations. In addition to the verification of the VPMMD method routing capability, the utility of the method for field applications was also investigated by simulating ten past recorded flood events of a 15 km reach between Pierantonia and Ponte Felcino stations of Tiber River in Central Italy. All the ten events, except one could be reproduced with the Nash-Sutcliffe efficiency η_q >99%, thus, demonstrating the immense usefulness of the method for routing floods in river reaches.

It was considered appropriate to investigate the applicability limits of the VPMMD routing method to bring out the practical limitations of the method. This was carried out by simulating 11200 hypothetical routing solutions based on the Saint-Venant equations and reproducing these 11200 benchmark solutions using the VPMMD method. This study

reveals that the VPMMD method is able to produce 95% of successful simulations of the discharge hydrograph solutions with 5% error in reproducing the pertinent characteristics of the benchmark solutions. Based on the applicability limit estimation study, the recommended criterion limit to be satisfied by the discharge hydrograph at the inlet of the reach is $(1/S_o)(\partial y/\partial x)_{\max} \le 0.57$, and for similar successful simulation of the benchmark stage hydrographs only, the criterion limit to be satisfied is $(1/S_o)(\partial y/\partial x)_{\max} \le 0.61$. These range of applicability limits of the VPMMD method brings out the immense practical usefulness of the VPMMD method. The reach-averaged channel flow and the cross-sectional information required for the estimation of the routing parameters of the VPMMD method was supplied in the tabular form by relating the flow depth uniquely with the discharge, velocity and the celerity, and the top width of the flow section. No in-between channel section information was used in the developed routing procedure which enables the channel routing between the upstream inflow section and the downstream outflow section, and enabling routing through the main and floodplain sections of the channel reach. Considering the practical usefulness of this routing procedure developed using the VPMMD method, a Variable Parameter McCarthy-Muskingum Discharge Real-time Flood-Forecasting (VPMMDRF) method is developed using the VPMMD method as a component model of a hydrometric data-based deterministic forecasting model for real-time flood forecasting, particularly considering routing through multiple sub reaches of a river reach. A two parameter autoregressive forecast error estimation model forms the other component of the VPMMDRF method. Extensive investigations were made to verify the suitability of the VPMMD method for real-time forecasting applications. Unlike, the simulation mode of routing, the routing is done by marching in time after routing along the entire routing reach for the current inflow discharge. This way of routing procedure is desirable especially for real-time flood operations in the river

reaches. In order to verify this method, an application study was conducted for the Pierantonio (upstream) and Ponte Felcino (downstream) reach of the Tiber River in Central Italy by studying 10 recent flood events in forecasting mode. The forecasting results were arrived at by considering the 15 km long Pierantonio and Ponte Felcino reach, first as a single reach, and secondly considering as 2 sub-reaches (each of 7.5 km). For all these forecasting experiments, the varied forecasting lead times such as 1.00 h, 1.50 h, 2.00 h, 2.50 h, and 3.00 h were used. The performance evaluation of the proposed model is carried out in conjunction with an error forecasting model developed based on a simple Autoregressive (AR) model. From all the investigation results obtained from this forecasting study, it is found that the model produces accurate forecasting results along with the corresponding stage estimates for a lead time up to 3.00 h, with the warm up period considered for developing the error forecast AR model being 5.00 h. Therefore, this newly proposed VPMMDRF model can be conveniently used for discharge forecasting up to 3.00 h lead time in the considered Pierantonio-Ponte Felcino reach.

ACKNOWLEDGEMENTS

I wish to express my indebtedness and heartfelt gratitude to my Ph. D. supervisors Dr. M. Perumal, Professor, Department of Hydrology, I.I.T. Roorkee, and Dr. D. K. Srivastava, Professor, Department of Hydrology, I.I.T. Roorkee, for their valuable guidance and encouragement throughout this thesis work. I feel my deep sense of respect, especially to my guide Dr. M. Perumal for his constant motivation, invaluable supervision, realistic advice, good teaching throughout my work, and for his in-depth knowledge with pioneering ideas without whom this thesis would not have been completed. He is the person who laid the foundation to pursue my research.

I am grateful to Dr. Himanshu Joshi, Professor and Head, Department of Hydrology, I.I.T. Roorkee, for his generous help in providing the infrastructure facilities required for my Ph. D. programme. I am also thankful to Prof. B. S. Mathur, Prof. N. K. Goel, Prof. D. C. Singhal, Prof. Ranvir Singh, Dr. D. S. Arya and Dr. M. K. Jain for their encouragement from time to time. I wish to thank the staff members of the Department of Hydrology, I.I.T.Roorkee, for their help and support.

I pay my heartfelt gratitude to Prof. Emeritus Roland. K. Price, Hydro Informatics, UNESCO-IHE, Institute for Water Education, 2601 DA Delft, The Netherlands, for providing the algorithm of four-point implicit finite difference scheme and invaluable guidance during his stay at the Department of Hydrology, I.I.T. Roorkee.

I wish to express my sincere thanks to Dr. Bhabagrahi Sahoo, Scientist, Agricultural Research Service (ARS), ICAR-NEH Region, Nagaland Centre, Nagaland, India, for his invaluable support from time to time. I am also thankful to Dr. T. Moramarco, Senior Researcher, and Dr. Silvia Barbetta, Fellowship, I.R.P.I., National Research Council, Italy, for providing the Tiber River data. Thanks are due to my co-research scholars, Mr. Harihar Mohanthi, Dr. Ravindra Vitthal Kale, Mr. Trivedi, Mr. M. K. Chowdari, Mr. Jajharia, Mr. Maske, Mr. Satish, Mr. Anil Kar, Mr. Merjanur Rehman, and Mr. Aravind, and MTech., students Mrs. Vaani Dubey and Mr. Prakash Singh for helping me directly or indirectly in my work and making my stay happy and memorable at I.I.T. Roorkee.

I wish my heartfelt gratitude to my wife, Smt. Pushpalatha, son, Mr. Raghunath, and daughter, Kum. Meghana, for their constant support, bearing my negligence, sharing my joy and sorrow moments throughout my Ph. D. work, without their help and encouragement, I would not have completed this thesis work.

I am grateful to my parents, Sri. Pandu Ranga Rao, and Smt. Meghalamani who are always a constant source of support and inspiration to me. I wish my heartfelt gratitude to my brothers Mr. Venkateswara Rao, and Mr. N. P. Kumar, and their family members, for their constant motivation, support and to keep morale high during difficult times. I wish to express my heartfelt appreciation to my brother-in-law Mr. Vijaya Babu and my sister Mrs. Bhagya Lakshmi for their moral support throughout my study. I also wish my sincere thanks to my uncle, Mr. Prabhakar Rao and my brother-in-law Murali and their family members, for their co-operation.

I would like to give my special thanks to my little angels, Kum. Devi Priyanka, Master. Ranganath Verma, Master. Narendra Kumar, Master Rajendra Kumar, Kum. Gayathri, and Kum. Srujana for their wholehearted well wishes.

I wish to express my heartfelt thanks to my late Grandparents both paternal and maternal, and late relatives for their showering of invaluable blessings. Though they are not physically alive, but alive in our memories forever and their blessings never are ignored.

I thank all my relatives and friends for their constant support and good wishes during my stay at I.I.T. Roorkee.

I wish to express my sincere thanks to the almighty GOD for blessing me always, without whom I would not have completed this thesis work.

I am grateful to the Principal and the Management of Kakatiya Institute of Technology and Science (KITS), Warangal, Andhra Pradesh, for sponsoring me to pursue my Ph. D. at I.I.T. Roorkee. I am also thankful to my other sponsoring organizations AICTE, New Delhi, and the QIP, I.I.T. Roorkee, for providing fellowship.

Last but not the least, I am also thankful to my colleagues and the staff of the Department of Civil Engineering, KITS, Warangal, for their encouragement, support and belief in me.

I dedicate this thesis book to my beloved parents and my teachers.

I.I.T. Roorkee — Chintalacheruvu Madhusudana Rao

September 19, 2011

TABLE OF CONTENTS

LIST OF FIGURES

LIST OF TABLES

NOTATIONS

The following symbols are used in this thesis:

A = cross-sectional area of flowing water (m^2);

A_M = cross-sectional area in the Muskingum sub-reach at the midsection M of the Figure 2.1 (m^2);

A_o = cross-sectional area of flowing water corresponding to Q_o (m^2); in Dooge [1973] equation (2.10);

$A(Q_o)$ = wetted cross-sectional area corresponding to Q_o for the synthetic channel shown in Figure 3.2 (m^2);

a_1 and a_2 = parameters of the autoregressive error estimation model;

B = semi bed width of the synthetic channel in Figure 3.2(m);

B_b = semi-bed width of the trapezoidal main section of synthetic channel in Figure 3.2(m);

B_c = channel semi surface width of the trapezoidal section of synthetic channel in Figure 3.2(m);

B_{fl} = semi surface width of synthetic channel when flow depth y =0 in Figure 3.2(m);

B_M = channel surface width in the Muskingum sub-reach at the midsection M of the Figure 2.1 (m);

B_t = semi bed width for tanh curve in Figure 3.2 (m);

B_x = semi-width of the channel at $y = -y_x$ in Figure 3.2 (m);

$B(Q_o)$ = surface width corresponding to Q_o (m);

b_f = bottom width of the floodplain channel in Figure 3.7 (m);

b_m = channel bottom width in Figure 3.7 (m);

c = wave celerity (m/s);

C_1, C_2, C_3 = coefficients of the Muskingum routing equation (-);

c_M = wave celerity in the Muskingum sub-reach at the midsection M of the Figure 2.1 (m/s);

c_{Mo} = normal wave celerity at midsection of the routing reach (m/s);

c_o = reference wave celerity corresponding to Q_o or y_o (m/s);

$c(Q_o)$ = wave speed corresponding to Q_o (ms^{-1});

D = Diffusion coefficient of flood wave (m/s^2) ;

$e_{f,(j+1)\Delta t+T_L}$ = forecast error (-);

$e_{obs,(j+1)\Delta t}$ = forecasting errors estimated at time $(j+1)\Delta t$;

$e_{obs,j\Delta t}$ = forecasting errors estimated at time $j\Delta t$;

F = Froude number (-);

F_o = Froude number corresponding to Q_o or y_o (-);

g = acceleration due to gravity (m/s^2);

I = inflow discharge (m^3/s);

K = travel time parameter of the Muskingum routing equation(s);

m = exponent which depends on friction law (i.e., the Manning's friction law or the Chezy's friction law used (-);

n = Manning's roughness coefficient ($m^{1/3}/s$);

N_c = number of characteristic reaches in the Kalinin-Milyukov method

O = outflow discharge (m^3/s);

P = wetted perimeter of the channel (m);

Q = discharge at any instant of time (m^3/s);

Q_3 = steady discharge in the Muskingum sub-reach at section 3 of Figure 2.1 (m^3/s);

Q_b = Initial steady discharge (m^3/s);

Q_M = discharge in the Muskingum sub-reach at the midsection M of the Figure 2.1 (m^3/s);

Q_o = reference discharge (m^3/s);

Q_p = peak discharge (m^3/s);

Q_u = upstream discharge in the Muskingum sub-reach at section 1 of Figure 2.1 (m^3/s);

Q_d = downstream discharge in the Muskingum sub-reach at the section 2 of the Figure 2.1 (m^3/s);

Q_{po} = peak of the outflow discharge hydrograph of the benchmark model (m^3/s);

$\hat{Q}$ = forecast discharge (m^3/s);

$Q_{u,(j+1)\Delta t}$ = upstream discharges at time $(j+1)\Delta t$ (m^3/s);

$Q_{d,(j+1)\Delta t}$ = downstream discharges at time $(j+1)\Delta t$ (m^3/s);

$Q_{u,j\Delta t}$ = upstream discharges at time $j\Delta t$ (m^3/s),

$Q_{d,j\Delta t}$ = downstream discharges at time $j\Delta t$ (m^3/s),

q_{per} = percentage error in peak discharge (-);

R = A/P = hydraulic radius (m);

S_o = channel bed slope (-);

S = storage volume in the channel (m^3);

S_f = energy slope of the water surface (-);

$(1/S_o)(\partial y/\partial x)_{\max}$ = maximum value of dimensionless longitudinal water surface gradient and also applicability criterion for selection of the variable parameter Muskingum routing method (-);

$(1/S_o)(\partial y/\partial x)$ = dimensionless longitudinal water surface gradient (-);

t = time (s);

T_L = forecast lead-time (s);

t_p = time-to-peak of the input hydrograph (s);

t_{pqer} = percentage error in time-to-peak discharge (-);

t_{pyer} = percentage error in time-to-peak stage (-);

v = flow velocity of water (m/s);

V_{Mo} = normal velocity in the Muskingum sub-reach at the midsection M of the Figure 2.1 (m/s);

$v(Q_o)$ = velocity corresponding to $Q_o(ms^{-1})$;

x = longitudinal space vector (m);

y = flow depth of water (m);

y_b = initial stage corresponding to initial steady discharge, Q_b (m);

y_u = upstream stage in the Muskingum sub-reach at section 1 of Figure 2.1 (m);

y_p = peak stage corresponding to peak inflow, Q_p (m);

y_{per} = percentage error in peak stage (-);

$\overline{y}_r$ = average hydraulic mean depth by Dooge [1973] to estimate routing parameter θ in equation (2.10) (m);

y_d = downstream stage in the Muskingum sub-reach at section 2 of Figure 2.1 (m);

y_M = flow depth at the midsection M of the Muskingum sub-reach in Figure 2.1 (m);

y_{fl} = flow depth of synthetic channel to y =0 in Figure 3.2(m);

y_m = height of the main channel in Figure 3.7;

y_x = flow depth from y =0 to where the *tanh* curve intersects with

		trapezoidal main channel in Figure 3.2 (m);
z	=	side slope of the channel (-);
z_1, z_2	=	side slopes of the main and floodplain channel sections, respectively in Figure 3.7 (-);
$(v/g)(\partial y/\partial x)$	=	convective acceleration gradient (-);
$(1/g)(\partial v/\partial t)$	=	local acceleration gradient(-);
$\partial Q/\partial x$	=	longitudinal discharge gradient (-);
$\partial y/\partial x$	=	longitudinal water surface gradient (-);
Δt	=	routing time step (s);
Δx	=	space step (m);
θ	=	spatial weighting parameter of the Muskingum routing (-);
β	=	dimension less correction factor in Muskingum-Cunge-Todini method;
γ	=	shape factor of inflow hydrograph (-);
η_q	=	Nash-Sutcliffe efficiency for discharge reproduction (%);
η_y	=	Nash-Sutcliffe efficiency for stage reproduction (%);
μ_q	=	percentage attenuation in peak discharge (-);
μ_y	=	percentage attenuation in peak stage (-);
$\varepsilon_{(j+1)\Delta t+T_L}$	=	random error (white noise);

ABBREVIATIONS

The following abbreviations are used in this thesis:

ACD	=	Approximate Convection–Diffusion;
ANFIS	=	Adaptive Neuro-Fuzzy Inference System;
ANGIS	=	Adaptive Neuro-Genetic Algorithm Integrated System;
ANN	=	Artificial Neural Networks;
API	=	Antecedent Precipitation Index;
AR	=	Autoregressive;
ARIMA	=	Auto-Regressive Integrated Moving Average;
ARMA	=	Auto-Regressive Moving Average;
ASCE	=	American Society of Civil Engineers;
DHI	=	Danish Hydraulic Institute;
DW	=	Diffusive Wave;
FL	=	Fuzzy Logic;
GA	=	Genetic Algorithm;
HEC	=	Hydrologic Engineering Centre;
HEC-HMS	=	HEC-Hydrologic Modeling System;
HEC-RAS	=	Hydrologic Engineering Centre -River Analysis System;
IUH	=	Instantaneous Unit Hydrograph;
KW	=	Kinematic Wave;
MA	=	Moving Average;
MC	=	Muskingum-Cunge;
MCT	=	Muskingum-Cunge-Todini;
MM	=	Multilinear Muskingum;
NAM	=	Nedbør-Afrstromnings-Model;
NERC	=	National Environment Research Council;

PC = Persistence Criterion;

TF = Transfer Function;

TFN = Transfer Function Noise;

UH = Unit Hydrograph;

UK = United Kingdom;

USACE = United States Army Corps of Civil Engineers;

VPD = Variable Parameter Diffusion;

VPMC = Variable Parameter Muskingum-Cunge;

VPMD = Variable Parameter Muskingum Discharge-routing method;

VPMMD = Variable Parameter McCarthy-Muskingum Discharge-routing method;

VPMMDRF = Variable Parameter McCarthy-Muskingum Discharge-routing based Real-time Flood-forecasting method;

VPMS = Variable Parameter Muskingum Stage-routing method;

WMO = World Meteorological Organization;

1 INTRODUCTION

1.1 GENERAL

From time immemorial, floods have been causing a lot of human misery. It is reported that floods and droughts kill more people and cause more damage than any other natural disaster [*WMO*, 1992]. The early efforts to reduce flood related deaths and damages, however, were primarily devoted to the structural measures of flood control, such as levees, dams and storage reservoirs. However, structural measures cannot eliminate completely the risk, given the impossibility of building larger structures to cope up with extremely low probability flood events. Therefore, an important role is left to the non-structural measures by which people are kept away from floods, rather than flood is being kept away from people using structural measures. Flood forecasting is one of the important components of non-structural measures of flood management. Forecasting in principle, attempts to estimate the crest of the hydrograph and its time of occurrence at predetermined locations along a river, where human interest is involved. Further, the temporal and spatial variability that characterizes a river system makes flow forecasting in real-time sense a very demanding task to help to anticipate extreme flood events which cost lives and damages to properties and services, and to allow sufficient time for action. To overcome all these losses, there is a need for models capable of efficiently forecasting water levels or discharges at desired locations along rivers.

Development of a flood forecasting system involves various sub-systems. These sub-systems deal with historical and real-time data collection, data transmission, data-base management, forecasting procedure (modeling), forecast dissemination, and evaluation

and updating. Technological advances in the field of forecasting under these sub-systems can be divided into three groups: the first associated with data collection, the second with transmission and the third with analysis for developing a forecasting model. Automatic collection of a range of data is now possible. These include automated rain gauges, river stage recorders, discharge measurements using ultrasonic flow meter, and the use of radar and remote sensing techniques to detect likely areas that would receive precipitation and its intensity. Transmission of data is achieved progressively by radio and telemetry. A detailed description of these technological components is beyond the scope of this thesis. The focus of this thesis is on the study of forecasting methods, specifically oriented to hydrometric data-based modeling involving only stream flow process. Apart from presenting a general overview of flood forecasting models in this chapter and describing the flood forecasting philosophy in the next chapter, the rest of the thesis presents the development of a flood routing component of a hydrometric data-based forecasting model for improved real-time forecasting. It may be clarified at this juncture that two interpretations prevail in the hydrological literature for the term " hydrometric data-based forecasting": 1) interpretation as given by *Nemec* [1985] from the perspective of using only the hydrometric data without involving the precipitation data like the case of using only the channel routing for forecasting, based on hydraulic or hydrological models, and 2) interpretation from the perspective of employing data-based models for linking input (precipitation, stream gauge or discharge) and output (outflow gauge or discharge) using empirical models such as the ANN models. In this study the term "hydrometric data-based forecasting" is used in the context of the former interpretation only.

1.2 FLOOD FORECASTING MODELS

Flood forecasting models make possible to simulate the watershed response to a given input at a given location under the existing catchment conditions. Forecasting models

generally operates on calibration (off-line) and operation (on-line) modes. The calibration mode tries to produce the watershed response for the past recorded precipitation or upstream flow input. This calibrated response is compared with the recorded response at the point of forecasting interest to check the matching of these two responses. If the matching is done satisfactorily the model structure or the model parameters need not be changed; otherwise, the model parameters need to be modified till the matching is done satisfactorily. Once the structure of the model frame work is finalized in the calibration mode, the model is said to be in operational mode and then the model can be used for the forecasting purposes.

In general, every forecasting model has two components of flow forecasting: 1) deterministic flow component and 2) stochastic flow component. The deterministic flow component is determined by the hydrologic/ hydraulic model; whereas, the stochastic flow component is determined based on the residual (error) series of the difference between the forecasted flow for a specified lead-time and the corresponding observed flow. The residual series reflects both the model error, due to the inability of the model used in the forecasting method to correctly reproduce the flow process, and the observational error that arise while measuring the flow.

Hydrological models used in the forecast are empirical, conceptual or combination of both. Empirical models use mathematical equations without relating to the physics of the system. Conceptual models use the hydrological concepts in order to simulate the basins behavior. Conceptual models usually have two main components: (a) rainfall-runoff module which transforms the rainfall into runoff through the water balance in the hydrological components such as interception, upper soil zone, ground water and over land flow; and (b) a routing module which simulates the flow in the rivers and reservoirs. Rainfall-runoff models can be lumped or distributed. Lumped models do not usually take

into account the spatial variability of rainfall, state variables and model parameters. For small basins, this type of model is very useful, since it has a simple structure and capability to easily update its parameters or state variables. In a distributed model the rainfall-runoff processes are considered as a function of time and space. It accounts the spatial variations of physical characteristics of the basin and rainfall conditions. In this distributed modeling approach the study area is divided into sub-units or zones, with different average parameters for each zone. As the emphasis of this study is on the forecasting methods, specifically oriented to hydrometric data-based modeling involving only stream flow process, the presentation of a general background of such type of forecasting models employed in the field is necessary.

1.3 ROUTING MODELS AS COMPONENTS OF FLOOD FORECASTING MODELS

In the past few decades, a wide variety of rainfall-runoff models have been developed and applied for flood forecasting. However, rainfall- runoff relationship is the most complex hydrological process to explain owing to tremendous spatial and temporal variability of the basin characteristics. *Thirumalaiah and Deo* [1998] pointed out that forecasting of stream flows during storms is usually very complex owing to the uncertainties and unpredictable nature of the rainfall event. Similar opinion was also expressed by *Bertoni et al.* [1992] stating that the real-time forecasts obtained by modeling rainfall-runoff processes are less accurate owing to the difficulties in modeling temporal and spatial variability of the within-basin processes than those obtained by channel routing of a hydrograph observed at an upstream gauging site. Further the reliability of forecasts involving only the channel routing process can be increased using the physically based models involving the equations governing the flow process, even in simplified forms.

Therefore, simplified flood routing methods have great potential for their use in the hydrometric data-based forecasting models.

The hydrometric data-based forecasting usually involves two phases: Firstly, the use of a flood routing model to obtain the flood discharge/stage and its time occurrence at a gauging station of forecast interest along the river reach. Secondly, the use of a forecasting error estimation model for further improvement of the flood routing model forecasted estimates. Broadly, these forecast errors may be categorized into two types: 1) model error, and 2) observational error. The first is due to the use of an inappropriate basic model which is incapable of correctly modeling the flow process, and the second is due to the observational and instrumental errors of flow/stage measurements. These errors affect the accuracy of flood forecasting estimates. Therefore, in order to arrive at the accurate forecast of a given lead-time, error estimate is separately forecasted which when summed up with the model forecasted estimate results in the forecasted flow/stage of specified lead-time. Therefore, it is necessary to use an appropriate model to reduce the model error. Forecasting methods employing the adaptive parameter estimation techniques based on the Kalman filtering technique [*Lee and Singh*, 1998], and other simple forecasting error estimation models such as autoregressive (AR) and Autoregressive-Moving Average (ARMA) models are already in use in field practices. Various researchers have applied the Kalman filtering algorithm to estimate the hydrological parameters for different river basins [*Szollosi- Nagy*, 1976; *Moll*, 1983; *Burn and McBean*, 1985; *Husain*, 1985; *Lee and Singh*, 1998 and *Neal et al.* 2007]. Some researchers have demonstrated the use of a second order linear autoregressive model for application to the estimation of forecasting errors [*Bergman and Delleur*, 1985a, b; *Refsgaard*, 1997; *Thirumalaiah and Deo*, 1998; *Chiu*, 1985 and *Perumal et al.*, 2011]. The adaptive parameter estimation methods employing the Kalman filtering technique

may not be worth the effort for real-time flood forecasting [*Ahsan and O'Connor*, 1994; *Huang*, 1999], when the hydrological models employed for forecasting is grossly inadequate to simulate past recorded floods [*Perumal et al.*, 2011]. In such a scenario, the application of the simplified physically based models along with the simple forecast error estimation techniques may be found useful for real-time flood forecasting. *Nash* [1980] reasoned that though the emphasis on the updating algorithms would be acceptable in an operational forecasting system, simple error updating techniques of the residuals could be used as a replacement of the complicated updating algorithms. The parameters of the 'physical' part of the model should be estimated independently of those of the error component, otherwise the error model tend to dominate. The essence of what *Nash* [1980] stated is that while the flow process is a highly nonlinear process, the same should be modeled using appropriate models which are able to take care of the nonlinearity. Very recently, *Price* [2009] applied a physically based simplified routing technique for flow forecasting in a synthetic river channel and for the Wye River in UK. In this, *Price* [2009] first calibrated the routing model and then applied it for forecasting the downstream flows. In order to reduce the forecast errors, Price [2009] forecasted the upstream discharge hydrograph before arriving at the actual downstream forecast. Very recently, *Perumal et al.* [2011] developed a real-time flood stage forecasting model using a Variable Parameter Muskingum Stage-routing (VPMS) method. But this method is limited to forecasting based on one single reach consideration of a given river reach, which does not serve the forecasting purpose in a realistic manner, particularly, the information required at the ungauged stations along the river reach.

Routing methods based on physical principles governing the flow movement in rivers enable to account for the non-linear behavior of the flood wave movement. However, a method accounting for non-linearity of the flow process and operating in both ways i.e.,

in simulation and forecasting mode, definitely serve the purpose of correct forecasting of stream flows in river channels. However, the use of such models is few in practice. One of the routing methods widely used in Eastern European countries, especially, for flood forecasting of the Danube River is the *Kalinin-Miliyukov* method proposed by the Russian hydraulic engineers [*Apollov et al.*, 1964]. The *Kalinin and Miliyukov* method [*Szollosi-Nagy*, 1976, 1982; *Szilagyi*, 2003, 2006] is based on linear theory in which the parameter, n, denoting number of sub-reaches, used for dividing the given routing reach into equal number of sub-reaches and K, the parameter defining the travel time of flood wave in a given sub-reach remain constant when the model is used for simulating a past recorded event (i.e., in off-line mode). But while applying this method for real-time forecasting, the parameters n and K are modified at every forecasting time interval using the updating algorithms such as the *Kalman* filters which is suitable for application in processes which involve high randomness. Since the flood flows of large rivers vary smoothly exhibiting more dependence among them in time sequence, the use of simple error updating algorithm may be appropriate rather than using the mathematically involved *Kalman* filter. However, to follow this strategy in real-time flood forecasting it is necessary to use a routing model which is capable of accounting for non-linearity in the routing process and yet maintain the simplicity of employing the linear form of the routing equation. This necessitates that the routing parameters vary while routing the flow at every routing time interval, unlike the available linear theory based routing models wherein the parameters are updated in real-time using the updating algorithm without involving the physical basis of varying the parameters. Therefore, if one can employ a physically based model, then the forecast error may only involve in a major way the observation error and the error due to unaccounted lateral flow between the upstream gauging station, where the inflow hydrograph is recorded, and the downstream gauging station of forecast interest. This

approach is based on the concept that the basic model employed in the real-time flood forecasting model should be a more appropriate one, rather than using a crude basic model and achieving the accuracy of forecast using complex updating algorithm such as Kalman filters.

In addition, most of the hydrodynamic routing methods operating on simulation and forecasting modes usually depend on the use of number of channel cross-sections at close intervals, besides using other morphometric details of a river such as the surface roughness along the river reach which are varying in space and time. Hydrodynamic principle based models such as MIKE11[*Danish Hydraulic Institute (DHI)-Water and Environment*, 2011] and HEC-RAS [*U.S. Army Corps of Civil Engineers (USACE)*, 2010] models can be used for river forecasting purposes, but at the cost of using hydrometric and morphometric data at closer temporal and special resolutions, respectively. However, cross-sectional data acquisition and stream gauging at the site of interest is often very difficult owing to the inaccessibility and spatial and temporal variations occur during high flows in natural rivers. The similar opinion was also expressed by *Birkhead and James* [1998] who stated that when the environmental requirements are being assessed, information is commonly required at a large number of locations which may be remote and inaccessible in natural rivers. Alternatively, replacing the channel cross-sectional details using only the normal rating curves and the associated channel cross-sectional information for their use in the simplified flood routing methods, simplifies the forecasting problem in the operational flood management. However, models which operate on such limited information have not been tested either in simulation or forecasting mode of flood studies, except by *Perumal et al.*, [2010]. Therefore, to fill this gap in the field of hydrological modeling and to apply a physically based simplified flood routing method, using only the rating curve information available at different gauging

stations of the river reach and the reach-averaged geometrical elements of the river reach cross-sections, an approach is proposed in this study to test the suitability of the Variable Parameter McCarthy-Muskingum Discharge-routing (VPMMD) Method and its subsequent application for forecasting in rivers. Here the VPMMD method originally developed by *Price and Perumal* [2011] for discharge routing in main channels of any prismatic type using cross-sectional information is replaced by using the reach averaged rating curve developed from the rating curves available at the inlet and outlet of the given routing reach. It is considered that there exists no lateral flow within the routing reach.

1.4 RELEVANCE OF SIMPLIFIED VARIABLE PARAMETER FLOOD ROUTING METHODS FOR HYDROMETRIC DATA-BASED FLOOD FORECASTING

In the light of the above discussion, the ability of investigating the simplified variable parameter flood routing methods for hydrometric data-based flood forecasting in river reaches can be briefly summarized as: 1)The alternate way of accurate runoff forecasting at the required river gauging stations without the use of channel cross-sectional details but by the use of actual rating curves available along the river reach and the associated cross-section information has not been extensively tested in hydrological practices and, therefore, the verification of this approach has a greater prospective for hydrological analyses. 2) The hydraulic methods, which generally use the full Saint-Venant equations, are of limited use primarily due to the non-availability of topological inputs required at smaller spatial resolutions and also due to the computational limitations of the numerical schemes adopted in the solution procedure. Another way of overcoming these data and computational problems is by using the simplified routing methods which are derived from the Saint-Venant equations, but at the same time, they are not data intensive. 3) Forecasting of stream flows during storms is usually very complex owing to the uncertain

and unpredictable nature of rainfall events. But forecasting at a river site using models based on hydrometric data only reduces such complexities and uncertainties, *albeit* at the cost of reduced forecast lead-time. Hydrometric data-based models mainly based on simplified flood routing methods not only possess these characteristics, but also less data intensive and use of such methods in real-time flood forecasting models helps the field engineers to anticipate the stream flows accurately. 4) Forecasting by the hydrometric data-based model of *Perumal et al.* [2011] used the off-line mode of routing procedure of the VPMS method (i.e., routing all the time ordinates of the given hydrograph before going into the next sub-reach) for real-time applications. Unlike the off-line mode of routing procedure, routing using the on-line mode (i.e., routing is done by completing all the space steps along the routing reach for the current inflow discharge) is desirable for the real-time flood forecasting applications. More clearly, conducting routing by marching in time after routing along the entire routing reach for the current inflow discharge is desirable for real-time flood forecasting. Further this type of novel attempt has not been employed in hydrological analyses. It may be inferred from the above discussion that the use of simplified variable parameter flood routing methods for hydrometric data-based real-time flood forecasting purposes have a great relevance for hydrological applications.

1.5 OBJECTIVES OF THE STUDY

The emphasis of this study is on the development of an improved volume conservative physically based simplified routing method suitable for flood forecasting in natural rivers without using the surveyed channel cross-sectional details, but by the use of existing normal rating curves and the associated cross-sectional information at the river gauging stations along a river reach. In this regard, the Variable Parameter McCarthy-Muskingum Discharge-routing (VPMMD) method advocated by *Price and Perumal* [2011] is

employed for its extension to routing in compound channels consisting of main and floodplain sections, and subsequently applied for real-time flood forecasting at a gauging site of Tiber River in Central Italy. However, before considering the use of this method as a basic component model of a real-time flood forecasting model, its potential for routing floods in simulation mode needs to be tested, in addition to ascertaining its range of applicability for accurately routing floods in channels and river reaches.

Considering the above discussed aspects, the present work is carried out with the following four objectives:

1. Developing a routing procedure using the VPMMD method for routing discharge in channel reaches by incorporating floodplain channel section as a two-step compound trapezoidal channel cross-section, as proposed by *Ackers* [1993] and adopted by *Tang et al.* [1999] and subsequently by *Sahoo* [2007], and comparing the VPMMD solutions with the corresponding benchmark solutions of the MIKE11model [*DHI,* 2008]. Also, applying the VPMMD routing method in a similar way for routing floods in synthetic uniform river channel reaches, introduced recently by *Price* [2009], characterized by channel sections closely resembling to those of natural river cross-sections and comparing these VPMMD solutions with the corresponding benchmark solutions of the Saint-Venant equations arrived at based on the four-point implicit and iterative finite difference scheme.

2. Investigation of the routing capability of the VPMMD method developed herein for field applications.

3. Development of the applicability criteria for the VPMMD routing method considering routing within main channels only.

4. Verification of the use of the VPMMD routing method developed herein as a component model of a hydrometric data-based deterministic forecasting model for real-time flood forecasting in a selected river reach, considering routing through single and multiple sub-reaches.

1.6 SCOPE OF THE STUDY

a) This study will bring out the alternate way of routing floods in channels and river reaches using the reach-averaged rating curve estimated by averaging only the upstream and downstream rating curves of the routing reach and the associated channel cross-section information without the need for using any in-between channel cross-section details.

b) The applicability criteria developed for the VPMMD method enable the hydrologists and field engineers to assess the suitability of applying this method for a given field routing problem. If found unsuitable based on the applicability criteria, the possibility of applying a higher level model say, the use of full Saint-Venant equations may be explored.

c) A Variable Parameter McCarthy-Muskingum Discharge Real-Time Flood forecasting henceforth VPMMDRF method is developed as a component model of a hydrometric data-based deterministic forecasting model. This proposed VPMMDRF method has a greater scope in handling the nonlinear behavior of flood wave movement in river reaches by updating its parameters at every routing time interval and conserving the mass more accurately.

1.7 LIMITATIONS OF THE STUDY

a) As the VPMMD method has been developed based on the assumption of no backwater effects, this method is not suitable when the routing reach is affected by downstream backwater flows.

b) The limitations of the proposed study also include the assumption of no lateral flow within the study reach. However, this simplified flood routing method can account for the point lateral flow in the form of flows from river tributaries, and not the distributed lateral flow.

1.8 THESIS LAYOUT

This thesis constitutes a total of six chapters. The relevance of simplified flood routing methods operating on simulation and forecasting mode for hydrological analyses are given in Chapter 1. The evaluation of different simplified flood routing methods and their applications both for simulation and forecasting are presented in Chapter 2.

Considering the first objective of the study, Chapter 3 presents the development of a routing procedure using the VPMMD method for routing discharge hydrograph in compound channel section reaches. The development of routing procedure using the VPMMD method for routing in compound channels, and the verification of it by routing hypothetical floods in hypothetical channels and comparing these results with the corresponding solutions of the full Saint-Venant equations are addressed in this chapter. The investigation of the routing capability of the extended VPMMD method for field application is also addressed in this chapter.

Chapter 4 presents, the applicability criteria proposed for the VPMMD method based on the numerical experiments conducted using this method in prismatic main channels.

In Chapter 5, the application of the VPMMD routing method for real-time flood forecasting in a selected river reach is presented. A Variable Parameter McCarthy-Muskingum Discharge Real-Time Flood Forecasting, henceforth, abbreviated as VPMMDRF method, is developed using the VPMMD routing method as the basic model, besides using a second-order linear autoregressive model as the forecast error estimating model.

Chapter 6 presents the conclusions of this study and the future recommendations.

The equations used for Price's synthetic river channel [*Price*, 2009] are given in Appendix I. The **FORTRAN 77** codes developed and used in this study for numerical routing experiments and field applications are given in the Appendices II and III, respectively.

2 REVIEW OF LITERATURE

2.1 GENERAL

As the future research in the area of flood forecasting is filled with new possibilities and challenges, it is appropriate to pause and determine the current status of research in this area. The earlier contributions blended naturally to evolve a synthesized body of knowledge on this topic. With the advent of computing skills in the recent years many researchers are trying to resolve the nonlinear complexity associated with real-time flood forecasting. As the research undertaken in this study focuses based on river routing, only the literature related to river routing methods employed for flood forecasting have been discussed herein.

2.2 NEED FOR FLOOD FORECASTING

Flood forecasting refers to the forecast of flood crest and its time of occurrence, and its logical extension to the flood stages of river above a specified water level called the warning level. Flood losses can be minimized by following two approaches, either independently or combined together: 1) Structural measures and 2) Non-structural measures. Using the former approach floods are kept away from people by providing levees, diversion of flood waters etc., and using the later approach, people are kept away from floods by the measures such as floodplain zoning, rising the dwelling levels, flood proofing, and real-time flood forecasting etc. The use of both these approaches for minimizing flood damages forms the effective flood management. The real-time flood forecasting is one of the most effective non-structural measures for flood management. The effectiveness of real-time flood forecasting systems in mitigating flood impact would

depend upon how accurately the estimation of expected stages or flow of the propagating flood and its time sequence at selected points along the river could be forecasted. Real-time flood forecasting systems are formulated for using the flood warning in real-time in order to prepare needed contingency measures during the formation of a flood. In addition, the following aspects necessitate the flood forecasting:

i) Warning of the approaching floods provides sufficient time for authorities for planning and to execute appropriate evacuation measures.
ii) To evacuate the affected or likely to be affected people to the safer places.
iii) To make an intense patrolling of the flood protection works.
iv) To regulate the barrages and reservoirs, so that the safety of these structures can be taken care of.
v) To operate the multipurpose reservoirs to safely accommodate the incoming flood and for the controlled release of water so as not to inundate the downstream river reaches taking into account the already prevailing conditions therein.
vi) To operate the city drains to prevent the back flow and flooding the areas drained by them.

2.3 CLASSIFICATION OF FLOOD FORECASTING MODELS

Flood forecasting can be performed using hydraulic or hydrologic models [*Li*, 1988; *Singh*, 1988, 1989, 1998; *Abbott and Refsgaard*, 1996]. It is necessary to stress that the classification of models for hydrological forecasting purposes not necessarily identical to the classification of models used for other purposes, such as for design, and estimation of missing data. Some models which are based on stochastic principles or statistical approaches may function as the deterministic models, when used for real-time forecasting. Hence, any model which is used for the real-time forecast, by definition, is a

deterministic model. A brief discussion on the classification of the flood forecasting models proposed by *Nemec* [1985] is as follows:

A. Purely Deterministic Forecasting Models:

(1) Hydrometric data-based forecasting models (involving only stream flow process)

(i) Correlation of stages and/or volumes (discharge)

(ii) Systems approach to stream flow (hydrologic routing)

(iii) Hydraulic/Simplified hydraulic routing using

- Dynamic wave model
- Diffusion analogy model and
- Kinematic wave model

(2) Hydrometeorological and hydrometric data-based forecasting models (involving rainfall-runoff and stream flow processes)

(i) Correlations using physical variables and parameters or indices (such as antecedent precipitation index (API))

(ii) Systems approach to study the basin response to rainfall,

(iii) Distributed parameter approaches (hydrological and hydraulic routing)

(iv) Conceptual moisture accounting using

a) Soil moisture indices

b) Implicit moisture accounting

c) Explicit moisture accounting

B. Hybrid-Deterministic-Stochastic Forecasting Models

1. Using only time series stochastic parameterization
2. Using systems approach to the basin response and time series stochastic parameterization.

Apart from the models described under the above classifications, there are some other classes of models developed with the passage of time like Artificial Neural Networks (ANN) models, fuzzy rule-based models, ANN-Fuzzy-Genetic Algorithm (GA) adaptive type models which are being currently used in the hydrological flood forecasting systems. A forecasting model consisting of any one of the above category model with a forecasting error updating model should be able to closely describe the behavior of the system being modeled. At the same time, it may be noted that a more mathematically involved hydrological model may not be suitable for operational flood forecasting purposes due to the requirements of intensive real-time data and, above all, the understanding of the forecasting model by the engineers involved in forecasting work.

2.3.1 Purely Deterministic Forecasting Models

The deterministic forecasting models are those models whose output is entirely determined by its initial state and input which yields unique output without involving random or stochastic component. Accordingly, the deterministic models used for hydrological forecasting may be classified into two major groups: 1) Hydrometric data-based models involving only stream flow process. These include simple gauge-to-gauge and discharge-to-discharge relationships. The formulation of forecast is only on the basis

of stage-discharge data; the basic data used are gauge and discharge data at various points along the river course. This model can be further classified as direct correlation between gauges or discharges of upstream station with downstream station, and stream flow routing by hydrologic and hydraulic models. The emphasis of this study is on the development of hydrometric data-based flood forecasting models involving only stream flow processes, therefore, the detailed description on the hydrologic and hydraulic routing models are given in later part of the literature review. The "hydrometric data-based forecasting" problem referred in this study has been addressed on this consideration only, without considering the other prospective of employing empirical models based on soft computing techniques as referred by *Lekkas* [2002]; 2) Hydrometeorological and hydrometric data-based models have been developed on the basis involving rainfall-runoff process and stream flow routing process. However, for catchments where the time of concentration is very less, the hydrometeorological data-based forecasting may not be of any use unless the rainfall itself is forecasted to get sufficient warning time about the impending flood. In addition, deterministic lumped and distributed hydrodynamic based models like NAM and MIKE SHE [*DHI*, 2011] are being used for flood forecasting studies. The NAM is a classical lumped conceptual model of the rainfall-runoff process [*More and Bell, 2001*] developed by DHI (1999). Based on rainfall and evaporation input data, the model produces catchment runoff which is split conceptually into overland flow, interflow and base flow components. Because it is a lumped model, each sub-catchment is treated as one unit with the parameters and variables thus represent effective values for the sub-catchment. Being a conceptual model, NAM is based upon physical structures and equations, together with semi-empirical equations. Thus, some of the parameters can be estimated from physical catchment data, but the final parameter estimation must be performed by calibration, employing concurrent input and output time series. For the

purpose of flood forecasting considering rainfall as input, a hydrological model of the NAM-type is believed to be appropriate [*Jønch-Clausen and Refsgaard,* 1984]. Researchers like *Chowdhury,* [2000]; *Paudyal,* [2002]; *Markar et al.,* [2004]; *Patro et al.,* [2009] have verified the use of lumped rainfall-runoff models for various river basins. Further, MIKE SHE models are also being used for flood forecasting studies. The MIKE SHE model is a comprehensive, deterministic distributed and physically based modeling system capable of simulating all major processes in the land phase of the hydrological cycle. However, there are also some important limitations to the applicability of comprehensive physically based models like MIKE SHE, particularly for flood forecasting [*Graham* and *Butts,* 2005]. They are: i) the data requirement can be significant and prohibitive in terms of cost, ii) complex processes representations may require substantial computing time, which may become important for flood forecasting or climate change modeling, iii) complex representations may lead to over parameterization for simpler applications like predicting basins outlet discharges, and iv) the representation process may not be valid on the grid scale of the model or sub-grid variability may not be represented adequately.

2.3.2 Hybrid-Stochastic-Deterministic Forecasting Models

This type of forecasting models use various linear univariate stochastic models, stationary and non-stationary, applied in conjunction with the conceptual models in order to forecast the discharge in rivers [*Brath et al.*, 1993; 1999]. Real-time flood forecasting in small and medium size basins are generally obtained by means of either conceptual or black-box models, because of their capability to be easily formulated in an adaptive framework. However, real-time discharge forecasts estimated using conceptual models are affected by model and observational errors which could be of significant magnitude. In order to get to an acceptable accuracy of the forecast estimate, the model parameters are updated in real-

time during the process of the flood event. This results in an "adaptive" calibration which could allow to optimize the forecasting performances taking into account the hydrological and meteorological characteristics of the ongoing flood event [*Barth and Rosso*, 1993]. Moreover, because of the simplified description of the physical process represented by the conceptual model, a strong autocorrelation in series of the forecast errors is generally present. This is the reason which led to the use of stochastic models in order to predict such forecast errors and, thereby, improving the forecasted estimates by combining the deterministic model output with the error [*WMO*, 1992]. Thus, the use of filtering techniques like Kalman filters and error estimation by Autoregressive (AR)/Autoregressive Moving Average (ARMA) models for the real-time flood forecasting resulted in the classification of deterministic-stochastic models [*Szollosi-Nagy*, 1976; *Husain*, 1985; *Moll*, 1983; *Lee and Singh*, 1998; *Perumal et al.*, 2011; and *Xiao-Ling Wu et al.*, 2011].

In addition, Transfer Function (TF) models are a class of time-series models popularized by Box and Jenkins [1970] are also being used for flood forecasting purposes. They are linear models using which an output variable can be forecasted as a linear weighted combination of past outputs and inputs. In a rainfall-runoff context, the output is usually flow and the input is rainfall. Any residual model error can be represented through a noise model which is normally of autoregressive moving average (ARMA) form. The overall model is termed a Transfer Function Noise (TFN) model. Although the TF model appears as a ''black-box'' type, it actually has the ability to reveal the underlying input-output mechanism in hydrological system [*Yang and Han*, 2006]. Much research has been done on transfer function models [*O*'Connell and Clarke, 1981; *Reed*, 1984; *Cluckie*, 1993; *Lees*, 2000*a*, 2000*b*; *Imrie et al.* 2000*b*; *Beven*, 2001; *Lekkas et al.*, 2001; *Yang and Han*, 2006] and it has played a very important role in real-time flood forecasting. In one

important sense, TF models provide a rather natural model form for hydrologists because the impulse response of a continuous-time TF model in hydrology is equivalent to the instantaneous unit hydrograph (IUH), while the discrete pulse response of the discrete time TF model is equivalent to the discrete time unit hydrograph (UH) [*Chow et al.*, 1988]. It should be pointed out that the well known Nash model is actually a special type of TF model [*Nash*, 1957]. Further, TF models have been used in real-time flood forecasting for many years, but enabling the TF model adaptive to different catchment states and storm characteristics is a complicated task. However, the most significant advancement in this field has been done using the Kalman filter to update the TF model's state and parameters by various researchers like *Todini*, 1978; *Cluckie and Harpin*, 1980; *Bras and Rodriguez-Iturbe*, 1985; *Ge*, 2001, *Yang and Han*, 2006.

2.3.3 ANN-Fuzzy-GA-Adaptive Models

In recent years soft computing techniques are being increasingly used for forecasting floods [*Mukerji et al.*, 2009]. Various researchers have successfully applied artificial neural networks (ANN) for forecasting floods for different lead times [*Dawson and Wilby*, 1998; *Thirumalaiah and Deo*, 1998, 2000; *Sajikumar* and *Thandaveswara*, 1999; *Lekkas*, 2002; *Sudheer et al.*, 2002; *Laio et al.*, 2003; *Sudheer*, 2005; *Chang et al.*, 2007; *Tayfur et al.*, 2007; *Kisi*, 2008; *Mukerji et al.*, 2009; *Partthajit et al.*, 2010] . Fuzzy Logic (FL) is another area that has been applied successfully in flood forecasting in recent years [*Nayak et al.*, 2005a; *Singh*, 2007]. Integrated approaches have also been developed such as an adaptive neuro-fuzzy inference system (ANFIS) for hydrologic time series modeling of river flow and subsequently used for flow forecasting [*Nayak et al.*, 2004]. *Jain and Srinivasulu* [2004] used real-coded Genetic Algorithm (GA) to train ANN rainfall-runoff models to predict daily flow more accurately than the ANN rainfall-runoff models trained using the back propagation method. A comprehensive study to compare the performances of ANN,

ANFIS, and adaptive neuro-GA integrated system (ANGIS) models for forecasting floods was made by *Mukerji et al.* [2009]. Although several studies indicate that ANN models have proven to be potentially useful tools in hydrology, their disadvantages should not be ignored [*American Society of Civil Engineers (ASCE) Task Committee on Application of Neural Networks in Hydrology,* 2000a, 2000b]. The major limitation of ANN models as pointed out by ASCE Committee is the lack of physical concepts and relations.

2.4 HYDROMETRIC DATA-BASED FLOOD FORECASTING MODELS

2.4.1 Hydrologic and Hydraulic Models

According to *Nemec* [1985] classification the hydrometric data-based forecasting models comes under the category of purely deterministic forecasting models involving only stream flow processes. It can be further divided into three major groups: 1) Correlation of stages and/or volumes (discharge) models, 2) Systems approach to stream flow (hydrologic routing) models, and 3) Hydraulic/Simplified hydraulic routing models. The correlation models develop the functional relationships between the different data sets. These models work based on gauge, to gauge or discharge to discharge correlation and are amenable for flood forecasting in large rivers. Further these methods are widely employed in the development of the stage-discharge relationships (rating curve development) at gauged or ungauged river stations. Hydrological models used for forecasting are semi-empirical, conceptual or combination of both. Semi-empirical models are developed based on observations linking the causative factors and the response of the system. While empirical models are developed using past input and output data, semi-empirical models are developed based on lumped continuity equation and storage relationships. Flow routing based on conceptual models use the system concept in order to simulate the flood propagation process in channel and river reaches. As stated by

Lekkas [2002], storage routing based on Muskingum routing, channel cascade routing (Nash model), lag and route model, and combinations like the multilinear discrete cascade model [*Perumal*, 1994] and the discrete multilinear-lag model [*Camacho and Lees*, 2000] are all different types of hydrological models used for flow routing. Hydraulic river routing models are based on the numerical integration of partial differential equations, describing the flood routing phenomenon such as the Saint-Venant equations governing the one-dimensional flood movement in rivers [*Lekkas*, 2002]. This approach concentrates on the detailed description and accurate simulation of internal sub-processes and physical mechanisms that govern in a channel reach. But for dealing with many practical situations, simplified models derived from the Saint-Venant equations may be sufficient. The most commonly used simplified hydraulic models are the kinematic wave and linear diffusion equation methods, and these methods are derived from the Saint-Venant equations. Recently *Perumal and Ranga Raju* [1999] have introduced a new simplified equation known as the Approximate Convective-Diffusion (ACD) equation which is directly derived from the Saint-Venant equations and governs the channel flow process in the transition range between the diffusion and kinematic waves, including the latter. *Price* [2009] demonstrated the successful application of a physically based simplified routing technique for flow forecasting in a synthetic river channel and subsequently for the Wye River in UK [*Price*, 2009]. *Perumal et al.* [2011] used the physically-based VPMS model for real-time forecasting applications to a reach of Tiber River in Central Italy.

2.4.2 Models Based on Soft Computing Techniques

For the past few decades, soft computing techniques are widely used for forecasting floods. Artificial Neural Networks (ANN) tool is one of the soft computing techniques successfully applied for forecasting floods. Usually, all the neural networks are arranged

in layers. There are three types of layers, each having a different role in the overall operation of the network: the input layer, where the data pattern is presented, the hidden layers and the output layer. Each layer is made up of several nodes, and the layers are interconnected by correlation weights. ANN models are more versatile because of the freedom available with the choice of number of hidden layers and the nodes associated with each of these layers [*ASCE*, 2000a]. *Thirumalaiah and Deo* [1998a, 1998b], *Campolo et al.* [1999], *Imrie and Durucan* [1999] and *Kisi* [2004, 2007, and 2008] applied the ANN models for real-time flood forecasting of streamflow studies. *Lekkas* [2002] developed the ANN hydrometric data-based flood forecasting model and compared its performance with that of the Transfer Function data-based flood forecasting model. *Lekkas et al.*, [2005] stated that the ANN models can be simple (small networks) and yet keep the non-linear characteristics required to predict the river flow. Although several studies point out that ANN models have proven to be potentially useful tools, their disadvantages should not be ignored. An extensive review of their use in hydrological field is given by *ASCE Task Committee on Application of Neural Networks in Hydrology* [2000a, 2000b]. The *ASCE Committee* also stated that the success of an ANN application depends on both the quality and quantity of data available and this requirement cannot be easily met, as many hydrological records do not go back far enough to verify that conditions remained homogeneous over the span of time. This makes the resulting ANN structure more complicated when they include the temporal effects. Yet, another major limitation of ANN models pointed out by the ASCE Committee is the lack of physical concepts and relations. This has been one of the main reasons for the skeptical attitude towards this methodology. As the ANN models are data intensive and are restricted to time-homogeneous cases, consequently, changes in land use, irrigation patterns, crop rotations, and others cannot be accommodated easily in the ANN model networks, and

further they will complicate the networks of ANN. In view of these deficiencies of the soft computing technique models, the physically based models are desirable in practice. These physically based models have proved to be very useful in handling many hydrological flood forecasting problems [*ASCE Task Committee*, 2000a].

2.5 FLOOD ROUTING METHODS SUITABLE FOR HYDROMETRIC DATA-BASED FORECASTING

The problem of flood routing is concerned with the modification of flood wave as it moves downstream from a fixed point A to a fixed point B. Thus *Chow* [1959] writes:

"*In engineering hydrology, flood routing is an important technique necessary for the complete solution of a flood control problem and for the satisfactory operation of a flood-prediction service. For such purposes flood routing is recognized as a procedure required in order to determine the hydrograph at one point on a stream from the known hydrograph at an upstream point*".

Two distinct modifications take place while the inflow hydrograph is routed downstream of a channel. They are:

(a) *Attenuation of the peak*: The peak of the routed hydrograph is less than or equal to the peak of the inflow hydrograph. The time base of the routed hydrograph is increased due to the combined effect of storage and channel friction.

(b) *Translation or lag of the peak*: The peak outflow hydrograph occurs sometime later than the peak of the inflow hydrograph. This is due to translation of the flood waves in the channel.

The flood is, therefore, said to be moderated while passing through a water course. Some important methods of routings are discussed herein:

All the methods available for routing floods in channels are broadly classified into two groups: (1) Hydrologic routing and (2) Hydraulic routing. Routing by lumped system methods is called hydrologic (lumped) routing, and routing by distributed system methods is called hydraulic (distributed) routing.

2.5.1 Hydrological routing methods

These hydrologic river routing methods assume the channel reach as a lumped system, and use the lumped continuity equation arrived from the distributed continuity equation and a storage equation as a substitute for the moment equation of the Saint-Venant equations which govern the one-dimensional flow in channels and rivers [*Barré de Saint-Venant*, 1871a, 1871b]. In hydrologic routing, only the hydrograph of the routed variable is estimated unlike the hydraulic routing method which estimates the outflow hydrograph of the routed variable along with the stage or discharge variable depending on the routing variable, either discharge or stage, respectively. On the basis of the type of storage equation used in the model framework, the hydrologic routing methods can be classified as linear or nonlinear. The widely used classical Muskingum routing method [*McCarthy*, 1938] is based on a linear storage routing concept. Similarly, the Nash model [*Nash*, 1960] based on routing through a series of equal linear reservoirs, by conceptualizing each of the successive small channel reaches as a linear reservoir, may also be considered as a lumped routing model [*Dooge*, 1973]. Various researchers like *Rockwood* [1958], *Laurenson* [1962, 1964] and *Mein et al.* [1974] proposed hydrologic methods with nonlinear storage equations. *Perumal* [1995] stated that the real distinction between the hydrologic and hydraulic methods should be on the basis of the estimation of the routing parameters of the method. In his opinion, if the parameters of the storage routing method are estimated using the recorded inflow, outflow, and the corresponding storage information only, then it may be categorized as the hydrologic method; and if, they are

estimated using the established relationships based on the channel and flow characteristics, then it may be categorized as the hydraulic routing method.

2.5.2 Hydraulic routing methods

Flood flow through a river reach always involves a varied flow problem and the flow is unsteady. Hydraulic (distributed) flow routings allow computation of the flow rate and water surface elevation (or depth) as a function of both space (location) and time. Hydraulic routing methods use two types of conservation equations: 1) the conservation of mass and 2) the conservation of momentum. Solution to the problem is arrived at using numerical methods. For unsteady flow conditions, the continuity and the momentum equations without considering lateral flow are, respectively written as:

$$\frac{\partial Q}{\partial x}+\frac{\partial A}{\partial t}=0 \tag{2.1}$$

$$S_f = S_o - \frac{\partial y}{\partial x} - \frac{v}{g}\frac{\partial v}{\partial x} - \frac{1}{g}\frac{\partial v}{\partial t} \tag{2.2}$$

$$(1) \quad (2) \quad (3)$$

where Q is the discharge, A is the flow area, S_o is the bed slope, S_f is the energy slope, g is the acceleration due to gravity, v is the average velocity over cross section, y is the depth of flow, and the notations x and t denote the space and time variables, respectively. The gradients in the momentum equation (2.2): $\partial y/\partial x$, $(v/g)(\partial y/\partial x)$, and $(1/g)(\partial v/\partial t)$ denote the longitudinal water surface gradient denoted as term (1), the convective and local acceleration gradients denoted as terms (2) and (3) respectively. No lateral flow is considered in the above equations. Equations (2.1) and (2.2) together are known as the Saint-Venant equations or full Saint-Venant equations. The hydraulic

methods of flood routing are based on the full Saint-Venant equations or their simplifications. For that reason, the hydraulic methods may be classified into two major groups: 1) the dynamic wave method based on the solution of the full Saint-Venant equations, and 2) the simplified hydraulic methods or the physically based hydrologic methods [*Sahoo*, 2007]. In the dynamic wave method, all the terms in the Saint-Venant's momentum equation are used. The simplified hydraulic methods are based on the continuity equation, which is either distributed or lumped, and a simplified momentum equation arrived at by truncating or approximating or linearizing the pressure and acceleration terms in the momentum equation of the full Saint-Venant equations. These simplified methods are useful for solving the computationally intensive hydrological land-surface schemes of the climate change models [*Sahoo*, 2007]. Flow problems solved using these two hydraulic approaches give better results. However, the application of the hydraulic routing method based on the full Saint-Venant equations requires high quality input data, cross-sectional data at closer intervals, and better understanding of this method by the field engineers dealing with flood forecasting. In the past, many researchers like *Henderson* [1966], *Kuchment* [1972], *Weinmann and Laurenson* [1979], [*Dooge*, 1980], *Zoppou and O'Neill* [1982], *Ferrick* [1985] carried out their studies to determine the magnitude of different terms in the Saint-Venant's momentum equation, such as the longitudinal water surface gradient, the convective and local acceleration gradients with the objective of understanding their effects on the propagation dynamics of the flood wave. It may be inferred from their findings that these different terms of the momentum equation may be truncated or approximated for many practical cases of flood routing, resulting in the simplified forms of momentum equation. It was also found that when the magnitudes of different terms in the momentum equation are widely varying, the dynamic wave equations become stiff leading to numerical stability problems and, in such a case,

the use of simplified momentum equation is inevitable [*Ferrick,* 1985]. *Woolhiser and Liggett* [1967], the British Flood Studies Report [*National Environment Research Council (NERC),* 1975], and *Ranga Raju et al.* [1993] also emphasize the need of using the simplified routing methods.

2.6 SIMPLIFIED HYDRAULIC FLOOD ROUTING METHODS

Perumal [1995] has classified the simplified hydraulic flood routing methods into two major groups: 1) directly derived simplified methods; and 2) indirectly derived simplified methods. The directly derived simplified flood routing methods are derived directly from the full Saint-Venant equations after truncating or approximating some of the terms in the momentum equation. The indirectly derived simplified methods use a lumped continuity equation in place of the distributed continuity equation of the Saint-Venant equations and a linear or nonlinear storage equation (usually in linear form). The storage equation expresses storage as a function of inflow and outflow in a channel reach; however, without describing how the storage is distributed within the reach [*Kulandaiswamy,* 1964]. The convection–diffusion equations [*Hayami,* 1951; *Price,* 1973], the approximate convection–diffusion (ACD) equations [*Perumal and Ranga Raju,* 1999], the kinematic wave equations [*Lighthill and Whitham,* 1955], and the linearized Saint-Venant equations of *Dooge and Harley* [1967] are some of the specific examples of the directly derived simplified methods. The convection–diffusion equation is considered as linear or nonlinear depending on whether the celerity *'c'* and diffusion *'D'* in this equation remain constant or vary over the entire routing process. The convection–diffusion equations in linear and nonlinear formulations may be solved by numerical techniques [*Thomas and Wormleaton,* 1970, 1971; *Price,* 1973; *NERC,* 1975; *Akan and Yen,* 1977; *Katapodes,* 1982]; and in linear formulation they may also be solved by analytical techniques [*Hayami,* 1951; *Dooge,* 1973]. Further, Kalinin–Milyukov method and the Muskingum

method are the specific examples of indirectly derived simplified flood routing methods. Many researchers like *McCarthy* [1938]; *Kalinin and Milyukov* [1958]; *Dooge* [1973]; *Price* [1973]; *Wong and Laurenson* [1983, 1984]; *Perumal* [1994a, b], *Perumal and Ranga Raju* [1998a, b], *Price* [2009], and *Price and Perumal* [2011] have significantly contributed to the area of simplified routing methods. However, the significance of the application of simplified methods for flood routing purposes was brought out by the British Flood Studies Report [*NERC*, 1975].

2.6.1 Kalinin-Milyukov routing method

The Kalinin–Milyukov routing method [*Kalinin and Milyukov*, 1958; *Apollov et al.*, 1964] is a conceptual linear storage routing method derived from the hydrodynamic principles in which a given prismatic channel reach is subdivided into a number of subreaches (characteristic reaches) wherein the storage is a linear function of the outflow discharge. This method is based on the assumption of a one-to-one relationship between the stage and the discharge during unsteady flow condition in which the discharge at any instant of time at the outlet of the reach is related to the stage at the middle of the reach. Hence, the discharge at any instant of time is a function of the depth of flow and the longitudinal gradient of the water surface at that section. During unsteady flow condition, it is assumed that the longitudinal gradient of the water surface remains constant over the length of the characteristic reach. Further, during the transformation of steady flow to unsteady flow, the discharge at the outflow section of the reach does not change. The number of characteristic reaches, N_c required for routing a discharge hydrograph in a given reach of length Δx using the Kalinin–Milyukov method is given by

$$N_c = \frac{S_0 B_0 c_0 \Delta x}{Q_0} \tag{2.3}$$

and the reservoir coefficient, K of each characteristic reach is

$$K = \frac{Q_0}{S_0 B_0 c_0^2} \tag{2.4}$$

where, Q_o is the reference discharge, B_o is the water surface width corresponding to Q_o, and c_o is the wave celerity corresponding to Q_o. Using the moment matching technique, *Dooge* [1973] linked the first and second moments of the instantaneous unit hydrograph (IUH) of the Nash model with the corresponding moments of the linearized Saint-Venant equations, when the Froude number, F = 0, and arrived at the same relationships for the number of linear reservoirs in series and the reservoir coefficient as given by equations (2.3) and (2.4), respectively. Note that when the Nash model parameter representing the number of linear reservoirs in a reach is an integer, the Nash model becomes a conceptual representation of the Kalinin–Milyukov method. Since the Nash model can operate on non-integer N_c values, the flood routing using the Nash model with the parameters estimated using equations (2.3) and (2.4) is more flexible than the Kalinin-Milyukov method. This avoids the interpolation of the outflow hydrograph when the last characteristic reach of the Kalinin-Milyukov method does not coincide with the outflow section of a given routing reach [*Koussis*, 1980]. *Kundzewicz* [1982] found that the routing solution of the Kalinin-Milyukov method, when compared with that of the Muskingum solution, was relatively insensitive to the variation in the reference discharge used for the estimation of the model parameters. Further, in order to enable the use of Kalinin-Milyukov (K-M) method for flood forecasting, the K-M method has been formulated using state-space analysis [*Szollosi-Nagy*, 1976]. State-space analysis of the K-M method enables easy use of the parameter updating algorithm such as the Kalman filter to improve the estimation of forecasted flood of a given lead time by minimizing the

errors between the model estimated flood and the corresponding observed flood up to the time of forecast.

2.6.2 The classical Muskingum routing method

The classical Muskingum method [*McCarthy,* 1938] of flood routing derived its name after its first application to the Muskingum River, a tributary of the Ohio River in the USA, is a linear storage routing method and it is widely used in practice [*Singh,* 1988] . This method models the flood storage of a given routing reach at any instant of time of the propagation of a flood event as a combination of wedge and prism storage. This method combines the lumped continuity equation

$$\frac{dS}{dt} = I - O \tag{2.5}$$

with the linear storage equation (i.e. storage is a linear function of inflow and outflow)

$$S = K\left[\theta I + (1-\theta)O\right] \tag{2.6}$$

to arrive at the difference equation which on simplification leads to the Muskingum routing equation as

$$O_{j+1} = C_1 I_{j+1} + C_2 I_j + C_3 O_j \tag{2.7}$$

where S is the storage volume, I is the inflow discharge, O is the outflow discharge, K is the travel time, θ is the weighting parameter, the suffix j denotes the time $j\Delta t$, where, Δt is the routing time interval, and the routing coefficients C_1, C_2, and C_3 are expressed as

$$C_1 = \frac{-K\theta + 0.5\Delta t}{K(1-\theta) + 0.5\Delta t} \tag{2.8a}$$

$$C_2 = \frac{K\theta + 0.5\Delta t}{K(1-\theta) + 0.5\Delta t} \tag{2.8b}$$

$$C_3 = \frac{K(1-\theta) - 0.5\Delta t}{K(1-\theta) + 0.5\Delta t} \tag{2.8c}$$

where $C_1 + C_2 + C_3 = 1.0$,which shows the mass conserving ability of the classical Muskingum method. Given an inflow hydrograph, an initial flow condition, a chosen time interval Δt , and the routing parameters K and θ , the routing coefficients can be calculated with equation (2.8) and subsequently the outflow hydrograph can be arrived at using equation (2.7). The routing parameters K and θ are related to flow and channel characteristics with K being interpreted as the travel time of the flood wave from upstream end where inflow hydrograph is applied to downstream end of the routing reach. The parameter θ is the weighting parameter used for weighting the prism and wedge storage to determine the equivalent prism storage of the reach at any instant of time. To calculate the value of θ, the storage S is plotted against the corresponding weighted discharge value $\left[\theta I + (1-\theta)O\right]$ in equation (2.6) for different trial values of θ resulting in various sizes of loops; and the value of θ which gives the narrowest loop of this plot is considered as the appropriate one for its use in the method. The effect of storage is to reduce the peak flow and spread the hydrograph over time and this effect introduces diffusion of the propagating flood wave resulting in peak attenuation. The successful application of the Muskingum method for real life routing problems led the hydrologists to think on the lines of linking the parameters K and θ to channel and flow characteristics. Subsequently, several attempts have been made by various researchers [*Dooge and Harley,* 1967; *Cunge,* 1969; *Dooge et al.,* 1982] to link the routing parameters K and θ of the classical Muskingum method with the flow and channel characteristics using the hydrodynamics principles to transform it into a physically based

method. Further, various attempts have been made for the physical interpretation of the classical Muskingum method by several researchers like *Apollov et al.* [1964]; *Cunge* [1969]; *Dooge* [1973]; *Koussis,* 1976; *Strupczewski and Kundzewicz* [1980]; *Dooge et al.,* [1982] *Kundzewicz* [1986]; *Perumal* [1992c; 1995].

2.6.2.1 Physically based Muskingum routing methods

For the past few decades, various attempts have been made for the physical interpretation of the classical Muskingum method. They may be broadly categorized as [*Kundzewicz,* 1986; *Perumal,* 1995]: i) direct interpretation [*Strupczewski and kundzewicz,* 1980], ii) matching the impulse response of the Muskingum method with that of the linearized Saint-Venant equations using the method of moments approach [*Dooge,* 1973], iii) matching difference schemes [*Cunge,* 1969; *Koussis,* 1976; *Dooge et al.,* 1982], and iv) the method based on the extension of the Kalinin-Milyukov method [*Apollov et al.,* 1964; *Perumal,* 1992c]. The salient features of each of these approaches are described below:

i) *Direct interpretation*: *Strupczewski and kundzewicz* [1980] attempted the interpretation of the Muskingum method directly from the Saint-Venant equations. Their interpretation of a one-to-one relationship between the stage and the discharge could not depict the storage equation of the Muskingum method as a linear function of the weighted discharge within the reach. Further, they could not express the parameters K and θ explicitly in terms of channel and flow characteristics.

ii) *Method based on the moment matching approach*: *Dooge* [1973] arrived at the following expressions for the routing parameters K and θ of the Muskingum method by matching the first and second moments of the IUH (Instantaneous Unit Hydrograph) of the linearized Saint-Venant equation with the corresponding moments of the Muskingum IUH. To arrive at the two parameters of the Muskingum method, he used the Chezy's and

Manning's friction law in wide rectangular channels. The parameters are expressed as:

$$K = \frac{\Delta x}{c_o} \tag{2.9}$$

$$\theta = \frac{1}{2} - \frac{Q_o \bar{y}_r}{2 S_o A_o c_o \Delta x}\left[1 - (m-1)^2 F_o^2\right] \tag{2.10}$$

where $\bar{y}_r$ =the average hydraulic mean depth; A_o =the area of cross-section corresponding to Q_o; c_o =wave celerity; F_o= Froude number corresponding to Q_o; and m =3/2 or 5/3 when Chezy's or Manning's friction law used, respectively.

iii) ***Method based on the matching difference schemes***: Although, *Dooge and Harley* [1967] presented the Muskingum parameter relationships with the wide rectangular channel and flow characteristics through the moment matching technique [*Nash,* 1960], *Dooge et al.,* [1982] latter arrived at the same for any shape of prismatic channel and for any type of friction law. However, it is the *Cunge's* [1969] matched diffusivity approach which has become more popular as the "Muskingum-Cunge (MC) method". It was *Price* [1973] who first coined the term "Muskingum-Cunge (MC) method". By matching the numerical diffusivity of the approximate linear kinematic wave equation, derived from the classical Muskingum difference equation, with the physical diffusivity of the linear convection-diffusion equation, *Cunge* [1969] arrived at the relationship for K as given in equation (2.9) and θ for wide rectangular channels as

$$\theta = \frac{1}{2} - \frac{Q_o}{2 S_o B_o c_o \Delta x} \tag{2.11}$$

Note that when the Froude number, $F_o = 0$, *Dooge et al.'s* [1982] expression for θ given by equation (2.10) reduces to *Cunge's* [1969] equation (2.11). *Perumal* [1992a] studied the differences in the routing results obtained using equations (2.10) and (2.11) for

varying Froude number cases and showed that the use of the former equation makes a very insignificant improvement on the estimated numerical value of θ over that of the latter equation. However, the use of equation (2.10) is advantageous as it retains the Vedernikov number [*Jolly and Yevjevich,* 1971; *Ponce,* 1991; *Perumal,* 1992a] which gives the amplification criterion of a flood wave while it moves downstream of a channel.

iv) ***Method based on the extension of the Kalinin-Milyukov method***: On the basis of the extension of the Kalinin-Milyukov method described by *Apollov et al.* [1964] for the interpretation of the Muskingum method, *Perumal* [1992c] brought out that only this method enables one to establish the reason behind the formation of negative or reduced outflow at the beginning of the Muskingum method solution. The parameter relationships for K and θ as established by this approach are the same as given by equation (2.9) and (2.11). *Wong* [1984] also independently made the interpretation of the Muskingum storage equation on the lines of *Apollov et al.* [1964].

2.6.3 Multilinear Methods

The multilinear flood routing methods, also known as the multiple input linear methods, multiple linearization methods, or nonlinear threshold methods [*Keefer and McQuivey,* 1974; *Becker,* 1976; *Kundzewicz,* 1984; *Becker and Kundzewicz,* 1987] attempt to account for the nonlinear effects in the flood wave propagation dynamics without rejecting the mathematical convenience of the linear systems. The principle of the multilinear routing technique is to discern different components on the input hydrograph, each of which is subsequently routed through a simple linear model. Depending upon the horizontal or vertical division of the inflow hydrographs, the multilinear routing methods can be broadly categorized as: 1) the amplitude distribution scheme-based multilinear methods, and 2) the time distribution scheme-based multilinear methods. The amplitude distribution scheme, in which the horizontal distinctions represent different zones of

discharge is more popular [*Keefer and McQuivey,* 1974; *Becker,* 1976; *Becker and Kundzewicz,* 1987] over the time distribution scheme [*Kundzewicz,* 1984; *Becker and Kundzewicz,* 1987] in which the vertical distinctions are introduced at fixed times. However, the time distribution scheme is more amenable for modeling the nonlinear dynamics of the flood routing process in a more efficient way than the amplitude distribution scheme. In the multilinear Muskingum discharge routing method developed by *Perumal* [1992b] based on the concept of time distribution scheme, the routing parameters of the linear sub-model is varied at every routing time step leading to a variable parameter flood routing method.

2.7 VARIABLE PARAMETER DISCHARGE ROUTING METHODS

The variable parameter flood routing methods are mainly developed for accounting the nonlinear dynamics of flood wave propagation by varying one or more routing parameters at every routing time step. While developing the variable parameter diffusion (VPD) routing method, *Price* [1973] proposed a way of accounting for the nonlinearity in the flood wave movement at every routing time interval, in which the parameters c and D of the convection–diffusion equation were defined as functions of the stage or discharge of the river. However, since the VPD method which is solved by the numerical methods is too restrictive on the size of space and time steps and there are practical difficulties in defining data curves for the c–D relationships, the British Flood Studies Report [*NERC,* 1975] suggested the development of a variable parameter Muskingum method. On the basis of this suggestion, *Price* [1985] and *Ponce and Yevjevich* [1978] developed the variable parameter Muskingum–Cunge (VPMC) method in which the parameters of the Muskingum method vary at every routing time step. As it was producing acceptable results and due to its wider applicability to the river routing problems, the U.S. Army Corps of Engineers has added this method in the HEC-HMS [*USACE,* 2010] model.

Some studies have also been conducted in the past for routing discharge hydrographs in compound channels using the VPMC method and its variants [*Garbrecht and Brunner*, 1991; *Tang et al.,* 1999b]. However, the VPMC method is unfortunately saddled by a small but perceptible loss of mass [*Ponce,* 1983; *Ponce and Chaganti*, 1994; *Tang et al.*, 1999a, b; *Perumal et al.,* 2001]. To overcome this deficiency, *Perumal* [1992b] proposed a Multilinear Muskingum (MM) method, and showed that the MM method scores better than the VPMC method in reproducing the solutions of the Saint-Venant equations closely. As an alternative interpretation for the Muskingum method, *Perumal* [1994a, 1994b] developed a Variable Parameter Muskingum Discharge-routing (VPMD) method and, on the same lines, a Variable Parameter Muskingum Stage-routing (VPMS) method [*Perumal and Ranga Raju,* 1998a, 1998b]. Both these methods were derived directly from the Saint-Venant equations for routing flood waves in semi-infinite rigid bed prismatic channels having any shape of cross-section, and for flow following either Manning's or Chezy's friction law. *Heatherman* [2004] found that the VPMD method is able to give physical justification for the Muskingum method better than the Muskingum-Cunge method advocated by *Cunge* [1969].The advantage of this simplified hydraulic routing method is that it allows the simultaneous computation of discharge as well as the corresponding stage hydrograph. Although, the problem of volume conservation of the VPMD method is less severe than the VPMC method [*Sahoo*, 2007], but it is still not fully volume conservative. The field applicability of the VPMD method was further demonstrated for routing floods in rivers including those flood events that inundated the floodplain. Some of these applications include routing in Tyne River in the United Kingdom [*Perumal et al., 2001*] and for reaches of Tiber River in Central Italy [*Perumal et al.,* 2007]. Recently *Perumal and Sahoo,* [2007] conducted a numerical experimental study to develop the applicability criteria of these VPMD and VPMS

methods in comparison with the Variable Parameter Muskingum-Cunge (VPMC) method. On the basis of this numerical study, *Perumal and Sahoo* [2007] suggested that the applicability of these methods assessed at the inlet of the reach for routing a given hydrograph in rectangular and trapezoidal channel reaches require to satisfy the following criteria:

VPMD method (for successful discharge routing and corresponding stage estimation) $(1/S_o)(\partial y/\partial x)_{\max} \le 0.43$

VPMS method (only for stage routing) $(1/S_o)(\partial y/\partial x)_{\max} \le 0.79$

VPMS method (for successful stage routing as well as discharge computation) $(1/S_o)(\partial y/\partial x)_{\max} \le 0.63$

VPMC method (discharge routing) $(1/S_o)(\partial y/\partial x)_{\max} \le 0.11$

where, $(1/S_o)(\partial y/\partial x)_{\max}$ is the longitudinal water surface gradient estimated at the inlet of the reach for the given input hydrograph .

To overcome the mass conservation problem of the variable parameter Muskingum method, recently, *Todini* [2007] proposed Muskingum-Cunge-Todini (MCT) method and tried to resolve the mass conservation inconsistency by converting the reach storage at any time during unsteady flow to that of the steady flow having the same storage. This equivalent storage interpretation resulted in the modification of the parameter K relationship as:

$$K = \frac{\Delta x}{\left(\frac{c}{\beta}\right)} \tag{2.12}$$

where β = a dimensionless correction coefficient; c = wave celerity. The parameter relationship for K given in equation (2.9) (established for the MC method) is different from the equation given in (2.12) (established for the MCT method). A correction factor β was introduced by *Todini* [2007] in order to replace wave celerity with flow velocity in the denominator term of the K equation.

Very recently, similar to the method proposed by *Todini* [2007], *Price* [2009] also developed a volume conservative variable parameter Muskingum method for a synthetic river cross-section which includes both main and floodplain sections. Based on the logical consideration of fully conserving the mass of the routed hydrograph, a simple way of developing a physically based Variable Parameter Muskingum method taking into account the McCarthy's [1938] storage concept has been proposed recently by *Price and Perumal* [2011]. This method known as the variable parameter McCarthy-Muskingum method has been developed for routing in-bank floods only. This fully mass conservative method has been extensively tested for its appropriateness. This method could be extended for the over-bank flow condition to improve the applicability of this method for river routing problems. Since, the VPMMD method is basically used in this thesis for its extension to routing floods in channel reaches with floodplains, it is considered necessary herein to give a detailed theoretical background of this method.

2.7.1 Theoretical Background of the VPMMD Method

The VPMMD method [*Price and Perumal*, 2011] is directly derived from the full Saint Venant equations describing the continuity and momentum of the one-dimensional unsteady flow. While the continuity equation has been used as it is, the momentum equation has been approximated using some assumptions. The parameters of the VPMMD vary at every routing time interval and they are related to the channel and flow

characteristics by a similar form of relationships as established for the physically based Muskingum method [*Apollov et al.*, 1964; *Cunge*, 1969; *Dooge et al.*, 1982; *Perumal*, 1994a, 1994b]. The description of the method is presented herein. The Saint-Venant equations governing the flow propagation in a channel reach without considering lateral flow are described by equations (2.1) and (2.2). The variables immediately above the terms (1), (2) and (3) of equation (2.2) denotes the longitudinal water surface gradient the gradients due to convective and local acceleration, respectively. Assuming the friction slope S_f is approximately constant over a small length of routing reach at any instant of time and $(1/S_o)\partial y/\partial x \ll 1$, one can arrive at the expression for simplified momentum equation using the Mannng's friction law as

$$\frac{\partial Q}{\partial x} = Bc\frac{\partial y}{\partial x} \tag{2.13}$$

where, $B = \partial A/\partial y$ is the water surface width corresponding to flow depth y; c is wave celerity expressed as

$$c = \left[1 + \frac{2}{3}\frac{(PdR/dy)}{dA/dy}\right]v \tag{2.14}$$

where, R is the hydraulic radius (A/P); and P is the wetted perimeter.

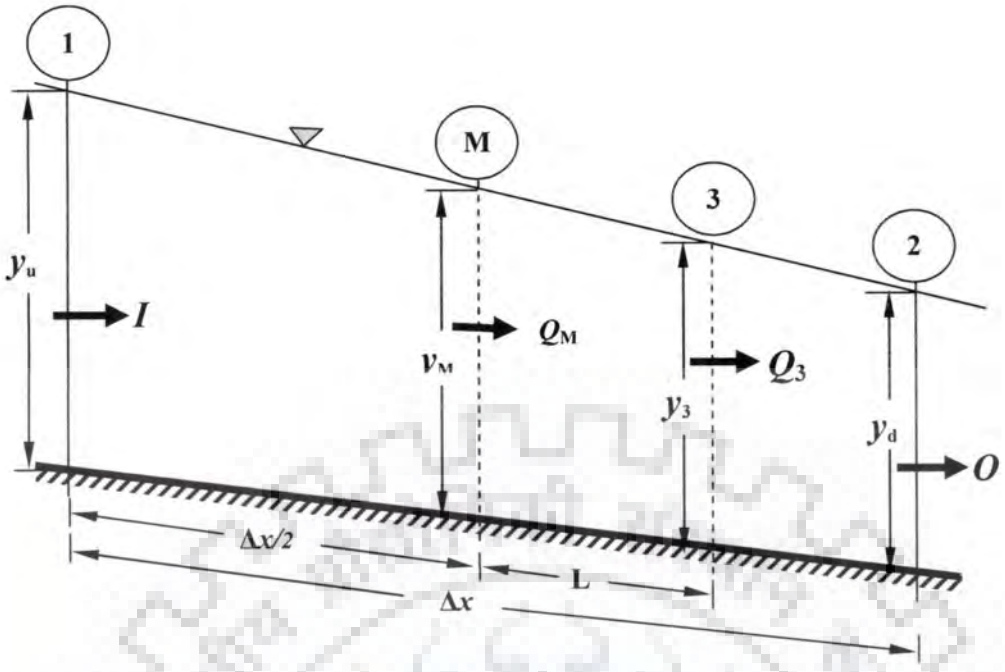

Figure 2.1 Definition sketch of the variable parameter McCarthy-Muskingum discharge-routing (VPMMD) method computational reach.

Using equations (2.1), (2.2) and (2.13) and (2.14) and the expression of discharge using the Manning's friction law, S_f can be expressed as

$$S_f = S_o \left\{ 1 - \frac{1}{S_o} \frac{\partial y}{\partial x} \left[1 - \frac{4}{9} F^2 \left(\frac{P dR/dy}{dA/dy} \right)^2 \right] \right\} \tag{2.15}$$

where F is the Froude number and is expressed as

$$F = \left(\frac{v^2 \, dA/dy}{gA} \right)^{\frac{1}{2}} \tag{2.16}$$

Using equation (2.15), the discharge Q_M at the middle of the computational channel reach (i.e. section M in Figure 2.1) can be expressed using the Manning's friction law as

$$Q_M = Q_3 \left\{ 1 - \frac{1}{S_o} \frac{\partial y}{\partial x} \left[1 - \frac{4}{9} F^2 \left(\frac{PdR/dy}{dA/dy} \right)^2 \right] \right\}_M^{\frac{1}{2}} \tag{2.17}$$

where Q_3 is the normal discharge corresponding to the flow depth y_M which passes at the weighted section 3 as shown in Figure 2.1

Q_3 can be expressed using equation (2.17) as

$$Q_3 = Q_M \left\{ 1 - \frac{1}{S_o} \frac{\partial y}{\partial x} \left[1 - \frac{4}{9} F^2 \left(\frac{PdR/dy}{dA/dy} \right)^2 \right] \right\}_M^{\frac{-1}{2}} \tag{2.18}$$

Approximating the right hand side of the above equation (2.18) using the binomial series expansion and using equation (2.13), Q_3 can be expressed as

$$Q_3 = Q_M + \frac{Q_M \left[1 - \frac{4}{9} F^2 \left(\frac{PdR/dy}{dA/dy} \right)^2 \right]_M}{2 S_o B_M c_M} \cdot \left. \frac{\partial Q}{\partial x} \right|_M \tag{2.19}$$

where B_M and c_M are the surface width and wave celerity, respectively, at midsection of the routing reach. It may be noted that the quotient adjacent to the term $\left. \frac{\partial Q}{\partial x} \right|_M$ denotes the distance between the mid-section and weighted section (i.e. section 3 in Figure 2.1), where the normal discharge corresponding to the flow depth at the mid-section of the reach passes.

The wave celerity c_M can also be expressed similar to equation (2.17) as

$$c_M = c_{Mo} \left\{ 1 - \frac{1}{S_o} \frac{\partial y}{\partial x} \left[1 - \frac{4}{9} F^2 \left(\frac{PdR/dy}{dA/dy} \right)^2 \right] \right\}_M^{\frac{1}{2}} \tag{2.20}$$

Replacing Q_M and c_M in the numerator and denominator of quotient of $(\partial Q/\partial x)_M$ in equation (2.19) by equation (2.17) and (2.20), respectively, leads to the modified expression as

$$Q_3 = Q_M + \frac{Q_3\left[1-\frac{4}{9}F^2\left(\frac{PdR/dy}{dA/dy}\right)^2\right]_M}{2S_o B_M c_{Mo}} \cdot \left.\frac{\partial Q}{\partial x}\right|_M \tag{2.21}$$

where c_{Mo} is the normal wave celerity at midsection of the routing reach.

Assuming approximate linear variation of discharge over the routing reach and expressing Q_M as the average of inflow, I and outflow, O, and $\partial Q/\partial x|_M = (O-I)/\Delta x$, Q_3 given in equation (2.21) can be expressed as

$$Q_3 = \theta I + (1-\theta)O \tag{2.22}$$

where θ is the weighting parameter of the Muskingum routing equation and is expressed as

$$\theta = \frac{1}{2} - \frac{Q_3\left[1-\frac{4}{9}F^2\left(\frac{PdR/dy}{dA/dy}\right)^2\right]_M}{2.S_o.B_M.c_{Mo}.\Delta x} \tag{2.23}$$

If inertial terms of the Saint-Venant equations are neglected, equation (2.23) can be expressed as

$$\theta = \frac{1}{2} - \frac{Q_3}{2.S_o.B_M.c_{Mo}.\Delta x} \tag{2.24}$$

Applying the hydraulic continuity equation (2.1) at the midsection of the Muskingum routing reach of length Δx, it can be written based on the computational grid network shown in Figure 2.2 as

$$\frac{\partial A_M}{\partial t} + \frac{\partial Q_M}{\partial x} = 0 \tag{2.25}$$

As the discharge Q_3 is passing at section 3 (Figure 2.1) during unsteady flow, it is uniquely related to flow depth y_M at the mid section of the routing reach (Kalinin-Milyukov concept), which in turn is uniquely related to the flow area A_M, then Q_3 can be expressed as

$$Q_3 = A_M V_{Mo} \tag{2.26}$$

where V_{Mo} is the normal velocity at the midsection of the routing reach.

Using equation (2.26) in equation (2.25), the continuity equation can be expressed as

$$\frac{\partial}{\partial t}\left(\frac{Q_3}{V_{Mo}}\right) + \frac{\partial Q_M}{\partial x} = 0 \tag{2.27}$$

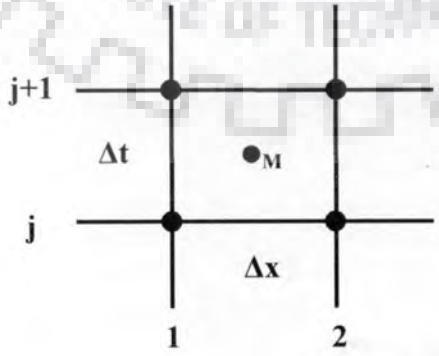

Figure 2.2 The Finite-difference grid representation of the VPMMD method computational scheme

Applying the above hydraulic continuity equation (2.27) at the midpoint of the finite-difference grid as shown in Figure 2.2 and expressing in finite difference form gives

$$\Delta x\left[\frac{Q_{3,j+1}}{V_{Mo,j+1}}-\frac{Q_{3,j}}{V_{Mo,j}}\right]=\Delta t\left[\frac{I_{j+1}+I_{j}}{2}-\frac{O_{j+1}+O_{j}}{2}\right] \tag{2.28}$$

The unknown O_{j+1} is to be determined from equation (2.28) using equation (2.22) in it and it can be expressed in the classical Muskingum routing equation form as

$$O_{j+1}=\frac{\Delta t-2.K_{j+1}.\theta_{j+1}}{\Delta t+2.K_{j+1}.\left(1-\theta_{j+1}\right)}.I_{j+1}+\frac{\Delta t+2.K_{j}.\theta_{j}}{\Delta t+2.K_{j+1}.\left(1-\theta_{j+1}\right)}.I_{j}+\frac{-\Delta t+2.K_{j}.\left(1-\theta_{j}\right)}{\Delta t+2.K_{j+1}.\left(1-\theta_{j+1}\right)}.O_{j} \tag{2.29}$$

where $$\frac{\Delta t-2.K_{j+1}.\theta_{j+1}}{\Delta t+2.K_{j+1}.\left(1-\theta_{j+1}\right)}=C_{1} \tag{2.30a}$$

$$\frac{\Delta t+2.K_{j}.\theta_{j}}{\Delta t+2.K_{j+1}.\left(1-\theta_{j+1}\right)}=C_{2} \tag{2.30b}$$

$$\frac{-\Delta t+2.K_{j}.\left(1-\theta_{j}\right)}{\Delta t+2.K_{j+1}.\left(1-\theta_{j+1}\right)}=C_{3} \tag{2.30c}$$

are the coefficients of the Muskingum routing equation

The Muskingum method travel time K and θ at the time level $(j+1)$ are expressed, respectively $$K_{j+1}=\frac{\Delta x}{V_{Mo,j+1}} \tag{2.31}$$

$$\theta_{j+1}=\frac{1}{2}-\frac{Q_{3,j+1}\left[1-\frac{4}{9}F_{j+1}{}^{2}\left(\frac{PdR/dy}{dA/dy}\right)_{j+1}^{2}\right]}{2S_{o}\left(B_{M}c_{Mo}\right)_{j+1}\Delta x} \tag{2.32}$$

The downstream stage y_d corresponding to the routed discharge O_{j+1} can be estimated as [*Perumal*, 1994a, 1994b].

$$y_d = y_M + \frac{\left(O_{j+1} - Q_M\right)}{\left.\frac{\partial Q}{\partial y}\right|_M} \tag{2.33}$$

where, y_M and Q_M are the stage and discharge at the midsection of the routing reach, respectively.

2.8 RELEVANCE OF THE VARIABLE PARAMETER ROUTING MODELS FOR HYDROMETRIC DATA-BASED FLOOD FORECASTING

While there are so many data driven models ranging from the traditional correlation based models to the recent neural network models, it is required to employ a forecasting model that is physically based, even though in a simplified form, than using a sophisticated black-box model such as that of a neural network model. The relevance of this statement would be recognized when significant changes take place in the catchments or when the upstream data collection station is washed away in floods or when the recorded flood is far exceeding the past floods based on which the parameters of the data driven model have been calibrated. Under such situations the use of black-box models, the parameters of which are estimated from the past data are not desirable. Therefore, a model accounting for the non-linearity of the flood propagation process based on physical consideration and capable of operating in simulation as well as forecasting mode is more desirable for forecasting purposes. However, many studies caution against the use of ANN based forecasting models indiscriminately [*Hill et al.* 1994]. The *ASCE Committee* also stated that the artificial neural networks cannot be considered as a panacea for hydrologic problems, nor can they be viewed as replacement for other modeling

techniques. Alternatively, in any real-time flood forecasting model it is desirable to employ a physically based basic model to describe the physical behavior of the system from the remaining part which describe the structure of the forecasting errors, also known as residuals, and the parameter of the "physical" part of the model should be estimated independently of those of the residual component in order to reduce the domination of the residual component or the error model over the basic model. While this concept is difficult to introduce in a flood forecasting model dealing with rainfall-runoff transformation process, it is amenable for incorporation in a hydrometric data-based flood forecasting models, mainly dealing with flood routing process only. Therefore, it is highly desirable to use physically based simplified routing model for flood forecasting purposes. However, the use of physically based simplified linear models for real-time flood forecasting purposes is also not desirable as it fails to take care of the non-linear characteristics of flood wave movement in channels resulting in large forecasting errors. While one can minimize these forecasting errors using Kalman filter (a complicated updating algorithm) by updating the routing parameters in real-time to arrive at the improved forecast, but these updated model parameters lose its physical relevance and simply serve only as the fitting parameters, though the forecasting errors could be minimized. Alternatively, simple error updating techniques of the residuals such as the autoregressive models could be used as a replacement of the complicated updating algorithms like the Kalman filter. If the parameters are estimated independent of the noise model, a simple Autoregressive (AR) updating algorithm is sufficient [*Ahsan and O' Conner,* 1994]. In essence, the following points may be highlighted from the above discussion about the relevance of variable parameter routing models as components of flood forecasting models:

(i) Use of simple basic models.

(ii) Linking the parameters of the model to channel and flow characteristics.

(iii)No numerical stability problem arises during real-time forecasting.

(iv)Applicable to steep to moderate slope river reaches.

(v) Applicable to forecast flood events that were not recorded in the past.

(vi)Enables the use of simple forecast error updating algorithm.

2.9 APPLICABILITY CRITERIA OF THE FLOOD ROUTING METHODS

It is difficult to identify a suitable simplified method for application to a given flood routing problem. Several researchers have attempted to resolve this difficulty by establishing applicability criteria for the selection of the appropriate flood routing methods for application to a given routing problem with or without considering downstream boundary condition. Among these criteria, the one introduced by *Ponce et al.* [1978] has found its place in standard text books. However, these criteria by *Ponce et al.* [1978] were established on the basis of at least 95% accuracy in the wave amplitude when compared with the dynamic wave after one propagation period. Since most of the flood waves have a small amount of physical diffusion, they are better represented by the diffusion waves rather than by the kinematic waves [*Ponce*, 1989]. Hence, the diffusion wave routing methods can be applied to a much wider range of practical flood routing problems than the kinematic wave-based methods [*Ponce*, 1989]. To know whether a wave is a diffusion wave (DW) or a kinematic wave (KW), the applicability criteria proposed by *Ponce et al.* [1978] which is based on the linear stability theory is widely used in practice. However, *Zoppou and O'Neill* [1982] studied the criteria of *Ponce et al.* [1978] for some typical flood waves in an Australian river Yarra, and proved the failure of these criteria. In a preliminary investigation of the applicability criteria for simplified flood routing methods, *Perumal and Sahoo* [2006] showed the failure of the criteria proposed by Ponce et al. [1978] and Fread [1985]. Based on the extensive study of the

VPMD and VPMS methods, *Perumal and Sahoo* [2007] have recently formulated the applicability criteria for the simplified routing methods based on the scaled water surface gradient $(1/S_o)(\partial y/\partial x)$, which are used for the classification of flood waves [*Henderson*, 1966; *NERC*, 1975] as kinematic, diffusive or approximately convective-diffusive. The scaled gradient can be estimated at every routing time level of the given inflow hydrograph at the inlet of the routing reach. *Perumal and Sahoo* [2007] applied this technique for developing the applicability criteria for both the VPMD and VPMS routing methods. The applicability limits of these two methods have already been described in Section 2.7.

2.10 CONCLUDING REMARKS

Based on the literature review presented in this chapter, the following conclusions are arrived at:

1. ANN based models cannot accommodate the significant changes that takes place in the channel geometry. However, when the trained ANN model is applied in operational mode, there is no certainty about estimating reliable forecast when dealing with flood scenarios beyond the range of magnitude of floods used in calibration of the ANN model. Therefore, these pitfalls of the ANN based models necessitates the use of simple physically based routing models for real-time applications.

2. The Variable Parameter McCarthy-Muskingum Discharge-routing (VPMMD) method introduced by *Price and Perumal* [2011] has the ability to compute both discharge and stage simultaneously and, therefore, can be applied for real-time forecasting in rivers.

3. It is a well-known fact that the autoregressive (AR) models and moving average (MA) models, or their mixed combinations, ARMA, ARIMA, model have found a fruitful application in describing the behavior of hydrological time series [*Szollosi-Nagy*, 1976].These stochastic models are widely used in real-time flood forecasting in stream flow estimation and also as a filtering techniques in the noise

models. These methods can be employed as alternatives to the complicated Kalman filter used for parameter updating.

4. The VPMMD method computes both discharge and stage simultaneously at any river cross-section for in-bank flows. Therefore, this method can be suitably extended for studying flood flow in channels with over-bank flows.

5. There is a need to develop applicability criteria for the simplified flood routing methods such as the Variable Parameter McCarthy-Muskingum Discharge-routing (VPMMD) method for its field applications., and

6. There is no simplified method available for routing floods in river channels based on the use of only upstream and downstream rating curves and cross-sectional information as an alternative to the conventional simplified routing methods which use the routing reach cross-sectional details.

3 THE VPMMD METHOD BASED CHANNEL ROUTING USING ONLY THE END-SECTIONS RATING CURVES AND CROSS-SECTIONS DATA

3.1 GENERAL

The cross-sectional data acquisition at the sites of interest in a river reach is often very difficult owing to their inaccessibility or involvement of huge expenditure or the both. This view point is substantiated by *Birkhead and James* [1998] who stated that when environmental requirements are being assessed in natural rivers, information is commonly required at large number of locations which may be remote and inaccessible. Moreover, the accuracy of most of the hydrodynamic routing methods depend on the use of a number of channel cross-sections information at closer spatial intervals, besides the other morphometric details of a river, such as the channel bed slope and surface roughness along the river reach which vary in space and time. The hydrodynamic models based on the solution schemes of the full Saint-Venant equations of continuity and momentum, such as the MIKE11 and HEC-RAS models can be used for flood routing in natural rivers, but at the cost of providing hydrometric and morphometric data at closer temporal and spatial resolutions. Alternatively, using only the end-sections rating curves and the associated cross-sections information simplifies the flood routing procedure in the operational flood management owing to the fact that these rating curves have inherited the flow and cross-section characteristics of the reach. Based on this consideration a routing method is developed herein using only the rating curves information available at different gauging stations and the information of the associated cross-sections along a river reach. In this context, the Variable Parameter McCarthy-Muskingum Discharge-routing (VPMMD) method advocated by *Price and Perumal* [2011] is employed for its

extension to routing in compound channels consisting of main and floodplain sections. This VPMMD method originally proposed for routing the in-bank flows with the model parameters estimated using the cross-sectional information is modified herein for incorporating the floodplain flows also. To enhance the practical utility of this method, the parameters K and θ of this method are estimated using only the reach-averaged rating curves established by overlapping the upstream and downstream rating curves, of the considered routing reach. This method has also the capability to estimate the stage hydrographs corresponding to the routed discharge hydrographs at any downstream river cross section. The capability of this routing approach is first demonstrated by routing a given hypothetical inflow hydrograph in two different types of hypothetical prismatic channel reaches, each characterized by different combinations of uniform roughnesses and bed slopes. The routing was carried out for a specified reach length of each of the hypothetical channels using the proposed VPMMD method, and the routed hydrographs and the estimated stage hydrographs at the end of the reach are compared with the corresponding benchmark hydrographs obtained using the numerical solutions of the full Saint-Venant equations. The study demonstrates that the hypothetical routing results of this VPMMD method closely reproduce the benchmark solutions of both discharge and stage hydrographs. The practical usefulness of this method is demonstrated by routing different flood events in two channel reaches of the upper Tiber River in Central Italy. However, the applicability of the method is restricted by the assumptions of no lateral flow and downstream effects in the reach.

3.2 THEORETICAL BACKGROUND OF THE VPMMD METHOD

The VPMMD method assumes that at any instant of time during unsteady flow, the steady flow relationship is applicable between the stage at the middle of the routing reach and the discharge passing somewhere downstream of it. This assumption is also

employed in the Kalinin-Milyukov method [*Apollov et al.*, 1964; *Miller and Cunge*, 1975]. Therefore, the normal discharge Q_3 passing just downstream of the midsection of the computational reach (section 3 in Figure 3.1) is uniquely related to the stage y_M at the midsection (section M in Figure 3.1) of the computational reach having the length of Δx.

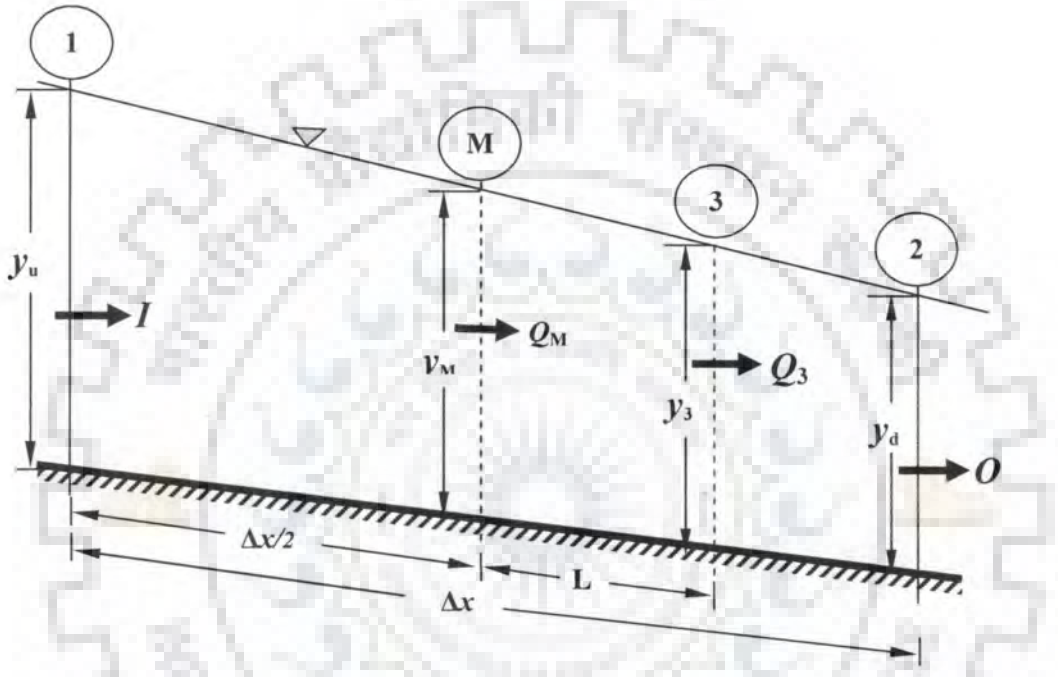

Figure 3.1 Definition sketch of the VPMMD routing reach

The governing finite difference equation of the VPMMD routing method derived as a simplification of the full Saint-Venant equations and developed on the basis of application of the hydraulic continuity equation at the midsection of the Muskingum routing reach of length Δx with no lateral flow can be given as [*Price and Perumal*, 2011]

$$\Delta x\left[\frac{Q_{3,j+1}}{V_{Mo,j+1}}-\frac{Q_{3,j}}{V_{Mo,j}}\right]=\Delta t\left[\frac{I_{j+1}+I_j}{2}-\frac{O_{j+1}+O_j}{2}\right] \tag{3.1}$$

where all the variables used in equation (3.1) have the usual connotations.

The explicit expression of the unknown variable of equation (3.1) leads to the classical Muskingum [*McCarthy*, 1938] routing equation as

$$O_{j+1} = C_1.I_{j+1} + C_2.I_j + C_3.O_j \tag{3.2}$$

where $C_1 = \dfrac{\Delta t - 2.K_{j+1}.\theta_{j+1}}{\Delta t + 2.K_{j+1}.\left(1-\theta_{j+1}\right)}$ (3.3a)

$$C_2 = \frac{\Delta t + 2.K_j.\theta_j}{\Delta t + 2.K_{j+1}.\left(1-\theta_{j+1}\right)} \tag{3.3b}$$

$$C_3 = \frac{-\Delta t + 2.K_j.\left(1-\theta_j\right)}{\Delta t + 2.K_{j+1}.\left(1-\theta_{j+1}\right)} \tag{3.3c}$$

and the travel time K at the time level (j+1) is expressed as

$$K_{j+1} = \frac{\Delta x}{V_{Mo,j+1}} \tag{3.4}$$

The weighting parameter, θ at the time level (j+1) can be given by

$$\theta_{j+1} = \frac{1}{2} - \frac{Q_{3,j+1}\left[1 - \frac{4}{9}F^2\left(\frac{PdR/dy}{dA/dy}\right)^2\right]_{M,j+1}}{2.S_o.B_{M,j+1}.c_{Mo,j+1}.\Delta x} \tag{3.5}$$

Assuming that the magnitudes of the inertial terms are negligible in natural flood waves [*Henderson,* 1966; *Price,* 1985], equation (3.5) can be modified assuming $F_M \approx 0$, as

$$\theta_{j+1} = \frac{1}{2} - \frac{Q_{3,j+1}}{2.S_o.B_{M,j+1}.c_{Mo,j+1}.\Delta x} \tag{3.6}$$

When a constant discharge is used as the reference discharge, the expressions for K and θ reduces to:

$$K = \frac{\Delta x}{V_{Mo}|_r} \tag{3.7}$$

$$\text{and, } \theta = \frac{1}{2} - \frac{Q_o}{2.S_o.B_M|_r.c_{Mo}|_r.\Delta x} \tag{3.8}$$

where, the suffix r of K and θ refers to the reference level discharge.

The downstream stage, y_d corresponding to the routed discharge, O_{j+1} can be estimated as [*Perumal*, 1994a; 1994b]

$$y_d = y_M + \frac{\left(O_{j+1} - Q_M\right)}{\left.\frac{\partial Q}{\partial y}\right|_M} \tag{3.9}$$

where y_M and Q_M are the stage and discharge variables at the midsection of the routing reach, respectively.

3.3 EXTENSION OF THE VPMMD METHOD FOR ROUTING IN FLOODPLAINS

The VPMMD method advocated by *Price and Perumal* [2011], originally developed for discharge routing in prismatic main channels using cross-sectional information, is extended for routing in compound channels consisting of main and floodplain channel sections, using only the upstream and downstream rating curves and the cross-sectional details at these sections. This approach proposed as an alternative to the methods which work on the basis of channel cross-sectional details can be considered as practically more useful when no other in-between cross-section information is available. This method also enables the estimation of stage hydrographs corresponding to the routed discharge hydrographs. The capability of this approach is demonstrated by routing a given

hypothetical inflow hydrograph in a number of hypothetical prismatic channel reaches characterized by different combinations of uniform roughness and bed slope values. The two types of hypothetical channel reaches used herein are defined by i) a channel section closely resembling to a natural river cross-section as proposed by *Price* [2009] and ii) a two-step compound trapezoidal channel cross-section as proposed by *Ackers* [1993] and subsequently used by *Tang et al.*[1999] and *Perumal et al.* [2007].

3.4 VPMMD ROUTING PROCEDURE USING RATING CURVE TABLES

The routing procedure of the VPMMD method applicable for routing flood waves in prismatic main channels without considering floodplain as proposed by *Price and Perumal* [2011] is revised herein by a new algorithm which works based on the reach-averaged rating curve and the end-sections information for routing flood waves in prismatic as well as in natural channels having any shape of cross-section with or without floodplains. This newly developed algorithm requires the preparation of normal rating curve tables or look-up tables of flow depth-discharge relationships, flow area $A(y)$, wave celerity $c(y)$, water surface width $B(y)$ and the flow velocity $v(y)$ generated at closer intervals of flow depth y. Subsequently, the look-up table for $A(Q_o), B(Q_o), c(Q_o)$ and $v(Q_o)$ corresponding to a given set of $A(y), B(y)$, $c(y)$ and $v(y)$ were developed by interpolating on these look-up tables for using in the newly developed routing procedure as mentioned below, where, Q_o is the normal discharge corresponding to y; $A(Q_o)$= wetted cross-sectional area (in m^2); $B(Q_o)$= surface width (in m); $c(Q_o)$= wave speed (in ms^{-1}) and $v(Q_o)$= velocity (in ms^{-1}).

The step-by-step procedure of discharge routing by the VPMMD method in the reach of length Δx is given below:

1. The initial values of K and θ are estimated for the initial steady flow in the reach using equations (3.7) and (3.8).

2. The unrefined discharge is estimated using the routing equation (3.2) with C_1, C_2, and C_3 estimated using K and θ estimated at the previous time level.

3. The normal discharge at section 3 (Figure 3.1) is computed as

$$Q_3 = \theta I_{j+1} + (1-\theta) O_{j+1} \tag{3.10}$$

4. Using Q_3 estimated at step 3, the stage at the mid section y_M is estimated by the interpolation of the normal rating curve relationship given in the look-up table.

5. Using the value of y_M estimated in step 4, the normal velocity, V_{Mo}, normal celerity, c_{Mo} and surface width, B_M are estimated from the look-up table.

6. The refined parameters K and θ are estimated using equations (3.4) and (3.6), respectively.

7. The refined discharge is estimated using the routing equation (3.2).

8. The discharge at the midsection of the routing reach is estimated as

$$Q_M = 0.5\left(I_{j+1} + O_{j+1}\right) \tag{3.11}$$

9. Using the refined discharge estimated at step 7, the normal discharge, Q_3 is again estimated using equation (3.10).

10. The refined flow depth y_M is computed again using this revised estimate of Q_3.

11. The downstream stage y_d is computed using equation (3.9).

12. Repeat the steps 2 to 11 until all the discharge hydrograph ordinates are completed for each space step.

3.5 PERFORMANCE EVALUATION CRITERIA

The following evaluation criteria were adopted to verify the performance of the VPMMD method in simulating the corresponding benchmark solutions:

3.5.1 Accuracy of the Simulated Outflow Peak and the Estimated Outflow Stage Peak

The percentage errors of peak estimates of the routed discharge hydrograph and the corresponding estimated stage hydrograph by the VPMMD method are given, respectively, as

$$q_{per} = \left(q_{pc}/q_{po} - 1\right) \times 100 \tag{3.12}$$

$$y_{per} = \left(y_{pc}/y_{po} - 1\right) \times 100 \tag{3.13}$$

where q_{pc} = peak of the routed discharge hydrograph at the outlet; q_{po} = peak of the benchmark or observed discharge hydrograph at the outlet; y_{pc} = peak of the computed stage hydrograph at the outlet; and y_{po} = peak of the computed benchmark or observed stage hydrograph at the outlet. The positive values of q_{per} and y_{per} indicate overestimation of the peaks of the benchmark or observed values, and the negative values of q_{per} and y_{per} indicate their underestimation.

3.5.2 Accuracy of the Time-to-Peak Estimate

The relative errors in time-to-peaks of the routed discharge hydrograph and the corresponding estimated stage hydrograph (in h) by the VPMMD method are given, respectively, as

$$t_{pqer} = t_{qpc} - t_{qpo} \tag{3.14}$$

$$t_{pyer} = t_{ypc} - t_{ypo} \tag{3.15}$$

where t_{qpc} = time-to-peak of the routed discharge hydrograph at the outlet (h); t_{qpo} = time-to-peak of the benchmark or observed discharge hydrograph at the outlet (h); t_{ypc} = time-to-peak of the estimated stage hydrograph at the outlet (h); and t_{ypo} = time-to-peak of the estimated benchmark or observed stage hydrograph at the outlet (h).

3.5.3 Accuracy of Conservation of Mass

The percentage error in the flow volume is expressed as

$$EVOL(\text{in}\%) = \left[\sum_{i=1}^{N} Q_{ci} \Big/ \sum_{i=1}^{N} I_i - 1 \right] \times 100 \tag{3.16}$$

where Q_{ci} = i^{th} ordinate of the computed discharge hydrograph routed by the VPMMD routing method; and $I_i = i^{\text{th}}$ ordinate of the inflow discharge hydrograph. A negative value of *EVOL* indicates loss of mass and positive value of *EVOL* indicates gain of mass. A value close to zero suggests mass conservation ability of the method.

3.5.4 Reproduction Capability of the Benchmark or Observed Hydrographs

The closeness with which the proposed method reproduces the benchmark solutions or observed hydrographs of both discharge and stage hydrographs, including the closeness of shape and size of the hydrograph, can be measured using the Nash-Sutcliffe criterion of variance explained [*Nash and Sutcliffe*, 1970], recommended by the *ASCE Task Committee* [1993]. The variance

explained in percentage for discharge and stage hydrographs reproductions are given, respectively, as

$$\eta_q = \left[1 - \sum_{i=1}^{N}\left(Q_{oi} - Q_{ci}\right)^2 \Big/ \sum_{i=1}^{N}\left(Q_{oi} - \overline{Q}_{oi}\right)^2\right] \times 100 \tag{3.17}$$

$$\eta_y = \left[1 - \sum_{i=1}^{N}\left(y_{oi} - y_{ci}\right)^2 \Big/ \sum_{i=1}^{N}\left(y_{oi} - \overline{y}_{oi}\right)^2\right] \times 100 \tag{3.18}$$

where Q_{oi} = i^{th} ordinate of the benchmark or observed discharge hydrograph at the outlet; $\overline{Q}_{oi}$ = mean of the benchmark or observed discharge hydrograph ordinates at the outlet; Q_{ci} = i^{th} ordinate of the routed discharge hydrograph by the VPMMD method ; y_{oi} = i^{th} ordinate of the benchmark or observed stage hydrograph at the outlet; $\overline{y}_{oi}$ = mean of the benchmark or observed stage hydrograph ordinates at the outlet; y_{ci} = i^{th} ordinate of the stage hydrograph computed corresponding to Q_{ci} of the VPMMD method; and N = total number of simulated discharge or stage hydrograph ordinates. One may consider the proposed routing method is more accurate when the variance explained for the hypothetical routing studies is estimated greater than 99%.

3.5.5 Attenuation of Peak Discharge

The percentage attenuation of peak discharge is expressed as

$$\mu_q = \left(1 - \frac{Q_{po}}{Q_{pi}}\right) \times 100 \tag{3.19}$$

where Q_{po} is the peak of the benchmark or observed outflow discharge hydrograph and Q_{pi} is peak of the inflow discharge hydrograph.

3.6 SYNTHETIC RIVER CHANNEL APPLICATIONS

3.6.1 Inflow Hydrograph for Routing in Price's [2009] Synthetic River Channel Reaches and Benchmark Solutions

In this case of the hypothetical routing study, both the inflow hydrograph and the hypothetical channel reaches as employed by *Price* [2009] for a similar study have been adopted. The inflow hydrograph used by him is based on the form of Pearson type-III distribution expressed as

$$Q(t) = Q_b + (Q_p - Q_b)\left(\frac{t}{t_p}\right)^{1/(\gamma-1)} \exp\left(\frac{1-t/t_p}{\gamma-1}\right) \tag{3.20}$$

where, the initial discharge, Q_b=100 m^3s^{-1}; peak discharge Q_p= 800 m^3s^{-1}; time-to-peak t_p = 24 h; and a shape factor $\gamma = 1.20$.

The benchmark solutions were obtained by routing the given inflow hydrograph in Price's synthetic channels by numerically solving the Saint-Venant equations based on the four-point implicit finite difference scheme. The algorithm used for estimating the benchmark solution was supplied by *Price R.K.* (Personal communication). The space and time increments used for solving the full Saint-Venant equations are 1000 m and 900 s, respectively. Further, the stage hydrograph of the VPMMD method for each case of the routing study was also estimated corresponding to that of the benchmark Saint- Venant solution.

3.6.2 Inflow Hydrograph for Routing in Two-Stage Compound Cross-Section Synthetic Channel Reaches and Benchmark Solutions

To verify the capability of the VPMMD method for routing in compound channels associated with varied size of floodplains, another type of synthetic river channel (i.e.,

two-stage trapezoidal compound channel proposed by *Ackers* [1993]) was considered for the study. The inflow hydrograph used for routing was characterized by the Pearson type III distribution as given by equation (3.20) with the base flow Q_b=10 m^3s^{-1}, peak discharge Q_p=150 m^3s^{-1}, time-to-peak t_p=10 h, shape factor $\gamma = 1.15$ .The benchmark solutions required for each of the proposed channel type, corresponding to each of the routed solutions of the proposed method, were obtained using MIKE11 [*DHI*, 2008] model. The space and time increments used in the calculations with the benchmark MIKE11 model are 1000 m and 300 s, respectively. Further the estimated stage hydrograph of the VPMMD method for each case of the routing study was also compared with the corresponding stage hydrograph of the MIKE11solutions.

3.6.3 Routing in Price's Synthetic River Channel Reaches

3.6.3.1 Channel reach details and look-up table preparation

The verification of the VPMMD method was attempted first by routing through synthetic prismatic channel reaches as used by *Price* [2009]. The length of the routing reach is 100 km with a uniform cross-section and the one-half of this symmetrical uniform cross-section is shown in Figure 3.2. This cross-section has a unique feature in that the floodplain is connected with the main channel section using a smooth transition resembling more to a natural channel section.

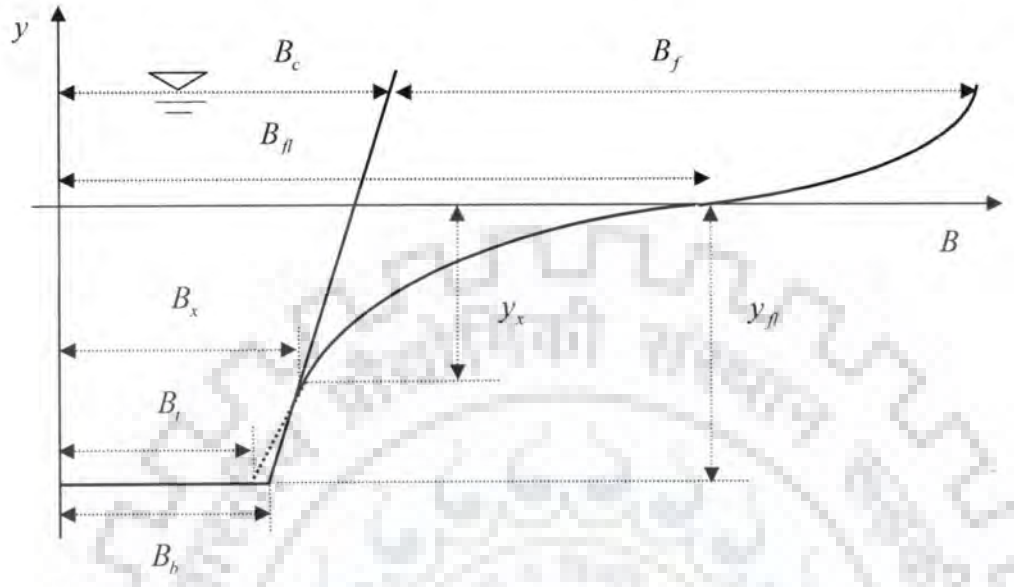

Figure 3.2 Semi-cross-section of Price's [*Price*, 2009] synthetic channel reach.

The main channel is trapezoidal with the semi-bed width, B_b (m), channel side slope, s and channel semi-surface width, B_c (m). The associated berms or floodplains to the left and right of the channel are defined by the semi-width B as

$$B = B_{fl} + \frac{\left(B_t - B_{fl}\right)\tanh\left(ky\right)}{\tanh\left(-ky_{fl}\right)} \tag{3.21}$$

where B_{fl} = semi-surface width of the synthetic channel when flow depth y =0 (m); B_t = semi-bed width for tanh curve (m) when $y = -y_{fl}$; k = parameter defining the shape of the tanh curve (m^{-1}); y = flow depth (m); y_{fl} = depth of the synthetic channel (m); B_b = actual semi-bed width of the channel with $B_b > B_t$ (m); B_x = semi-width of the channel at

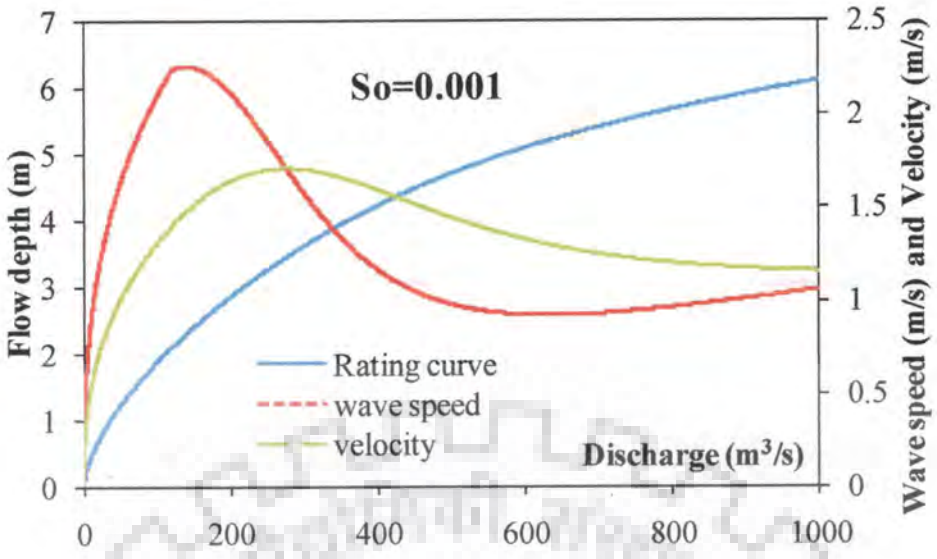

Figure 3.3 Typical channel relationships between the normal depth, discharge, wave speed, and velocity for Price's synthetic river reach with $S_o = 0.001$.

3.6.3.2 Results and discussion

The routing of the inflow hydrograph given by equation (3.20) was carried out in all the ten hypothetical channels following the procedure outlined in Section (3.4). The verification of the proposed VPMMD routing method for routing the inflow hydrograph for a reach length of 100 km in *Price's* [2009] synthetic river channel as discussed in Section 3.6.1 and 3.6.3.1 was carried out by comparing its routing results with the corresponding benchmark solutions arrived at by solving the full Saint-Venant equations using the four-point implicit and iterative (non-linear) finite difference scheme. In order to arrive at accurate results by the proposed VPMMD method for the hypothetical routing cases in Price's synthetic channel, the rating curves developed for this channel reaches were defined at closer intervals of flow depth. The summary of performance criteria showing the reproduction of the pertinent characteristics of the Saint-Venant solutions by the VPMMD method using the spatial step of $\Delta x = 2$ km (i.e., 50 sub-reaches consideration) in routing through the 100 km Price's synthetic channel reaches are

presented in Table 3.1. Similar results are given in Table 3.2 corresponding to the results obtained for the routing spatial step of Δx = 12.5 km (i.e., 8 sub-reaches consideration). Tables 3.1 and 3.2 present the details of channel types and the performance evaluation measures of the routing results related to the reproduction of pertinent characteristics of the Saint-Venant solutions by the VPMMD method, i.e., the estimates of Nash-Sutcliffe criterion, η_q (in %) and η_y (in %), error in volume estimated in reproducing the discharge hydrograph ($EVOL$ in %), errors in peak discharge reproduction (q_{per} in %) and it's time-to-peak (t_{pqer} in h), and the peak stage (y_{per} in %) and it's time-to-peak (t_{pyer} in h).

Figures 3.4(a) to 3.4(t) and Figures 3.5(a) to 3.5(t) show the routed discharge and the corresponding estimated stage hydrographs simulated by the VPMMD method and their comparison with the Saint-Venant solutions for routing in channel types 1 to 10 of the synthetic river channels using two different space steps of $\Delta x = 2km$ (50 sub-reaches) and $\Delta x = 12.5km$ (8 sub-reaches), respectively.

Figure 3.6 (a) shows the comparison between the peak discharges of the routing results of the VPMMD method and the corresponding benchmark solutions of the Saint-Venant equations for the routing experiments in channel reaches corresponding to the spatial steps of Δx = 2 km (50 sub-reaches) and Δx = 12.5 km (8 sub-reaches) considerations. Figure 3.6 (b) shows a similar comparison of the corresponding peak stage estimates.

Discharge reproduction: It is evident from the performance evaluation measures given in Table 3.1 and 3.2 that the VPMMD method is highly volume conservative with $|EVOL| \approx 0$ for routing in the entire channel types studied. It is also seen from Tables 3.1 and 3.2 that the VPMMD method performs very well for discharge hydrograph reproduction with η_q > 99.27% for all the channel types, except that of channel type-10

characterized by a very mild slope of $S_o = 0.0001$ for which the estimated η_q are 95.57% and 96.53%, respectively, corresponding to routings in the 100 km length using the spatial steps Δx =2 km and Δx =12.5 km. Figures 3.4 (a, c, e, g, i, k, m, o, q, and s) and Figures 3.5 (a, c, e, g, i, k, m, o, q, and s) illustrate the routed discharge hydrograph reproductions by the VPMMD method in Price's synthetic channel types 1 to 10 corresponding to 50 (Δx = 2 km) and 8 (Δx = 12.5 km) sub-reaches consideration, respectively. The corresponding benchmark Saint-Venant solutions are also shown in these figures. The VPMMD method could very closely reproduce the benchmark discharge hydrographs of the Saint-Venant solutions with no volume loss estimated for all the numerical experiments. It is further seen from Tables 3.1 and 3.2 that the performance estimates $|q_{per}|$ and $|t_{pqer}|$ of the VPMMD method are less than 3.42% and 3.5 h, respectively, for all the channel types, except for that of the channel type-10 characterized by $S_o = 0.0001$ for which the estimates $|q_{per}|$ and $|t_{pqer}|$ are 9.33% and 9.50 h, and 8.34% and 8.00 h corresponding to routings using Δx = 2 km and Δx = 12.5 km, respectively. It was brought out by *Perumal* [1994a, 1994b], and *Perumal and Sahoo* [2007] that the close reproduction of the benchmark discharge and stage hydrographs by the variable parameter Muskingum discharge routing method depends on the magnitude of the scaled water surface gradient $(\partial y/\partial x)$ with reference to the channel bed slope, S_o. It can be seen from Tables 3.1 and 3.2 that the estimates of $|(1/S_o)(\partial y/\partial x)|_{\max}$ increase significantly with the decrease in the magnitudes of channel bed slopes S_o, reaching the higher magnitude $|(1/S_o)(\partial y/\partial x)|_{\max}$ = 0.6119 corresponding to $S_o = 0.0001$. It can be inferred from Figure 3.6(a) that the reproduction of the peak discharges of the Saint-Venant

solutions by the VPMMD method is indeed remarkable both for the cases of routing using $\Delta x = 2$ km (50 sub-reaches) and $\Delta x = 12.5$ km (8 sub-reaches).

Table 3.1 Summary of performance criteria showing the reproduction of pertinent characteristics of the Saint-Venant's solutions by the VPMMD method for routing in Price's synthetic river channel reaches using 50 sub-reaches.

					Discharge Routing				Stage Computation		
Channel Type	Bed gradient	μ_q (%)	μ_y (%)	$(1/S_o)(\partial y/\partial x)_{max}$	*EVOL* (%)	η_q (%)	q_{per} (%)	t_{pqer} (h)	η_y (%)	y_{per} (%)	t_{pyer} (h)
1	0.001	6.40	2.28	0.036561	-0.000009	99.98	0.72	0.00	99.95	0.28	0.00
2	0.0009	7.60	2.67	0.044139	0.000000	99.98	0.70	0.00	99.94	0.27	0.00
3	0.0008	9.16	3.17	0.054217	0.000000	99.98	0.67	0.00	99.93	0.26	0.00
4	0.0007	11.21	3.83	0.068129	0.000009	99.98	0.60	0.50	99.91	0.24	0.00
5	0.0006	13.98	4.71	0.088051	0.000009	99.97	0.49	0.00	99.88	0.20	0.00
6	0.0005	17.81	5.95	0.117949	0.000000	99.95	0.29	0.50	99.85	0.14	0.50
7	0.0004	23.18	7.74	0.165778	-0.000009	99.91	-0.15	1.00	99.80	0.01	1.00
8	0.0003	30.97	10.40	0.247392	0.000054	99.78	-1.12	2.00	99.72	-0.28	2.00
9	0.0002	42.49	14.50	0.392190	0.000000	99.27	-3.42	3.50	99.47	-1.01	3.50
10	0.0001	59.55	20.90	0.611900	-0.029465	95.57	-9.33	9.50	97.13	-2.88	11.00

μ_q is the attenuation in peak discharge by the Saint-Venant method computed by equation (3.19), and μ_y is the corresponding attenuation in peak stage, computed by equation (3.19) after replacing the discharge value with the corresponding stage value.

Table 3.2 Summary of performance criteria showing the reproduction of pertinent characteristics of the Saint-Venant's solutions by the VPMMD method for routing in Price's synthetic river channel reaches using 8 sub-reaches.

					Discharge Routing				Stage Computation		
Channel Type	Bed gradient	μ_q (%)	μ_y (%)	$(1/S_o)(dy/dx)_{max}$	*EVOL* (%)	η_q (%)	q_{per} (%)	t_{pqer} (h)	η_y (%)	y_{per} (%)	t_{pyer} (h)
1	0.001	6.40	2.28	0.036561	-0.000009	99.61	0.13	-1.00	99.72	0.12	-1.00
2	0.0009	7.60	2.67	0.044139	0.000018	99.61	0.00	-0.50	99.68	0.10	-1.00
3	0.0008	9.16	3.17	0.054217	0.000018	99.62	-0.05	-1.00	99.65	0.09	-1.00
4	0.0007	11.21	3.83	0.068129	0.000000	99.65	-0.11	-0.50	99.61	0.10	-1.00
5	0.0006	13.98	4.71	0.088051	0.000000	99.70	-0.10	-1.00	99.58	0.13	-1.00
6	0.0005	17.81	5.95	0.117949	0.000009	99.77	-0.06	-0.50	99.55	0.19	-1.00
7	0.0004	23.18	7.74	0.165778	0.000009	99.87	-0.04	-0.50	99.53	0.25	-0.50
8	0.0003	30.97	10.40	0.247392	0.000036	99.96	-0.39	0.00	99.55	0.25	0.00
9	0.0002	42.49	14.50	0.392190	0.000036	99.79	-2.15	1.50	99.56	-0.16	1.50
10	0.0001	59.55	20.90	0.611900	-0.040462	96.53	-8.34	8.00	98.27	-1.97	7.50

Stage reproduction: The estimated stage hydrographs by the VPMMD method could reproduce the corresponding benchmark solutions very closely as shown in Figures 3.4 (b, d, f, h, j, l, n, p, r, and t) for the case of $\Delta x = 2$ km; and Figures 3.5 (b, d, f, h, j, l, n, p, r, and t) for the case of $\Delta x = 12.5$ km. The performance evaluation measures as shown in Tables 3.1 and 3.2 confirm this inference with the variance explained in reproducing the benchmark solutions $\eta_y > 99.47\%$ for all channel types, except for that of the channel type-10 characterized by a very mild slope of $S_o = 0.0001$ for which the estimated η_y are 97.13% and 98.27% corresponding to the cases of routing with $\Delta x = 2$ km and $\Delta x = 12.5$ km, respectively. Further, it is observed while routing in reaches with $S_o \geq 0.0005$ and with $\Delta x = 12.5$ km, a slight formation of hump is seen in the recession limbs of the estimated stage hydrographs immediately after the peak (Figures 3.5 (b, d, f and h)). However, these formations are not seen with the routing results of the mild slope channels (Figures 3.5 (n, p, r and t)). Further, such formations are also not seen with the simulation results obtained using $\Delta x = 2$ km. It can be surmised from Tables 3.1 and 3.2 that the estimates of performance evaluation measures $|y_{per}|$ and $|t_{pyer}|$ of the VPMMD method are less than 1.01% and 3.50 h, respectively, for all the channel types, except for that of the channel type-10 characterized by $S_o = 0.0001$ for which the estimates $|y_{per}|$ and $|t_{pyer}|$ are 2.88% and 11.00 h, and 1.97% and 7.50 h corresponding to routings with $\Delta x = 2$ km and $\Delta x = 12.5$ km, respectively. Figure 3.6(b) shows the comparison between the peak stages of the routing results of the VPMMD method and the corresponding benchmark solutions for the routing experiments corresponding to $\Delta x = 2$ km and $\Delta x = 12.5$ km. It can be inferred from Figure 3.6(b) that the VPMMD method is able to reproduce the benchmark peak stages very closely for channel reaches characterized by channel slope >0.0005, but

slightly underestimates the peaks of the benchmark solutions for channel slopes characterized by S_o <0.0005.

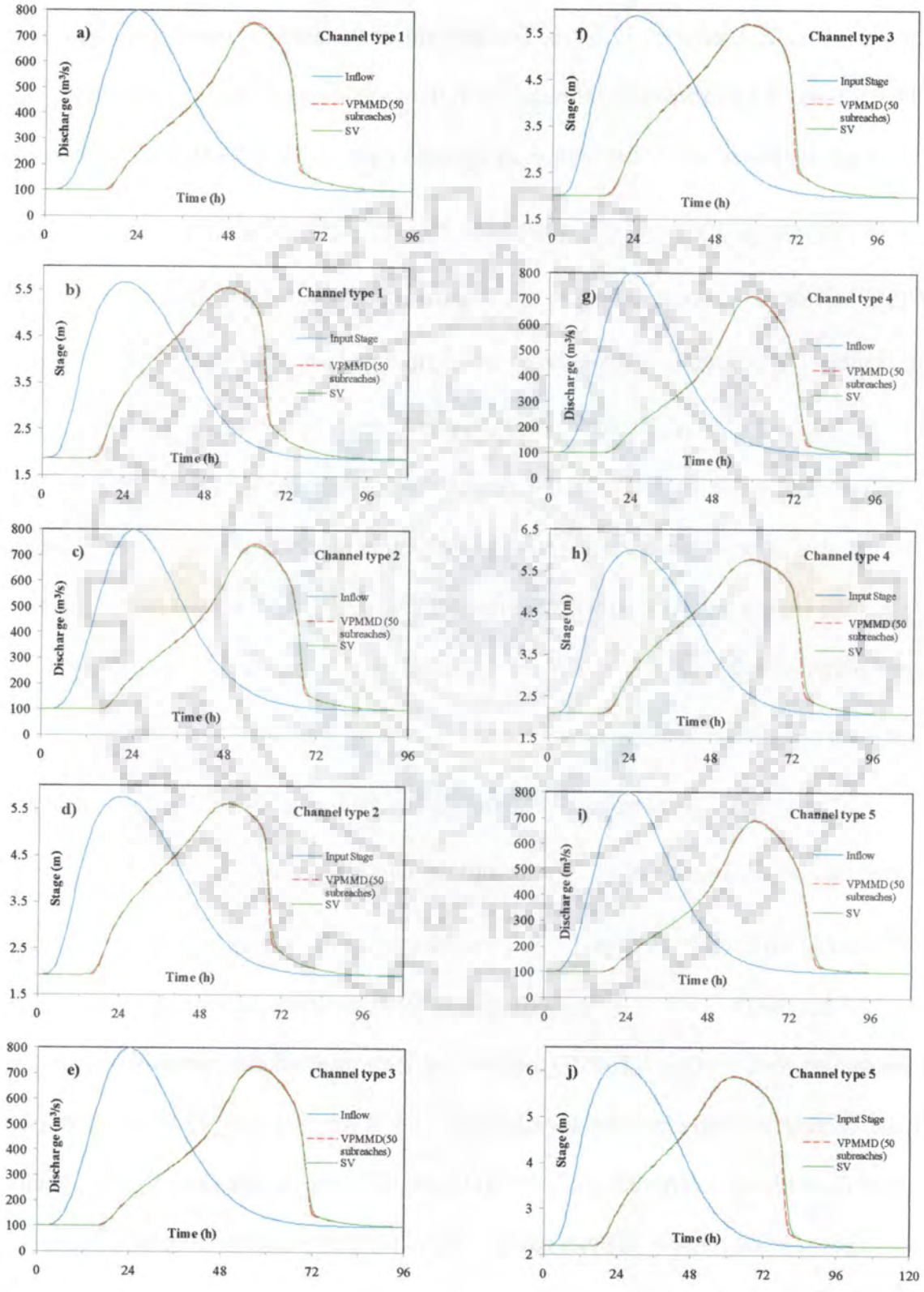

Fig. 3.4(i)

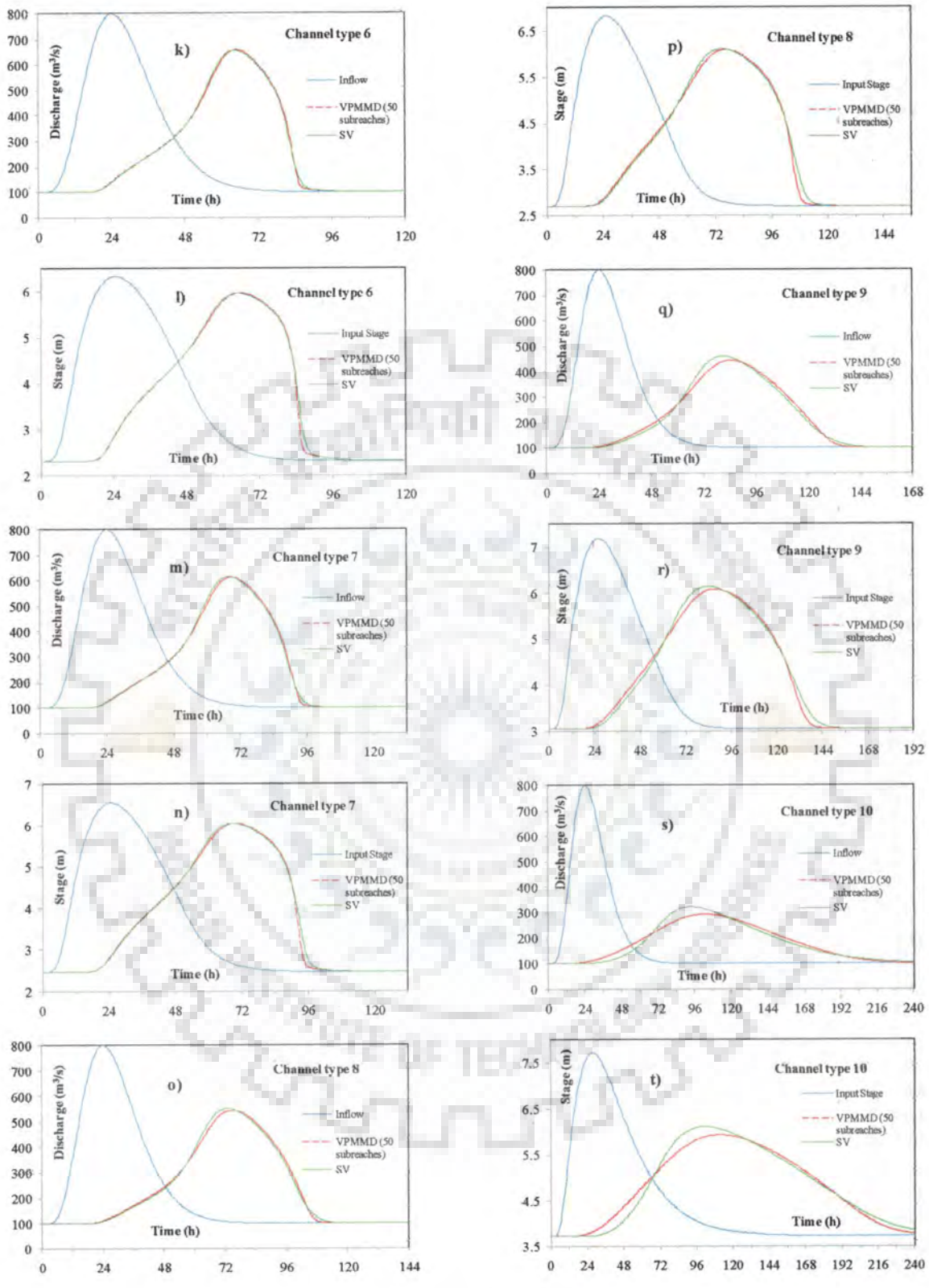

Fig. 3.4(ii)

Figure 3.4 Reproductions of routed discharge and estimated stage hydrographs by the VPMMD method for routing in channel types 1 to 10 of Price's synthetic river channels considering 50 sub-reaches.

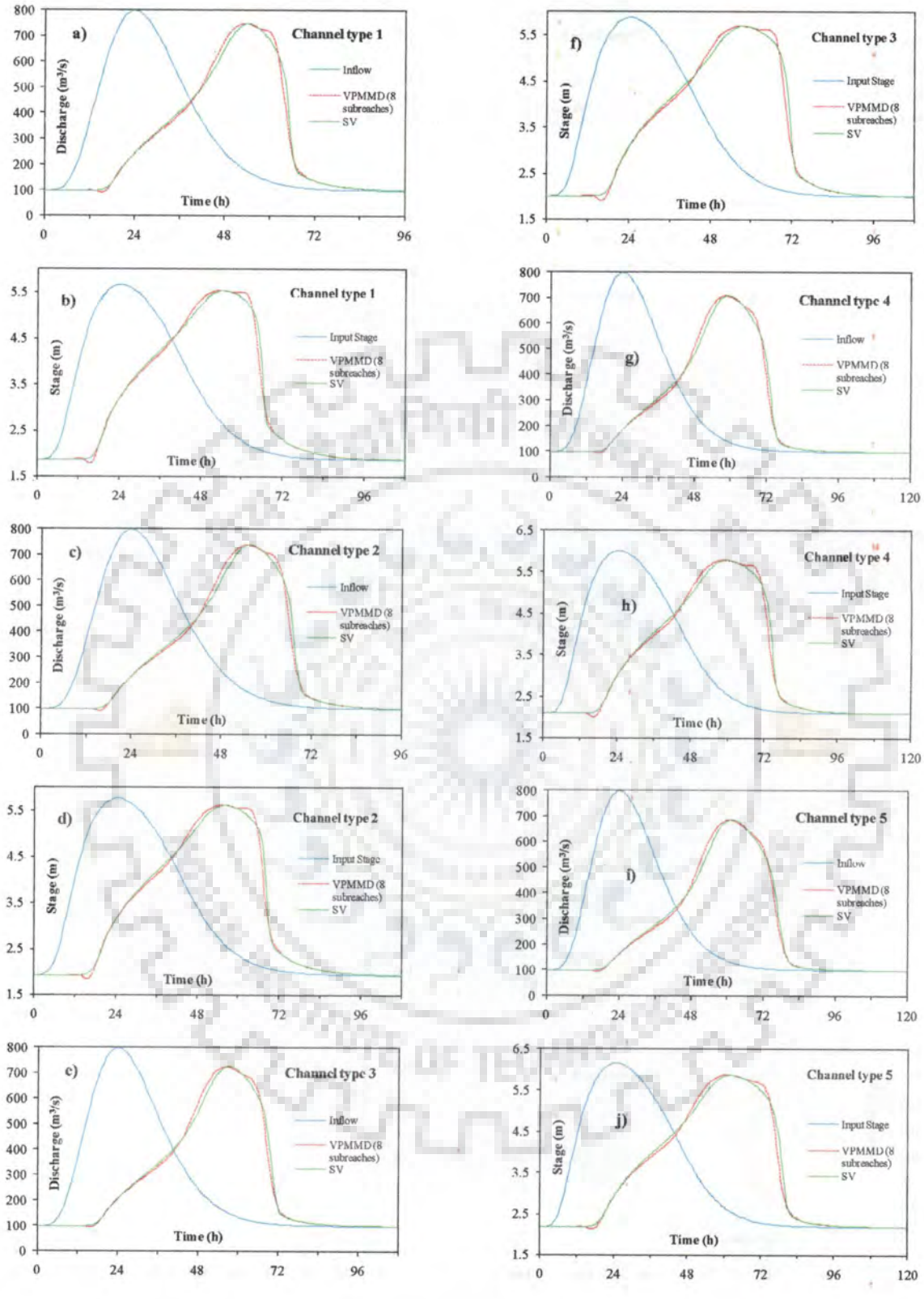
a)
Channel type 1
Discharge (m³/s)
Time (h)
Inflow
VPMMD (8 subreaches)
SV
b)
Channel type 1
Stage (m)
Time (h)
Input Stage
VPMMD (8 subreaches)
SV
c)
Channel type 2
Discharge (m³/s)
Time (h)
Inflow
VPMMD (8 subreaches)
SV
d)
Channel type 2
Stage (m)
Time (h)
Input Stage
VPMMD (8 subreaches)
SV
e)
Channel type 3
Discharge (m³/s)
Time (h)
Inflow
VPMMD (8 subreaches)
SV
f)
Channel type 3
Stage (m)
Time (h)
Input Stage
VPMMD (8 subreaches)
SV
g)
Channel type 4
Discharge (m³/s)
Time (h)
Inflow
VPMMD (8 subreaches)
SV
h)
Channel type 4
Stage (m)
Time (h)
Input Stage
VPMMD (8 subreaches)
SV
i)
Channel type 5
Discharge (m³/s)
Time (h)
Inflow
VPMMD (8 subreaches)
SV
j)
Channel type 5
Stage (m)
Time (h)
Input Stage
VPMMD (8 subreaches)
SV

Fig. 3.5(i)

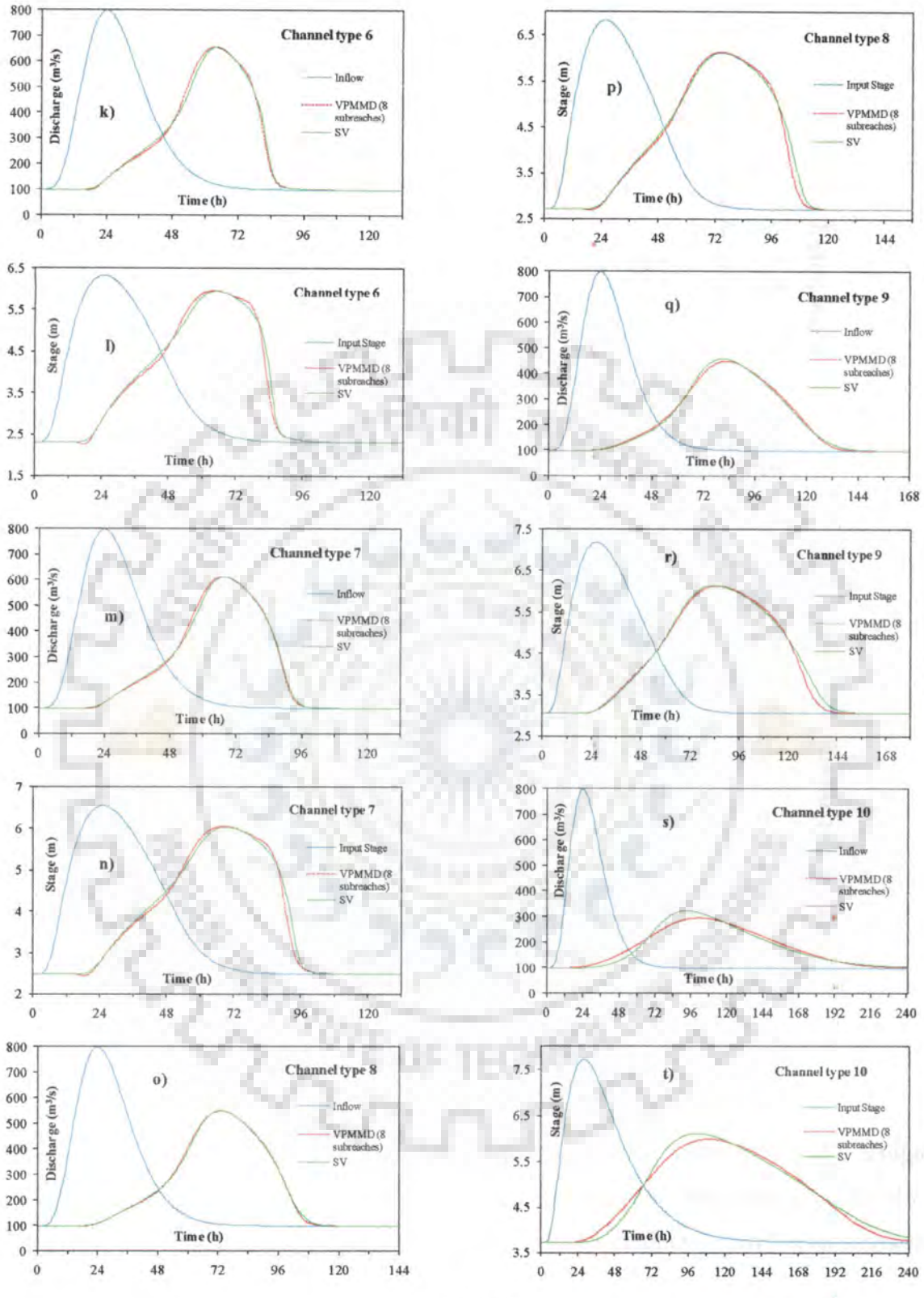

Fig. 3.5(ii)

Figure 3.5 Reproductions of routed discharge and estimated stage hydrographs by the VPMMD method for routing in channel types 1 to 10 of Price's synthetic river channels considering 8 sub-reaches.

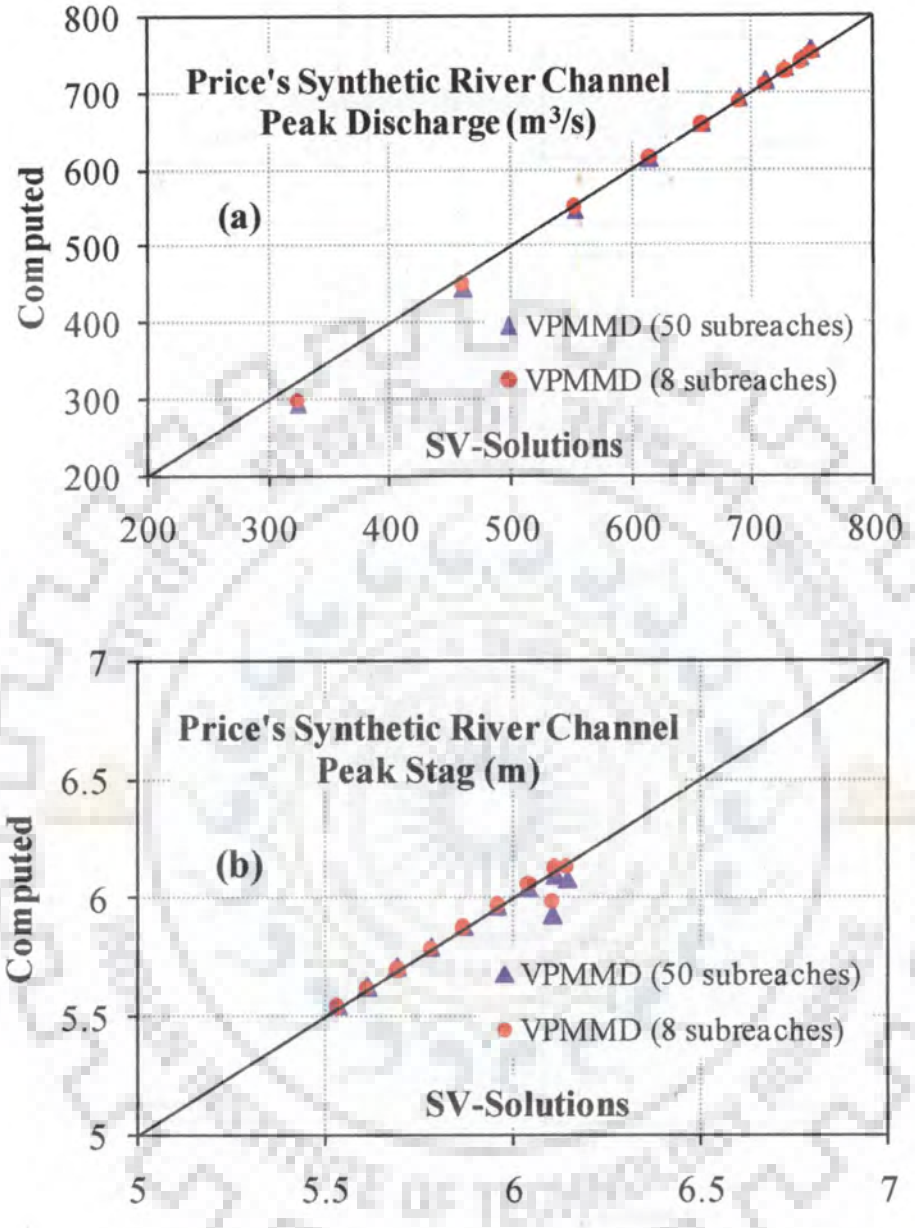

Figure 3.6 Comparison between the peak discharges of the routing results of the VPMMD method and the corresponding Saint-Venant solutions for the routing experiments in Price's synthetic river channel reaches considering 50 and 8 sub-reaches.

3.6.4 Routing in a Two-Stage Compound Channel Reaches

3.6.4.1 Channel reach details and look-up table preparation

An additional evaluation was conducted to verify the proposed routing procedure of the VPMMD method by routing in channel reaches characterized by a two-stage uniform compound cross-section with a trapezoidal main channel flow section and an extended trapezoidal floodplain channel section as shown in Figure 3.7. This compound channel section (Figure 3.7) proposed by *Ackers* [1993] was also adopted by *Tang et al.* [1999] and subsequently by *Perumal et al.* [2007] to verify their respective proposed simplified routing methods.

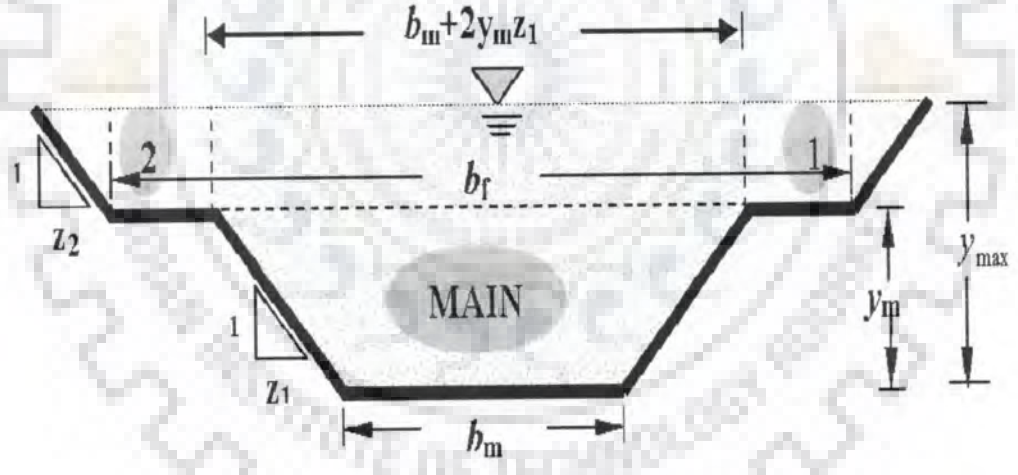

Figure 3.7 Shape of the two-stage compound channel section reach adopted in the study (b_m=15 m, y_m=1.5 m, $z_1 = z_2 = 1.0$) [after *Ackers*, 1993].

A number of different compound channels were used, each characterized by a bed width of main channel $b_m = 15$ m, bank full level $y_m = 1.5$ m, side slope of the main channel z_1=1, and side slope of the flood plains z_2=1, but different uniform floodplain channel sections defined by the ratio of b_f/b_m = 1.5, 2.0, 2.5, 3.0, 3.5, and 4.0. The notation of b_f denotes the bottom width of the floodplain. Corresponding to each b_f/b_m ratio, twelve channel configurations characterized by two different roughnesses Manning's values of n = 0.04 and 0.025, and six varying channel bed slopes, S_o = 0.003, 0.002, 0.001, 0.0005, 0.0003, and 0.0002 were employed. A routing reach length of 40 km was considered for each of the compound channel. It is, further, assumed that the entire channel reach is characterized by a uniform or representative Manning's roughness coefficient irrespective of the main or floodplain channel. This assumption may not be strictly valid in practice. However, as the main objective herein is to develop a simplified hydraulic routing method using discharge as the main routing variable, such an assumption helps to reduce complications in the verification of the methodology. The given inflow discharge hydrograph was routed using the proposed method in different two-stage symmetrical trapezoidal compound cross-section channel reaches for a length 40 km, each having different size of floodplains. Two sets of test runs were carried out using the proposed routing method in each of the 72 channel types considered, by routing in a channel reach length of 40 km with the consideration of 40 equal sub-reaches (Δx =1 km) and 10 equal sub-reaches (Δx =4 km). A uniform routing time interval of Δt =1800 s was used for all the test runs, except in the case of routing in channel reaches with bed slopes of 0.001, 0.002 and 0.003, wherein a routing time interval, Δt =300 s was used. Use of a larger Δt in such cases resulted in wiggles while simulating the recession limb of the discharge hydrograph at 40 km.

As was stated earlier, the proposed routing procedure of the VPMMD method uses the normal depth tables or look-up tables of y *vs* $A(y), B(y)$, $c(y)$ and $v(y)$ prepared at 0.002 m increments of normal flow depth y. Further, tables of $A(Q_o), B(Q_o), c(Q_o)$ and $v(Q_o)$ were developed by interpolating on the look-up tables. These look-up tables of the two-stage compound channel section were developed using the output data of MIKE11 model generated information while developing the benchmark solutions for each of the channel type. The following steps were followed for the development of these look-up tables.

i) rating curve and the stage-flow area relationships generated by the MIKE11 model were extracted for each channel type while developing the benchmark solutions.

ii) water surface widths (dA/dy) were extracted from the established stage-flow area relationship using the first order backward difference scheme, and

iii) wave celerity (dQ/dA) and the flow velocity $v(y)$ were extracted from the discharge-flow area relationships.

A sample case of developing the look-up tables for a typical case of channel type 62 is illustrated in Figure 3.8. It can be seen from Figures 3.8(b) and 3.8(c) that at the bank-full level of y_m=1.5 m and at the discharge corresponding to the bank-full level, there is a sudden drop in celerity when the main channel section suddenly expands to the floodplain section. This unique form of wave speed-discharge relationship established at any section of the river reach is in conformity with the general form of wave speed-discharge relationship for natural rivers as established by *Price* [1973], and *Wong and Laurenson* [1983, 1984].

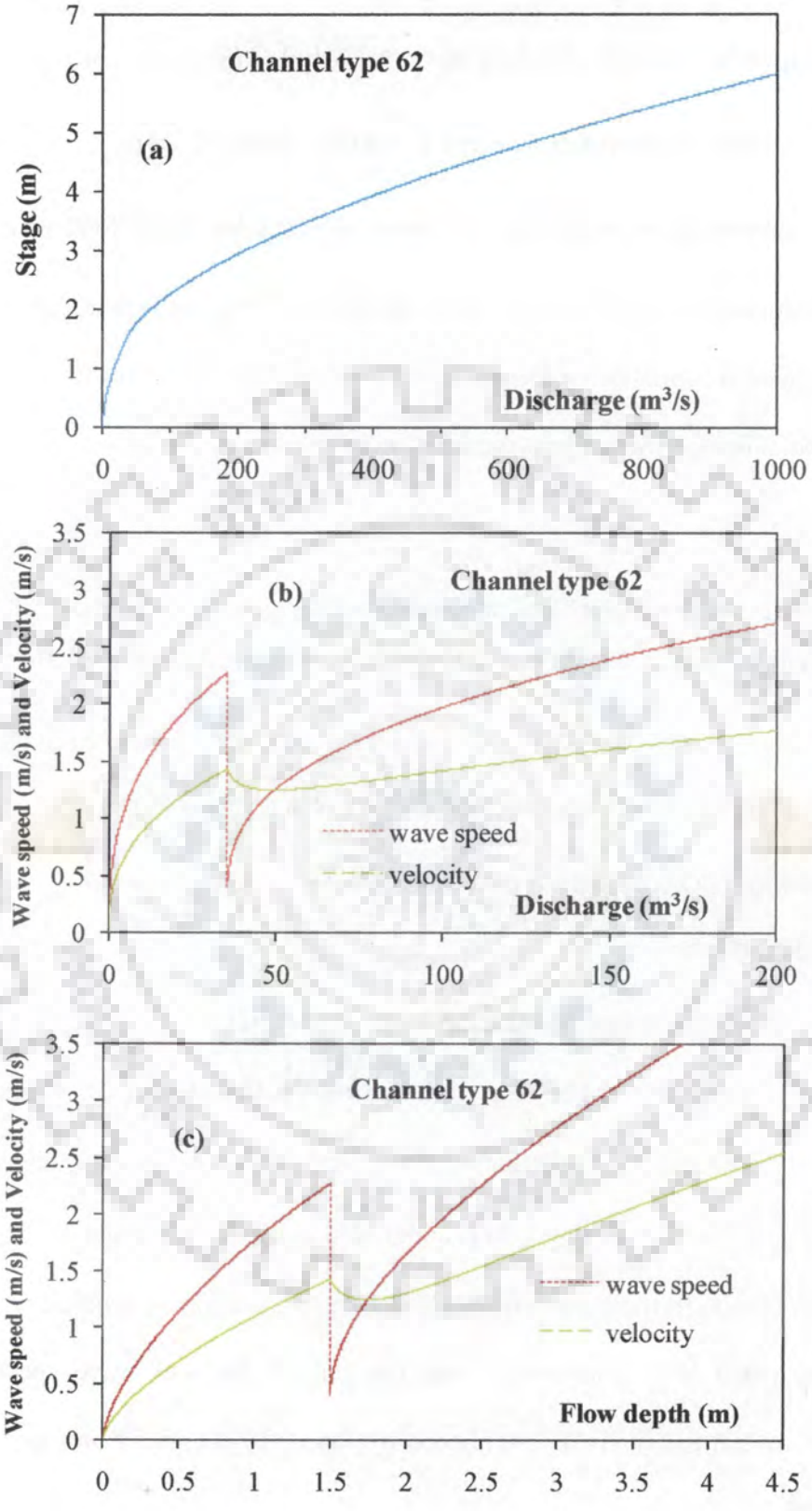

Figure 3.8 Characteristic relationships between the normal depth *vs* discharge, *vs* wave celerity and velocity for channel type 62.

3.6.4.2 Results and Discussion

A similar verification study of the proposed routing procedure of the VPMMD method was made for routing inflow hydrograph, as discussed in the Section 3.6.2 and 3.6.4.1, in two-stage compound cross-section channel reaches of 40 km reach length each, and the results were compared with the corresponding benchmark solutions given by the MIKE11 [*DHI*, 2008] model. In order to arrive at accurate results of the hypothetical routing cases in two-stage compound channels by the VPMMD method, the rating curves developed for these channel reaches were defined at closer intervals of flow depth. The summary of performance criteria showing reproduction of the pertinent characteristics of the MIKE11 solutions by the VPMMD method for 40 sub-reaches consideration (Δx = 1 km) and for 10 sub-reaches consideration (Δx = 4 km) are presented in Tables 3.3 and 3.4, respectively. Figure 3.9(a) to 3.9(v) demonstrates the reproduction of some of the typical routed discharge and computed stage hydrographs by the VPMMD method along with the corresponding MIKE11 solutions (benchmark solutions) arrived at for routing in channel reaches of 40 km length using 40 sub-reaches consideration (Δx = 1 km) and 10 sub-reaches consideration (Δx = 4 km). These typical routing solutions were obtained for channel reaches with b_f/b_m = 2.0 (channel types 14, 17, 18 and 23) and b_f/b_m = 4.0 (channel types 62, 65, 66, 71 and 72).

Figure 3.10 illustrates the reproduction of the peak discharges and their corresponding peak stages by the VPMMD method (with 40 sub-reaches and 10 sub-reaches consideration) in comparison with the corresponding MIKE11 solutions.

Discharge reproduction: It can be seen from Tables 3.3 and Table 3.4 that the VPMMD method as applied in this study is highly volume conservative with $|EVOL| \approx 0$ for routing

in all the channel types studied herein. It can also be seen from Tables 3.3 and 3.4 that the estimates of performance evaluation measures of discharge reproduction η_q, $|q_{per}|$ and $|t_{pqer}|$ by the VPMMD method in two-stage compound channel reaches considering sub-reach lengths of Δx = 1 km and Δx = 4 km are: >98.54%, <7.72%, and <1.5 h; and >96.43%, <6.20%, and <1.5 h, respectively. These evaluation measures imply that the VPMMD method is able to reproduce the discharge hydrographs of the MIKE11 solutions very closely. Figures 3.9 (a, c, e, g, i, k, m, o, q, s and u) demonstrates the reproduction of some of these typical routed discharge hydrographs by the VPMMD method along with the corresponding benchmark MIKE11solutions. These typical routing solutions were obtained at the end of 40 km of the routing reach using the space steps of Δx = 1 km and 4 km for the channel sizes of b_f/b_m = 2.0 (channel types 14, 17, 18 and 23) and b_f/b_m = 4. 0 (channel types 62, 65, 66, 71 and 72). It is seen from the Figures 3.9(a) and 3.9(k) that there is a tendency of formation of wiggles in the simulated hydrograph whenever there is a sudden rise of the hydrograph in steep channels. Further, these wiggle formations are generated when the routing using the VPMMD method is carried out for long sub-reaches in steep slope channels $(S_o \geq 0.001)$. *Nash* [1959] was the first researcher who brought out this deficiency of the Muskingum routing solution, and the wiggle appears due to the formation of "initial dip" or "negative initial flow" and its sequential routing through the cascade of Muskingum sub-reaches. Further, *Perumal,* [1992] also pointed out that the size of the wiggle depends directly on the steepness of the bed slope, steepness of the rise or fall of the input discharge hydrograph and the magnitude of the roughness coefficient. In essence, when the input discharge hydrograph experiences a large variation in magnitude of $(1/S_o)(\partial y/\partial x)$, while routing in steep slope channels, the tendency for the formation of wiggle is strong. However, the effect of the

wiggle on the hydrograph can be minimized by increasing the number of sub-reaches used for routing. That is, increasing from 10 sub-reaches (Δx = 4 km) to 40 sub-reaches (Δx = 1 km), or, if not sufficient, further increase of sub-reaches resulted in the complete elimination of the wiggle formation. This is evident from Figure 3.9(u) (channel type 62) simulated with 80 sub-reaches (Δx = 0.5 km) consideration to avoid the wiggle formation. Further, one can also notice that the effect of wiggle impacts the solution results only locally and does not affect the entire solution significantly, such as the peak and time-to-peak characteristics of the hydrograph. In addition, it is also noticed that the size of the wiggle is less pronounced in the discharge hydrograph routing solution, as compared to that of the estimated stage hydrograph while routing using the VPMMD method. However, the overall performance of the VPMMD method can be considered good given the fact that even when the input discharge hydrograph has completely entered into the channel reach, typically as seen in Figures 3.9(m) and 3.9(o) (corresponding to channel types 65 and 66, respectively), with no significant response at the outlet of the reach, the VPMMD method could closely reproduce the MIKE11 solutions with η_q >98.54%. Further, the MIKE11 solutions considered herein are characterized by a maximum attenuation of μ_q = 39% and μ_y =19% for discharge and stage hydrographs reproductions, respectively, and these benchmark solutions could be reproduced very well by the VPMMD method in all aspects. Further, it can be inferred from Figure 3.10(a) that the VPMMD method also performs better in reproducing the MIKE11 peak discharges using the sub-reach lengths of Δx = 1 km and Δx = 4 km with a routing time intervals of Δt = 300 s for channels characterized by $S_o \geq 0.001$ and Δt = 1800 s in channels characterized by $S_o \leq 0.0005$. Further, these peak discharge reproductions of the benchmark MIKE11 solutions by the VPMMD method are again verified with a routing time intervals of Δt =

300 s. These results reveal that the VPMMD method reproduces the peak discharges of the MIKE11 solutions very closely as depicted in Figure 3.11(a).

Stage reproduction: Tables 3.3 and 3.4 reveal that the performance evaluation measures η_y, $|y_{per}|$ and $|t_{pyer}|$ by the VPMMD method in reproducing the benchmark solutions for $\Delta x = 1$ km and $\Delta x = 4$ km considerations, are: >98.50%, <3.98%, and <1.5 h; and >89.68%, <3.42%, and <1.5 h, respectively. The typical estimated stage hydrograph reproductions by the VPMMD method for routings using $\Delta x = 1$ km and $\Delta x = 4$ km can be considered to closely reproduce the benchmark MIKE11 solutions as illustrated in Figures 3.9 (b, d, f, h, j, l, n, p, r, t and v). It is also surmised that the wiggle formation in the estimated stage hydrograph is more pronounced for channels with bed gradient ≥ 0.001 (e.g., Figures 3.9 (b and l)) and is less in channels having $S_o \leq 0.0005$. (e.g., Figures 3.9 (d, n, p, r, and t)) with 10 sub-reaches ($\Delta x = 4$ km) consideration. However, as described earlier, the problem of wiggle formation is minimized by increasing the number of sub-reaches, i.e., with smaller Δx, in a given channel reach as evident from Figures 3.9 (b, d, f, h, j, l, n, p, r, and t) with $\Delta x = 1$ km and also seen from Figure 3.9(v) (channel type 62) simulated for $\Delta x = 0.5$ km (80 sub reaches). Further, it can be inferred from Figure 3.10(b) while comparing the estimated peak stages with the corresponding benchmark solutions, the VPMMD method closely reproduces peak stages of the MIKE11 solutions while routing in channel reaches with sub-reach lengths of $\Delta x =$ 1 km and $\Delta x = 4$ km with a routing time intervals of $\Delta t = 300$ s for channels having $S_o \geq 0.001$ and $\Delta t = 1800$ s for channels having $S_o \leq 0.0005$. Further, the use of smaller Δt does not affect the estimated peak stages reproductions of the benchmark solutions by the VPMMD method, as evident from Figure 3.11(b).

Table 3.3 Summary of performance criteria showing reproduction of pertinent characteristics of the MIKE11 results by the VPMMD method for routing in two-stage compound channel reaches using 40 sub-reaches.

Channel Type	b_f/b_m	S_o	n	μ_q (%)	μ_y (%)	Discharge Routing				Stage Comutation		
						EVOL (%)	η_q (%)	q_{per} (%)	t_{pqer} (h)	η_y (%)	y_{per} (%)	t_{pyer} (h)
1	1.5	0.003	0.04	0.42	0.21	0.002236	99.93	0.29	0.00	99.70	0.16	0.08
2	1.5	0.002	0.04	0.78	0.40	0.001205	99.98	0.32	0.00	99.88	0.18	0.08
3	1.5	0.001	0.04	2.75	1.45	0.001170	99.99	0.47	0.00	99.91	0.30	0.08
4	1.5	0.0005	0.04	10.15	5.35	-0.001491	99.75	3.29	0.00	99.61	2.14	0.00
5	1.5	0.0003	0.04	20.36	11.02	0.000897	99.61	0.81	0.50	99.53	1.83	0.50
6	1.5	0.0002	0.04	29.57	16.05	-0.000793	98.94	-4.91	1.00	99.19	0.08	1.50
7	1.5	0.003	0.025	0.25	0.13	-0.000286	99.98	0.21	0.00	99.93	0.12	0.00
8	1.5	0.002	0.025	0.40	0.20	0.002187	99.97	0.24	0.00	99.90	0.12	0.08
9	1.5	0.001	0.025	1.19	0.63	-0.000334	99.99	0.31	0.00	99.94	0.18	0.08
10	1.5	0.0005	0.025	4.35	2.29	-0.000876	99.89	1.83	0.00	99.81	1.18	0.00
11	1.5	0.0003	0.025	10.64	5.75	-0.000594	99.83	2.27	0.00	99.75	1.92	0.00
12	1.5	0.0002	0.025	18.10	9.79	0.001439	99.64	-0.25	0.50	99.61	1.48	0.50
13	2.0	0.003	0.04	0.48	0.22	0.002236	99.91	0.32	0.00	99.64	0.14	0.00
14	2.0	0.002	0.04	0.85	0.40	0.001205	99.96	0.37	0.00	99.84	0.17	0.00
15	2.0	0.001	0.04	2.97	1.42	0.001177	99.81	0.64	-0.17	99.90	0.32	0.08
16	2.0	0.0005	0.04	10.93	5.56	-0.001491	99.63	4.39	-0.50	99.52	2.67	0.00
17	2.0	0.0003	0.04	21.97	11.58	0.000897	99.46	1.85	0.50	99.39	2.20	0.00
18	2.0	0.0002	0.04	31.80	16.87	-0.000782	98.81	-3.82	1.00	99.05	0.60	1.50
19	2.0	0.003	0.025	0.34	0.18	-0.000286	99.96	0.28	0.00	99.91	0.14	0.08
20	2.0	0.002	0.025	0.48	0.25	0.002194	99.96	0.29	0.00	99.88	0.15	0.08
21	2.0	0.001	0.025	1.29	0.63	-0.000348	99.99	0.35	0.00	99.93	0.19	0.08
22	2.0	0.0005	0.025	4.71	2.31	-0.000886	99.84	2.30	-0.50	99.80	1.37	0.00
23	2.0	0.0003	0.025	11.58	5.93	-0.000605	99.74	2.95	0.00	99.70	2.15	0.00
24	2.0	0.0002	0.025	19.78	10.18	0.001429	99.50	0.37	1.00	99.52	1.69	0.50
25	2.5	0.003	0.04	0.51	0.23	0.002236	99.89	0.35	0.00	99.61	0.15	0.08
26	2.5	0.002	0.04	0.89	0.38	0.001198	99.94	0.39	0.00	99.76	0.17	0.08
27	2.5	0.001	0.04	3.06	1.42	0.001170	99.98	0.66	-0.08	99.88	0.33	0.00
28	2.5	0.0005	0.04	11.74	5.79	-0.001491	99.53	5.35	-0.50	99.44	3.11	0.00
29	2.5	0.0003	0.04	23.52	12.00	0.000886	99.34	2.62	0.50	99.27	2.53	0.50
30	2.5	0.0002	0.04	33.87	17.50	-0.000793	98.71	-2.78	1.00	98.93	0.96	1.00
31	2.5	0.003	0.025	0.42	0.19	-0.000286	99.84	0.32	0.00	99.78	0.16	0.08
32	2.5	0.002	0.025	0.54	0.26	0.002187	99.95	0.32	-0.08	99.86	0.15	0.17
33	2.5	0.001	0.025	1.38	0.62	-0.000341	99.98	0.38	0.00	99.91	0.20	0.08
34	2.5	0.0005	0.025	5.14	2.34	-0.000876	99.79	3.36	-0.50	99.75	1.68	-0.50
35	2.5	0.0003	0.025	12.52	6.11	-0.000594	99.67	3.57	0.00	99.67	2.31	0.00
36	2.5	0.0002	0.025	21.19	10.55	0.001449	99.41	0.97	0.50	99.47	1.86	0.50

μ_q is the attenuation in peak discharge by the MIKE11 model computed by equation (3.19), and μ_y is the corresponding attenuation in peak stage, computed by equation (3.19) after replacing the discharge value with the corresponding stage value.

Contn... of Table 3.3 for $\Delta x = 1$ km (40 Sub-reaches)

Channel Type	b_f/b_m	S_o	n	μ_q (%)	μ_y (%)	Discharge Routing				Stage Comutation		
						EVOL (%)	η_q (%)	q_{per} (%)	t_{pqer} (h)	η_y (%)	y_{per} (%)	t_{pyer} (h)
37	3.0	0.003	0.04	0.55	0.24	0.002229	99.75	0.38	0.00	99.50	0.17	0.08
38	3.0	0.002	0.04	0.95	0.40	0.001205	99.92	0.43	0.00	99.79	0.18	0.08
39	3.0	0.001	0.04	3.26	1.45	0.001170	99.98	0.78	-0.08	99.85	0.39	0.00
40	3.0	0.0005	0.04	12.62	6.04	-0.001481	99.43	6.17	-0.50	99.39	3.50	0.00
41	3.0	0.0003	0.04	24.96	12.40	0.000897	99.26	3.40	0.50	99.19	2.75	0.50
42	3.0	0.0002	0.04	35.75	18.00	-0.000803	98.64	-1.85	1.50	98.83	1.32	1.00
43	3.0	0.003	0.025	0.46	0.19	-0.000286	99.93	0.34	0.00	99.88	0.16	0.17
44	3.0	0.002	0.025	0.59	0.26	0.002194	99.93	0.35	-0.08	99.83	0.16	0.17
45	3.0	0.001	0.025	1.47	0.64	-0.000341	99.97	0.43	0.00	99.88	0.20	0.17
46	3.0	0.0005	0.025	5.67	2.45	-0.000887	99.74	4.34	-0.50	99.72	2.12	-0.50
47	3.0	0.0003	0.025	13.44	6.31	-0.000605	99.63	4.14	0.00	99.63	2.45	0.00
48	3.0	0.0002	0.025	22.54	10.86	0.001449	99.35	1.47	0.50	99.43	1.98	0.50
49	3.5	0.003	0.04	0.60	0.24	0.002236	99.56	0.42	-0.08	99.44	0.17	0.08
50	3.5	0.002	0.04	0.99	0.41	0.001198	99.82	0.46	-0.08	99.75	0.19	0.08
51	3.5	0.001	0.04	3.48	1.51	0.001170	99.97	0.91	-0.17	99.82	0.44	0.00
52	3.5	0.0005	0.04	13.52	6.26	-0.001481	99.39	6.99	0.00	99.32	3.77	0.00
53	3.5	0.0003	0.04	26.42	12.69	0.000907	99.20	4.07	0.50	99.13	2.81	0.50
54	3.5	0.0002	0.04	37.37	18.41	-0.000793	98.59	-1.19	1.00	98.71	1.55	1.50
55	3.5	0.003	0.025	0.51	0.19	-0.000293	99.86	0.39	-0.08	99.85	0.14	0.00
56	3.5	0.002	0.025	0.63	0.22	0.002194	99.92	0.37	0.00	99.83	0.14	0.08
57	3.5	0.001	0.025	1.56	0.62	-0.000348	99.94	0.46	0.00	99.76	0.19	0.08
58	3.5	0.0005	0.025	5.94	2.58	-0.000876	99.68	5.08	-0.50	99.64	2.41	-0.50
59	3.5	0.0003	0.025	14.34	6.48	-0.000605	99.59	4.66	0.00	99.60	2.55	0.00
60	3.5	0.0002	0.025	23.82	11.12	0.001429	99.31	1.91	0.50	99.41	2.06	1.00
61	4.0	0.003	0.04	0.61	0.21	0.002236	99.14	0.41	0.00	99.16	0.15	0.08
62	4.0	0.002	0.04	1.03	0.38	0.001205	99.60	0.49	-0.08	99.64	0.18	0.00
63	4.0	0.001	0.04	3.74	1.56	0.001177	99.97	1.06	-0.17	99.80	0.48	0.00
64	4.0	0.0005	0.04	14.42	6.45	-0.001481	99.36	7.72	0.00	99.28	3.98	0.00
65	4.0	0.0003	0.04	27.62	12.97	0.000897	99.15	4.48	0.50	99.07	2.97	0.50
66	4.0	0.0002	0.04	38.90	18.72	-0.000834	98.54	-0.32	1.00	98.50	1.73	1.00
67	4.0	0.003	0.025	0.55	0.20	0.001915	99.57	0.41	-0.08	99.66	0.15	0.00
68	4.0	0.002	0.025	0.68	0.27	0.002194	99.85	0.40	-0.08	99.81	0.16	0.17
69	4.0	0.001	0.025	1.64	0.60	-0.000341	99.97	0.51	0.00	99.85	0.20	0.00
70	4.0	0.0005	0.025	6.33	2.59	-0.000887	99.62	6.33	-0.50	99.58	2.69	-0.50
71	4.0	0.0003	0.025	15.22	6.65	-0.000594	99.57	5.13	0.00	99.59	2.61	0.00
72	4.0	0.0002	0.025	25.01	11.31	0.001439	99.27	2.32	0.50	99.38	2.12	0.50

Table 3.4 Summary of performance criteria showing reproduction of pertinent characteristics of the MIKE11 results by the VPMMD method for routing in two-stage compound channel reaches using 10 sub-reaches.

Channel Type	b_f/b_m	S_o	n	μ_q (%)	μ_y (%)	Discharge Routing				Stage Comutation		
						EVOL (%)	η_q (%)	q_{per} (%)	t_{pqer} (h)	η_y (%)	y_{per} (%)	t_{pyer} (h)
1	1.5	0.003	0.04	0.42	0.21	0.002075	99.91	0.30	0.00	99.63	0.17	0.08
2	1.5	0.002	0.04	0.78	0.40	0.000968	99.94	0.31	0.00	99.79	0.18	0.08
3	1.5	0.001	0.04	2.75	1.45	0.000996	99.89	0.37	0.00	99.57	0.30	0.08
4	1.5	0.0005	0.04	10.15	5.35	-0.00147	99.80	3.43	0.00	99.38	2.36	0.00
5	1.5	0.0003	0.04	20.36	11.02	0.000876	99.73	0.94	0.50	99.54	2.31	0.50
6	1.5	0.0002	0.04	29.57	16.05	-0.000876	99.08	-4.66	1.00	99.32	0.77	1.50
7	1.5	0.003	0.025	0.25	0.13	-0.000453	99.98	0.25	0.00	99.93	0.14	0.00
8	1.5	0.002	0.025	0.40	0.20	0.002006	99.95	0.26	0.00	99.84	0.14	0.08
9	1.5	0.001	0.025	1.19	0.63	-0.000543	99.97	0.29	0.00	99.85	0.20	0.08
10	1.5	0.0005	0.025	4.35	2.29	-0.000866	99.88	2.11	0.00	99.66	1.41	0.00
11	1.5	0.0003	0.025	10.64	5.75	-0.000605	99.87	2.40	0.00	99.70	2.18	0.00
12	1.5	0.0002	0.025	18.10	9.79	0.001418	99.71	-0.10	0.50	99.64	1.90	0.50
13	2.0	0.003	0.04	0.48	0.22	0.002075	99.69	0.32	0.00	99.29	0.15	0.00
14	2.0	0.002	0.04	0.85	0.40	0.001003	99.67	0.34	0.00	99.39	0.17	0.00
15	2.0	0.001	0.04	2.97	1.42	0.001024	99.33	0.47	-0.17	99.32	0.29	0.08
16	2.0	0.0005	0.04	10.93	5.56	-0.00146	99.76	4.33	-0.50	99.38	2.79	0.00
17	2.0	0.0003	0.04	21.97	11.58	0.000907	99.65	1.99	0.50	99.44	2.74	0.00
18	2.0	0.0002	0.04	31.80	16.87	-0.000866	99.01	-3.56	1.00	99.22	1.31	1.00
19	2.0	0.003	0.025	0.34	0.18	-0.000432	99.95	0.28	0.08	99.91	0.14	0.08
20	2.0	0.002	0.025	0.48	0.25	0.002061	99.90	0.30	0.00	99.77	0.16	0.08
21	2.0	0.001	0.025	1.29	0.63	-0.000543	99.92	0.32	0.00	99.77	0.19	0.08
22	2.0	0.0005	0.025	4.71	2.31	-0.000907	99.88	2.57	0.00	99.75	1.57	0.00
23	2.0	0.0003	0.025	11.58	5.93	-0.000574	99.82	3.03	0.00	99.71	2.37	0.00
24	2.0	0.0002	0.025	19.78	10.18	0.001439	99.61	0.54	0.50	99.59	2.14	0.50
25	2.5	0.003	0.04	0.51	0.23	0.002089	99.27	0.33	0.00	98.86	0.15	0.08
26	2.5	0.002	0.04	0.89	0.38	0.000989	99.16	0.33	0.00	98.78	0.16	0.08
27	2.5	0.001	0.04	3.06	1.42	0.001017	99.32	0.37	0.00	98.32	0.25	0.08
28	2.5	0.0005	0.04	11.74	5.79	-0.00146	99.74	4.98	-0.50	99.14	3.08	0.00
29	2.5	0.0003	0.04	23.52	12.00	0.000886	99.60	2.61	0.50	99.32	2.93	0.50
30	2.5	0.0002	0.04	33.87	17.50	-0.000845	98.97	-2.53	1.00	99.11	1.71	1.00
31	2.5	0.003	0.025	0.42	0.19	-0.000474	99.84	0.32	0.00	99.82	0.16	0.08
32	2.5	0.002	0.025	0.54	0.26	0.002013	99.74	0.31	-0.08	99.65	0.15	0.17
33	2.5	0.001	0.025	1.38	0.62	-0.000529	99.77	0.33	0.00	99.61	0.20	0.08
34	2.5	0.0005	0.025	5.14	2.34	-0.000897	99.87	3.37	-0.50	99.74	1.69	-0.50
35	2.5	0.0003	0.025	12.52	6.11	-0.000605	99.79	3.56	0.00	99.70	2.49	0.00
36	2.5	0.0002	0.025	21.19	10.55	0.001397	99.56	1.06	0.50	99.56	2.32	0.50

Contn... of Table 3.4 for $\Delta x = 4$ km (10 Sub-reaches)

Channel Type	b_f/b_m	S_o	n	μ_q (%)	μ_y (%)	Discharge Routing				Stage Comutation		
						EVOL (%)	η_q (%)	q_{per} (%)	t_{pqer} (h)	η_y (%)	y_{per} (%)	t_{pyer} (h)
37	3.0	0.003	0.04	0.55	0.24	0.002082	98.61	0.33	0.00	98.27	0.15	0.08
38	3.0	0.002	0.04	0.95	0.40	0.000982	98.40	0.34	0.00	97.95	0.15	0.08
39	3.0	0.001	0.04	3.26	1.45	0.000996	98.64	0.34	0.00	96.67	0.24	0.08
40	3.0	0.0005	0.04	12.62	6.04	-0.00147	99.67	5.48	-0.50	98.75	3.29	0.00
41	3.0	0.0003	0.04	24.96	12.40	0.000928	99.60	3.36	0.50	99.20	3.16	0.50
42	3.0	0.0002	0.04	35.75	18.00	-0.000865	98.97	-1.65	1.50	99.00	1.99	1.00
43	3.0	0.003	0.025	0.46	0.19	-0.000494	99.63	0.33	0.00	99.72	0.16	0.17
44	3.0	0.002	0.025	0.59	0.26	0.002103	99.44	0.33	-0.08	99.43	0.16	0.17
45	3.0	0.001	0.025	1.47	0.64	-0.000543	99.50	0.33	0.00	99.36	0.19	0.17
46	3.0	0.0005	0.025	5.67	2.45	-0.000876	99.86	4.10	-0.50	99.70	1.97	-0.50
47	3.0	0.0003	0.025	13.44	6.31	-0.000594	99.78	4.02	0.00	99.67	2.58	0.00
48	3.0	0.0002	0.025	22.54	10.86	0.001429	99.54	1.57	0.50	99.53	2.46	0.50
49	3.5	0.003	0.04	0.60	0.24	0.002075	97.91	0.35	-0.08	97.70	0.15	0.08
50	3.5	0.002	0.04	0.99	0.41	0.000926	97.47	0.32	-0.08	96.87	0.14	0.17
51	3.5	0.001	0.04	3.48	1.51	0.000926	97.77	0.28	0.00	94.18	0.22	0.08
52	3.5	0.0005	0.04	13.52	6.26	-0.001481	99.61	5.88	0.00	98.19	3.38	0.00
53	3.5	0.0003	0.04	26.42	12.69	0.000907	99.61	4.04	0.50	99.02	3.25	0.00
54	3.5	0.0002	0.04	37.37	18.41	-0.000813	98.99	-0.91	1.00	98.85	2.22	1.00
55	3.5	0.003	0.025	0.51	0.19	-0.000481	99.22	0.36	-0.08	99.49	0.13	0.00
56	3.5	0.002	0.025	0.63	0.22	0.002138	99.07	0.33	0.00	99.21	0.13	0.08
57	3.5	0.001	0.025	1.56	0.62	-0.000501	99.11	0.32	0.00	99.03	0.16	0.08
58	3.5	0.0005	0.025	5.94	2.58	-0.000887	99.84	4.24	0.00	99.62	2.12	-0.50
59	3.5	0.0003	0.025	14.34	6.48	-0.000594	99.80	4.40	0.00	99.62	2.61	0.00
60	3.5	0.0002	0.025	23.82	11.12	0.001439	99.54	2.02	0.50	99.47	2.55	0.50
61	4.0	0.003	0.04	0.61	0.21	0.002062	97.07	0.31	0.00	97.05	0.11	0.08
62	4.0	0.002	0.04	1.03	0.38	0.00101	96.43	0.28	-0.08	95.66	0.11	0.08
63	4.0	0.001	0.04	3.74	1.56	0.000926	96.70	0.23	0.00	89.68	0.19	0.17
64	4.0	0.0005	0.04	14.42	6.45	-0.001481	99.54	6.20	-0.50	97.30	3.42	0.00
65	4.0	0.0003	0.04	27.62	12.97	0.000897	99.63	4.31	0.00	98.77	3.29	0.00
66	4.0	0.0002	0.04	38.90	18.72	-0.000834	99.02	-0.15	1.00	98.58	2.36	1.00
67	4.0	0.003	0.025	0.55	0.20	0.001839	98.59	0.35	-0.08	99.14	0.13	0.00
68	4.0	0.002	0.025	0.68	0.27	0.002131	98.54	0.34	0.00	98.90	0.14	0.17
69	4.0	0.001	0.025	1.64	0.60	-0.000495	98.56	0.30	0.00	98.53	0.14	0.08
70	4.0	0.0005	0.025	6.33	2.59	-0.000887	99.77	4.53	-0.50	99.50	2.03	0.00
71	4.0	0.0003	0.025	15.22	6.65	-0.000563	99.80	4.72	0.00	99.52	2.71	-0.50
72	4.0	0.0002	0.025	25.01	11.31	0.00145	99.53	2.36	0.50	99.42	2.55	0.00

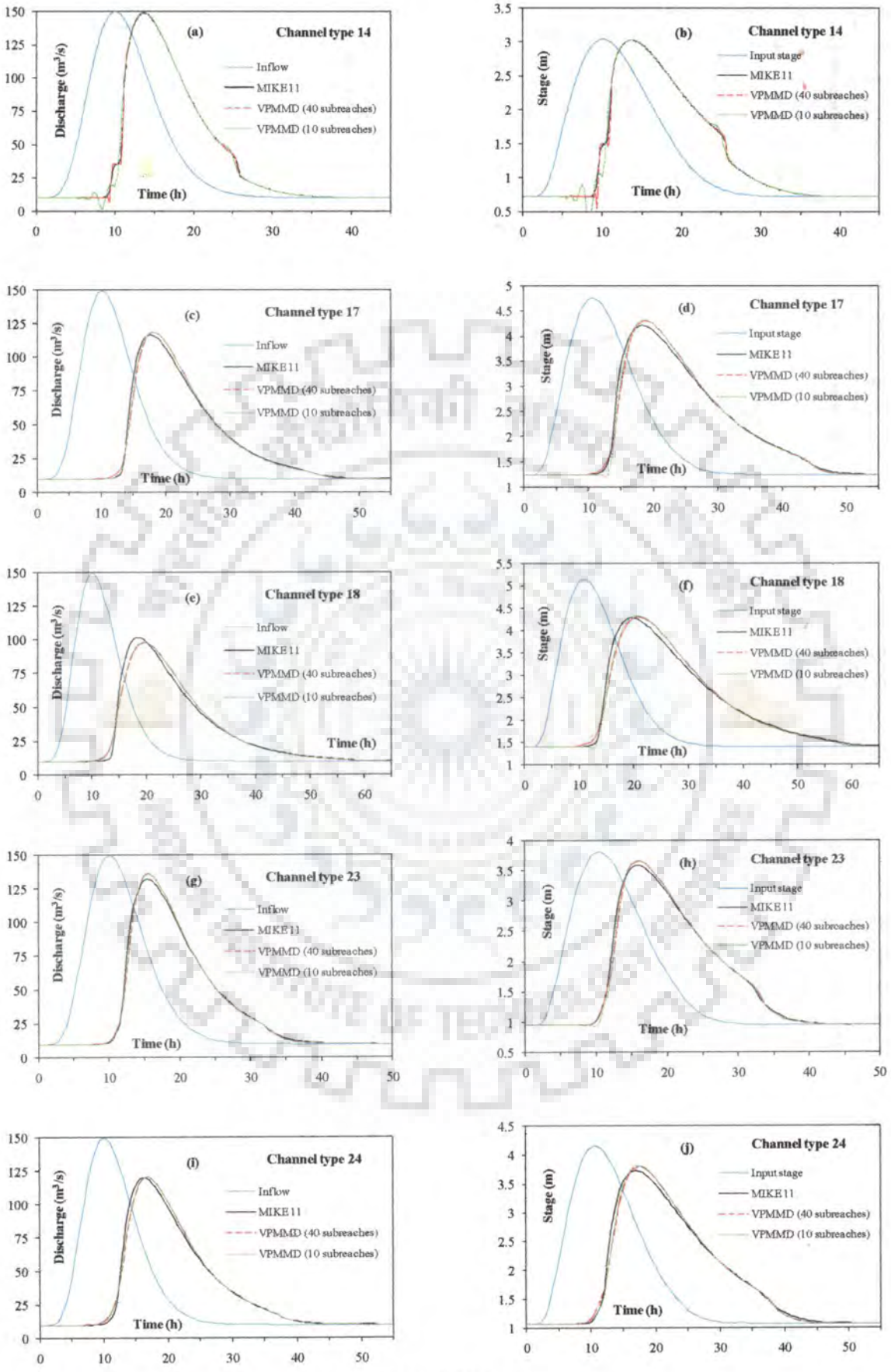
(a)
Channel type 14
Discharge (m³/s)
Time (h)
Inflow
MIKE11
VPMMD (40 subreaches)
VPMMD (10 subreaches)
(b)
Channel type 14
Stage (m)
Time (h)
Input stage
MIKE11
VPMMD (40 subreaches)
VPMMD (10 subreaches)
(c)
Channel type 17
Discharge (m³/s)
Time (h)
Inflow
MIKE11
VPMMD (40 subreaches)
VPMMD (10 subreaches)
(d)
Channel type 17
Stage (m)
Time (h)
Input stage
MIKE11
VPMMD (40 subreaches)
VPMMD (10 subreaches)
(e)
Channel type 18
Discharge (m³/s)
Time (h)
Inflow
MIKE11
VPMMD (40 subreaches)
VPMMD (10 subreaches)
(f)
Channel type 18
Stage (m)
Time (h)
Input stage
MIKE11
VPMMD (40 subreaches)
VPMMD (10 subreaches)
(g)
Channel type 23
Discharge (m³/s)
Time (h)
Inflow
MIKE11
VPMMD (40 subreaches)
VPMMD (10 subreaches)
(h)
Channel type 23
Stage (m)
Time (h)
Input stage
MIKE11
VPMMD (40 subreaches)
VPMMD (10 subreaches)
(i)
Channel type 24
Discharge (m³/s)
Time (h)
Inflow
MIKE11
VPMMD (40 subreaches)
VPMMD (10 subreaches)
(j)
Channel type 24
Stage (m)
Time (h)
Input stage
MIKE11
VPMMD (40 subreaches)
VPMMD (10 subreaches)

Fig. 3.9(i)

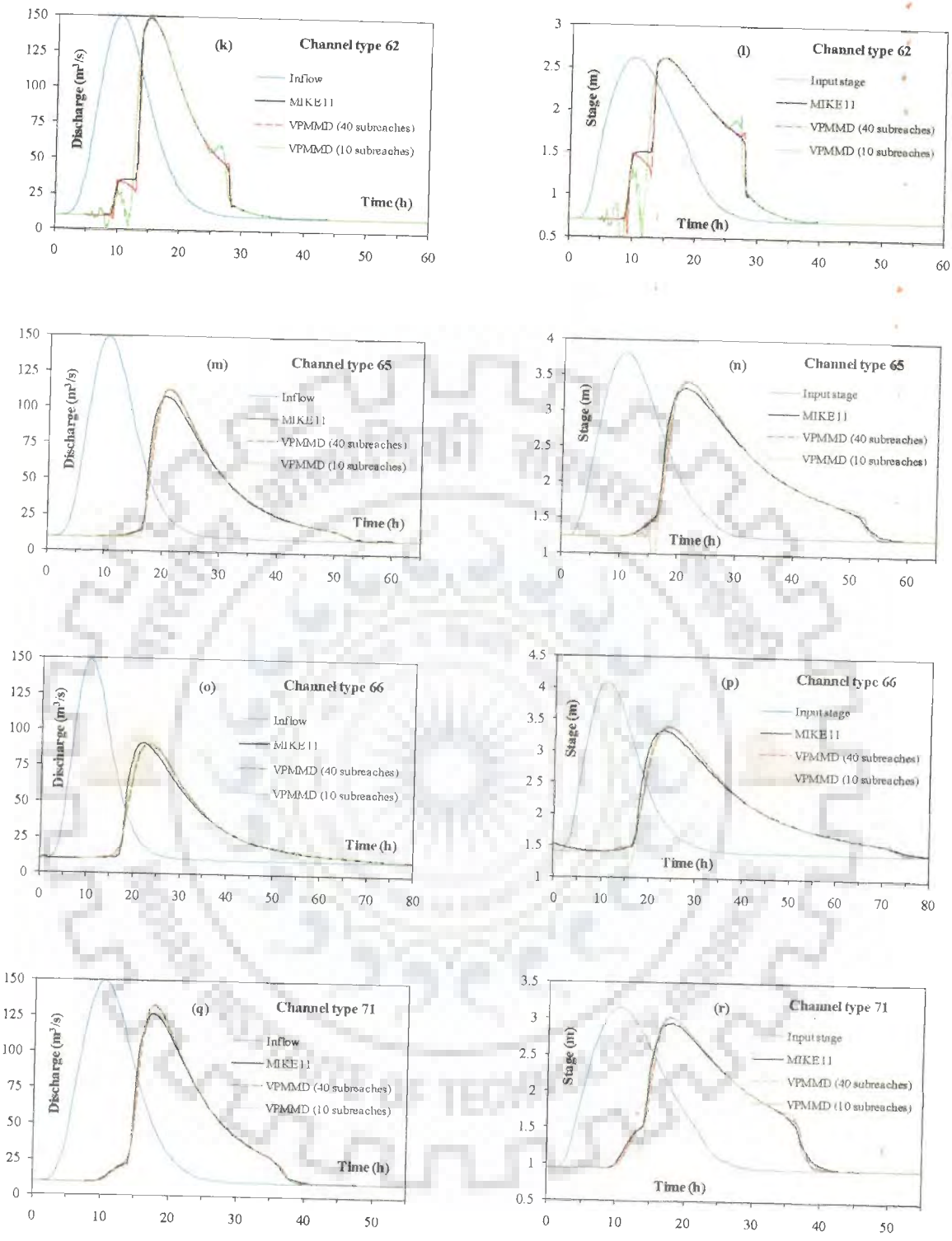
(k)
Channel type 62
Discharge (m³/s)
Inflow
MIKE11
VPMMD (40 subreaches)
VPMMD (10 subreaches)
Time (h)
(l)
Channel type 62
Stage (m)
Input stage
MIKE11
VPMMD (40 subreaches)
VPMMD (10 subreaches)
Time (h)
(m)
Channel type 65
Discharge (m³/s)
Inflow
MIKE11
VPMMD (40 subreaches)
VPMMD (10 subreaches)
Time (h)
(n)
Channel type 65
Stage (m)
Input stage
MIKE11
VPMMD (40 subreaches)
VPMMD (10 subreaches)
Time (h)
(o)
Channel type 66
Discharge (m³/s)
Inflow
MIKE11
VPMMD (40 subreaches)
VPMMD (10 subreaches)
Time (h)
(p)
Channel type 66
Stage (m)
Input stage
MIKE11
VPMMD (40 subreaches)
VPMMD (10 subreaches)
Time (h)
(q)
Channel type 71
Discharge (m³/s)
Inflow
MIKE11
VPMMD (40 subreaches)
VPMMD (10 subreaches)
Time (h)
(r)
Channel type 71
Stage (m)
Input stage
MIKE11
VPMMD (40 subreaches)
VPMMD (10 subreaches)
Time (h)

Fig. 3.9(ii)

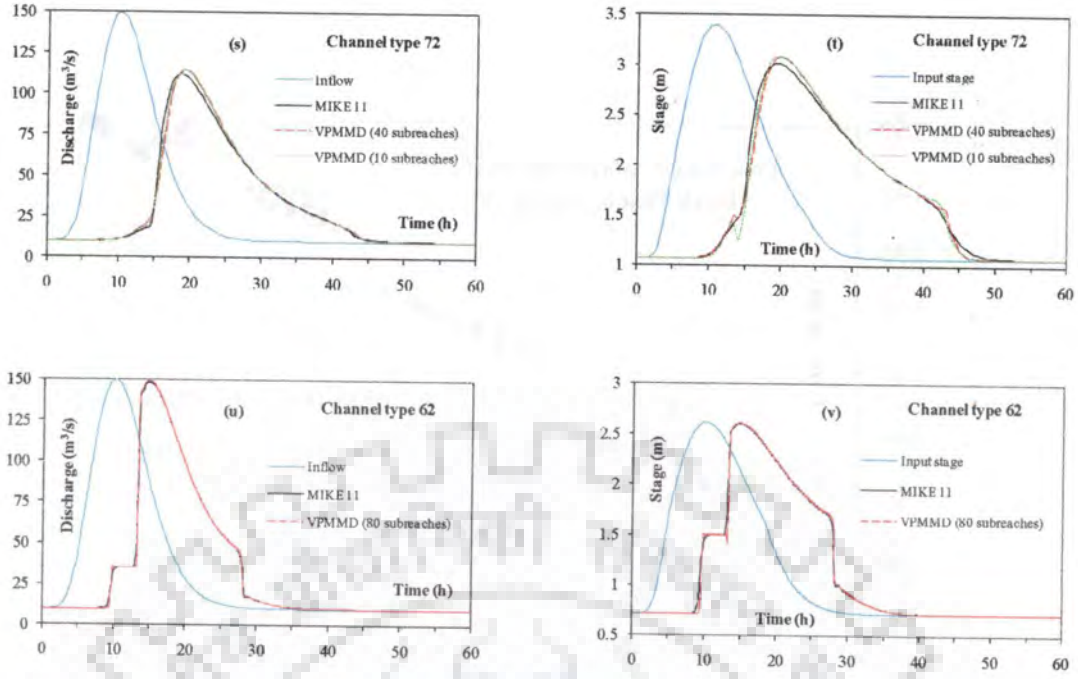

Fig. 3.9(iii)

Figure 3.9 Reproductions of some typical routed discharge and estimated stage hydrographs by the VPMMD method and the MIKE11 model in two-stage compound channel reaches considering 10 and 40 sub-reaches routing and for channel sizes $b_f / b_m = 2.0$ and 4.0.

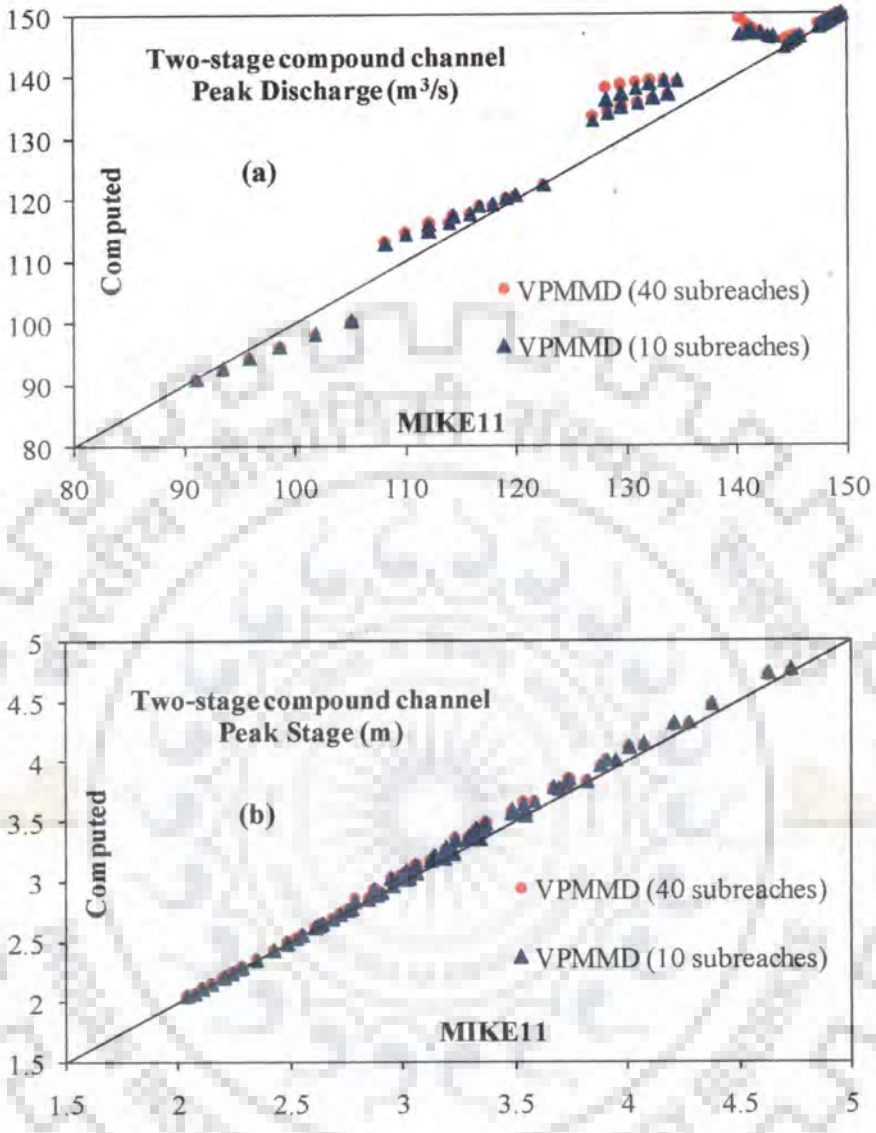

Figure 3.10 Comparison between the peak discharges and peak stages of the routing results of the VPMMD method and the corresponding MIKE11 solutions for the routing experiments in two-stage compound channel reaches considering10 and 40 sub-reaches and with a routing time interval of $\Delta t = 300$ s for channels with $S_o \geq 0.001$ and $\Delta t = 1800$ s for channels with $S_o \leq 0.0005$.

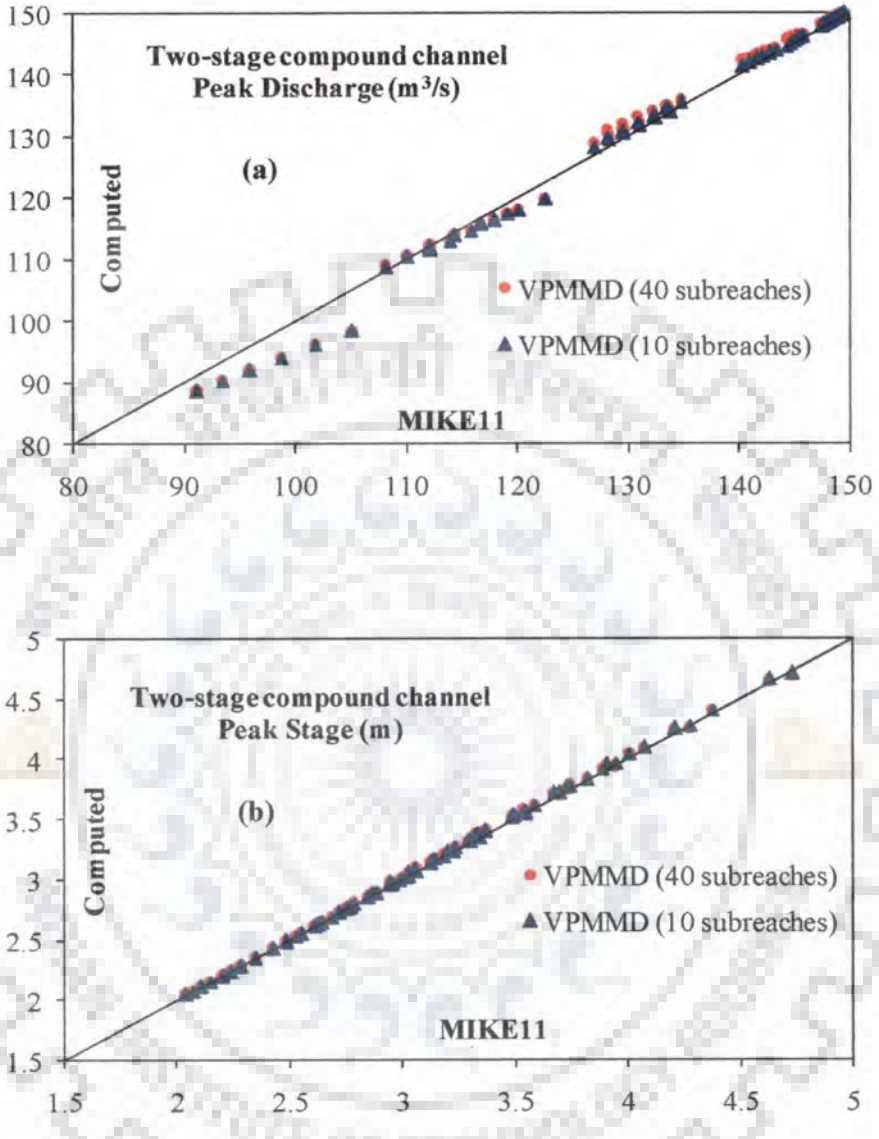

Figure 3.11 Comparison between the peak discharges and the peak stages of the routing results of the VPMMD method and the corresponding MIKE11solutions for the routing experiments in two-stage compound channel reaches considering 10 and 40 sub-reaches and with a routing time interval of $\Delta t = 300$s.

3.7 FIELD APPLICATION

3.7.1 River Reach Details

The acceptable solutions of most of the hydrodynamic routing methods depend on the use of number of channel cross-sections at closer intervals, hydrometric data at closer temporal intervals besides using other morphometric details of a river such as the surface roughness along the river reach which vary in space and time. The hydrodynamic principle based MIKE11 and HEC-RAS are such models that work at the cost of intensive data requirement of the morphometric and hydrometric data at closer spatial and temporal resolutions, respectively. Many underdeveloped and developing countries face difficulties in acquiring reliable stage-discharge data, leave alone the impossibility of measuring hydrometric and morphometric data at closer temporal and spatial intervals. Under such conditions, the application of models such as MIKE11, HEC-RAS and similar hydrodynamic routing models become difficult. The gauging sites where stream flow rating curves are available may be located at far apart distances. Considering such practical limitations of developing countries, a novel approach is proposed herein to simplify the routing process in natural river reaches using the VPMMD method. This study introduces an alternative routing procedure using a simplified hydraulic routing method based only on the use of the actual rating curves and the associated cross-section information available at the two ends of the routing reach, without directly involving any cross-sectional information in-between the reach. The establishment of reach-averaged rating curve enables the prismatic representation of the selected routing reach which is an essential assumption in the development of the VPMMD method. Such an approach of reach averaging of upstream and downstream rating curves of the considered routing reach avoids the complexities involved in the establishment of equivalent prismatic section envisaged by *Perumal et al.*, [2007; 2010] while routing using the VPMS stage

hydrograph routing method. In addition to the establishment of the reach-averaged rating curve, the reach-averaged flow cross-section, obtained using the cross-sections at the end sections, *versus* flow depth was also established for estimating the top width of the water surface required for estimating the weighting parameter θ expressed by the equation (3.5).

The VPMMD method developed based on the above lines is verified for ten recent flood events in the 15 km reach length of Pierantonio-Ponte Felcino reach characterized by negligible lateral flows. The proposed routing approach was also field tested for demonstrating its capability for routing in a long reach. For this purpose, the routing reach of length 50 km between Santa Lucia and Ponte Felcino of the Tiber River in Central Italy was considered. However, this reach experiences significant lateral flows. As the VPMMD method has been developed considering no lateral flow in the routing reach, it was considered logical to use a synthetic flood hydrograph defined by a four parameter Pearson type-III distribution given by equation (3.20) for routing using the MIKE11 model in this Santa Lucio-Ponte Felcino reach using the actual morphometric information. This reach has rich morphometric information with 200 cross-sections at 0.25 km intervals. The Pierantonio-Ponte Felcino reach forms the downstream part of the Santa Lucia-Ponte Felcino reach as shown in Figure 3.12.

Figure 3.12 Index map of the upper Tiber River in Central Italy.

The reach-averaged bed slope S_o for the selected river reaches were estimated as 0.0016 and 0.0014 for the Pierantonio-Ponte Felcino and Santa-Lucia-Ponte Felcino reaches, respectively. The discharge hydrograph routing and the corresponding stage hydrograph estimation capability using the VPMMD method were investigated by routing floods in these two different channel reaches separately.

3.7.2 Performance Evaluation of the VPMMD Method in Pierantonio-Ponte Felcino Reach

3.7.2.1 Establishment of reach-averaged rating curve and stage-mean flow area relationship

The existing actual rating curves at the Pierantonio (upstream) and the Ponte Felcino (downstream) stations were averaged to arrive at the reach-averaged rating curve for the entire Pierantonio-Ponte Felcino reach. The stage-mean flow area relationship of the Pierantonio-Ponte Felcino reach developed by *Perumal et al.*, [2010] was used directly in this study and the same is reproduced in Figure 3.13 The water surface widths (dA/dy) were extracted from the established stage-flow area relationship using the first order backward difference scheme. Similarly, the wave celerity, (dQ/dA) and the flow velocity, $v(y)$ were extracted from the discharge-flow area relationships. Therefore, the required normal depth *vs* reach-averaged channel reach and flow characteristics (dQ/dA, dA/dy and v) tables or look-up tables were generated using the reach-averaged rating curve and the stage-mean flow area information. One can estimate the stage hydrograph at the outlet of the reach corresponding to the routed discharge hydrograph arrived at that section using the VPMMD method. It may be noted that the assumption of prismatic channel reach behind the development of the VPMMD method does not affect the routed discharge hydrograph at the outlet, as discharge is a volume conserving variable. However, the stage variable is sensitive to the local geometrical variations and, therefore, a conversion equation is needed to convert the estimated stage hydrograph at a section to the corresponding actual stage hydrograph at that section. Therefore, the stage conversion equation as developed by *Perumal et al.* [2010] for the Pierantonio-Ponte Felcino reach

was used. This conversion equation: $y_{actual} = 0.927 * y_{equivalent} + 0.062$ already developed by *Perumal et al.* [2010] is adopted herein to enable the conversion of equivalent stage hydrograph value to that of the actual stage value at the outlet of the reach.

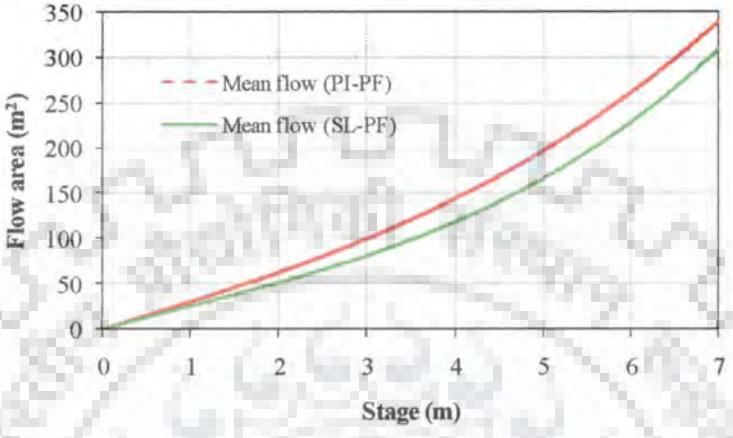

Figure 3.13 The mean flow depth *vs* cross-section area relationships of the Pierantonio-Ponte Felcino reach and the Santa Lucia-Ponte Felcino reach.

3.7.2.2 Results and discussion

The practical applicability of the VPMMD method to route flood hydrographs in natural rivers was tested by routing flood hydrographs in the 15 km river stretch between Pierantonio-Ponte Felcino gauging stations of the Tiber River in Central Italy. This reach is characterized by a bed slope of $S_o = 0.0016$ with negligible lateral flows. The discharge hydrograph routing and the corresponding stage hydrograph computation capability of the VPMMD method for routing in this reach was investigated using the reach-averaged rating curve (as discussed in Section 3.7.2.1). Ten recorded flood events comprising of floods of December 1996, April 1997, November 1997, February 1999, December 2000, April 2001, November 2005, 03rd December 2005, 05th December 2005, and 30th December 2005 were used. Out of all these floods, two flood events such as those of

December 2000 and November 2005 recorded significant lateral flows [see, Table 3.5]. All these flood events were routed from Pierantonio to Ponte Felcino station by the VPMMD method using a space step of $\Delta x = 1$ km (i.e., 15 sub-reaches) and a routing time interval of $\Delta t = 1800$ s. The pertinent characteristics of these simulated events are given in Table 3.5.

Table 3.5 Summary of performance criteria showing reproduction of pertinent characteristics of the ten flood events of the Pierantonio-Ponte Felcino reach by the VPMMD method.

Sl.No.	Flood Event	Discharge Routing				Stage Computation			Lateral Inflow (%)
		q_{per} (%)	$EVOL$ (%)	η_q (%)	t_{pqer} (h)	y_{per} (%)	η_y (%)	t_{pyer} (h)	
1	Dec, 1996	3.46	-1.56	99.59	0.00	-2.06	98.79	0.00	1.90
2	Apr, 1997	-0.58	-0.92	99.55	-2.00	-4.01	98.48	-2.00	6.50
3	Nov, 1997	8.23	-0.95	99.08	-1.00	0.93	98.84	-0.50	5.40
4	Feb, 1999	10.36	-1.13	95.30	0.00	1.64	98.02	0.00	4.40
5	Dec, 2000	9.48	-1.18	92.53	-1.50	1.47	97.78	-1.50	Flooding
6	Apr, 2001	6.93	-1.47	96.32	0.00	4.64	93.26	0.00	0.20
7	Nov, 2005	-12.29	-0.86	91.04	-5.50	-8.95	94.10	-5.50	Flooding
8	03Dec, 2005	1.98	-0.53	98.15	-0.50	4.49	96.77	-0.50	3.60
9	05Dec, 2005	0.55	-0.33	98.90	-0.50	4.22	97.72	-0.50	5.70
10	30 Dec, 2005	2.46	-1.17	98.95	0.00	4.51	97.94	0.50	1.90

It can be seen from Table 3.5 that the VPMMD method is almost volume conservative from practical consideration with $|EVOL| < 1.56\%$ for routing all these ten flood events studied. It is further seen that this method has a tendency to slightly underestimate the volume of the routed hydrograph. Further, it can be seen from Table 3.5 that all the discharge hydrographs could be reproduced with $\eta_q > 95.30\%$, except those of December 2000 and November 2005 flood events for which the variance explained are $\eta_q < 95\%$, but >90%. As noted earlier, these two floods recorded significant lateral flows as given

in Table 3.5. The errors in peak discharge reproduction $|q_{per}|$< 3.50% for the five flood events out of ten floods routed, and $|q_{per}|$>3.46%, but < 12.30% for the remaining flood events (viz., from Table 3.5). The errors of time-to-peak discharge $|t_{pqer}|$< 2.00 h for all the flood events routed except that of November 2005 event, for which $|t_{pqer}|$=5.50 h was estimated. Figures 3.14(a) to 3.14(t) demonstrate the comparisons between the routed discharge and the computed stage hydrographs along with the respective observed hydrographs at the Ponte Felcino station. It can be inferred from these figures and Table 3.5 that the routed discharge hydrographs of the VPMMD method and the corresponding estimated stage hydrographs are able to reproduce the respective observed hydrographs closely for all the flood events studied, except those events of December 2000 and November 2005 which were affected by flooding conditions along the routing reach. Similarly, the performance estimates of the simulated end section stage hydrographs, arrived at using the conversion equation: $y_{actual} = 0.927 * y_{equivalent} + 0.062$, in reproducing the actual observed stage hydrographs at the Ponte Felcino station are: η_y> 96.77% for all the flood events, except those of November 2005 and April 2001 floods, for which η_y<95%, η_y= 94.10% and 93.26%, respectively. The errors in peak stage reproduction $|y_{per}|$<4.64% for all the floods studied, except that for November 2005 flood for which $|y_{per}|$= 8.95%. The errors in peak stage time $|t_{pyer}|$<2.00 h for all the flood events, except that of November 2005, for which $|t_{pyer}|$=5.50 h. Therefore, the performance of the reproductions of the routed discharge and estimated stage hydrographs by the VPMMD method using rating curve information may be considered to be well acceptable for all the practical purposes.

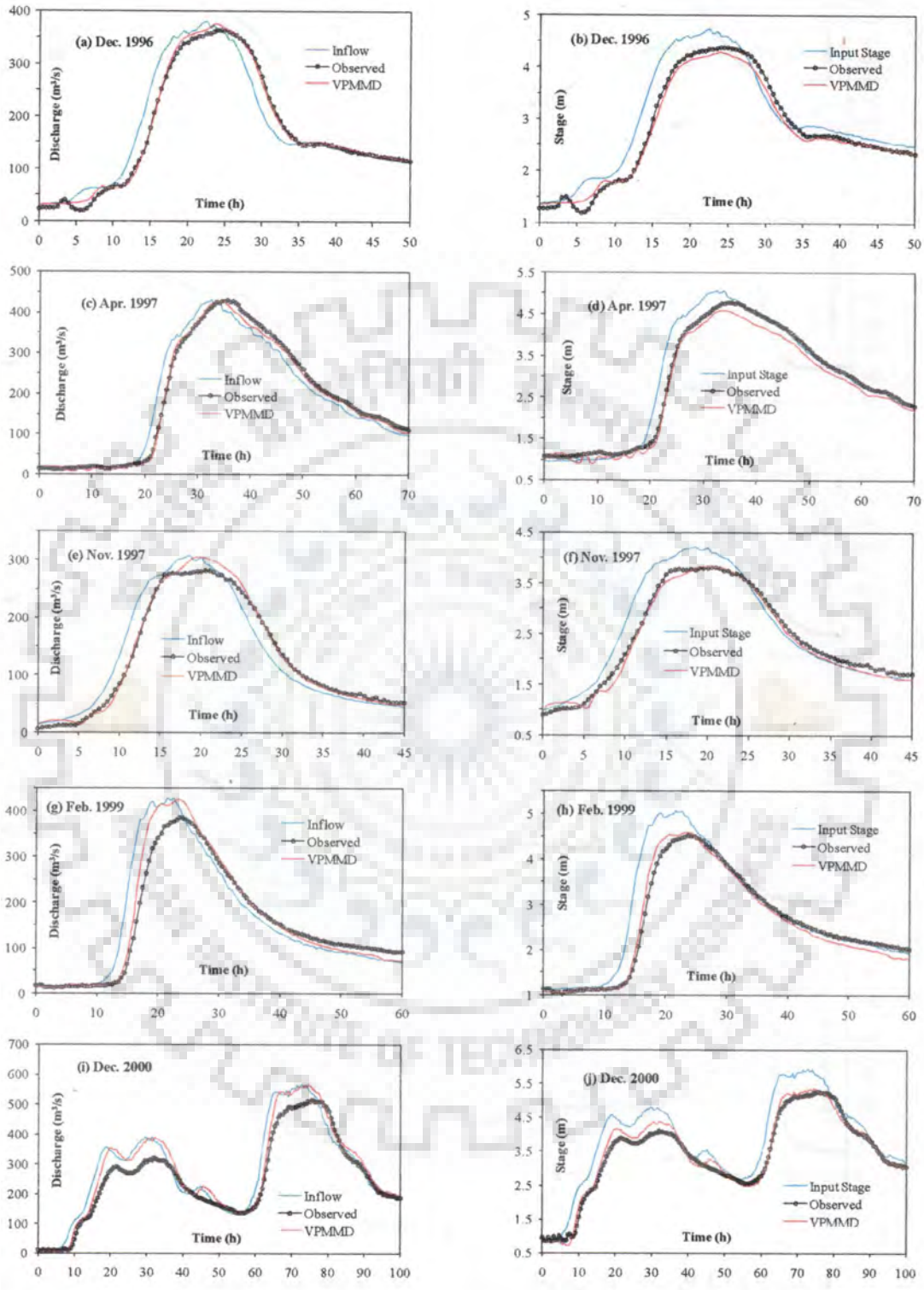
(a) Dec. 1996
Discharge (m³/s)
Time (h)
Inflow
Observed
VPMMD
(b) Dec. 1996
Stage (m)
Input Stage
(c) Apr. 1997
(d) Apr. 1997
(e) Nov. 1997
(f) Nov. 1997
(g) Feb. 1999
(h) Feb. 1999
(i) Dec. 2000
(j) Dec. 2000

Fig.3.14 (i)

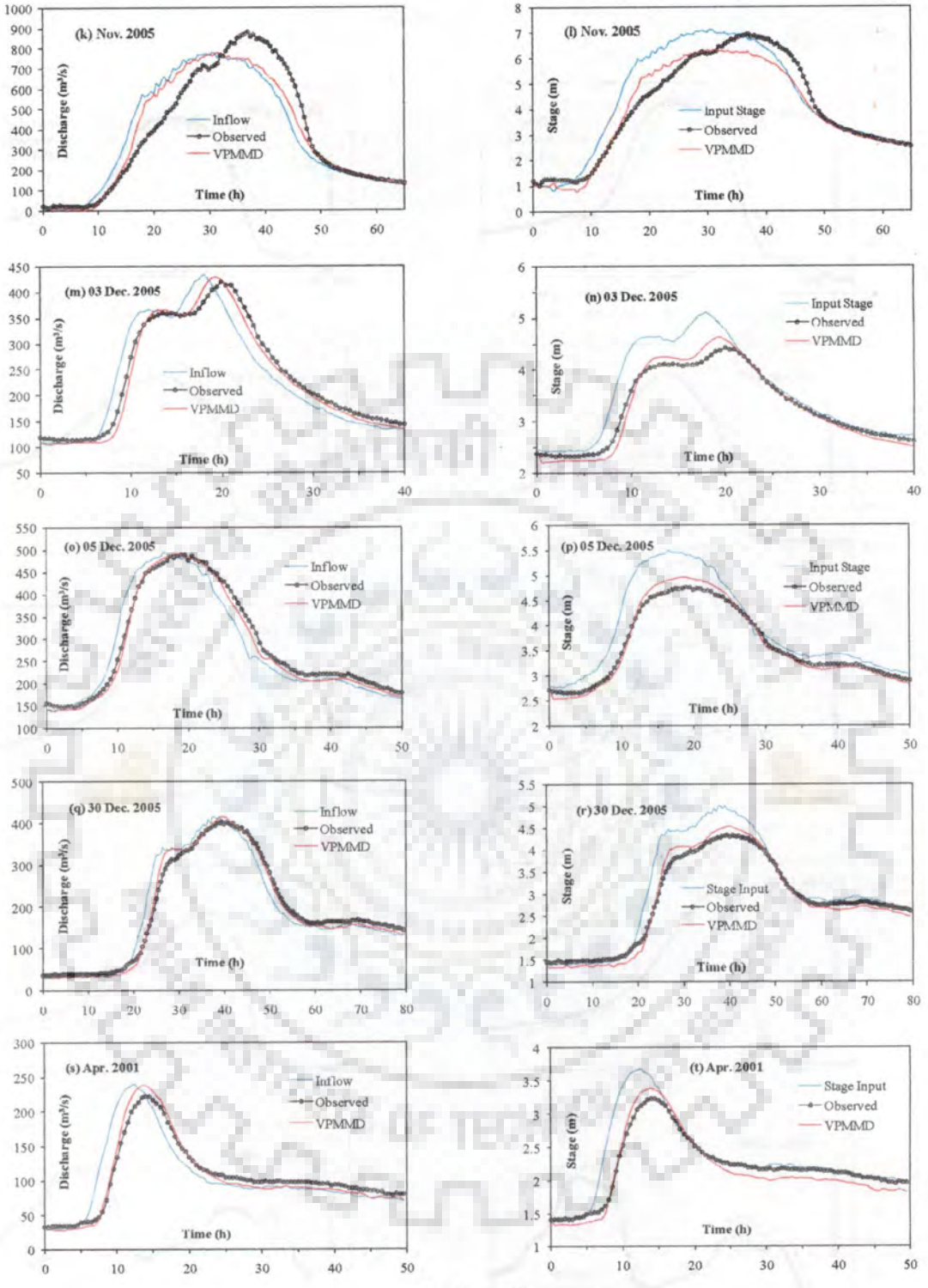

Fig.3.14 (ii)

Figure 3.14 Routed discharge and the corresponding estimated stage hydrographs by the VPMMD method at the Ponte Felcino station for ten flood events of the Pierantonio-Ponte Felcino reach.

3.7.3 Performance Evaluation of the VPMMD Method in Santa Lucia-Ponte Felcino Reach

3.7.3.1 Establishment of reach-averaged rating curve and stage-mean flow area relationship

All the three existing actual rating curves at Santa Lucia (upstream), Pierantonio (in between) and the Ponte Felcino (downstream) stations were used in arriving at the reach-averaged rating curve for the entire Santa Lucia-Ponte Felcino reach. To develop this reach-averaged rating curve, the existing rating curve at Santa Lucia gauging station and the mean rating curve of the downstream Pierantonio-Ponte Felcino reach were averaged. Similar procedure was also adopted for developing the stage-mean flow area relationships for the Santa Lucia-Ponte Felcino reach. The developed stage-mean flow area curve is given in Figure 3.13. The water surface widths (dA/dy) were extracted from the established stage-flow area relationship using the first order backward difference scheme. Similarly, the wave celerity (dQ/dA) and the flow velocity $v(y)$ were extracted from the discharge-flow area relationships. Therefore, the required normal depth tables or look-up tables were generated using the reach-averaged rating curve, (dA/dy), (dQ/dA) and $v(y)$ information. Since the stage variable is sensitive to the local variations of the cross-sectional flow area of the river reach, the stage hydrograph arrived at the site of interest is affected by the subjectivity of the assumed prismatic channel section between the two end sections of the routing reach. Therefore, a stage conversion equation: $y_{actual} = 0.741 * y_{equivalent} + 0.462$ for Santa Lucia-Ponte Felcino reach is developed by correlating the flow depth $(y_{equivalent})$ of the reach-averaged prismatic section and the actual flow depth (y_{actual}) at the Ponte Felcino outlet station.

The existing rating curves of Santa Lucia, Pierantonio, and Ponte Felcino gauging stations and the reach-averaged rating curves for the Santa Lucia-Ponte Felcino and Pierantonio-Ponte Felcino reaches are shown in Figure 3.15.

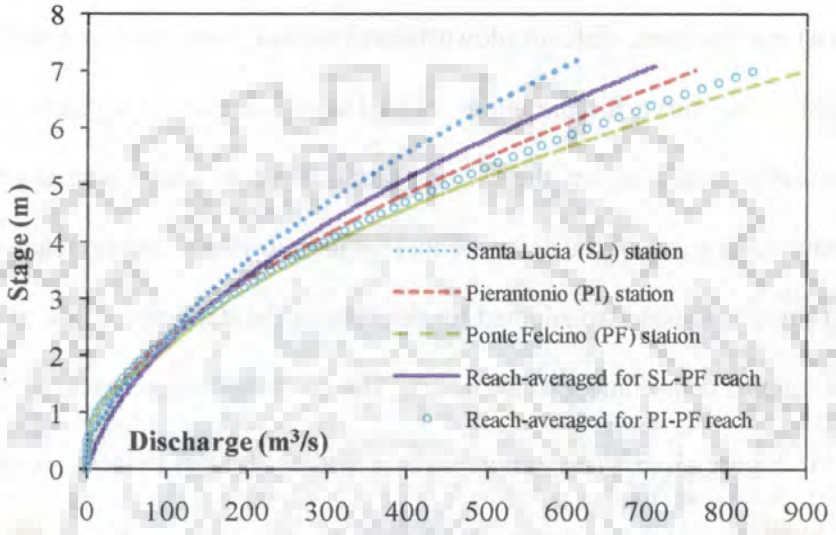

Figure 3.15 Existing rating curves at Santa Lucia, Pierantonio and Ponte Felcino gauging stations and the reach-averaged rating curves for the Santa Lucia-Ponte Felcino, and Pierantonio-Ponte Felcino reaches.

3.7.3.2 Results and discussion

The practical applicability of the VPMMD method is again tested for 50 km long river stretch between Santa Lucia-Ponte Felcino gauging stations. This reach is characterized by a bed slope of $S_o = 0.0014$. This reach experiences significant lateral flows and un-accounting of these lateral flows by the VPMMD method can affect the routed hydrographs at the outlet section of the considered routing reach. On the contrary, the present VPMMD method assumes no lateral flow within the routing reach. Therefore, an

alternative way of evaluating the suitability of the VPMMD method for routing in longer river reaches without lateral flow was considered by routing hypothetical inflow hydrographs in real channel reaches both for the benchmark and VPMMD solutions. Four-different synthetic floods characterized by four-parameter Pearson type-III distribution were generated using equation (3.20) using the parameters given in Table 3.6.

Table 3.6 Parameters of synthetic inflow hydrographs used for generating benchmark solutions at Ponte Felcino of the Santa Lucia-Ponte Felcino reach[#].

Synthetic Floods	Q_b (m^3/s)	Q_p (m^3/s)	t_p (h)	γ
Flood 1	5	200	10	1.5
Flood 2	5	800	12	1.3
Flood 3	5	1100	10	1.2
Flood 4	5	1400	15	1.2

[#]Q_b = base flow; Q_p = peak discharge; t_p = time to peak; γ = shape factor.

Four benchmark solutions were obtained at the outlet of the Santa Lucia-Ponte Felcino reach using the MIKE11 model by routing the considered synthetic floods at the Santa Lucia station. It may be mentioned herein that 200 measured cross-sections (at a space step of 0.25 km) are available within the Santa Lucia-Ponte Felcino reach and the MIKE11 simulations used all these cross-sections information to arrive at the four benchmark solutions. All the four-synthetic flood hydrographs were routed from Santa Lucia to Ponte Felcino by the VPMMD method using a space step of $\Delta x = 1$ km (50 sub-reaches) and a routing time interval of $\Delta t = 1800$ s. The pertinent characteristics of these simulated synthetic flood events are given in Table 3.7.

Table 3.7 Summary of performance criteria showing reproduction of pertinent characteristics of synthetic floods at Ponte Felcino of the Santa Lucia-Ponte Felcino reach using the VPMMD method.

Floods	Discharge Routing				Stage Routing		
	$EVOL$ (%)	η_q (%)	q_{per} (%)	t_{pqer} (h)	η_y (%)	y_{per} (%)	t_{pyer} (h)
Flood 1	-0.81	99.36	-0.01	0.50	95.38	-1.55	1.00
Flood 2	-0.27	99.81	-1.28	0.50	99.28	0.19	0.50
Flood 3	-0.12	99.57	-4.28	0.50	99.27	-0.14	1.00
Flood 4	-0.22	98.81	-3.95	2.50	99.13	2.89	2.50

Table 3.7 reveals that the performance estimates of the simulated discharge hydrograph reproductions η_q, $|q_{per}|$, $|t_{pqer}|$ and $|EVOL|$ by the VPMMD method for routing the four synthetic floods in Santa Lucia-Ponte Felcino reach are: >98.81%, <4.28%, <2.5 h and <0.81%, respectively; whereas the performance estimates of the simulated end-section stage hydrographs, arrived at by using the conversion equation $y_{actual} = 0.741 * y_{equivalent} + 0.462$, in reproducing the actual observed hydrographs at the Ponte Felcino station are: η_y, $|y_{per}|$ and $|t_{pyer}|$ are: >95.38%, <2.89% and <2.5 h, respectively. It is seen from Figures 3.16(a) to 3.16(h) that the VPMMD method performs very well in reproducing the discharge and computed stage hydrographs of the four synthetic floods studied for the Santa Lucia-Ponte Felcino reach.

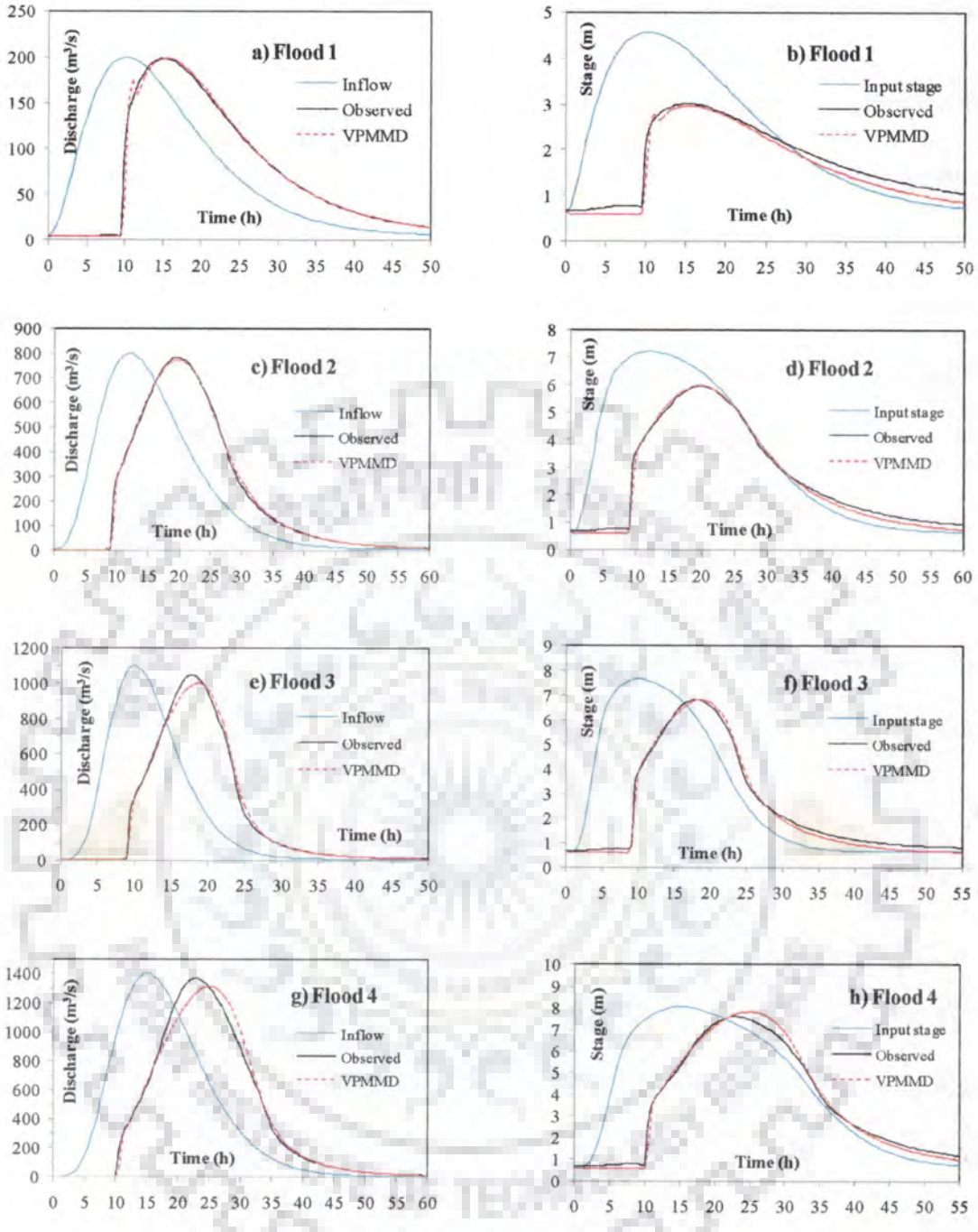

Figure 3.16 Routed discharge and the corresponding estimated stage hydrographs by the VPMMD method at the Ponte Felcino station for the synthetic floods of the Santa Lucia-Ponte Felcino reach.

3.8 SUMMARY AND CONCLUDING REMARKS

An extended VPMMD method suitable for routing flood discharge hydrographs in channels using only the reach-averaged rating curve and cross-section was developed. This method also enables the estimation of stage hydrographs corresponding to the routed discharge hydrographs. This method has been extensively tested for routing floods in synthetic river channels consisting of main and floodplain sections.

The first evaluation for verifying the proposed routing procedure using the VPMMD method was conducted by routing a given synthetic inflow hydrograph in Price's synthetic river channels characterized by uniform compound section comprising of main and floodplain sections [*Price,* 2009] having reach length of 100 km each. The routing results of the VPMMD method simulated for Price's synthetic channels were compared with the benchmark solutions obtained using the full Saint-Venant equations based on the four-point implicit finite difference scheme.

A second evaluation of this method was conducted by routing a given inflow hydrograph in channel reaches of 40 km length, each characterized by a two-stage uniform trapezoidal compound cross-section comprising of main channel section and an extended floodplain section [*Ackers,* 1993]. The benchmark solutions required for each of these 72 channels were obtained using the MIKE11 model. The study reveals that the VPMMD method is able to reproduce almost all the benchmark solutions closely with the variance explained >99% for all the simulations, except that of the channel characterized by S_o=0.0001.

In addition to the verification of the method using hypothetical studies, the field applicability of the method was also demonstrated by routing four synthetic floods in longer (50 km) and ten real flood events in shorter (15 km) length river reaches of the

Upper Tiber River in Central Italy. These routed results reveal that the proposed VPMMD method based on the use of reach-averaged rating curve and cross-section information only along the river reaches is capable of accurately routing the discharge hydrographs, and computing the corresponding stage hydrographs at the required downstream gauging stations. This method is totally volume conservative. It can be inferred from the field application studies that to arrive at good reproduction results of the observed hydrographs, the reach-end rating curves used for establishing the reach-averaged rating curve applicable for routing using the VPMMD method should not vary significantly from each other. Further, the look-up table of the depth *versus* discharge developed from the reach-averaged rating curve should be defined at closer intervals of flow depth. Therefore, based on the approach adopted herein, it may be concluded that the VPMMD method could be used for routing floods in natural river channels with no cross-section information between the well established gauging stations, where only the rating curves and cross-section details are available.

4 APPLICABILITY CRITERIA OF THE VPMMD METHOD

4.1 GENERAL

Over the years, the hydrological literature is proliferated with a number of routing methods for application to flood routing problems. The selection of a suitable method(s) for application to a given flood routing problem is a difficult task for field engineers and hydrologists as they always look for routing methods with minimum data requirement, as always the case with the field problems, and computationally simple and stable methods. The variable parameter simplified hydraulic routing methods directly developed from the Saint-Venant equations are suitable for their application to field flood routing problems as they satisfy these requirements. In view of this fact, it is proposed herein to develop criteria for the application of the variable parameter McCarthy-Muskingum discharge-routing (VPMMD) method studied herein. The applicability criteria of the VPMMD method are developed by routing a number of hypothetical inflow hydrographs in different rectangular and trapezoidal prismatic channel reaches for a specified reach length, and evaluating the performance of the routing results with the corresponding benchmark solutions given by the Saint-Venant equations based on appropriate performance evaluation measures.

4.2 AVAILABLE APPLICABILITY CRITERIA

Many researchers in the past have developed criteria for the selection of a suitable method for the application to a given routing problem with and without considering any downstream boundary conditions [*Henderson*,1966; *Ponce et al.*,1978; *Fread*,1985;

Ferrick,1985; *Price*,1985; *Dooge and Napiorkowski*,1987; *Marsalek et al.*,1996; *Moussa and Bocquillon*,1996; *Singh*,1996; *Tsai*,2003; and *Perumal and Sahoo*,2007]. Among these criteria the one developed by *Ponce et al.* [1978] is widely referred in standard text books [*French*, 1986; *Ponce*, 1989; *Chaudhry*, 1993; *Viessman and Lewis*, 1996; *Singh*, 1996]. In order to develop these criteria for the kinematic wave (KW) and diffusive wave (DW) type of floods, *Ponce et al.* [1978] used the linear stability theory. Many researchers [*Zoppou and O'Neill*, 1982; *Ferrick and Goodman*, 1998; *Cargo and Richards*, 2000; and *Perumal and Sahoo*, 2007] pointed out the deficiencies of the linear stability theory used in the development criteria by *Ponce et al.* [1978]. These researchers argued that the linear stability theory is valid for small perturbations from the reference flow, but the real world flood waves are frequently very large in amplitude. Further, the linear criteria primarily assume a wide rectangular channel and a sinusoidal wave of arbitrary amplitude which is in contradiction with the nonlinear behavior of flood waves propagate in natural rivers.

Considering the above limitations of the criteria *of Ponce et al.* [1978], there is a necessity to propose alternative criteria accounting for the physical significance of the nonlinear characteristics of flood wave propagation in natural rivers. In this context, *Price* [1985] advocated the use of an applicability criteria for the simplified routing methods using the scaled longitudinal gradient of the water surface $(1/S_o)(\partial y/\partial x)$ (where S_o is the channel slope and $\partial y/\partial x$ is the longitudinal gradient of water surface) which is used for the classification of flood waves [*Henderson*, 1966; *NERC*, 1975] as kinematic or diffusive. The inflow hydrograph characterized by a significant magnitude of $(1/S_o)(\partial y/\partial x)$ indicates a diffusive flood wave, while its near absence signifies a kinematic flood wave [*NERC*, 1975]. But the applicability criterion advocated by *Price*

[1985] for the variable parameter Muskingum-Cunge method proposed by Price (1978) as $\left|(1/S_o)(\partial y/\partial x)\right| \le 0.05$ is too restrictive. Adopting the same idea as advocated by *Price* [1985], *Perumal and Sahoo* [2007] also developed applicability criteria both for the variable parameter Muskingum stage-routing (VPMS) and the variable parameter Muskingum discharge-routing (VPMD) methods by carrying out an extensive numerical study on these two methods. They estimated $(1/S_o)(\partial y/\partial x)$ at every routing time level of the given hydrograph at the inlet of the routing reach. Their findings suggest that the applicability of the VPMS method to be assessed at the inlet of the reach for routing a given stage hydrograph in rectangular and trapezoidal channel reaches requires the fulfilment of the criteria $(1/S_o)(\partial y/\partial x)_{\max} \le 0.79$ for routing stage hydrograph only, and $(1/S_o)(\partial y/\partial x)_{\max} \le 0.63$ for both stage hydrograph routing and the corresponding discharge hydrograph estimation. Similarly, the applicability of the VPMD method for routing a given discharge hydrograph in rectangular and trapezoidal channel reaches requires to satisfy the criterion $(1/S_o)(\partial y/\partial x)_{\max} \le 0.43$ at the inlet of the reach both for the discharge hydrograph routing and the corresponding stage hydrograph estimation. *Perumal and Sahoo* [2007] compared the solutions of the VPMS and VPMD methods arrived at the end of the specified routing reaches of the rectangular and trapezoidal prismatic main channels with the corresponding numerical solutions of the Saint-Venant equations considered as the benchmark solutions. Further, in proposing the applicability criteria of the VPMS and VPMD methods, based on the magnitude of $(1/S_o)(\partial y/\partial x)_{\max}$ estimated for the hydrograph to be routed, *Perumal and Sahoo*, [2007] have considered a minimum performance level of 95% or a maximum error level of 5% in reproducing all the pertinent characteristics of the benchmark solutions by the routed solutions of the VPMS and VPMD methods, including that of the mass conservation. It is

pertinent to note herein that the VPMMD method is fully mass conservative as the routing equation has been developed directly using the distributed continuity equation. Accordingly, there is no need to consider mass conservation as one of the pertinent characteristics for the development of applicability criteria of the VPMMD method. However, as the routing equation of the VPMD method has been developed without directly using the distributed continuity equation unlike that of the VPMMD method studied herein, its routed solution is not fully mass conservative and, therefore, the mass conservation error was incorporated as one of the pertinent characteristics for determining the applicability criteria of the VPMS and VPMD methods [*Perumal and Sahoo*, 2007].

4.3 FORMULATION OF APPLICABILITY CRITERIA

Similar to the applicability criteria developed by *Perumal and Sahoo* [2007] for the VPMD and VPMS routing methods, in this study also it is proposed to develop the applicability criteria for the VPMMD method based on the magnitude of $\left|(1/S_o)(\partial y/\partial x)\right|_{\max}$ estimated for the inflow hydrograph to be routed. Even though the classification of flood waves has been well established on the basis of magnitudes of $(1/S_o)(\partial y/\partial x)$ [*Hendeson*, 1966; *Ferrick*, 1985], the same concept has not been exploited effectively for formulating applicability criteria of the simplified methods, except the one prepared by Price [1985]. The same is used herein for the development of applicability criteria of the VPMMD method as described below:

Using the assumption employed in the Kalinin-Milyukov method [*Apollov et al.*, 1964; *Miller and Cunge*, 1975] that at any instant of time during the passage of a flood wave in river reach, the discharge passing at section 3 located (denoted as Q_3) just downstream of the midsection of the computational reach (See Figure 3.1) is uniquely related to the stage

or flow depth y_M existing at the midsection of the reach, the relationship between Q_3 and the discharge at the midsection of the reach can be expressed as

$$Q_M = Q_3 \left\{ 1 - \frac{1}{S_o} \frac{\partial y}{\partial x} \left[1 - \frac{4}{9} F^2 \left(\frac{P\, dR/dy}{dA/dy} \right)^2 \right] \right\}_M^{\frac{1}{2}} \tag{4.1}$$

where, Q_M is the discharge passing at the midsection of the reach denoted by the subscript M, A is the water flow area, P is the wetted perimeter, R is the hydraulic radius, x is the distance along the channel and F is the Froude number of flow passing at the midsection of the routing reach.

Rearranging equation (4.1), we get

$$Q_3 = Q_M \left\{ 1 - \frac{1}{S_o} \frac{\partial y}{\partial x} \left[1 - \frac{4}{9} F^2 \left(\frac{P\, dR/dy}{dA/dy} \right)^2 \right] \right\}_M^{\frac{-1}{2}} \tag{4.2}$$

Under the assumption that when the magnitude of $(1/S_o)(\partial y/\partial x) \ll 1$, equation (4.2) may be expanded using the binomial series and after assuming the magnitude of the second and higher order terms to be negligible, we get

$$Q_3 = \left\{ Q_M + \frac{Q_M}{2.S_o} \frac{\partial y}{\partial x} \left[1 - \frac{4}{9} F^2 \left(\frac{P\, dR/dy}{dA/dy} \right)^2 \right] \right\}_M \tag{4.3}$$

Perumal and Ranga Raju [1998a] has stated that the inertial terms approximated in terms of $\left[F(PdR/dy)/(dA/dy) \right]$ in equation (4.3) can be ignored, as it has a minor contribution towards the computational accuracy of discharge. Hence equation (4.3) can be modified as

$$Q_3 = Q_M + \frac{Q_M}{2.S_o}\frac{\partial y}{\partial x}\bigg|_M \tag{4.4}$$

Rearranging equation (4.4), we get

$$Q_M = Q_3 - \frac{Q_M}{2.S_o}\frac{\partial y}{\partial x}\bigg|_M \tag{4.5}$$

It can be inferred from equation (4.5) that during unsteady flow the discharge $Q_M = f\{y_M, \partial y/\partial x|_M\}$ passing at the midsection and the normal discharge $Q_3 = f\{y_M\}$ passing at some location downstream of the midsection of the computational reach, where $f\{\bullet\}$ denotes a function, are related to each other by $(1/S_o)(\partial y/\partial x)$. The significant magnitude of the water surface gradient $(1/S_o)(\partial y/\partial x)$ in equation (4.5) implies the flood wave to be diffusive resulting in attenuation of the flood wave, and its insignificance implies a kinematic wave (KW) characterized by insignificant attenuation of flood peak [*Henderson,* 1966; *NERC,* 1975]. Further, based on equation (4.5) that when the magnitude of the water surface gradient $\left|(1/S_o)(\partial y/\partial x)\right|_{\max} \ll 1$, the flood wave can be classified as Approximate Convection-Diffusion (ACD) wave [*Perumal and Ranga Raju,* 1999]. Based on the truncation error analysis of the binomial series expansion, *Perumal and Sahoo* [2007] opined that the applicability criteria of the VPMD and VPMS methods are restricted by the positive values of $(1/S_o)(\partial y/\partial x)$. In accordance with this consideration the criteria developed for the VPMMD method are also restricted by the magnitudes of positive value of $(1/S_o)(\partial y/\partial x)_{\max}$ subjected to the requirement of $\left|(1/S_o)(\partial y/\partial x)\right| \le 1$.

4.3.1 Strategy for Determining $(1/S_o)(\partial y/\partial x)$

Assuming that the inertial terms are insignificant, the unsteady flow discharge at any location of the channel reach can be expressed as [*Henderson,* 1966].

$$Q = Q_o\left[1-\frac{1}{S_o}\frac{\partial y}{\partial x}\right]^{\frac{1}{2}} \tag{4.6}$$

where, Q_o is normal flow corresponding to flow depth y.

Rearranging equation (4.6), the longitudinal water surface gradient can be expressed as

$$\frac{1}{S_o}\frac{\partial y}{\partial x} = 1-\left(\frac{Q}{Q_o}\right)^2 \tag{4.7}$$

Since the successful application of the VPMMD method depends on the magnitude of the longitudinal water surface gradient $(1/S_o)(\partial y/\partial x)$, the same is estimated at the inlet section at every routing time level of the inflow hydrograph to be routed. As the attenuation of the flood wave over the routing reach causes reduction in the magnitude of $(1/S_o)(\partial y/\partial x)$ at any location downstream of the inlet section compared with the corresponding estimates at the inlet section, the applicability criteria for VPMMD method needs to be established at the inlet of the routing reach only. As the magnitude of longitudinal water surface gradient $(1/S_o)(\partial y/\partial x)$ depends on the characteristics of inflow stage (or discharge) hydrograph and that of the routing channel reach, one can express

$$(1/S_o)(\partial y/\partial x) = f\left\{S_o, n, y_b(orQ_b), y_p(orQ_p), t_p, \gamma, z\right\} \tag{4.8}$$

where, S_o = bed slope; n = Manning's roughness coefficient; y_b = initial stage; Q_b = initial steady discharge; y_p = peak stage; Q_p = peak discharge of the inflow hydrograph; t_p =time-to-peak; γ = shape factor of hydrograph, z = side slope of the channel, and $f\{\bullet\}$ denotes a function.

Predefined form of input stage hydrographs were used for routing in a number of hypothetical channels using the Saint-Venant equations to arrive at the benchmark solutions at the end of the specified reach length of the hypothetical channels considered in this study. The discharge hydrograph estimated at the inlet of each of the channel reach was used as the inflow hydrograph for the hypothetical routing studies of the VPMMD method.

The equation of the input stage hydrograph used for arriving at the benchmark routing solutions in uniform rectangular and trapezoidal channels, and for estimating the inflow hydrograph required for the VPMMD routing application, can be expressed as:

$$y(0,t) = y_b + \left[y_p - y_b\right]\left[\frac{t}{t_p}\right]^{\gamma/(\gamma-1)} \exp\left[\frac{1-t/t_p}{\gamma-1}\right] \tag{4.9}$$

where, $y(0,t)$ is stage at the upstream end $(x=0)$ at any instant of time t, y_b = is initial stage, y_p = peak stage, t_p =time-to-peak, and γ = shape factor.

4.4 NUMERICAL EXPERIMENTS

The strategy proposed above for developing the applicability criteria of the VPMMD method for successfully routing discharge hydrographs in prismatic rectangular and trapezoidal channel reaches and for the estimation of stage hydrographs corresponding to the routed discharge hydrographs was implemented by conducting a number of

hypothetical routings using different input stage hydrographs of the form given by equation (4.9). The values of different parameters of input stage hydrographs used in this study, which also influence the range of values of the applicability criterion variable $(1/S_o)(\partial y/\partial x)$ as per equation (4.8), are given in Table 4.1.

Table 4.1 Different combinations of input stage hydrograph parameters used for numerical experiments.

Parameters	Values
Gamma γ	1.05, 1.15, 1.25, 1.50
Bed slope S_o	0.002, 0.001, 0.0008, 0.0005, 0.0004, 0.0002, 0.0001
Manning's roughness n	0.01, 0.02, 0.03, 0.04, 0.05
Initial discharge Q_b	100 m^3/s
Peak stage y_p	5.0 m, 8.0 m, 10.0 m, 12.0 m, 15.0 m
Time to peak t_p	5.0 h, 10.0 h, 15.0 h, 20.0 h
Bottom width b	100 m
Side slope z	0, 1.0, 3.0, 5.0

Different input stage hydrographs formulated by different combinations of the parameters given in Table 4.1 were routed in a number of hypothetical rectangular and trapezoidal prismatic channels for a reach length of 40 km in each of the channels. No lateral flow was considered for all the hypothetical routings. The discharge hydrograph estimated at the inlet of each of channel reaches by the benchmark solution of the Saint-Venant equations formed the inflow hydrograph required for the routing study of the VPMMD method. The solutions of the Saint-Venant equations were obtained using the explicit numerical scheme. The input discharge hydrographs estimated at the inlet section of the reach corresponding to different input stage hydrographs were characterized by different peak discharges. The applicability criteria for successfully arriving at the routed discharge hydrograph using the VPMMD method and the corresponding computed stage hydrograph were estimated by comparing the solutions of the VPMMD method with the

corresponding benchmark solutions. The comparison was made based on reproducing some pertinent characteristics of the benchmark solutions such as the overall reproduction of the benchmark solution assessed by the Nash-Sutcliffe (N-S) efficiency in percent, and peak and time-to-peak of discharge and stage hydrographs. Note that the error in volume is not considered as one of the pertinent characteristics as the VPMMD method is fully mass conservative as described in Section 4.2. In this study it was considered that a successful VPMMD method routing solution should reproduce all the pertinent characteristics of the benchmark solutions within the specified error limit of 5% and with the N-S efficiency of at least 95%. All the estimated evaluation measures were compared with the magnitudes of the criterion variable $(1/S_o)(\partial y/\partial x)_{\max}$. An initial discharge of Q_b=100 m^3/s was considered for all the hypothetical routings, and the corresponding y_b was computed using the Newton-Raphson method. A total of 11,200 routing simulations of benchmark solutions were made in the considered rectangular and trapezoidal channel reaches by routing input stage hydrographs defined by different combinations of parameters as given in Table 4.1 using the Saint-Venant equations. All the inflow discharge hydrographs estimated from these benchmark solutions were routed in the respective channels by the VPMMD method to arrive at the routed solutions for their comparison with the benchmark solutions. Out of these 11,200 routing simulations made following the above described approach, a total of 2,800 runs pertain to simulations in different configurations of rectangular channel reaches and the remaining 8,400 simulations pertain to different combinations of trapezoidal channel reaches. More number of simulations made in trapezoidal channels could be attributed to the use of 3 different side slopes of the trapezoidal section channel reaches. A space step of Δx = 1 km and the routing time interval of Δt = 300 s were used for all the benchmark simulations conducted in this study.

4.5 PERFORMANCE EVALUATION

The evaluations of the VPMMD method solutions in reproducing all the pertinent characteristics of the benchmark solutions were made based on the evaluation measures as described in Section 3.4.

4.6 RESULTS AND DISCUSSION

To establish the applicability criteria of the VPMMD method, the performance of all hypothetical discharge and stage hydrograph solutions arrived at using this method at the end of 40 km reach length of each of the considered rectangular and trapezoidal hypothetical channels were evaluated based on the criteria specified in reproducing the pertinent characteristics of the corresponding benchmark solutions. For each of the successful benchmark solutions, the magnitude of $(1/S_o)(\partial y/\partial x)_{\max}$ of the inflow hydrograph estimated using equation (4.7) was noted for establishing its relationship with the corresponding simulation performance evaluation measures of the pertinent characteristics such as $\eta_q, \eta_y, q_{per}, y_{per}, t_{qper}$ and t_{yper}.

4.6.1 Reproduction of Pertinent Characteristics of Benchmark Solutions

Table 4.2 presents the percentage of the VPMMD solutions which fall within the selected error level up to a maximum of 5% error, in reproducing the pertinent characteristics of the benchmark solutions and the same is illustrated in the form of chart shown in Figure 4.1. The percentage of the VPMMD solutions which satisfy the specified pertinent characteristics criterion is calculated against the total number of 10,523 successful benchmark solutions out of 11,200 input stage hydrographs routing simulations attempted. The total failure of 677 simulations of benchmark solutions (6.05% failure runs) can be attributed to the instability problems developed in the execution of the

explicit numerical scheme solutions of the Saint-Venant equations. Among the 10523 successful benchmark Saint-Venant solutions, some of them corresponding to the range of $0.1 < (1/S_o)(\partial y/\partial x)_{\max} < 0.2$ were characterized by many oscillations due to numerical stability problems, though the solutions did not fail from the computational perspective, but can be considered as failure from the perspective of using them as a benchmark solution for evaluating the corresponding VPMMD method solution. The plotted points of such stability affected oscillatory solutions can be clearly seen in Figures 4.2 to 4.7, appearing as outliers from the trend of rest of the plotted points and these points have been encircled in these figures. However, such deviations are very few in comparison with the total successful runs of 10523, may be about 40 simulation runs, and, therefore, they have been ignored from the inference of the analysis of results. It can be inferred from Table 4.2 that at 1% error level, 10.17% of VPMMD solutions performed with the N-S efficiency (η_q in %) less than 99%, while at 5% error level only 1.74% of VPMMD solutions performed with $\eta_q \leq 95\%$. This inference implies that almost all the 10523 VPMMD method simulations, except 183 simulations, perform with an overall reproduction efficiency of $\eta_q \geq 95\%$. Similarly, it can be seen from Table 4.2 that at 1% error level only nearly 7% of the estimated stage hydrographs performed with the N-S efficiency η_y (in %) less than 99% in reproducing the corresponding benchmark solutions, while at 5% error level only 0.18% of the estimated stage hydrographs performed with $\eta_y \leq 95\%$. Again this inference implies that almost all the stage hydrograph simulations reproduce the benchmark solutions with the efficiency of $\eta_y \geq 95\%$. Figures 4.2 and 4.3 lend support to the discussion presented regarding the efficiencies of reproduction of the discharge and stage hydrographs by the VPMMD method based on the inference of the results given in Table 4.2. It is clearly seen from

these figures that a dense clustering of the plotted points can be observed up to $(1/S_o)(\partial y/\partial x)_{\max} = 0.4$, and beyond which sparse clustering of these points can be seen up to $(1/S_o)(\partial y/\partial x)_{\max} = 0.6$. However, these points are plotted very sparsely beyond $(1/S_o)(\partial y/\partial x)_{\max} = 0.6$ and also deviating away from 100% efficiency level both for the discharge and stage hydrographs reproductions. It can be inferred from the relative comparison of the efficiencies of both the discharge and stage hydrographs as presented in Table 4.2, and as shown in Figures 4.2 and 4.3, that even though the stage hydrographs were estimated from the corresponding routed discharge hydrograph solutions of the VPMMD method, the efficiency of reproducing the benchmark solution of the stage hydrograph is higher than that of the corresponding discharge hydrograph. One may attribute the reasoning for this behavior to the better adherence of the linear variation assumption of the water surface profile at any instant of time over the routing reach (i.e., $\partial y/\partial x \rightarrow$ constant) than the assumption of linear variation of discharge over the routing reach (i.e., $\partial Q/\partial x \rightarrow$ constant) considered for the development of the VPMMD method. Figure 4.4 shows the variation of error in peak discharge q_{per} (in %) arrived at using equation (3.12) in estimating the difference between the peaks of the routed discharge hydrographs of the VPMMD method and that of the corresponding benchmark solutions with reference to the $(1/S_o)(\partial y/\partial x)_{\max}$ estimate of the inflow hydrograph. Similarly Figure 4.5 shows the variation of error in peak of the estimated stage hydrograph, y_{per} (in %) of the corresponding routed discharge hydrograph, arrived at using equation (3.13) with reference to the $(1/S_o)(\partial y/\partial x)_{\max}$ estimate of the inflow hydrograph. The same inference that has been arrived for the plotted points of Figures 4.2 and 4.3 about the distribution of cluster points, i.e., dense cluster of points up to $(1/S_o)(\partial y/\partial x)_{\max} = 0.4$,

sparse clustering between $(1/S_o)(\partial y/\partial x)_{\max} = 0.4$ to 0.6, and very sparse clustering beyond $(1/S_o)(\partial y/\partial x)_{\max} = 0.6$, can be arrived for the Figures 4.4 and 4.5. Figure 4.5 clearly shows that y_{per} (in %) is nearly zero up to $(1/S_o)(\partial y/\partial x)_{\max} = 0.4$, while q_{per} (in %) is nearly zero up to $(1/S_o)(\partial y/\partial x)_{\max} = 0.3$ as shown in Figure 4.4. This once again highlights the already arrived inference that the stage hydrograph reproduction is closer to the benchmark solution than the corresponding discharge hydrograph arrived at using the VPMMD method. This inference is verified from the results given in Table 4.2 that 11.26% successful simulation runs of the VPMMD method results estimate error level beyond 5% in comparison with the corresponding stage hydrograph simulations which estimate on error level of only 2.69 %. Further, it can be inferred from these figures that in most of the routing solutions obtained using the VPMMD method, the tendency to underestimate the peak discharge prevails, while the corresponding stage hydrographs solutions display a mixed tendency of overestimation as well as underestimation of the peak stages in comparison with the corresponding benchmark solutions. Figures 4.6 and 4.7 display the variation between the time-to-peaks of the simulated discharge hydrographs and the corresponding estimated stage hydrographs of the VPMMD method, respectively, with reference to $(1/S_o)(\partial y/\partial x)_{\max}$ of the inflow hydrograph. Similar qualitative inference as arrived at for the other performance evaluation measures as depicted in Figures 4.2 to 4.5 can be reached about the clustering of the plotted points of these figures also. It can be seen that both Figures 4.6 and 4.7 display that the peak estimates of the discharge and stage hydrographs of the VPMMD method arrive later than the corresponding benchmark solution estimates. Accordingly, almost all the error estimates of time-to-peak errors of discharge and stage hydrographs are positive as seen from Figures 4.6 and 4.7, respectively, with time-to-peak error estimates of the stage

hydrograph displaying a tendency of higher errors than that of the corresponding discharge hydrograph peak error estimates.

Figure 4.8 shows the comparison between the attenuations of peak discharge Q_p of the VPMMD method solutions with that of the corresponding solutions of the Saint-Venant equations at the end of 40 km routing reach of the channels of all the routing simulations. A similar comparison for peak stage attenuations of all the simulations is shown in Figure 4.9. It can be inferred from Figure 4.8 that the VPMMD method has a tendency to underestimate the peak discharge of the benchmark solutions, i.e., showing over attenuation of peak discharge in comparison with that of the benchmark solutions, though this tendency may be considered small for the attenuation of the benchmark solutions in the range of 0 to 30% when $0 < (1/S_o)(\partial y/\partial x)_{\max} < 0.4$ as seen from Figure 4.10. This figure also shows the relationship between $(1/S_o)(\partial y/\partial x)_{\max}$ and the attenuation of the routed discharge hydrographs of the 10523 simulations of benchmark as well as VPMMD routing method arrived at the end of 40 km reach length of all the channels as discussed earlier. These pairs of discharge attenuation values of the VPMMD method and the benchmark solution against the corresponding simulation maximum surface gradient $(1/S_o)(\partial y/\partial x)_{\max}$ estimates show a wide spread but with a systematic variation of increasing attenuation with increasing $(1/S_o)(\partial y/\partial x)_{\max}$ estimate. It can be seen that while the attenuation estimates of the routing solutions of the VPMMD method and that of the corresponding Saint-Venant solutions are closer to each other in the upper range of attenuation, relatively these estimates are not close in the lower range of the attenuation curve with underestimation of attenuation when $0 < (1/S_o)(\partial y/\partial x)_{\max} \le 0.2$ and over-estimation when $0.2 \le (1/S_o)(\partial y/\partial x)_{\max} < 0.6$. Figure 4.9 reveals a mixed tendency of

overestimation and underestimation of the attenuation of the simulated peak stages of the VPMMD method in comparison with the corresponding benchmark solutions up to an attenuation of 20%. Similar to the trend of relationship shown in Figure 4.10, Figure 4.11 displays the relationship between the pairs of stage hydrograph attenuation values of the solution of the VPMMD method and the Saint-Venant equations with reference to the corresponding pairs $(1/S_o)(\partial y/\partial x)_{\max}$ estimates of the inflow hydrographs of all the 10523 successful simulation runs. It is seen from this figure that the attenuation of routed stage hydrograph is small relatively in comparison with the attenuation of routed discharge hydrograph. It is inferred from this figure that the pairs of both attenuation estimates seem to plot closely up to 20% attenuation in the range of $0 < (1/S_o)(\partial y/\partial x)_{\max} < 0.4$, beyond which these pair of values plot sparsely up to an attenuation of 25% between the ranges of $0.4 \le (1/S_o)(\partial y/\partial x)_{\max} \le 0.6$. Figure 4.11 also displays a minimum attenuation enveloping curve ranging from nearly zero to 5% corresponding to the range of $0.2 \le (1/S_o)(\partial y/\partial x)_{\max} \le 0.6$. Beyond $(1/S_o)(\partial y/\partial x)_{\max} = 0.6$, a sparse distribution of pair of attenuation estimates could be seen with the attenuation of VPMMD solution overestimates the corresponding estimate of the solution of the Saint-Venant equations. A comparison of Figures 4.10 and 4.11 shows that within the upper and lower enveloping curves of the pairs of attenuation points, the pair of stage attenuation points seem to plot closely in comparison with the corresponding pair of discharge attenuation points.

Table 4.2 Percentage of the successful VPMMD solutions in reproducing the pertinent characteristics of the benchmark solutions at the selected error levels.

Parameter	Total no. of successful runs	Error Level											
		>0.5%		>1%		>2%		>3%		>4%		>5%	
		No. of runs	%	No. of runs	%	No. of runs	%	No. of runs	%	No. of runs	%	No. of runs	%
η_q	10523	1559	14.82	1070	10.17	641	6.09	417	3.96	289	2.75	183	1.74
|Qper|	10523	3017	28.67	2473	23.50	1945	18.48	1599	15.20	1374	13.06	1185	11.26
|Tpqer|	10523	4072	38.7	3149	29.92	1950	18.53	1333	12.67	928	8.82	671	6.38
η_y	10523	1270	12.07	733	6.97	303	2.88	138	1.31	51	0.48	19	0.18
|Yper|	10523	2834	26.93	1406	13.36	776	7.37	548	5.21	376	3.57	283	2.69
|Tpyer|	10523	3941	37.45	3193	30.34	2193	20.84	1676	15.93	1335	12.69	1029	9.78

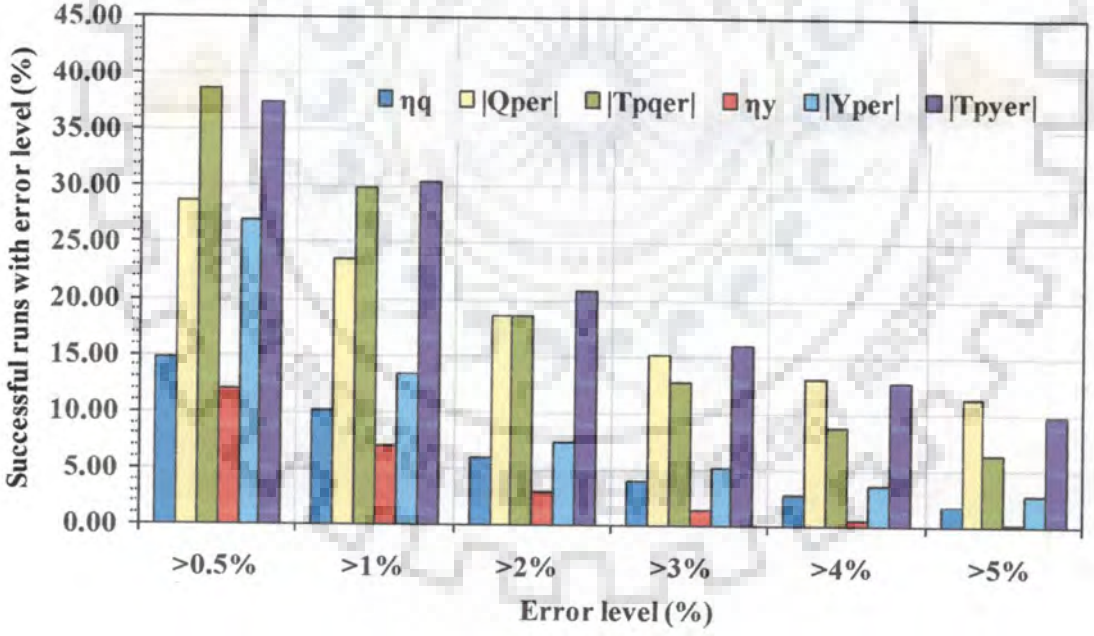

Figure 4.1 Percentage of successful VPMMD solutions in reproducing the pertinent characteristics of the benchmark solutions at the selected error levels.

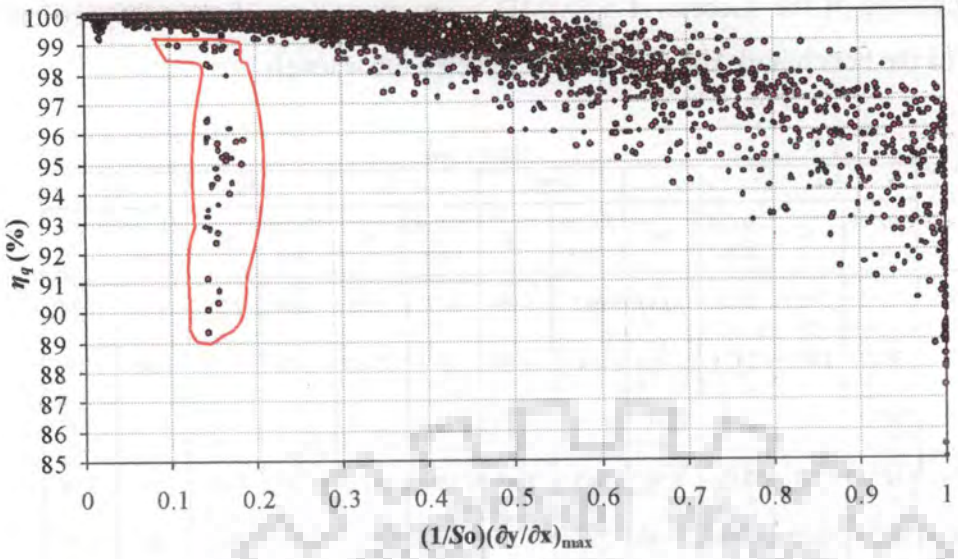

Figure 4.2 Variation of N-S efficiency (η_q in %) of the routed discharge hydrograph of the VPMMD method in reproducing the benchmark solutions of rectangular and trapezoidal channel reaches (shape factor γ=1.05, 1.15, 1.25 and 1.50; side slope z = 0, 1, 3 and 5).

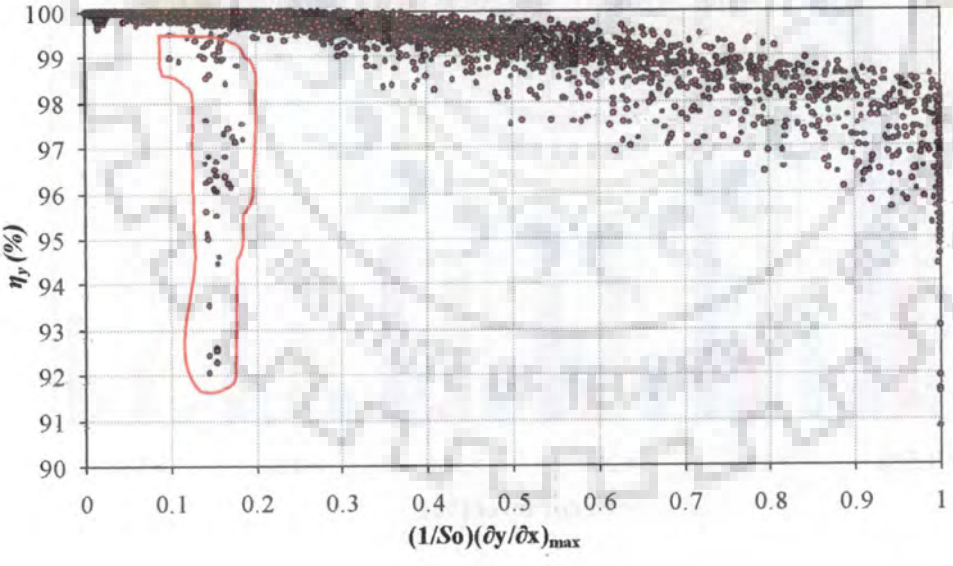

Figure 4.3 Variation of N-S efficiency (η_y in %) of the stage hydrograph estimated by the VPMMD method in reproducing the benchmark solutions of rectangular and trapezoidal channel reaches (shape factor γ=1.05, 1.15, 1.25 and 1.50; side slope z = 0, 1, 3 and 5).

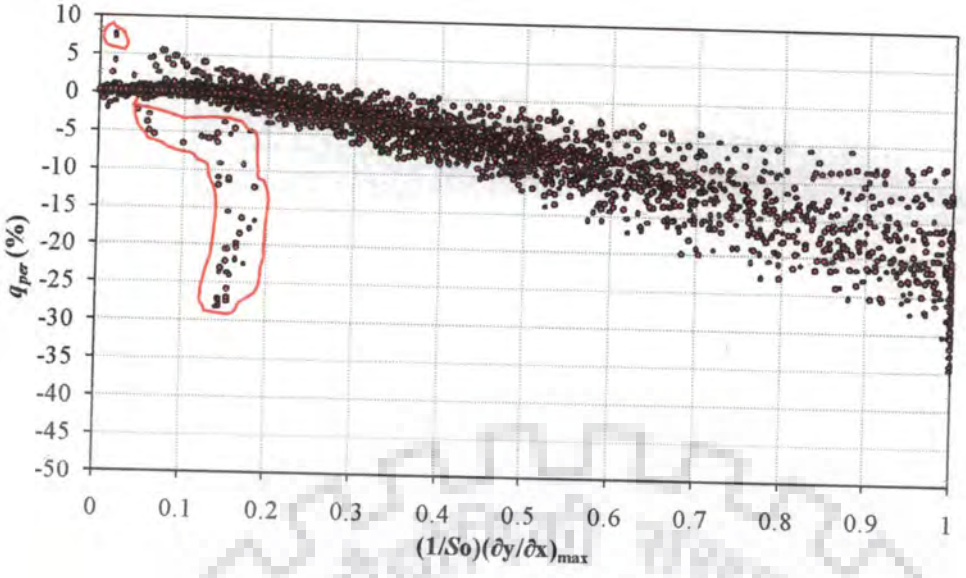

Figure 4.4 Variation of error of peak of the routed discharge hydrograph (q_{per} in %) of the VPMMD method.

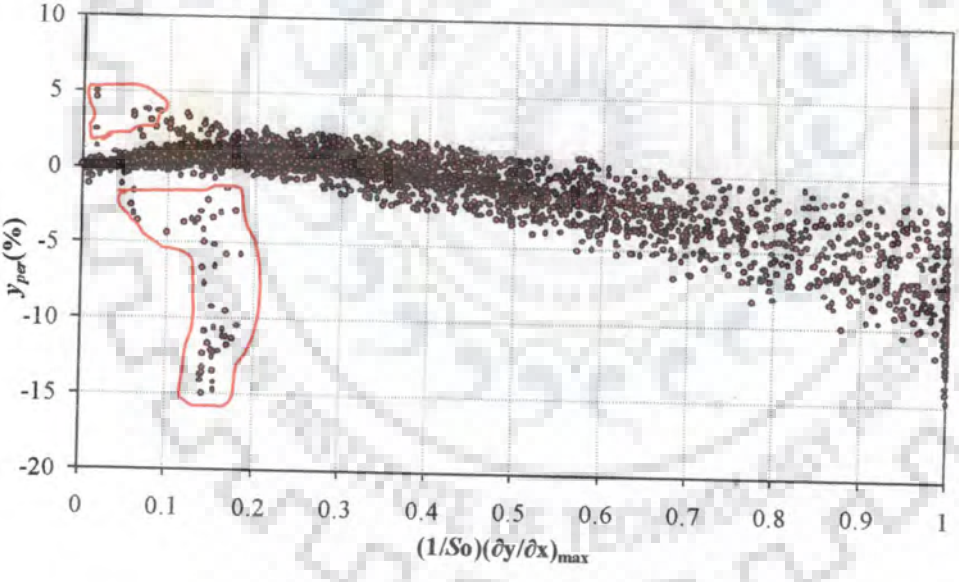

Figure 4.5 Variation of error of peak of the stage hydrograph (y_{per} in %) estimated by the VPMMD method.

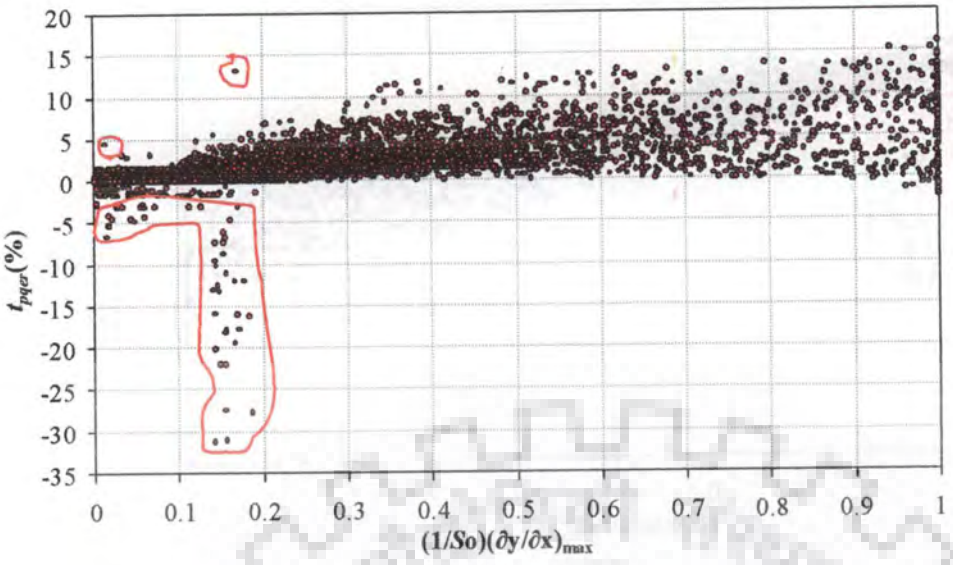

Figure 4.6 Variation of error in time-to-peak discharge of routed discharge hydrograph (t_{qper} in %) of the VPMMD method.

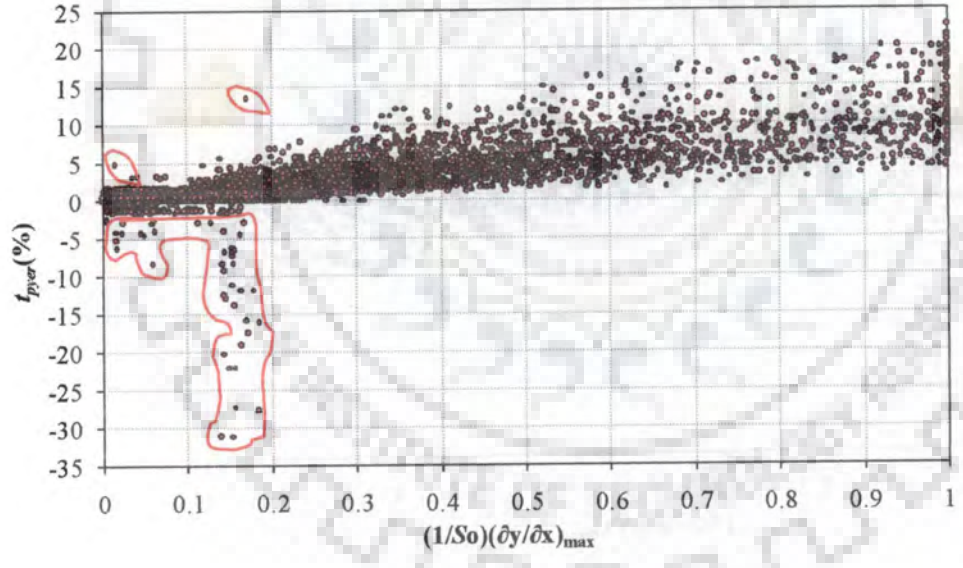

Figure 4.7 Variation of error in time-to-peak stage hydrograph (t_{yper} in %) estimated by the VPMMD method.

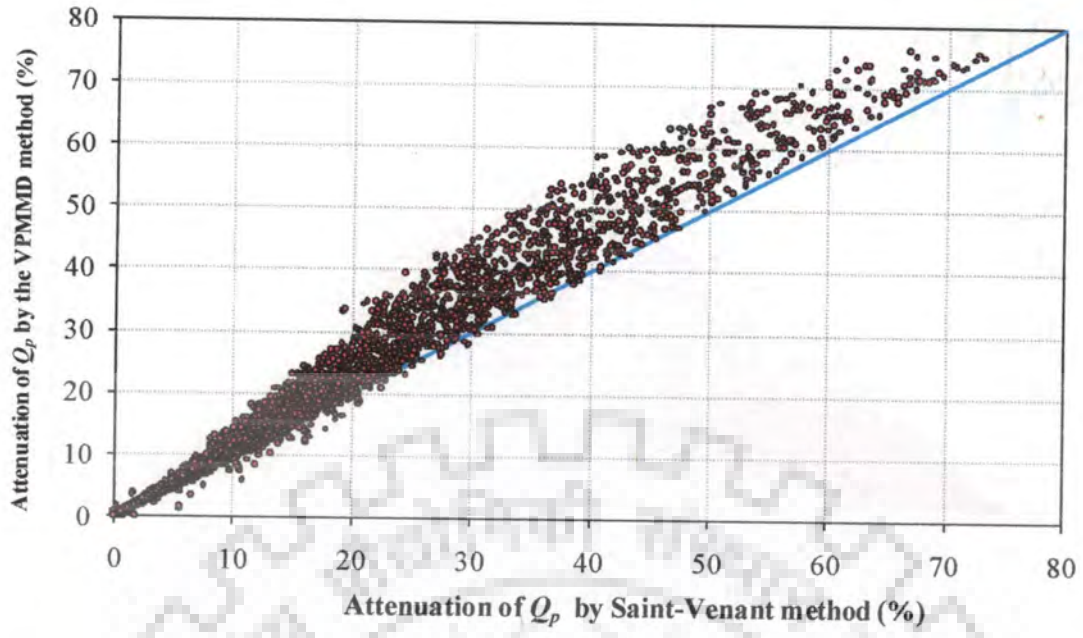

Figure 4.8 Comparison of peak discharge Q_p attenuation of the VPMMD method solution with that of the Saint-Venant solutions.

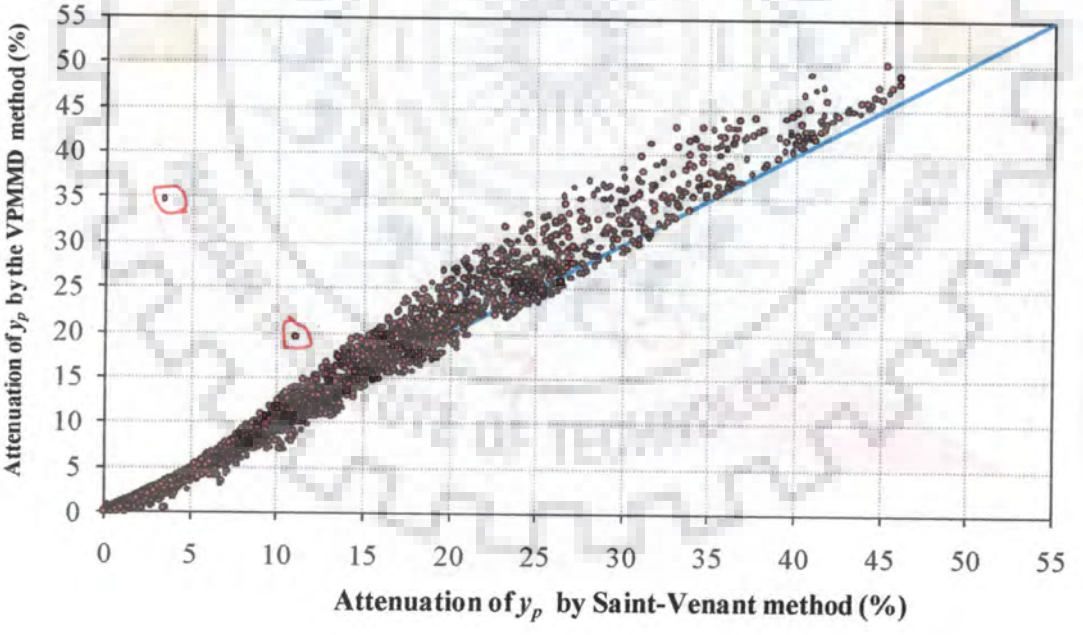

Figure 4.9 Comparison of peak stage y_p attenuation by the VPMMD method solution with that of the Saint-Venant solutions.

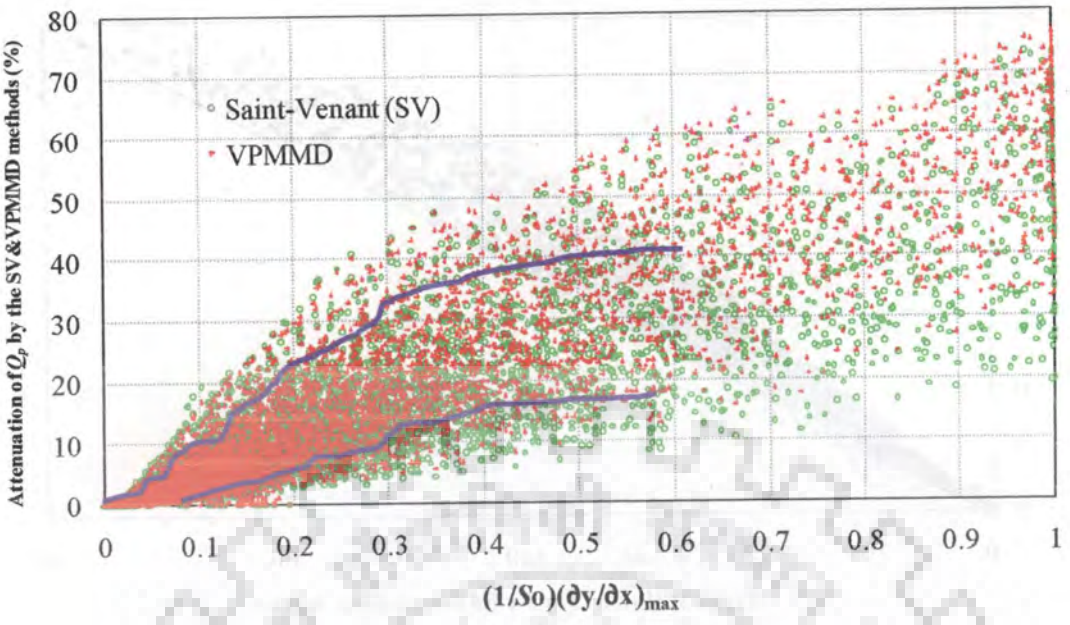

Figure 4.10 Variation of the routed discharge hydrograph attenuation values of all the 10523 solutions of the VPMMD method and the Saint-Venant equations.

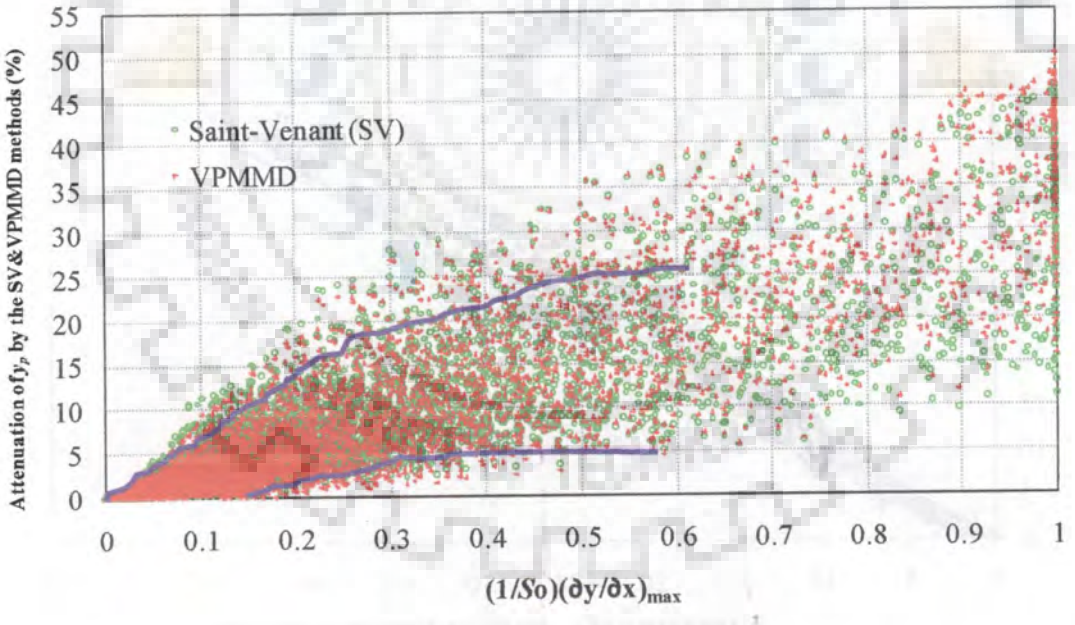

Figure 4.11 Variation of the stage hydrograph attenuation values of all the 10523 solutions of the VPMMD method and the Saint-Venant equations.

Some of the typical routed discharge and their corresponding estimated stage hydrograph reproductions of the Saint-Venant solutions by the VPMMD method in rectangular and trapezoidal channel reaches are illustrated in Figures 4.12 to 4.15 in order to support the inferences arrived from the analysis of the results given in Table 4.2 and Figures 4.2 to 4.11.

Figure 4.12 demonstrates the discharge and stage hydrographs reproductions of the benchmark solutions by the routing solution of the VPMMD method for a typical case of routing the discharge hydrograph in a trapezoidal channel reach characterized by z = 1, S_o= 0.0004 and n= 0.05 and for routing the discharge hydrograph of the input stage hydrographs characterized by the parameters Q_b= 100 m^3/s (y_b= 1.736 m), y_p= 5 m (Q_p= 632.25 m^3/s), t_p= 5 h and γ = 1.15. It can be seen from this figure that even when the inflow at upstream section is almost ceased entering into the reach, the VPMMD method could reproduce the discharge and computed stage hydrographs very well, and the reproductions of the pertinent characteristics are also well within the specified error limits of 5% except for the aspect of time-to-peak estimation. The performance evaluation estimates of the simulation case shown Figure 4.12 are: η_q = 98.81%, η_y = 99.19%, $|q_{per}|$ = 3.65%, $|t_{pqer}|$ = 6.38%($\geq$ 5%), $|y_{per}|$ = 0.54%, and $|t_{pyer}|$ = 6.08%($\geq$ 5%). Further, the inflow hydrograph of this hydrograph was characterized by the estimate of $(1/S_o)(\partial y/\partial x)_{\max}$ = 0.3653 and the benchmark solutions of discharge and stage hydrographs were characterized by the attenuation of Q_p = 45.09%, and the attenuation of stage y_p = 26.75%, respectively.

Figure 4.13 demonstrates the discharge and stage hydrographs reproductions of the benchmark solutions by the VPMMD method for another case of routing a discharge hydrograph in a trapezoidal channel reach characterized by z = 5, S_o= 0.001 and n= 0.05,

and for routing the discharge hydrograph of the input stage hydrograph characterized by the parameters Q_b= 100 m^3/s (y_b= 1.299 m), y_p= 15 m (Q_p= 8208.74 m^3/s), t_p= 5 h and γ = 1.15. The following are the estimates of the evaluation measures of reproduction of the pertinent characteristics of the benchmark solutions: η_q = 99.50%, η_y = 99.64%, $|q_{per}|$ = 1.89%, $|t_{pqer}|$ = 2.17%, $|y_{per}|$ = 0.35%, and $|t_{pyer}|$ = 2.11% . Further, the inflow hydrograph was characterized by the estimate of $(1/S_o)(\partial y/\partial x)_{\max} = 0.3108$, and the benchmark solutions of the discharge and stage hydrographs were characterized by the attenuation of Q_p = 25.15%, and the attenuation of stage y_p = 12.30%, respectively.

Figure 4.14 reveals the discharge and stage hydrographs reproductions of the benchmark solutions by the solution of the VPMMD method for a typical case of routing the discharge hydrograph in a trapezoidal channel reach characterized by z = 5, S_o= 0.0002 and n= 0.03 and for routing the discharge hydrograph of the input stage hydrographs characterized by the parameters Q_b= 100 m^3/s (y_b= 1.545 m), y_p= 15 m (Q_p= 6361.59 m^3/s), t_p= 20 h and γ = 1.15. The evaluation estimates of the reproductions of pertinent characteristics are well within the specified error limits of 5%, and these estimates are: η_q = 99.67%, η_y = 99.62%, $|q_{per}|$ = 4.63%, $|t_{pqer}|$ = 1.14%, $|y_{per}|$ = 0.21%, and $|t_{pyer}|$ = 2.87%. Further, the inflow hydrograph was characterized by an estimate of $(1/S_o)(\partial y/\partial x)_{\max} = 0.5172$, and the benchmark solutions of the discharge and stage hydrographs were characterized by the attenuation of Q_p = 15.21%, and the attenuation of stage y_p = 5.87%, respectively.

Figure 4.15 show the discharge and stage hydrographs reproductions of the benchmark solutions by the solution of the VPMMD method for yet another case of routing a discharge hydrograph in a trapezoidal channel reach characterized by z = 1, S_o= 0.0002

and n= 0.01 and for routing the discharge hydrograph of the input stage hydrographs characterized by the parameters Q_b= 100 m^3/s (y_b= 0.813 m), y_p= 15 m (Q_p= 13170.44 m^3/s), t_p= 15 h and γ = 1.15. The evaluation estimates of the reproduction of pertinent characteristics of this case are well within the 5% error level and they are: η_q = 100%, η_y = 99.98%, $|q_{per}|$ = 0.35%, $|t_{pqer}|$ = 0.54%, $|y_{per}|$ = 1.12%, and $|t_{pyer}|$ = 0.54% . Further, the inflow hydrograph was characterized by an estimate of $(1/S_o)(\partial y/\partial x)_{\max} = 0.1849$, and the benchmark solutions of the discharge and stage hydrographs were characterized by the attenuation of Q_p = 2.43%, and the attenuation of stage y_p = 0.40%, respectively.

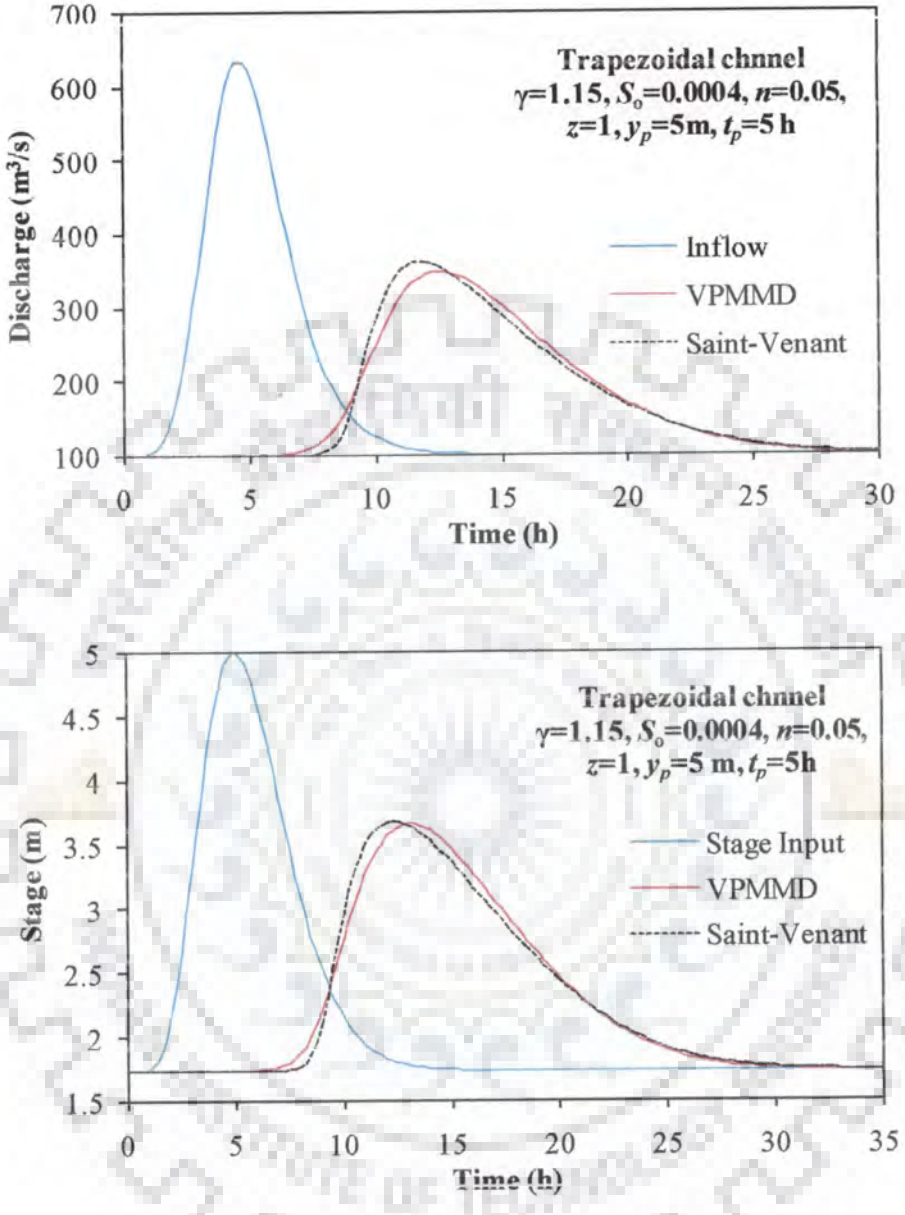

Figure 4.12 A typical discharge and stage hydrographs reproductions of the Saint-Venant solutions by the VPMMD method for S_o= 0.0004, n= 0.05, Q_b= 100 m^3/s (y_b= 1.736 m), y_p= 5 m (Q_p= 632.25 m^3/s), t_p= 5 h and γ = 1.15 in a trapezoidal channel reaches (z = 1).

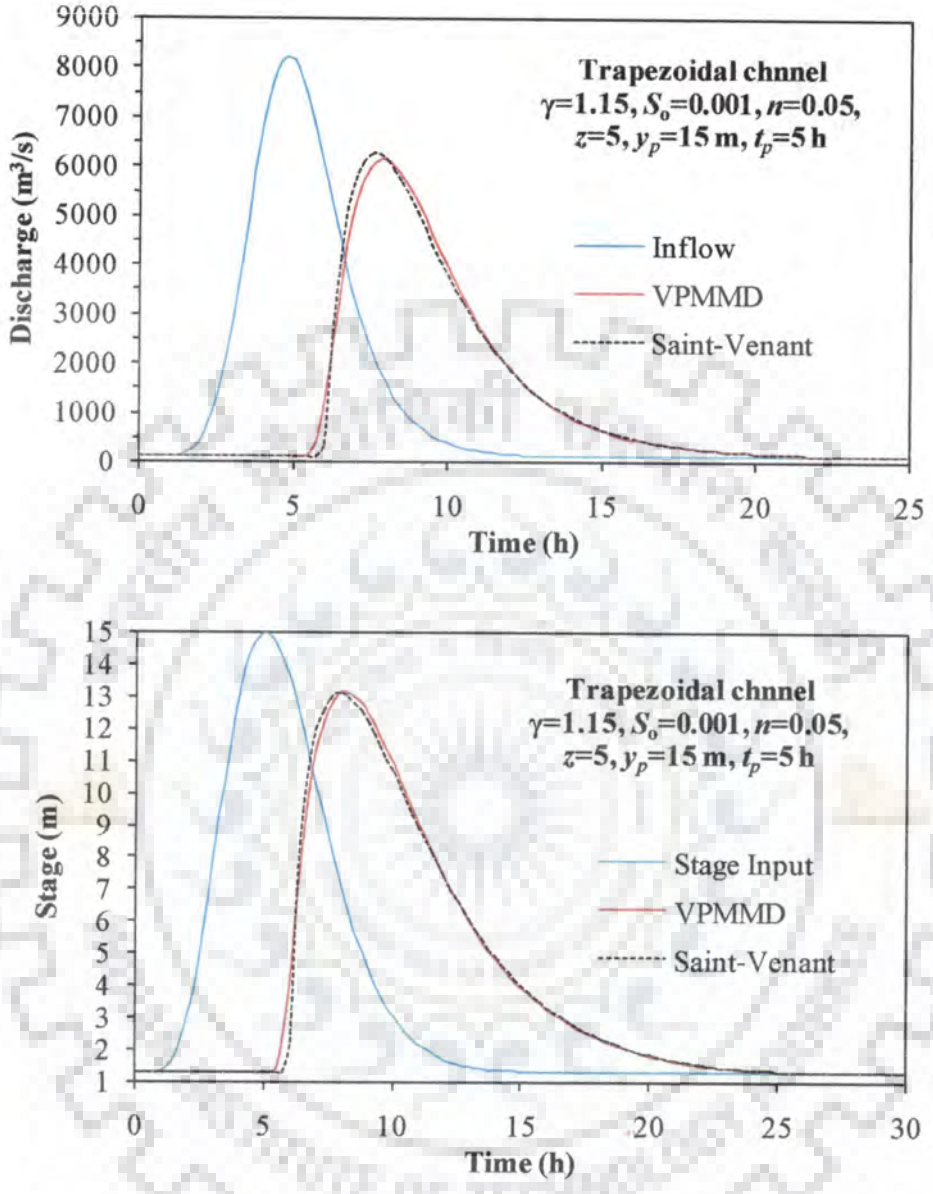

Figure 4.13 A typical discharge and stage hydrographs reproductions of the Saint-Venant solutions by the VPMMD method for S_o= 0.001, n= 0.05, Q_b= 100 m^3/s (y_b= 1.299 m), y_p= 15 m (Q_p= 8208.74 m^3/s), t_p= 5 h and γ = 1.15 in a trapezoidal channel reaches (z = 5).

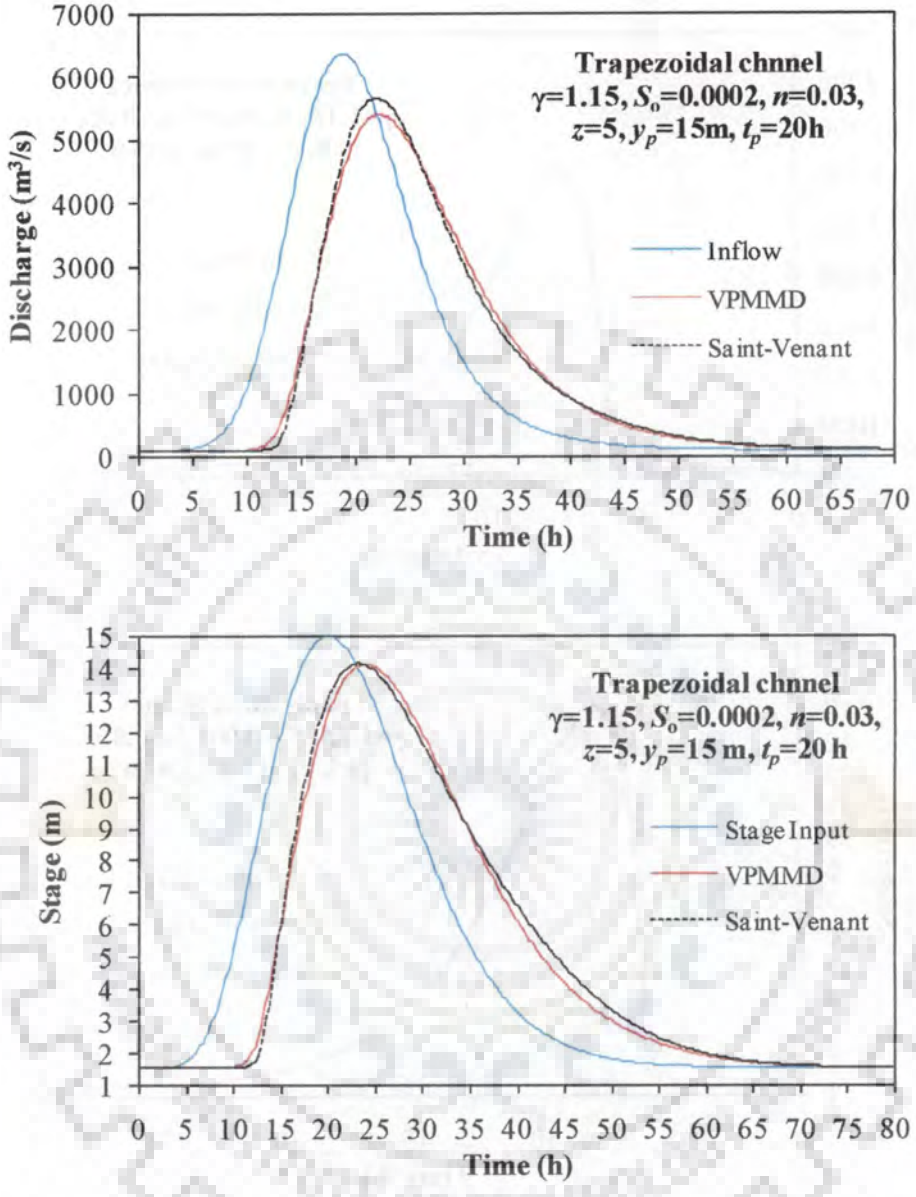

Figure 4.14 A typical discharge and stage hydrographs reproductions of the Saint-Venant solutions by the VPMMD method for S_o= 0.0002, n= 0.03, Q_b= 100 m^3/s (y_b= 1.545 m), y_p= 15 m (Q_p= 6361.59 m^3/s), t_p= 20 h and γ = 1.15 in a trapezoidal channel reaches (z = 5).

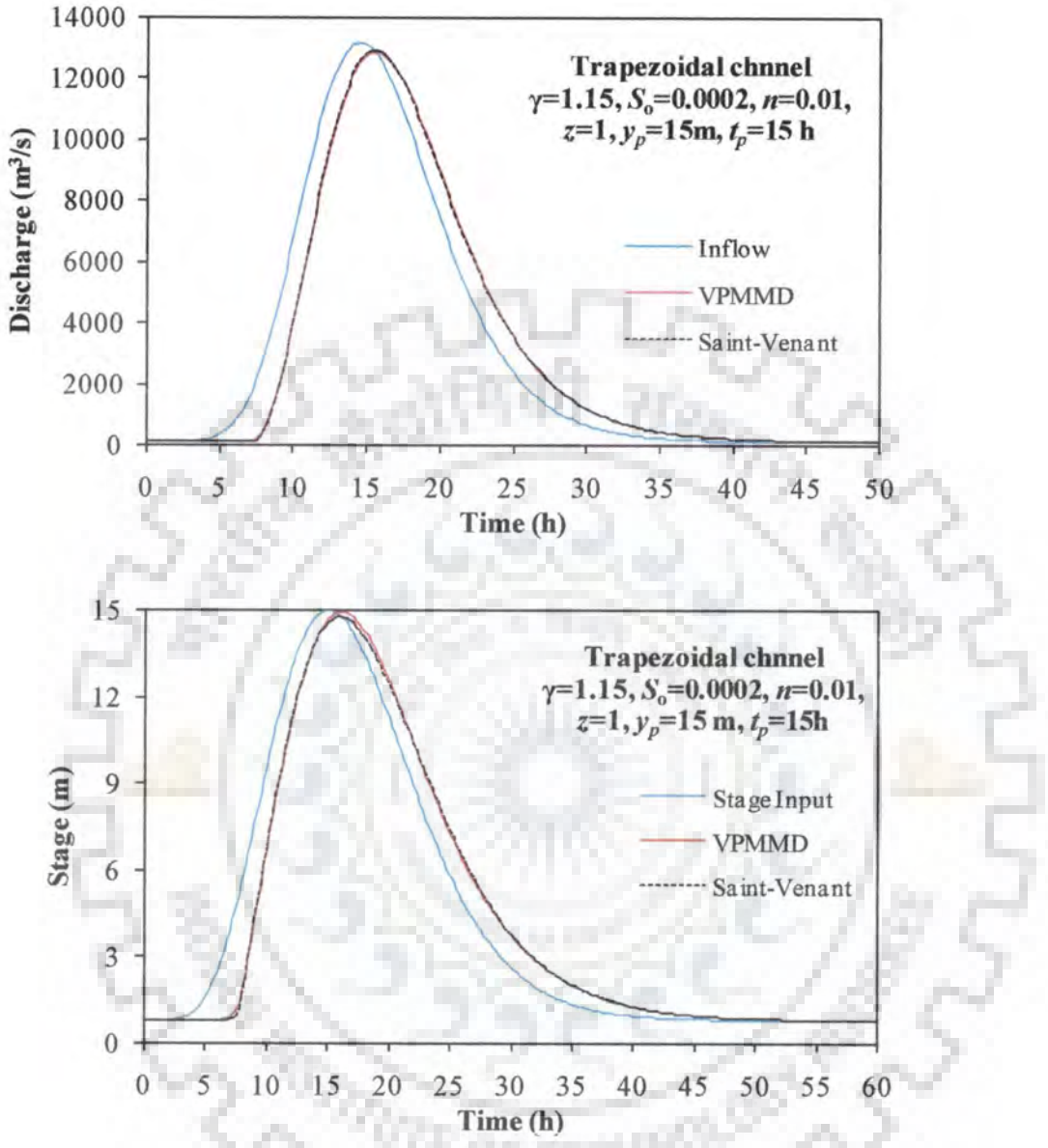

Figure 4.15 A typical discharge and stage hydrographs reproductions of the Saint-Venant solutions by the VPMMD method for S_o= 0.0002, n= 0.01, Q_b= 100 m^3/s (y_b= 0.813 m), y_p= 15 m (Q_p= 13170.44 m^3/s), t_p= 15h and γ = 1.15 in a trapezoidal channel reaches (z = 1).

Recommendations of Applicability Criteria

A consolidated approach of identifying the applicability limits of the VPMMD method for its successful application for routing the discharge hydrograph and the subsequent estimation of the corresponding stage hydrograph in rectangular and trapezoidal channels are brought out in Figures 4.16 and 4.17. These limits are determined on the basis of 95% simulations of this method perform with ≤5% error limit in reproducing all the considered pertinent characteristics of the benchmark solutions. For this purpose, the percentage of successful runs satisfying the error level criterion ≤5% of each of the evaluation measures against the total number of simulation runs upto any specified magnitude of $(1/S_o)(\partial y/\partial x)_{\max}$ is estimated. Figure 4.16 shows the variation of percentage of successful runs satisfying the 5% error limit criterion of each of the evaluation measures of the pertinent characteristics reproduction out of the total number of all simulation runs made up to a specified magnitude of $(1/S_o)(\partial y/\partial x)_{\max}$, which is considered as the variate of the abscissa. A similar variation is shown in Figure 4.17 based on the analysis of the estimated stage hydrograph simulation results. It can be seen from Figure 4.16 that the reproduction of the pertinent characteristics of the benchmark discharge hydrographs by the solutions of the VPMMD routing method measured by η_q, $|q_{per}|$ and $|t_{pqer}|$ show that 100% simulation runs satisfy the error limit of 5% of the considered evaluation measures in the range of $(1/S_o)(\partial y/\partial x)_{\max} \le 0.15$, and beyond which the error measure curves deviate away from 100% successful runs. Similar inference can also be arrived at from Figure 4.17 with reference to the reproduction of the pertinent characteristics of benchmark stage hydrographs, estimated from the corresponding VPMMD method solutions, evaluated by the measures of η_y, $|y_{per}|$, and $|t_{pyer}|$. A careful study of Figure 4.16 brings out the fact that almost all the simulation runs (nearly 100% of runs) falling

within the limits of $(1/S_o)(\partial y/\partial x)_{\max} \le 0.8$ satisfy the N-S efficiency criterion $\eta_q \ge 95\%$ and then slightly deviate away from the line of 100% successful runs to ultimately reach the limit of 98.26%, i.e., 1.74% successful runs of all the successful simulations fail to satisfy the criterion of $\eta_q \ge 95\%$ as seen from the Table 4.2. However, the other two measures of pertinent characteristics of reproduction, viz., $|q_{per}|$, and $|t_{pqer}|$ could nearly maintain 100% successful runs for the considered error limit of 5% of these measures, up to $(1/S_o)(\partial y/\partial x)_{\max} \le 0.30$. But beyond this limit, the percentage of successful runs characterized by the error limits $\le 5\%$ of the measures $|q_{per}|$, and $|t_{pqer}|$ start falling drastically, with 95% successful runs achieved when $(1/S_o)(\partial y/\partial x)_{\max} \le 0.57$ and 0.85 for the former and latter, respectively. Considering the least of all the three $(1/S_o)(\partial y/\partial x)_{\max}$ magnitudes corresponding to the error limits of $\le 5\%$ of the evaluation measures, it is seen that the error limit of 5% of peak discharge reproduction with at least 95% successful runs is reached when $(1/S_o)(\partial y/\partial x)_{\max} \le 0.57$. This sets the applicability limit of the VPMMD method for successfully routing the discharge hydrographs in rivers and channels. However, to know the applicability limit of the VPMMD method for successfully estimating the stage hydrograph corresponding to the routed discharge hydrograph within the error limits of $\le 5\%$ of all the reproduction measures, a similar analysis as carried out for the discharge hydrograph reproduction using Figure 4.16 was performed on the basis of results presented in Figure 4.17. Based on such analysis of reproduction measures of the N-S efficiency η_y, $|y_{per}|$, and $|t_{pyer}|$ at 5% error limit, it is seen that the evaluation measure of $|t_{pyer}|$ reaches early with at least 95% runs satisfying all the evaluation measures with 5% error limit when

$(1/S_o)(\partial y/\partial x)_{max} \leq 0.61$. This sets the applicability limit for the VPMMD routing method for successfully reproducing the stage hydrographs. However, for successful reproduction of both discharge and the corresponding stage hydrographs, the applicability limit of VPMMD routing method is restricted by the magnitude of $(1/S_o)(\partial y/\partial x)_{max} \leq 0.57$.

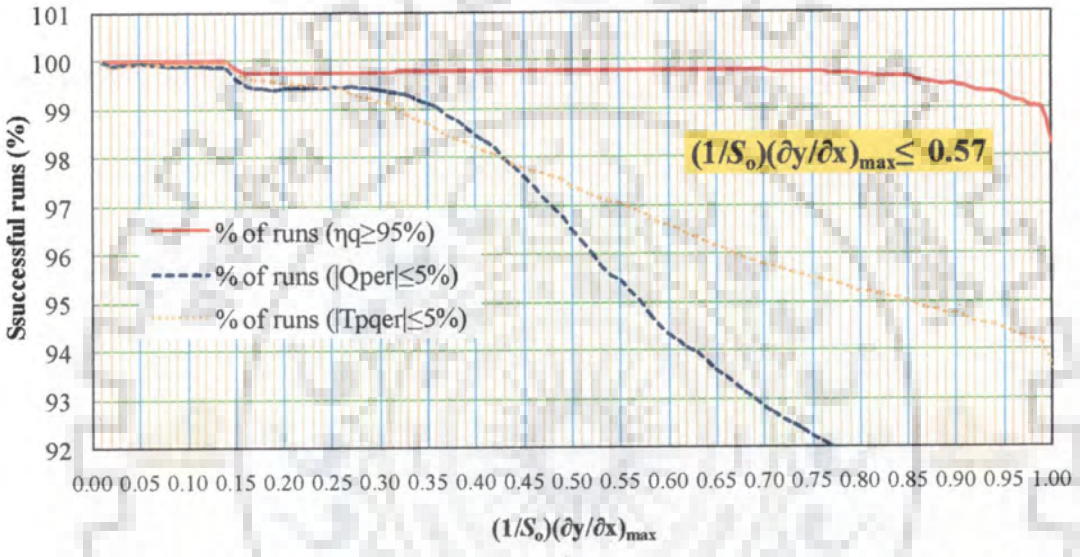

Figure 4.16 Plot required for determining the applicability limits of VPMMD method for discharge hydrograph routing.

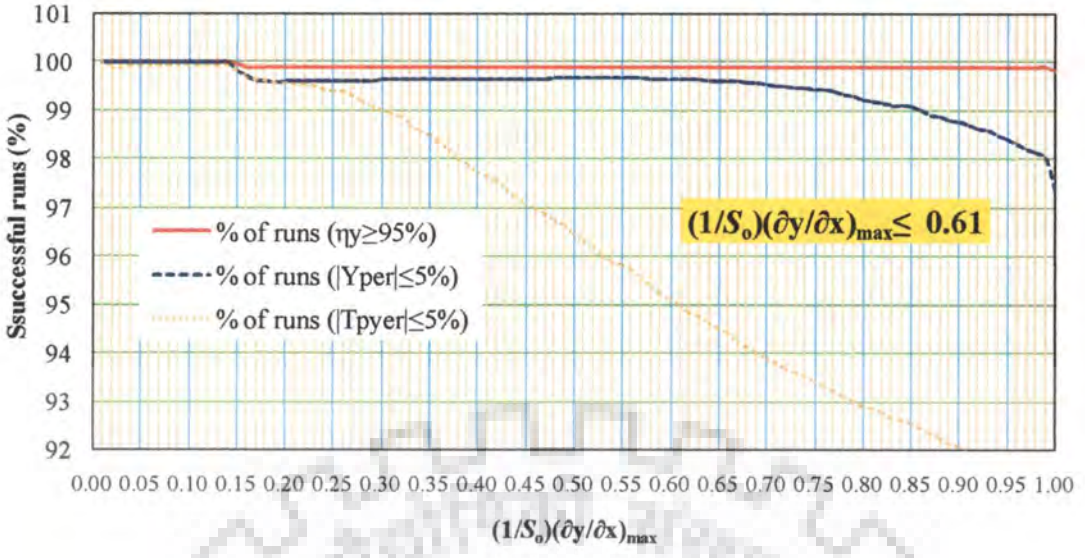

Figure 4.17 Plot required for determining the applicability limits of VPMMD method for stage hydrograph estimation.

4.7 SUMMARY AND CONCLUDING REMARKS

An investigation has been carried out to arrive at the applicability limit of the VPMMD method for successfully routing discharge hydrograph and for the simultaneous estimation of the corresponding stage hydrograph in uniform prismatic rectangular and trapezoidal main channel reaches. The appropriateness of using the scaled longitudinal water surface gradient $(1/S_o)(\partial y/\partial x)_{max}$ estimated for the inflow hydrograph as the applicability criterion for determining the applicability limits of the VPMMD method is brought out. A number of numerical experiments covering a wide range of combinations of channel characteristics (i.e., channel bed slope and Manning's roughness coefficients) and inflow characteristics (i.e., peak discharge, time-to-peak discharge, and shape factor) were conducted for simulating benchmark routing solutions of both discharge and stage hydrographs using the Saint-Venant equations, and for subsequent reproductions of these hydrographs using the respective solution of the VPMMD method with the objective of

establishing the applicability criteria of the VPMMD method for the successful reproductions of the benchmark solutions by the respective VPMMD method. The ability to reproduce the benchmark solutions by the VPMMD method was studied on the basis of assessing the close reproduction of some pertinent characteristics of the former solutions by the latter solutions. Accordingly, the applicability criteria of the VPMMD method for close reproduction of the benchmark solutions were determined on the basis of almost 95% simulations of this method performs with $\leq 5\%$ error limit in reproducing all the considered pertinent characteristics of the benchmark solutions for the given magnitude of $(1/S_o)(\partial y/\partial x)_{max}$ estimate for the inflow hydrograph to be routed. Based on the study conducted on these considerations, it is revealed that the applicability of the VPMMD method evaluated on the basis of the estimate $(1/S_o)(\partial y/\partial x)_{max}$ of the inflow hydrograph requires to satisfy the following criteria:

For successful discharge hydrograph routing using the VPMMD method as well as for the subsequent successful stage hydrograph estimation, the applicability criterion to be satisfied is $(1/S_o)(\partial y/\partial x)_{max} \leq 0.57$ estimated for the given inflow hydrograph. However, only for stage hydrograph estimation using the VPMMD routing method, the applicability criterion to be satisfied is $(1/S_o)(\partial y/\partial x)_{max} \leq 0.61$.

5 APPLICATION OF THE VPMMD METHOD FOR HYDROMETRIC DATA-BASED REAL-TIME FLOOD FORECASTING

5.1 GENERAL

River routing is one of the hydrological component processes that can be simulated accurately in comparison with the simulation of the runoff process using the causative rainfall. This could be attributed to the confinement of flood flow within the channel section which possible to be monitored relatively easily, contrary to the runoff generation process caused by spatially and temporally distributed rainfall process. Consequently, the uncertainties associated with flood movement process in rivers are less in comparison with the rainfall-runoff process. Therefore, real-time flood forecasting based only on the channel routing process is expected to be more reliable than that based on the rainfall based forecasting, though at the cost estimating forecast with short lead-time. The reliability of river forecasting can be enhanced using models developed based on equations governing the flow process in channels rather than using empirical or black-box models. In this regard the simplified routing models can be considered more attractive due to their applicability with limited data, especially the channel geometry data, in comparison with the applicability of the full Saint-Venant equations. Therefore, it is considered worthwhile herein to examine the suitability of a simplified physically based model like the variable parameter McCarthy-Muskingum discharge-routing (VPMMD) method studied herein for real-time forecasting at a river gauging station. The present study focuses mainly to verify the suitability of the VPMMD method as a component model of a hydrometric data-based forecasting model in conjunction with a two-parameter linear autoregressive forecast error estimation model for real-time flood forecasting applications in natural river channels. The river reach of 15 km length

between Pierantonio and Ponte Felcino, the upstream and downstream gauging stations, respectively, of the Tiber river in Central Italy is considered for the application of this model for real-time forecasting at the Ponte Felcino station, knowing the evolving flood at the Pierantonio station.

5.2 BACKGROUND OF THE PROPOSED HYDROMETRIC DATA-BASED REAL-TIME FLOOD FORECASTING

In hydrological literature, the term "hydrometric data-based forecasting" is interpreted in two forms: 1) interpretation as given by *Nemec* [1985] from the perspective of using only the hydrometric data without involving the precipitation data, like the case of employing only the channel routing methods for forecasting based on hydraulic or hydrological models, and 2) interpretation from the perspective of employing data-based models for linking input (stream gauge or discharge) and output (outflow gauge or discharge) using empirical models such as the ANN models. Based on ANN models, one can also use evolving rainfall event for flood forecasting in river reaches. Such a consideration is not accommodated using the first form of the model. Therefore, in this study the term "hydrometric data-based forecasting" is used in the context of the first interpretation only. The process of estimating the expected stages or flows and their time sequences at selected vulnerable points along the river course during floods is called "Real-Time Flood Forecasting". Real-time flood forecasting systems are formulated for issuing flood warning in real-time in order to prepare the evacuation plan for safe-guarding the lives of humans and livestock, and movable properties of the people during floods. Experiences have shown that the loss of human life and property can be reduced to a considerable extent by giving reliable advance information about the expected floods. The effectiveness of real-time flood forecasting system in reducing flood damages would depend upon how accurately the estimation of the yet to arrive stages or flows of flood

and its time sequence at selected points along the river could be forecasted during the propagation of the evolving causative input. Therefore, there is a need for methods or models capable of efficiently forecasting water levels or discharges at desired locations along rivers. Efficient forecasting requires that the structure of the model should be simple, easy to be understood and handled by flood control engineer and it should not have excessive input requirements, but at the same time the forecast must be accurate enough to serve the intended purpose. Typically, the flood forecasting models make possible to simulate the response of the system to a given input at a given location under the existing system conditions. The forecasting models generally operate on calibration (off-line) and operation (on-line) modes. The calibration mode tries to produce the response of the system for the past recorded precipitation or upstream flow input. This calibrated response is compared with the recorded response at the point of forecasting interest to check the matching of these two responses. If the matching is done satisfactorily the model structure or the model parameters need not be changed, otherwise the model parameters are to be modified till the matching is done satisfactorily. Once the structure of the model frame work is finalized in the calibration mode, the model can be adopted for operational mode of using it for the forecasting purposes. While the basic structure of the model is not changed in the operational mode, the parameters are changed considering the current catchment conditions due to the evolving input. To effectively accounting this evolving scenario, forecasting models have two components: 1) deterministic flow component and 2) stochastic flow component. The deterministic flow component is determined by the identified hydrologic or hydraulic mode; whereas, the stochastic flow component is determined based on the residual forecast error series of the difference between the forecasted flow of a specified lead-time and the corresponding observed flow. While forecast error reflects both the model error, due to the inability of

the model used for forecasting to correctly reproduce the flow process and the observational error while measuring the flow. Hydrodynamic principle based models such as MIKE11 and HEC-RAS models can be used as deterministic flow component models, but at the cost of using hydrometric and morphometric data at close temporal and spatial resolutions. These models are not suitable to serve the purpose of flood routing in rivers where detailed topographical surveys of channel cross-sections and roughness at close intervals are not available [*Barbetta et al.*, 2011]. Alternatively, implementing a channel routing method developed only based on normal rating curves and the cross-sectional details available at the end-sections of the reach, corresponding to where forecast is made and forecast is required, simplifies the forecasting problem of the operational flood management.

Under the above requirement, the application of a physically based simplified flood routing method as a component model of a hydrometric data-based deterministic forecasting model along with a simple autoregressive forecast error estimation model may be found useful for real-time flood forecasting applications.

5.3 APPLICATION OF THE VPMMD METHOD FOR REAL-TIME FLOOD FORECASTING

As the objective herein is to apply the proposed routing procedure of the VPMMD method for flow forecasting at the desired location of a river reach knowing the discharges of an evolving event at an upstream station, the forecast estimated by the VPMMD method using the latest available inflow forms the deterministic flow component of the forecast model. Based on this consideration, an approach is developed herein for the application of the VPMMD method as a component model of a hydrometric data-based deterministic forecasting model along with a two-parameter linear

autoregressive error estimating model for real-time flood forecasting at the end of a river reach considered for forecasting.

The routing equation of the VPMMD method is written as:

$$Q_{d,(j+1)\Delta t} = C_1 Q_{u,(j+1)\Delta t} + C_2 Q_{u,j\Delta t} + C_3 Q_{d,j\Delta t} \tag{5.1}$$

where $Q_{u,(j+1)\Delta t}$ and $Q_{d,(j+1)\Delta t}$ denote the observed upstream and the estimated downstream discharges at time $(j+1)\Delta t$, respectively; and, $Q_{u,j\Delta t}$ and $Q_{d,j\Delta t}$ denote the observed upstream and downstream discharges at time $j\Delta t$, respectively. The notation Δt denotes the routing time interval, and the coefficients C_1, C_2 and C_3 are expressed as

$$C_1 = \frac{\Delta t - 2.K_{j+1}.\theta_{j+1}}{\Delta t + 2.K_{j+1}.\left(1-\theta_{j+1}\right)} \tag{5.2a}$$

$$C_2 = \frac{\Delta t + 2.K_j.\theta_j}{\Delta t + 2.K_{j+1}.\left(1-\theta_{j+1}\right)} \tag{5.2b}$$

$$C_3 = \frac{-\Delta t + 2.K_j.\left(1-\theta_j\right)}{\Delta t + 2.K_{j+1}.\left(1-\theta_{j+1}\right)} \tag{5.2c}$$

where K and θ are the travel time and weighting parameter, respectively, of the VPMMD method as described in Chapter (3).

In order to apply the VPMMD method for real-time forecasting purposes, the routing equation given by equation (5.1) is suitably modified considering the forecast lead-time, T_L as

$$\hat{Q}_{d,(j+1)\Delta t+T_L} = C_1 \hat{Q}_{u,(j+1)\Delta t+T_L} + C_2 \hat{Q}_{u,j\Delta t+T_L} + C_3 \hat{Q}_{d,j\Delta t+T_L} + e_{f,(j+1)\Delta t+T_L} \tag{5.3}$$

where $\hat{Q}$= denotes the forecast discharge; $e_{f,(j+1)\Delta t+T_L}$ = forecast error (i.e., the difference between the observed discharge and the corresponding forecasted discharge at the site of forecast interest); $(j+1)\Delta t$ = time of forecast. In order to get the forecast estimate of the downstream discharge with a lead-time T_L, one should have the three different forecast quantities mentioned in the above equation (5.3) such as $\hat{Q}_{u,(j+1)\Delta t+T_L}$, $\hat{Q}_{u,j\Delta t+T_L}$ and $\hat{Q}_{d,j\Delta t+T_L}$. However, only the last one is known, being the forecast estimate of the downstream discharge assessed at the previous time of forecast $j\Delta t$. Therefore, in order to apply equation (5.3) for the estimation of $\hat{Q}_{d,(j+1)\Delta t+T_L}$, the following assumption has to be made on the basis of no-model hypothesis:

$$\hat{Q}_{u,(j+1)\Delta t+T_L} = \hat{Q}_{u,j\Delta t+T_L} = Q_{u,(j+1)\Delta t} \tag{5.4}$$

where $Q_{u,(j+1)\Delta t}$ is the last upstream observed discharge. The similar assumption was also adopted by *Perumal et al.*, [2011] while using the VPMS method for real-time flood forecasting applications.

Using equation (5.4) in equation (5.3), the final forecasting model is expressed as

$$\hat{Q}_{d,(j+1)\Delta t+T_L} = C_1 Q_{u,(j+1)\Delta t} + C_2 Q_{u,(j+1)\Delta t} + C_3 \hat{Q}_{d,j\Delta t+T_L} + e_{f,(j+1)\Delta t+T_L} \tag{5.5}$$

In equation (5.5), the minimum lead-time is Δt, the routing time interval at which the flow measurements are made, and this corresponds to one time-interval ahead forecast. The flood routing models allow for the forecast at an extreme end of the river reach, and the lead-time is limited by the flood wave travel time [*Barbetta et al.*, 2011]. Therefore, the maximum lead-time that can be adopted depends on the accuracy of the obtained forecast which may nearly corresponds to the travel time of the upstream discharge to

arrive at the site of forecast interest. The use of a larger lead-time beyond this approximate travel time would lead to poorer accuracy of the forecast. The error of forecast $e_{f,(j+1)\Delta t+T_L}$ in equation (5.5) is estimated using a second order autoregressive error estimation model and is added to the model estimated forecast for a given lead-time, thus, yielding the final forecasted discharge at the site of interest. The following form of model is used for forecasting the error at time $(j+1)\Delta t+T_L$:

$$e_{f,(j+1)\Delta t+T_L} = a_{1,(j\Delta t)} e_{obs,(j+1)\Delta t} + a_{2,(j\Delta t)} e_{obs,j\Delta t} + \varepsilon_{(j+1)\Delta t+T_L} \quad (5.6)$$

where $e_{obs,(j+1)\Delta t}$ and $e_{obs,j\Delta t}$ are the forecasting errors estimated at time $(j+1)\Delta t$ and $j\Delta t$, respectively, and $\varepsilon_{(j+1)\Delta t+T_L}$ is the random error (white noise). Further, the above equation (5.6) is used after the lapse of certain initial period of the forecasting event, known as the warm-up period. The difference between the observed discharge and the VPMMD routed discharge in the warm-up period is considered as the actual error and its series is assumed to be stochastic in nature. The initial parameters a_1 and a_2 of the error estimation model are assessed using this error series estimated in the warm-up period. The duration of the initial warm-up period considered for developing the error forecast model should not be too long to avoid the forecasting exercise becomes of no practical relevance for forecasting the given event, and at the same time, it should not be too short resulting in numerical problem while estimating the parameters a_1 and a_2 using the least squares approach. Utilization of the latest available observed data to improve the performance of a real-time forecasting system is called updating [*Lekkas et al.*, 2001]. If an operational flow forecasting model produces forecasts that consistently do not agree with the observed flow resulting in forecasting error, then corrective action should be taken in order to modify the future forecasts in an attempt to improve the performance.

However, in this study the error estimation model given by equation (5.6) has been applied without generating the random error component. It may be noted that the parameters a_1 and a_2 are updated on real-time basis taking into account the latest available discharge observation. It may be noted that no attempt was made herein to study the sensitivity of the order of the stochastic error model and the initial warm-up period on the estimates of the forecast.

The solution of the VPMMD method can be obtained by two routing approaches:

1) Routing the entire hydrograph over the considered sub-reach of length Δx, and in this way sequentially through a cascade of sub-reaches. This approach is more suitable for off-line mode application such as in the case of design flood estimation studies and routing model calibration studies.

2) Routing a given inflow discharge at a given time to estimate the corresponding outflow discharge at the same time by routing through a cascade of sub-reaches, and then subsequently move to the next time level by the time step Δt to route the next inflow discharge in the similar manner along each of the spatial step node points till the forecast at the outlet of the forecasting river reach is estimated. In this study the latter approach is adopted due to the feasibility of employing multiple sub-reaches required for routing during real-time forecasting.

In order to apply this routing procedure for real-time forecasting purpose, the simulation mode of the routing procedure of the VPMMD method given in Section 3.4 is modified. The numerical grid network of this solution scheme is depicted in Figure 5.1.

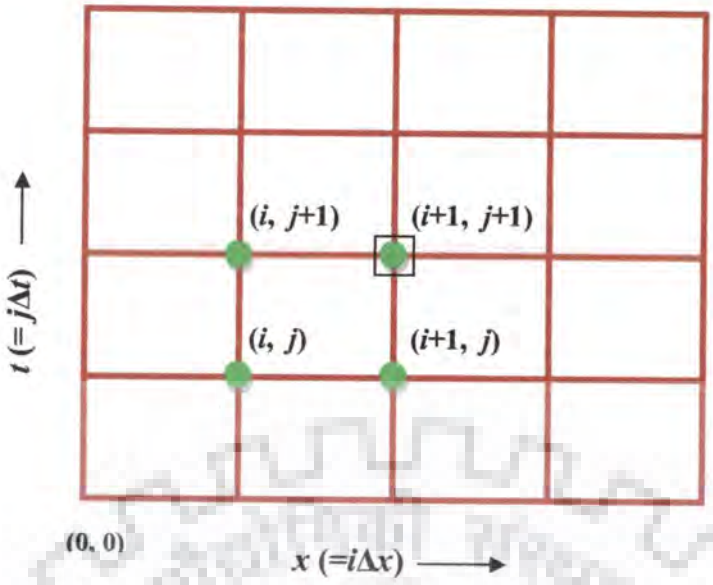

Figure 5.1 The x-t solution grid network for real-time application

The Variable Parameter McCarthy-Muskingum Discharge-routing based Real-time Flood-forecasting method, henceforth, abbreviated as VPMMDRF method comprises of the VPMMD routing method and the forecast error estimation model based on the second-order linear autoregressive model. The description of the application of the VPMMDRF method for field forecasting problems is illustrated in the following pages.

5.3.1 The VPMMDRF Algorithm

Similar to the VPMMD method, the VPMMDRF method also does not use the in-between channel cross-sectional details, but uses the rating curves information and the cross-sections details available at these end-sections. For this purpose the preparation of normal tables or look-up tables, which consist of discharge-normal flow depth relationships, water surface widths, flow area-depth relationships, wave celerity and the velocity-discharge relationships are necessary to interpolate the required flow/sectional variables while using the proposed real-time forecasting algorithm. As the VPMMDRF method is intended for multi sub-reach analysis, the two-dimensional computational

scheme as shown in Figure 5.1 is generated considering space x ($=i\,\Delta x$) as abscissa and time t ($= j\Delta t$) as ordinate of the computational scheme.

The step-by-step procedure of real-time forecasting by the VPMMDRF method over the river reach between the gauging station, where forecast is made, and the gauging station for which the forecast is needed is given below:

1. Start of time step j =1 (initial time)
2. The initial values of K and θ are estimated for the initial steady flow in the reach using equations (3.7) and (3.8).
3. Supply the forecast lead-time, T_L and the warm-up time period.
4. Routing time step = $j+1$
5. Start of space step
6. Compute unrefined flow using routing equation (5.5)
7. Estimate normal discharge at section 3 (see, Figure 3.1) as

$$Q_3 = \theta Q_{u,(j+1)\Delta t} + (1-\theta)\hat{Q}_{d,(j+1)\Delta t+T_L} \tag{5.7}$$

8. Using Q_3 estimated at step 7, estimate stage y_M at the midsection of the sub-reach by the interpolation of the normal stage-discharge relationship given in the look-up table.
9. Using the value of y_M estimated in step 8, estimate the normal velocity, V_{Mo}, normal celerity, c_{Mo} and surface width, B_M by interpolation of the respective values from the look-up tables.

10. Estimate the refined parameters K and θ using equations (3.4) and (3.6), respectively.

11. Estimate the refined discharge using the routing equation (5.5).

12. Go to step 5 for routing through the next space step until the routing through all the space steps are completed.

13. Estimate the forecast error using equation (5.6). (The parameters a_1 and a_2 of the autoregressive error estimate model given by equation (5.6) are assessed using the actual forecast error series estimated in the warm-up period immediately prior to the last flow observation. Actual forecast error = observed flow - flow estimated by the VPMMDRF method).

14. Compute the forecasted discharge as summation of the discharge estimated by the VPMMD method and that of the corresponding forecast error discharge estimated by the autoregressive model.

15. The downstream stage y_d is computed using equation (3.9).

16. The above steps 4 to 15 are repeated for issuing new forecast of the considered lead-time as soon as the next inflow information becomes available.

5.4 FIELD APPLICATION

The proposed VPMMDRF method is demonstrated for real-time flood forecasting application over the 15 km long Pierantonio-Ponte Felcino reach of the Tiber River in Central Italy. Ten recorded flood events, most of them characterized by negligible lateral flow over the considered river reach were studied. All these events were studied by *Perumal et al.*, [2011] for stage forecasting using the VPMS method considering the

entire 15 km reach as a single reach. Information regarding the lateral flow contribution of these studied flood events is given in Table 5.1. As the VPMMDRF method uses the upstream and downstream rating curves information for analyzing the given flood event for real-time forecasting, the reach-averaged rating curve already developed for the Pierantonio-Ponte Felcino reach was directly used in the forecasting model (See, Section 3.7.2.1) and the same is presented in Figure 5.2 for the ready reference along with upstream and downstream rating curves of the reach. Further, the look-up tables of the reach averaged variables such as the surface width (dA/dy), wave celerity (dQ/dA) and flow velocity $v(y)$ required for routing floods in this reach, as presented in Section 3.7.2.1 were directly used in this forecasting study. As the stage variable is sensitive to the local geometrical variations, the conversion equation $y_{actual} = 0.927 * y_{equivalent} + 0.062$ as given in Section 3.7.2.1 for converting the estimated stage, $y_{equivalent}$ at the station of forecast interest to the corresponding actual stage, y_{actual} was used herein.

Table 5.1 Wave travel times and lateral flows of different flood events studied for Pieranto-Ponte Felcino reach (Adopted from *Perumal et al.*, 2011).

Sl. No.	Flood Event	Wave travel time (h)	Lateral Inflow (%)
1	December, 1996	1.50	1.90
2	April, 1997	1.50	6.50
3	November, 1997	1.00	5.40
4	February, 1999	2.00	4.40
5	December, 2000	2.00	Flooding
6	Apr. 2001	2.00	0.20
7	November, 2005	2.50	Flooding
8	03 Dec.2005	1.00	3.60
9	05 Dec. 2005	1.00	5.70
10	30 Dec. 2005	2.00	1.90

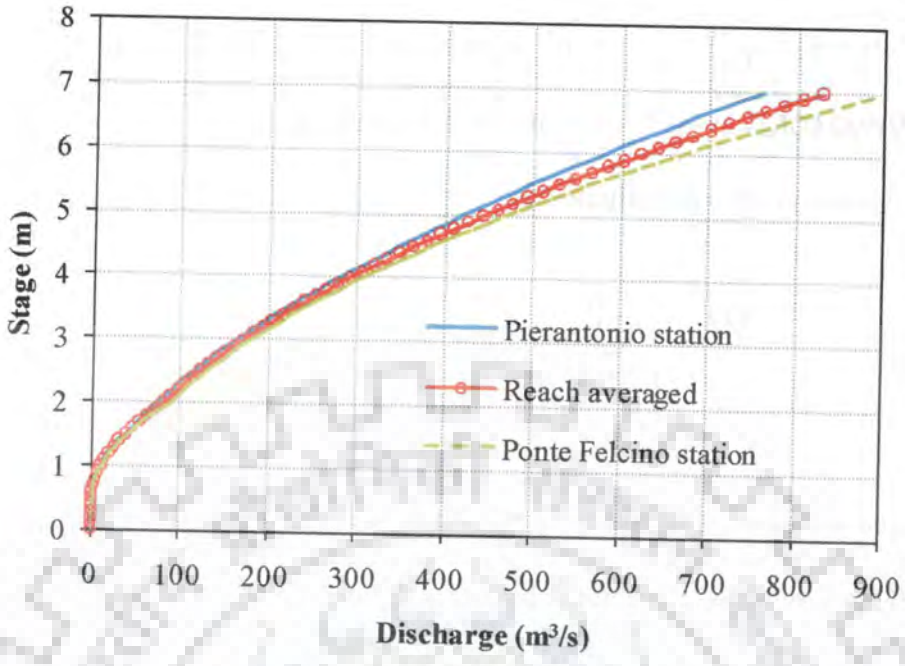

Figure 5.2 Rating curves at the Pierantonio and Ponte Felcino stations and the developed reach averaged rating curve for the Pierantonio-Ponte Felcino reach.

The ability of the proposed VPMMDRF method to serve its purpose was studied for five different forecast lead-times 1.0, 1.5, 2.0, 2.5, and 3.0 hours considering a warm-up period of 5 hours. The forecast error is estimated using a two-parameter autoregressive model with its parameters updated at every routing time interval $\Delta t = 1800$ s based on the latest actual inflow and outflow discharge observations available over the window of the warm-up period. Two cases of space steps of $\Delta x = 15$ km (single reach consideration) and $\Delta x = 7.5$ km (2 sub-reaches consideration) were used to arrive at the forecasted discharge hydrographs and the corresponding computed stage forecast hydrographs at the Ponte-Felcino station. Further sub-division of the reach causes accumulation of forecast errors leading to numerical instability in the solution of the proposed model. The efficiency of the forecast was evaluated using two criteria: 1) the well known Nash-Sutcliffe (N-S)

efficiency criterion; and 2) the Persistence-Criterion (PC) as used by *Moramarco et al.* [2006] and *Barbetta et al.* [2011]. In order to evaluate the efficacy of forecast of the proposed VPMMDRF model over no-model forecast of the same lead-time, the Persistence-Criterion (PC) is evaluated as:

$$PC = \left(1 - \frac{\sum_i \left(Q_{i\Delta t} - \hat{Q}_{i\Delta t} \right)^2}{\sum_i \left(Q_{i\Delta t} - Q_{(i\Delta t - T_L)} \right)^2} \right) \times 100 \tag{5.8}$$

where, Q and $\hat{Q}$ denote the observed and the forecasted discharge values, respectively. The Persistence-Criterion is estimated based on the consideration that the latest observed discharge at the site of forecast interest is sustained till the lead-time and, thus, becoming the forecast flow at that site. This essentially implies that the best forecast one could make under no-model scenario is to sustain the latest observed flow to be the forecasted flow of the considered lead-time.

5.5 RESULTS AND DISCUSSIONS

The efficacy of the VPMMDRF method for its suitability of application for hydrometric data-based forecasting of floods in a river reach can be analyzed from the forecasting results obtained by its application in studying the ten past recorded events in the Pierantonio-Ponte Felcino reach of the Tiber River in Central Italy. Tables 5.2 to 5.6 show the reproduction of the pertinent characteristics of the observed discharge and stage hydrographs by the forecasted discharge and the corresponding estimated stage hydrographs arrived at using the VPMMDRF method, by considering the entire routing reach as a single reach, i.e., Δx = 15 km. Similar reproduction results of forecasting based on the same ten flood events, but based on the consideration two sub-reaches of this 15 km reach are shown in Tables 5.7 to 5.11.

Tables 5.2 to 5.11 show the details of performance evaluation measures of the forecasting results of the VPMMDRF method with reference to the reproductions of pertinent characteristics of the observed discharge and stage hydrographs measured by the N-S efficiencies, η_q (in %), η_y (in %), and PC (in %) of the forecasted discharge hydrograph, errors in peak discharge and peak stage reproductions measured by q_{per} (in %) and y_{per} (in %), respectively, and the errors of their respective time-to-peaks, *viz.*, t_{pqer} (in h), and t_{pyer} (in h). These tables present the results of ten investigated events for all the considered lead-times. The relevance of these performance evaluation measures of reproductions of the pertinent characteristics of the simulated or forecasted hydrographs were discussed in Section 3.5.

Figure 5.3 (a, c, e, g, i, k, m, o, q, and s) demonstrates the comparison of the forecasted discharge hydrographs of different flood events and for different lead-times, obtained at the Ponte Felcino station using the single reach application of the VPMMDRF method along with the corresponding observed discharge hydrographs. Similarly, the forecasted stage hydrographs estimated at the Ponte Felcino station using the corresponding forecasted discharge hydrographs are shown in Figure 5.3 (b, d, f, h, j, l, n, p, r, and t) along with the respective event observed stage hydrographs.

Figure 5.4 illustrates the comparison between the 3.00 h lead-time forecasted discharge hydrographs of the December, 1996 and November, 1997 flood events with the corresponding observed discharge hydrographs. These forecasts were obtained using the VPMMDRF method for single routing reach consideration, with and without considering the forecast error estimates.

Figure 5.5 (a, c, e, g, i, k, m, o, q, and s) shows the forecasted results at the Ponte Felcino station similar to that of Figure 5.3, but for routing using two sub-reaches consideration (i.e., $\Delta x = 7.5$ km). The corresponding forecasted stage hydrographs estimated at the

Ponte Felcino station using the respective forecasted discharge hydrographs given in Figure 5.5 (a, c, e, g, i, k, m, o, q, and s) are shown in Figure 5.5 (b, d, f, h, j, l, n, p, r, and t) along with the respective event observed stage hydrographs.

Table 5.2 Forecasting results of the VPMMDRF method for a lead-time of 1.00 hour and a space step of Δx= 15 km (single reach).

Sl. No.	Flood Event	Discharge Forecast				Computed Stage Forecast		
		q_{per} (%)	t_{pqer} (h)	η_q (%)	PC (%)	y_{per} (%)	t_{pyer} (h)	η_y (%)
1	December, 1996	0.76	-0.50	99.87	95.98	-3.52	-0.50	98.67
2	April, 1997	-0.07	-0.50	99.94	95.78	-3.74	-0.50	99.11
3	November, 1997	2.76	-3.00	99.81	94.29	-1.82	-3.00	98.84
4	February, 1999	-0.28	-0.50	99.75	91.60	-3.83	-0.50	98.94
5	December, 2000	-1.92	-0.50	99.63	81.98	-4.40	1.50	98.07
6	Apr. 2001	-1.39	0.50	99.50	93.58	0.12	0.50	98.99
7	November, 2005	-0.06	0.00	99.75	83.55	-1.91	0.00	99.29
8	03 Dec.2005	-2.36	1.00	99.73	94.82	2.24	1.00	98.83
9	05 Dec. 2005	-0.34	0.50	99.81	93.59	3.71	0.50	98.09
10	30 Dec. 2005	-0.18	-1.00	99.87	89.69	3.01	-1.00	99.48
	Mean value			**99.77**	**91.49**			**98.83**

Table 5.3 As in Table 5.2, but for a lead-time of 1.50 hour

Sl. No.	Flood Event	Discharge Forecast				Computed Stage Forecast		
		q_{per} (%)	t_{pqer} (h)	η_q (%)	PC (%)	y_{per} (%)	t_{pyer} (h)	η_y (%)
1	December, 1996	1.50	0.00	99.82	97.41	-3.13	0.00	98.72
2	April, 1997	-0.76	0.00	99.92	97.55	-4.10	0.00	99.11
3	November, 1997	4.80	-2.50	99.77	96.87	-0.73	-2.50	98.83
4	February, 1999	0.82	0.50	99.75	96.31	-3.28	0.50	98.96
5	December, 2000	-1.37	0.00	99.44	87.28	-4.12	-3.50	97.96
6	Apr. 2001	1.06	0.00	99.48	96.93	1.46	0.00	98.80
7	November, 2005	-0.84	1.00	99.44	83.06	-2.32	1.00	99.11
8	03 Dec.2005	-1.83	-0.50	99.25	93.31	2.17	-0.50	98.21
9	05 Dec. 2005	0.17	0.00	99.73	95.89	3.99	0.00	97.69
10	30 Dec. 2005	1.98	0.00	99.85	94.73	4.25	0.00	99.40
	Mean value			**99.65**	**93.93**			**98.68**

Table 5.4 As in Table 5.2, but for a lead-time of 2.00 hour

Sl. No.	Flood Event	Discharge Forecast				Computed Stage Forecast		
		q_{per} (%)	t_{pqer} (h)	η_q (%)	PC (%)	y_{per} (%)	t_{pyer} (h)	η_y (%)
1	December, 1996	2.69	0.50	99.41	95.10	-2.51	0.50	98.53
2	April, 1997	0.66	-1.50	99.76	95.56	-3.35	-1.50	99.05
3	November, 1997	6.03	-1.50	99.48	95.98	-0.15	-1.50	98.60
4	February, 1999	1.34	0.50	99.71	97.49	-3.00	0.50	99.14
5	December, 2000	-0.27	-8.50	99.16	88.99	-3.50	-8.50	97.90
6	Apr. 2001	5.29	0.00	98.89	96.18	3.74	0.00	97.84
7	November, 2005	-1.46	1.00	99.03	83.15	-2.77	1.00	98.87
8	03 Dec.2005	1.50	0.00	97.36	86.24	4.12	0.00	95.88
9	05 Dec. 2005	1.47	-3.00	99.16	92.71	4.86	-3.00	96.74
10	30 Dec. 2005	2.39	0.50	99.74	94.72	4.48	0.50	99.20
	Mean value			**99.17**	**92.61**			**98.17**

Table 5.5 As in Table 5.2, but for a lead-time of 2.50 hour

Sl. No.	Flood Event	Discharge Forecast				Computed Stage Forecast		
		q_{per} (%)	t_{pqer} (h)	η_q (%)	PC (%)	y_{per} (%)	t_{pyer} (h)	η_y (%)
1	December, 1996	4.00	1.00	98.16	90.03	-1.83	1.00	97.79
2	April, 1997	2.92	-1.50	99.17	90.05	-2.13	-1.50	98.62
3	November, 1997	8.58	-2.50	98.49	92.33	1.29	-2.50	97.83
4	February, 1999	5.00	-2.00	98.97	94.23	-1.08	-2.00	98.77
5	December, 2000	4.93	-8.00	98.25	84.94	-0.78	-8.00	97.39
6	Apr. 2001	10.97	0.50	95.56	89.92	6.77	0.50	94.28
7	November, 2005	-1.82	2.00	98.42	82.11	-2.96	2.00	98.49
8	03 Dec.2005	5.21	-7.50	92.03	72.23	6.94	-7.50	90.80
9	05 Dec. 2005	6.18	-4.00	97.50	85.88	7.72	-4.00	94.81
10	30 Dec. 2005	3.59	2.00	99.29	90.72	5.13	2.00	98.64
	Mean value			**97.58**	**87.24**			**96.74**

Table 5.6 As in Table 5.2, but for a lead-time of 3.00 hour

Sl. No.	Flood Event	Discharge Forecast				Computed Stage Forecast		
		q_{per} (%)	t_{pqer} (h)	η_q (%)	PC (%)	y_{per} (%)	t_{pyer} (h)	η_y (%)
1	December, 1996	10.20	-3.00	95.36	82.07	1.57	-3.00	95.89
2	April, 1997	5.20	-0.50	97.96	82.66	-0.96	-0.50	97.71
3	November, 1997	14.98	-3.50	96.13	86.10	4.64	-3.50	95.99
4	February, 1999	12.38	-1.50	96.88	87.60	2.69	-1.50	97.42
5	December, 2000	10.46	-8.50	96.40	77.91	2.25	-8.50	96.09
6	Apr. 2001	18.02	1.00	86.39	77.71	10.39	1.00	85.92
7	November, 2005	-2.26	2.50	97.72	81.71	-3.20	2.50	97.92
8	03 Dec.2005	13.88	-6.50	82.62	55.94	11.67	-6.50	82.66
9	05 Dec. 2005	13.21	-3.50	94.30	77.15	11.71	-3.50	91.30
10	30 Dec. 2005	4.40	0.00	98.45	85.58	5.64	0.00	97.70
	Mean value			**94.22**	**79.44**			**93.86**

It can be inferred from the results of all the ten flood events studied in the forecasting mode to verify the forecasting capability of the VPMMDRF method, as brought out by Tables 5.2 to 5.11 and shown in Figure 5.3 and 5.5, that the method is capable of forecasting the discharge hydrographs and the subsequent estimation of the stage hydrograph very closely for lead-times up to 3 hours. Comprehensive details regarding the performance of the VPMMDRF method in forecasting the considered flood events for lead-times of 1.00 h, 1.50 h, 2.00 h, 2.50 h and 3.00 h are presented as mean values of the performance evaluation measures of all the events studied in each of these tables.

It can be seen from the evaluation measures presented in Tables 5.2 to 5.6 of the forecasted results obtained at the Ponte Felcino station based on single reach routing consideration shows that the mean values of N-S efficiency for discharge hydrograph forecasting obtained for the considered lead-times of 1.00 h, 1.50 h, 2.00 h, 2.50 h and 3.00 h are 99.77%, 99.65%, 99.17%, 97.58% and 94.22%, respectively. Similarly, the N-S efficiencies of the corresponding stage hydrograph forecasting obtained are 98.83%, 98.68%, 98.17%, 96.74% and 93.86%, respectively. These results with systematic

decrease of N-S efficiency estimates demonstrate the inaccuracy of the forecasted floods with the increase of lead-time. It is also seen from Tables 5.2 to 5.6 that the mean Persistence-Criteria (PC) values estimated for discharge forecasting with the lead-times of 1.00 h, 1.50 h, 2.00 h, 2.50 h and 3.00 h are 91.49%, 93.93% 92.61%, 87.24% and 79.44%, respectively. As the N-S efficiency estimates of the VPMMDRF discharge forecasts are significantly larger than the PC estimates, one may conclude that the VPMMDRF method to be efficient for forecasting.

It can be seen from the evaluation measures presented in Tables 5.7 to 5.11 corresponding to the forecasting results obtained using two sub-reaches consideration that these measures display reduced efficiency of the forecast in comparison with those corresponding estimates based on single reach routing, as brought out by the overall range of the mean values of these measures as η_q=99.79 % to 74.42%, η_y=98.77% to 77.56%, and PC=91.60% to 13.11%, except for the cases of forecasts with one hour lead-time for which the efficiency of the forecasts based on two sub-reaches may be considered to be very insignificantly improved over those results based on single reach based routing. All these results, in general, demonstrate the systematic decrease of N-S efficiency estimates with the increase of forecasting lead-time values and with increased sub-reach routing considerations. This observation can also be seen again with reference to other evaluation measures such as peak discharge (q_{per} in %) and peak stage y_{per} (in %) reproductions of the observed peaks as given in Tables 5.2 to 5.11. For the smaller forecasting lead-time hours the VPMMDRF method shows slightly under estimation of the observed peak discharges and the observed peak stages in most of the flood events studied, while for the higher values of lead-times the VPMMDRF method show over estimation. Further, the Persistence-Criterion estimates are lower than the N-S efficiencies of the forecasted hydrographs in all the results obtained which, as described earlier, show the efficacy of

the VPMMDRF method for hydrometric data-based forecasting. It is inferred from this discussion that the over all performance of the VPMMDRF method is good for single reach consideration compared with that of the two sub-reaches consideration for all the lead-time hours studied. Therefore, it can be further inferred from these results that the VPMMDRF method can be confidently applied for discharge forecasting at Ponte Felcino station up to a lead-time of 3.00 h on the basis of single reach routing.

It can be inferred from Tables 5.2 to 5.11 that the forecasted hydrographs of the VPMMDRF method performs better even for those flood events such as December 2000 and November 2005 which received significant lateral flows (as given in Table 5.1). With reference to the performance of the autoregressive forecast error model is concerned that it could effectively minimize the forecasting errors even for those floods associated with the lateral flows. Therefore, it can be inferred from these results that the VPMMDRF model comprising the VPMMD method and the two-parameter autoregressive forecast error estimation model, enables to arrive at an accurate real-time forecasting discharge hydrographs and, subsequently, the estimation of the forecasted stage hydrographs at the Ponte Felcino station for all the ten flood events and for the lead-times up to 2.00 h. However, real-time forecasting results with lead-times of 2.50 h and 3.00 h yield mixed results of accurate and acceptable results, especially near the crest of the flood events analyzed.

Flood forecasting, in general, considered important for forecasting the rising phase of the hydrograph, especially the crest of the hydrograph and its time of occurrence, and to a lesser extent for forecasting the recession phase of the hydrograph. It is evident from Figures 5.3 (a, c, e, g, i, k, m, o, q, and s) and 5.5 (a, c, e, g, i, k, m, o, q, and s), respectively for single and two sub-reaches routing considerations, that the rising phase of the observed discharge hydrographs could be forecasted closely by the VPMMDRF

method for the forecast lead-times up to 2.00 h. Similar behavior can also be seen from Figures 5.3 (b, d, f, h, j, l, n, p, r, and t) and 5.5 (b, d, f, h, j, l, n, p, r, and t), respectively for single and two sub-reaches routing considerations in reproducing the stage forecasted hydrographs by the VPMMDRF method. However, the peak phases of the forecasted discharge and the corresponding computed stage forecast hydrographs show oscillation behavior for the single reach routing consideration forecasting results and to a great extent for the two sub-reaches routing consideration.

It can be inferred from the analysis of the forecasting results that closer forecasting were made for lead-time up to 2.00 h and this aspect could be linked to the travel time of the flood waves over the Pierantonio-Ponte Felcino reach, i.e., the forecast error developed due to the deterministic routing model on account of non availability of input information during the lead-time could be easily modeled by the forecast error model to yield forecast errors required for close reproduction of the observed hydrograph. However, when the lead-time increases beyond 2.00 h in the Pierantonio-Ponte Felcino reach, the forecast error model becomes a crude model without the actual input information and, therefore, the forecast results on the rising part of the hydrograph to be forecasted become inferior.

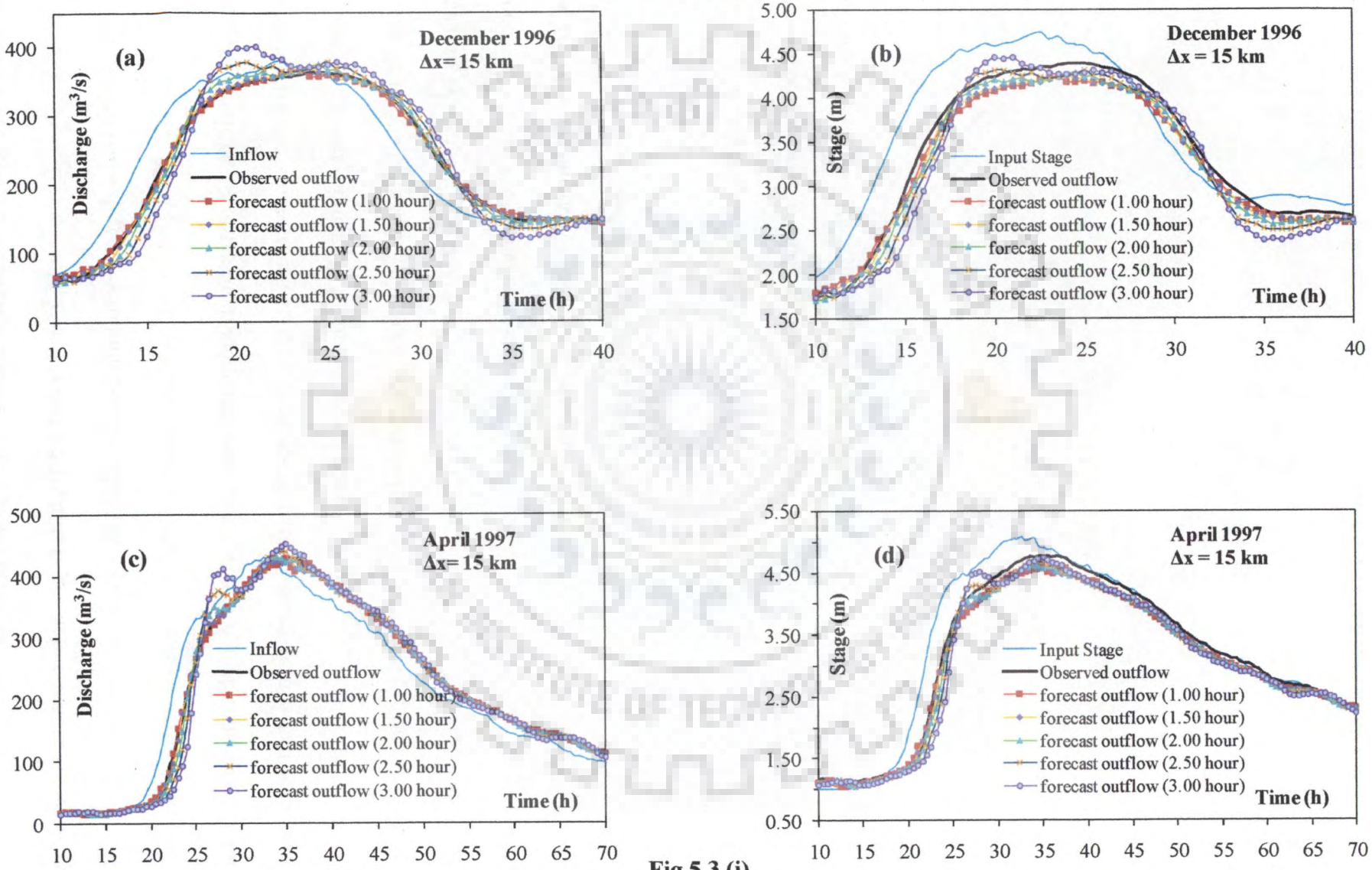
(a)
December 1996
Δx= 15 km
Discharge (m³/s)
Time (h)
Inflow
Observed outflow
forecast outflow (1.00 hour)
forecast outflow (1.50 hour)
forecast outflow (2.00 hour)
forecast outflow (2.50 hour)
forecast outflow (3.00 hour)
(b)
December 1996
Δx = 15 km
Stage (m)
Input Stage
(c)
April 1997
Δx= 15 km
(d)
April 1997
Δx = 15 km

Fig 5.3 (i)

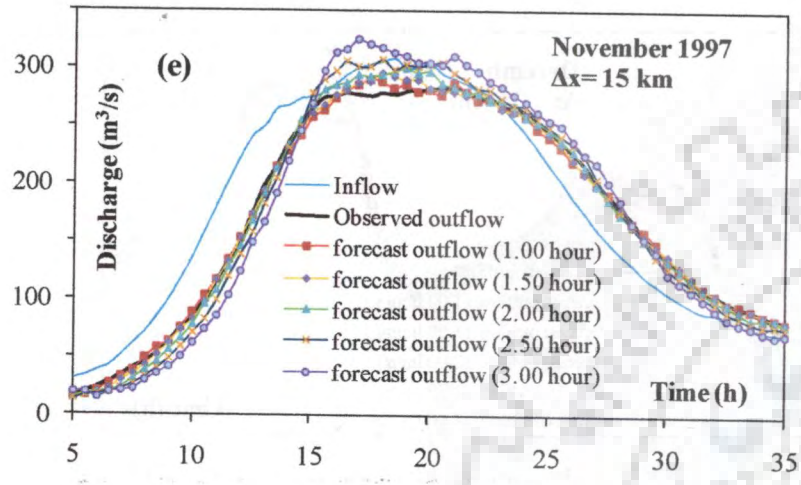
(e)
November 1997
Δx= 15 km
Discharge (m³/s)
Time (h)
Inflow
Observed outflow
forecast outflow (1.00 hour)
forecast outflow (1.50 hour)
forecast outflow (2.00 hour)
forecast outflow (2.50 hour)
forecast outflow (3.00 hour)

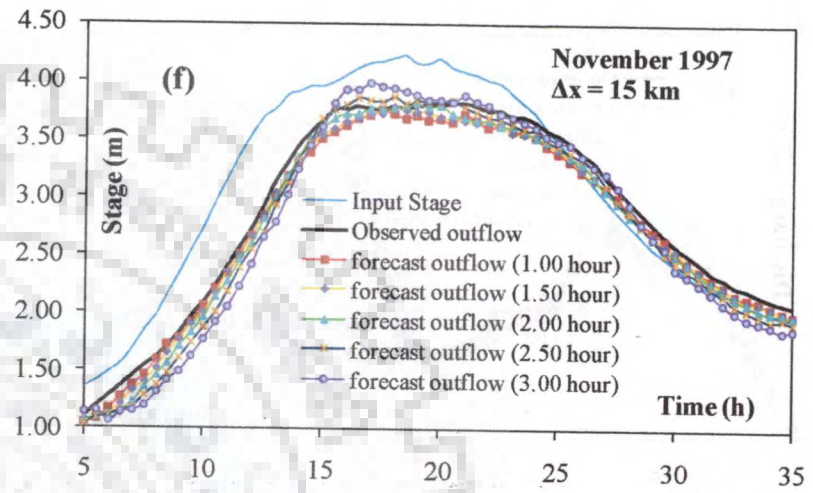
(f)
November 1997
Δx = 15 km
Stage (m)
Time (h)
Input Stage
Observed outflow
forecast outflow (1.00 hour)
forecast outflow (1.50 hour)
forecast outflow (2.00 hour)
forecast outflow (2.50 hour)
forecast outflow (3.00 hour)

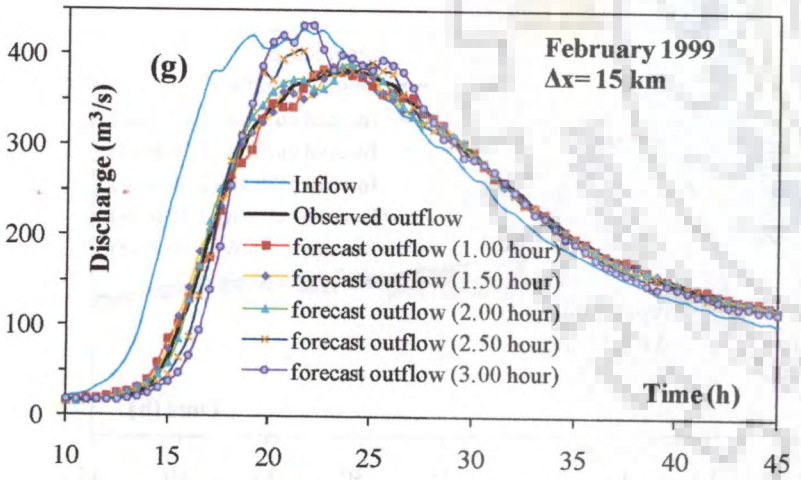
(g)
February 1999
Δx= 15 km
Discharge (m³/s)
Time (h)
Inflow
Observed outflow
forecast outflow (1.00 hour)
forecast outflow (1.50 hour)
forecast outflow (2.00 hour)
forecast outflow (2.50 hour)
forecast outflow (3.00 hour)

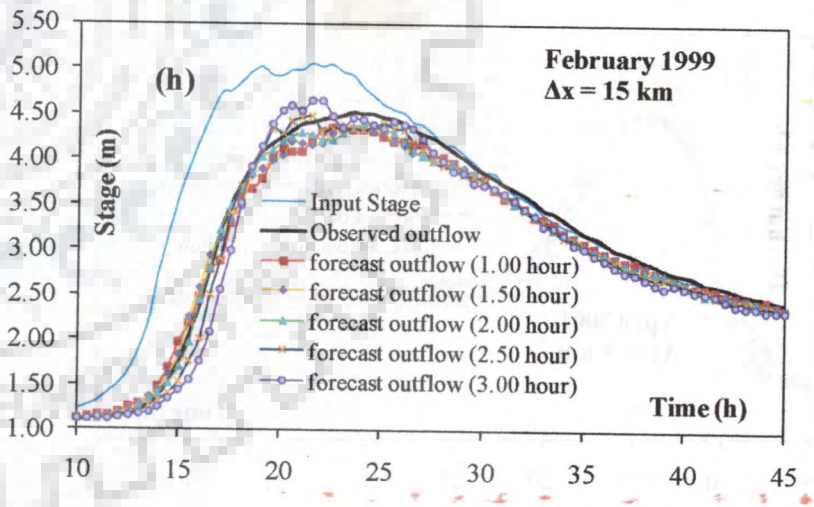
(h)
February 1999
Δx = 15 km
Stage (m)
Time (h)
Input Stage
Observed outflow
forecast outflow (1.00 hour)
forecast outflow (1.50 hour)
forecast outflow (2.00 hour)
forecast outflow (2.50 hour)
forecast outflow (3.00 hour)

Fig 5.3 (ii)

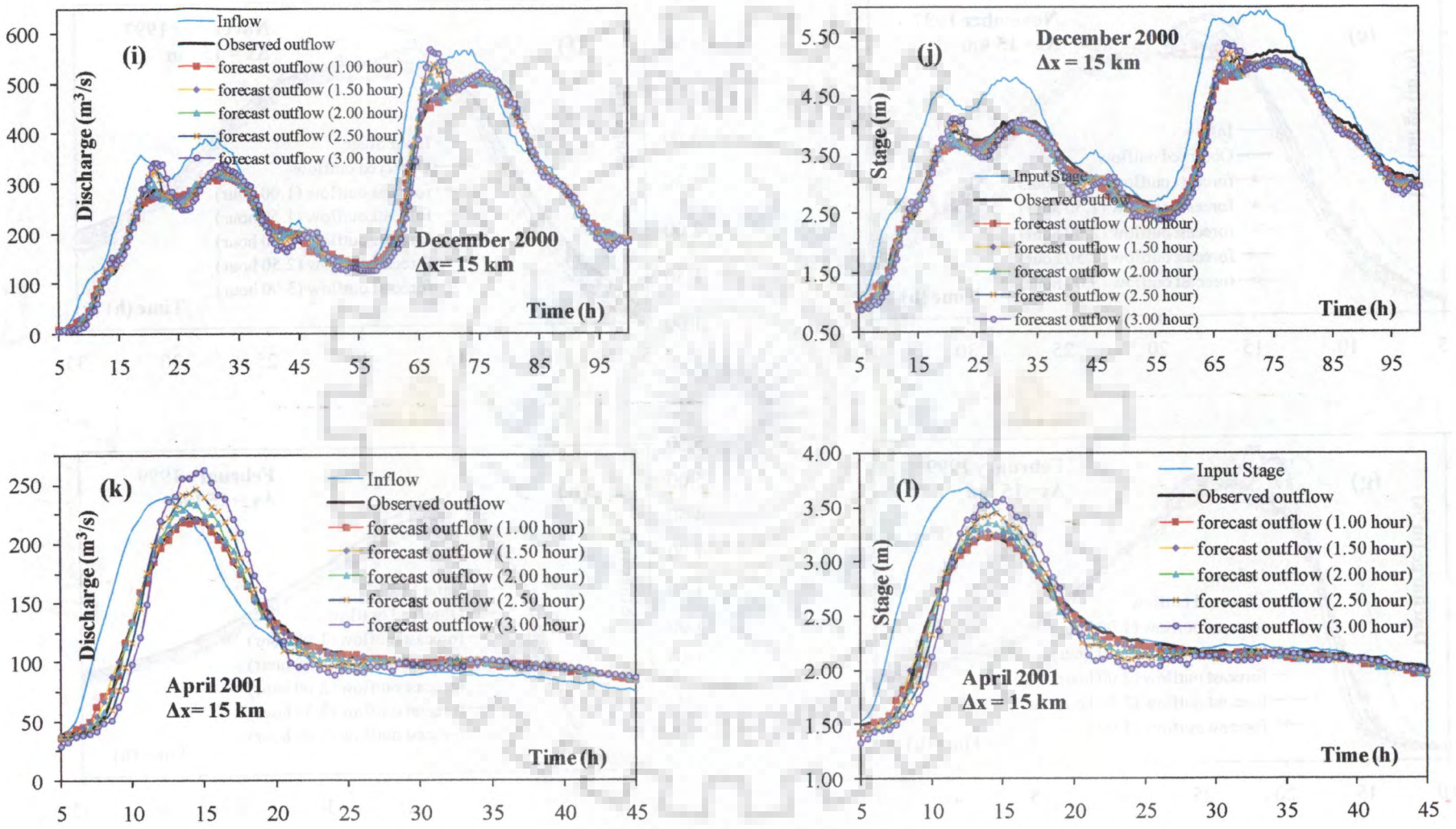
(i)
Inflow
Observed outflow
forecast outflow (1.00 hour)
forecast outflow (1.50 hour)
forecast outflow (2.00 hour)
forecast outflow (2.50 hour)
forecast outflow (3.00 hour)
Discharge (m³/s)
December 2000
Δx= 15 km
Time (h)
(j)
December 2000
Δx = 15 km
Stage (m)
Input Stage
Observed outflow
forecast outflow (1.00 hour)
forecast outflow (1.50 hour)
forecast outflow (2.00 hour)
forecast outflow (2.50 hour)
forecast outflow (3.00 hour)
Time (h)
(k)
Inflow
Observed outflow
forecast outflow (1.00 hour)
forecast outflow (1.50 hour)
forecast outflow (2.00 hour)
forecast outflow (2.50 hour)
forecast outflow (3.00 hour)
Discharge (m³/s)
April 2001
Δx= 15 km
Time (h)
(l)
Input Stage
Observed outflow
forecast outflow (1.00 hour)
forecast outflow (1.50 hour)
forecast outflow (2.00 hour)
forecast outflow (2.50 hour)
forecast outflow (3.00 hour)
Stage (m)
April 2001
Δx = 15 km
Time (h)

Fig 5.3 (iii)

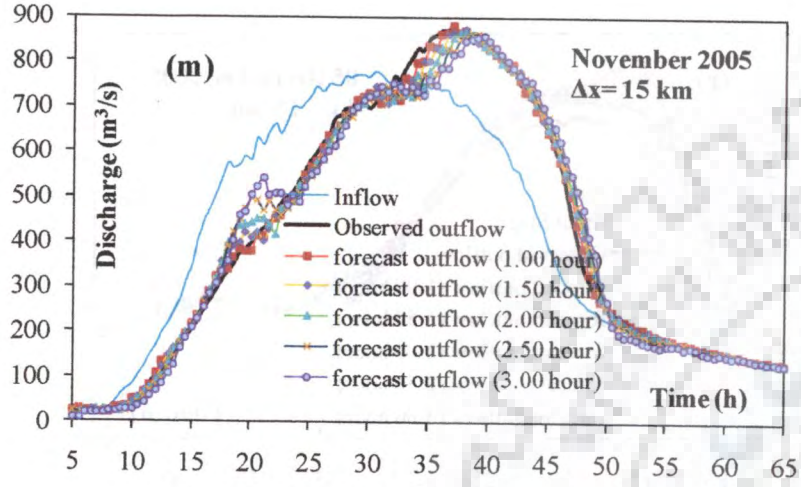
(m)
November 2005
Δx= 15 km
Discharge (m³/s)
Time (h)
Inflow
Observed outflow
forecast outflow (1.00 hour)
forecast outflow (1.50 hour)
forecast outflow (2.00 hour)
forecast outflow (2.50 hour)
forecast outflow (3.00 hour)

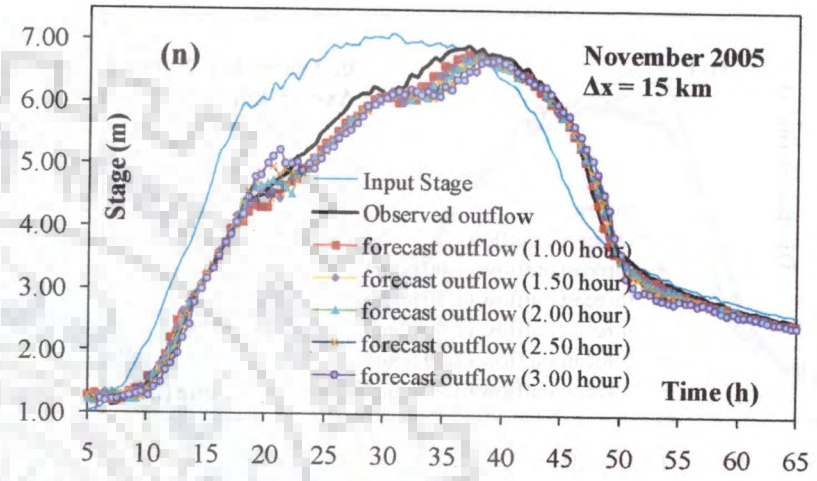
(n)
November 2005
Δx = 15 km
Stage (m)
Time (h)
Input Stage
Observed outflow
forecast outflow (1.00 hour)
forecast outflow (1.50 hour)
forecast outflow (2.00 hour)
forecast outflow (2.50 hour)
forecast outflow (3.00 hour)

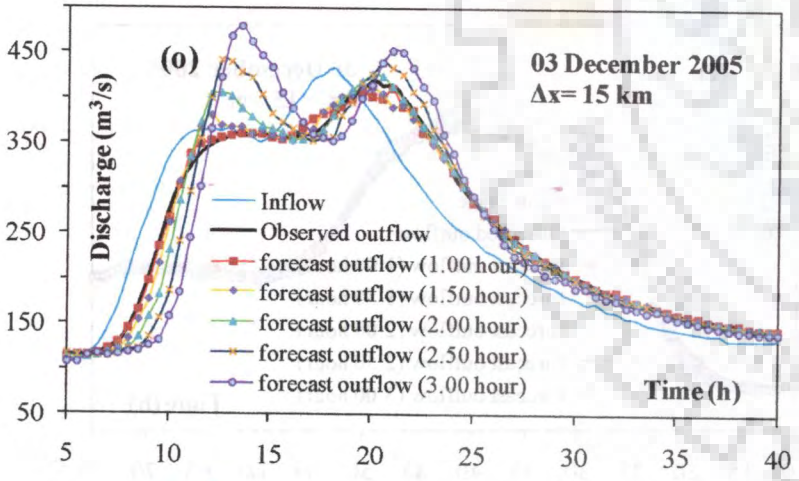
(o)
03 December 2005
Δx= 15 km
Discharge (m³/s)
Time (h)
Inflow
Observed outflow
forecast outflow (1.00 hour)
forecast outflow (1.50 hour)
forecast outflow (2.00 hour)
forecast outflow (2.50 hour)
forecast outflow (3.00 hour)

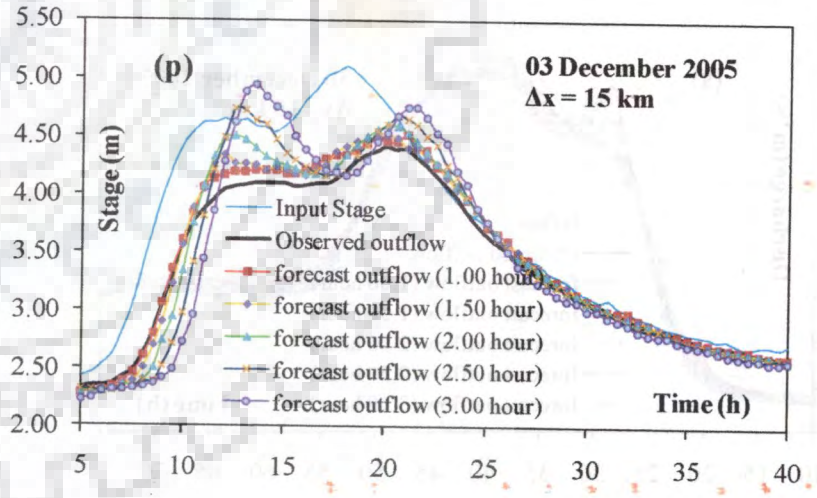
(p)
03 December 2005
Δx = 15 km
Stage (m)
Time (h)
Input Stage
Observed outflow
forecast outflow (1.00 hour)
forecast outflow (1.50 hour)
forecast outflow (2.00 hour)
forecast outflow (2.50 hour)
forecast outflow (3.00 hour)

Fig 5.3 (iv)

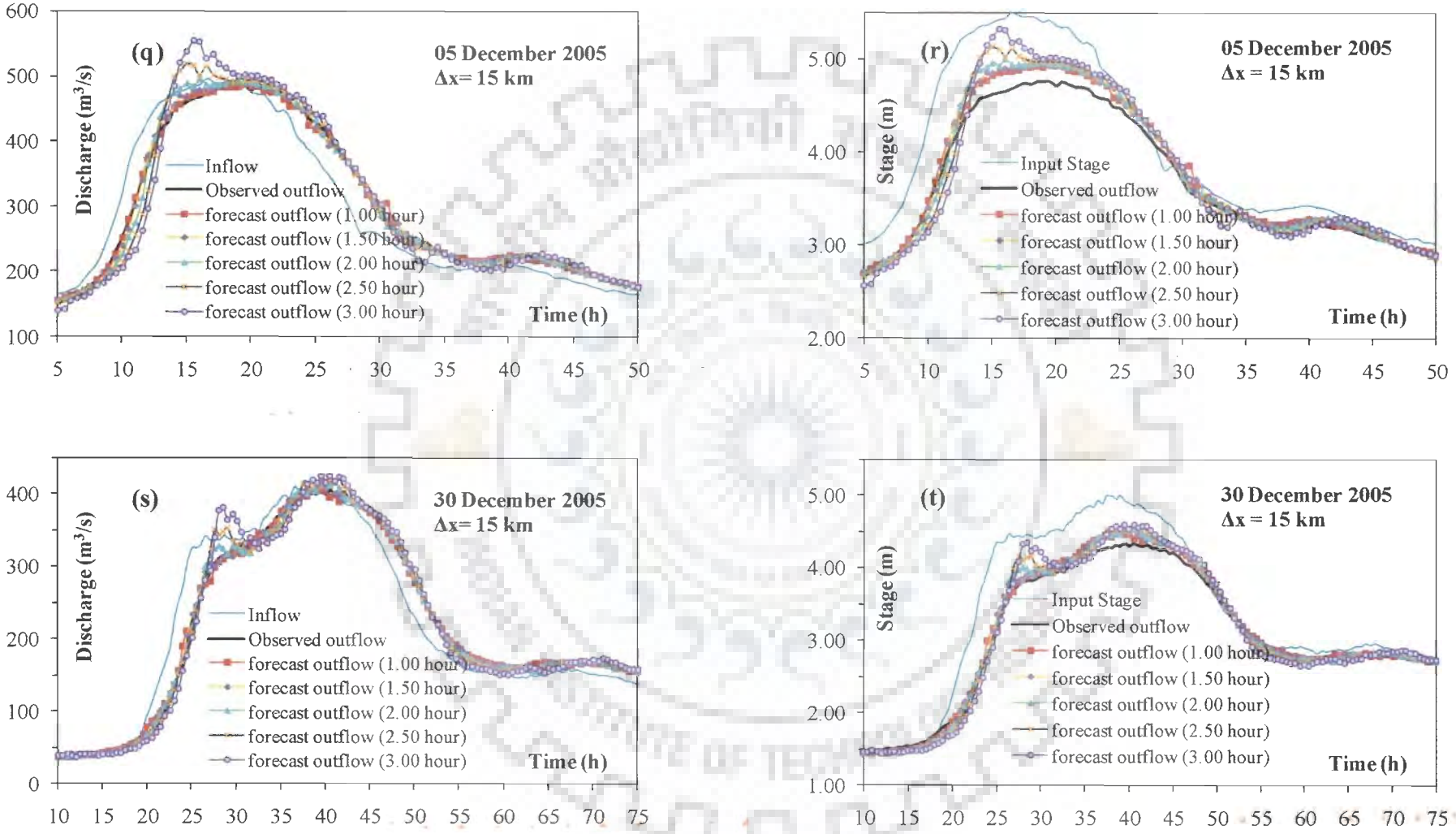

Figure 5.3 Discharge and the computed stage forecast hydrographs by the VPMMDRF method at the Ponte Felcino station of the Pierantonio-Ponte Felcino reach for different flood events arrived at using a single reach routing (Δx= 15 km).

Figure 5.4 shows that the forecasting hydrographs estimated by the VPMMDRF method with the consideration of the autoregressive error estimates closely reproduce the observed hydrograph, whereas the forecasting hydrograph estimated without considering the forecast error estimates produce lagged forecasted hydrographs in comparison with the observed hydrographs. This inference has been arrived at by employing a single reach consideration of the Pierantonio-Pote Felcino reach with a lead-time of 3.00 h for the flood events that occurred on (a) December 1996 and (b) November 1997 at Ponte Felcino gauging station.

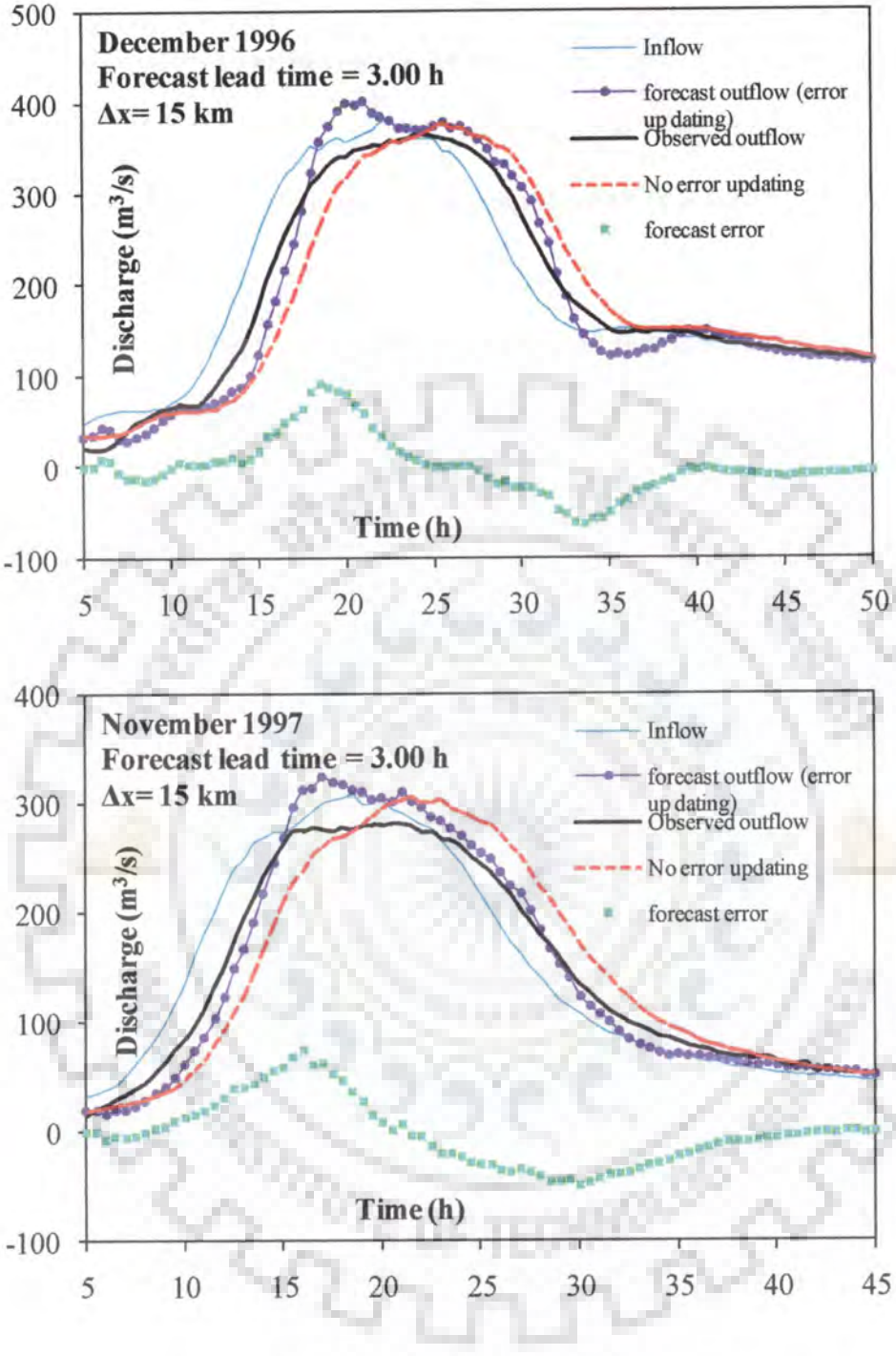

Figure 5.4 Observed discharge hydrograph at the Ponte Felcino station and the corresponding forecasted discharge hydrograph by the VPMMDRF method for a lead-time of 3.00 h with and without considering the error estimation model, and considering single reach routing.

Table 5.7 Forecasting results of the VPMMDRF method for a lead-time of 1.00 hour and a space step of Δx= 7.5 km (2 sub-reaches).

Sl. No.	Flood Event	Discharge Forecast				Computed Stage Forecast		
		q_{per} (%)	t_{pqer} (h)	η_q (%)	PC (%)	y_{per} (%)	t_{pyer} (h)	η_y (%)
1	December, 1996	1.56	0.00	99.88	96.00	-3.10	0.00	98.90
2	April, 1997	0.14	0.50	99.92	94.07	-3.62	0.50	99.14
3	November, 1997	3.05	-1.50	99.85	95.53	-1.71	-1.50	98.94
4	February, 1999	0.79	0.50	99.83	94.52	-3.43	0.50	99.09
5	December, 2000	-0.55	0.50	99.65	82.65	-3.86	0.50	98.06
6	Apr. 2001	1.25	0.50	99.69	96.02	1.47	0.50	98.88
7	November, 2005	0.31	1.00	99.70	80.35	-1.42	1.00	99.27
8	03 Dec.2005	0.11	0.00	99.64	93.04	3.22	0.00	98.38
9	05 Dec. 2005	0.94	-0.50	99.82	93.93	4.41	-0.50	97.66
10	30 Dec. 2005	1.73	0.50	99.87	89.84	4.09	0.50	99.39
	Mean value			**99.79**	**91.60**			**98.77**

Table 5.8 As in Table 5.7, but for a lead-time of 1.50 hour

Sl. No.	Flood Event	Discharge Forecast				Computed Stage Forecast		
		q_{per} (%)	t_{pqer} (h)	η_q (%)	PC (%)	y_{per} (%)	t_{pyer} (h)	η_y (%)
1	December, 1996	4.14	1.50	99.08	86.72	-1.75	1.50	98.47
2	April, 1997	2.89	-1.00	99.53	84.88	-2.10	-1.00	98.92
3	November, 1997	5.77	-4.00	99.27	90.03	0.14	-4.00	98.49
4	February, 1999	2.57	1.00	99.24	88.69	-2.52	1.00	98.87
5	December, 2000	2.51	-7.50	98.93	75.87	-2.02	-7.50	97.67
6	Apr. 2001	8.64	-0.50	97.00	82.26	5.89	-0.50	95.40
7	November, 2005	-0.10	1.50	99.36	80.86	-1.69	1.50	99.10
8	03 Dec.2005	3.99	0.00	96.31	67.01	5.77	0.00	94.60
9	05 Dec. 2005	2.11	-4.50	98.68	80.10	6.22	-4.50	95.89
10	30 Dec. 2005	2.77	1.00	99.56	84.52	4.72	1.00	98.88
	Mean value			**98.70**	**82.09**			**97.63**

Table 5.9 As in Table 5.7, but for a lead-time of 2.00 hour

Sl. No.	Flood Event	Discharge Forecast				Computed Stage Forecast		
		q_{per} (%)	t_{pqer} (h)	η_q (%)	PC (%)	y_{per} (%)	t_{pyer} (h)	η_y (%)
1	December, 1996	8.87	-4.00	95.83	65.36	1.73	-4.00	96.03
2	April, 1997	6.13	0.00	98.16	66.04	-0.38	0.00	97.89
3	November, 1997	15.78	-3.50	96.65	73.89	5.55	-3.50	96.64
4	February, 1999	14.65	-2.50	96.46	69.77	4.36	-2.50	96.95
5	December, 2000	10.56	-7.00	96.44	53.61	2.36	-7.00	95.70
6	Apr. 2001	18.56	0.00	86.23	52.74	11.43	0.00	84.88
7	November, 2005	-0.78	2.00	98.65	76.54	-2.05	2.00	98.51
8	03 Dec.2005	8.96	1.00	85.98	26.83	9.92	-6.50	85.17
9	05 Dec. 2005	11.74	-4.00	95.22	58.68	12.21	-4.00	91.74
10	30 Dec. 2005	4.21	1.00	98.46	68.82	5.63	1.00	97.52
	Mean value			**94.81**	**61.23**			**94.10**

Table 5.10 As in Table 5.7, but for a lead-time of 2.50 hour

Sl. No.	Flood Event	Discharge Forecast				Computed Stage Forecast		
		q_{per} (%)	t_{pqer} (h)	η_q (%)	PC (%)	y_{per} (%)	t_{pyer} (h)	η_y (%)
1	December, 1996	17.77	-3.00	88.93	39.85	6.39	-3.00	91.02
2	April, 1997	8.03	0.50	95.50	45.94	0.89	-7.00	95.90
3	November, 1997	27.34	-3.00	90.40	51.27	11.44	-3.00	91.87
4	February, 1999	23.68	-1.50	89.54	41.53	9.31	-2.00	92.28
5	December, 2000	19.06	-7.00	91.54	27.38	7.14	-7.00	91.96
6	Apr. 2001	27.70	0.50	60.89	11.19	16.51	0.50	63.28
7	November, 2005	-0.81	2.50	97.44	71.11	-2.12	2.50	97.24
8	03 Dec.2005	17.03	-5.50	68.46	-9.88	14.88	-5.50	70.49
9	05 Dec. 2005	21.89	-2.50	89.11	38.51	17.73	-2.50	85.11
10	30 Dec. 2005	5.85	1.00	96.18	49.73	6.80	-9.50	94.99
	Mean value			**86.80**	**36.66**			**87.42**

Table 5.11 As in Table 5.7, but for a lead-time of 3.00 hour

Sl. No.	Flood Event	Discharge Forecast				Computed Stage Forecast		
		q_{per} (%)	t_{pqer} (h)	η_q (%)	PC (%)	y_{per} (%)	t_{pyer} (h)	η_y (%)
1	December, 1996	26.57	-1.50	77.85	14.34	10.67	-1.50	83.05
2	April, 1997	16.56	-5.50	91.70	29.33	6.23	-5.50	93.13
3	November, 1997	35.31	-2.00	79.58	26.75	15.40	-2.00	83.40
4	February, 1999	39.71	-1.50	77.92	12.21	17.63	-1.50	84.84
5	December, 2000	28.84	-5.50	84.01	1.98	11.85	-5.50	86.39
6	Apr. 2001	42.41	1.00	18.03	-34.17	24.30	1.00	29.82
7	November, 2005	-2.58	2.00	95.55	64.33	-3.12	2.00	95.03
8	03 Dec.2005	24.56	-4.00	47.09	-34.17	18.72	-4.00	52.26
9	05 Dec. 2005	27.33	-2.00	79.97	19.76	21.00	-2.00	75.58
10	30 Dec. 2005	11.55	-8.50	92.55	30.78	10.85	-8.50	91.13
	Mean value			**74.42**	**13.11**			**77.46**

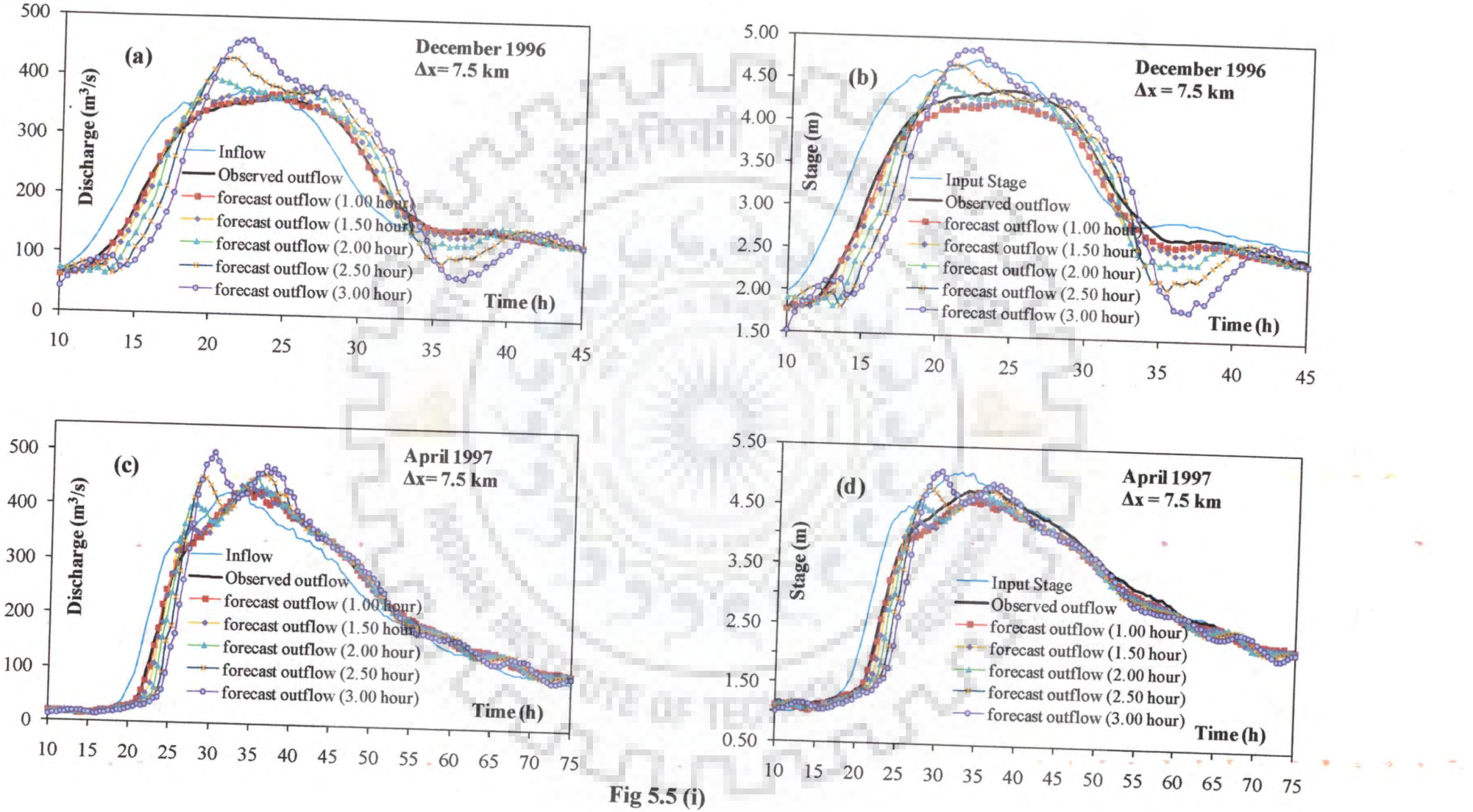
(a)
December 1996
Δx= 7.5 km
Discharge (m³/s)
Time (h)
Inflow
Observed outflow
forecast outflow (1.00 hour)
forecast outflow (1.50 hour)
forecast outflow (2.00 hour)
forecast outflow (2.50 hour)
forecast outflow (3.00 hour)
(b)
December 1996
Δx = 7.5 km
Stage (m)
Time (h)
Input Stage
Observed outflow
forecast outflow (1.00 hour)
forecast outflow (1.50 hour)
forecast outflow (2.00 hour)
forecast outflow (2.50 hour)
forecast outflow (3.00 hour)
(c)
April 1997
Δx= 7.5 km
Discharge (m³/s)
Time (h)
Inflow
Observed outflow
forecast outflow (1.00 hour)
forecast outflow (1.50 hour)
forecast outflow (2.00 hour)
forecast outflow (2.50 hour)
forecast outflow (3.00 hour)
(d)
April 1997
Δx = 7.5 km
Stage (m)
Time (h)
Input Stage
Observed outflow
forecast outflow (1.00 hour)
forecast outflow (1.50 hour)
forecast outflow (2.00 hour)
forecast outflow (2.50 hour)
forecast outflow (3.00 hour)

Fig 5.5 (i)

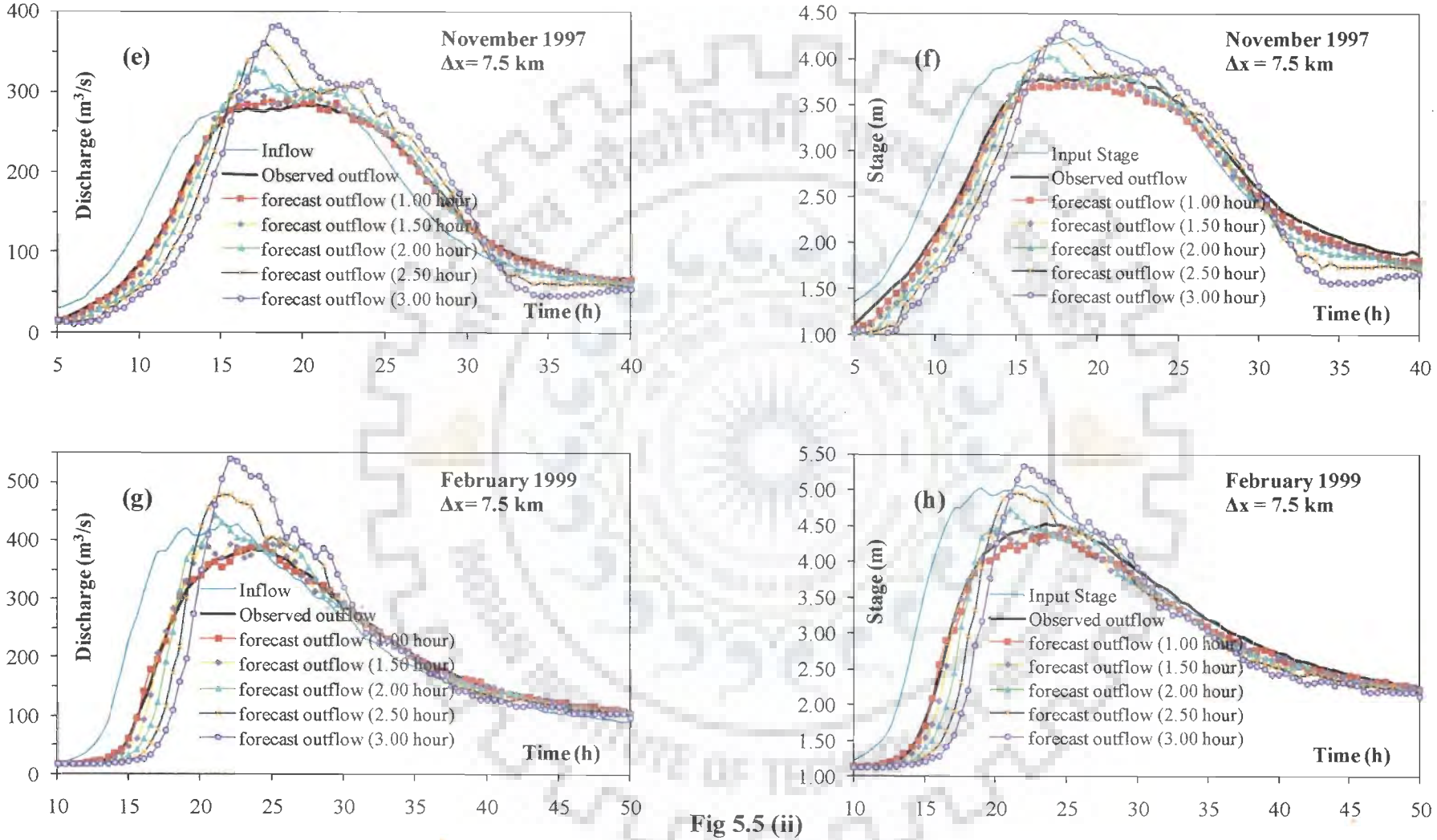
(e)
November 1997
Δx= 7.5 km
Discharge (m³/s)
Time (h)
Inflow
Observed outflow
forecast outflow (1.00 hour)
forecast outflow (1.50 hour)
forecast outflow (2.00 hour)
forecast outflow (2.50 hour)
forecast outflow (3.00 hour)
(f)
November 1997
Δx = 7.5 km
Stage (m)
Time (h)
Input Stage
Observed outflow
forecast outflow (1.00 hour)
forecast outflow (1.50 hour)
forecast outflow (2.00 hour)
forecast outflow (2.50 hour)
forecast outflow (3.00 hour)
(g)
February 1999
Δx= 7.5 km
Discharge (m³/s)
Time (h)
Inflow
Observed outflow
forecast outflow (1.00 hour)
forecast outflow (1.50 hour)
forecast outflow (2.00 hour)
forecast outflow (2.50 hour)
forecast outflow (3.00 hour)
(h)
February 1999
Δx = 7.5 km
Stage (m)
Time (h)
Input Stage
Observed outflow
forecast outflow (1.00 hour)
forecast outflow (1.50 hour)
forecast outflow (2.00 hour)
forecast outflow (2.50 hour)
forecast outflow (3.00 hour)

Fig 5.5 (ii)

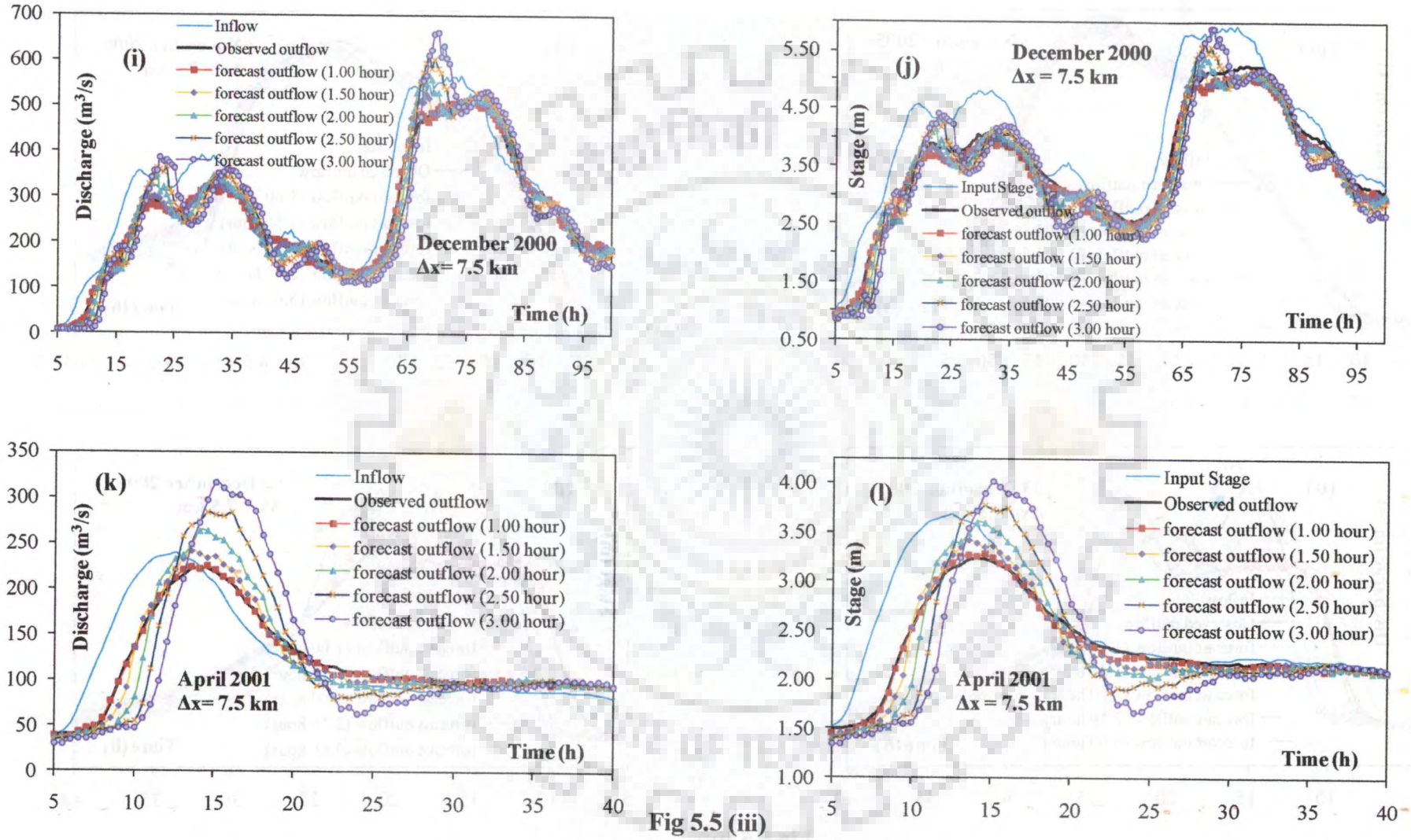
(i)
Inflow
Observed outflow
forecast outflow (1.00 hour)
forecast outflow (1.50 hour)
forecast outflow (2.00 hour)
forecast outflow (2.50 hour)
forecast outflow (3.00 hour)
Discharge (m³/s)
December 2000
Δx= 7.5 km
Time (h)
(j)
December 2000
Δx = 7.5 km
Stage (m)
Input Stage
Observed outflow
forecast outflow (1.00 hour)
forecast outflow (1.50 hour)
forecast outflow (2.00 hour)
forecast outflow (2.50 hour)
forecast outflow (3.00 hour)
Time (h)
(k)
Inflow
Observed outflow
forecast outflow (1.00 hour)
forecast outflow (1.50 hour)
forecast outflow (2.00 hour)
forecast outflow (2.50 hour)
forecast outflow (3.00 hour)
Discharge (m³/s)
April 2001
Δx= 7.5 km
Time (h)
(l)
Input Stage
Observed outflow
forecast outflow (1.00 hour)
forecast outflow (1.50 hour)
forecast outflow (2.00 hour)
forecast outflow (2.50 hour)
forecast outflow (3.00 hour)
Stage (m)
April 2001
Δx = 7.5 km
Time (h)

Fig 5.5 (iii)

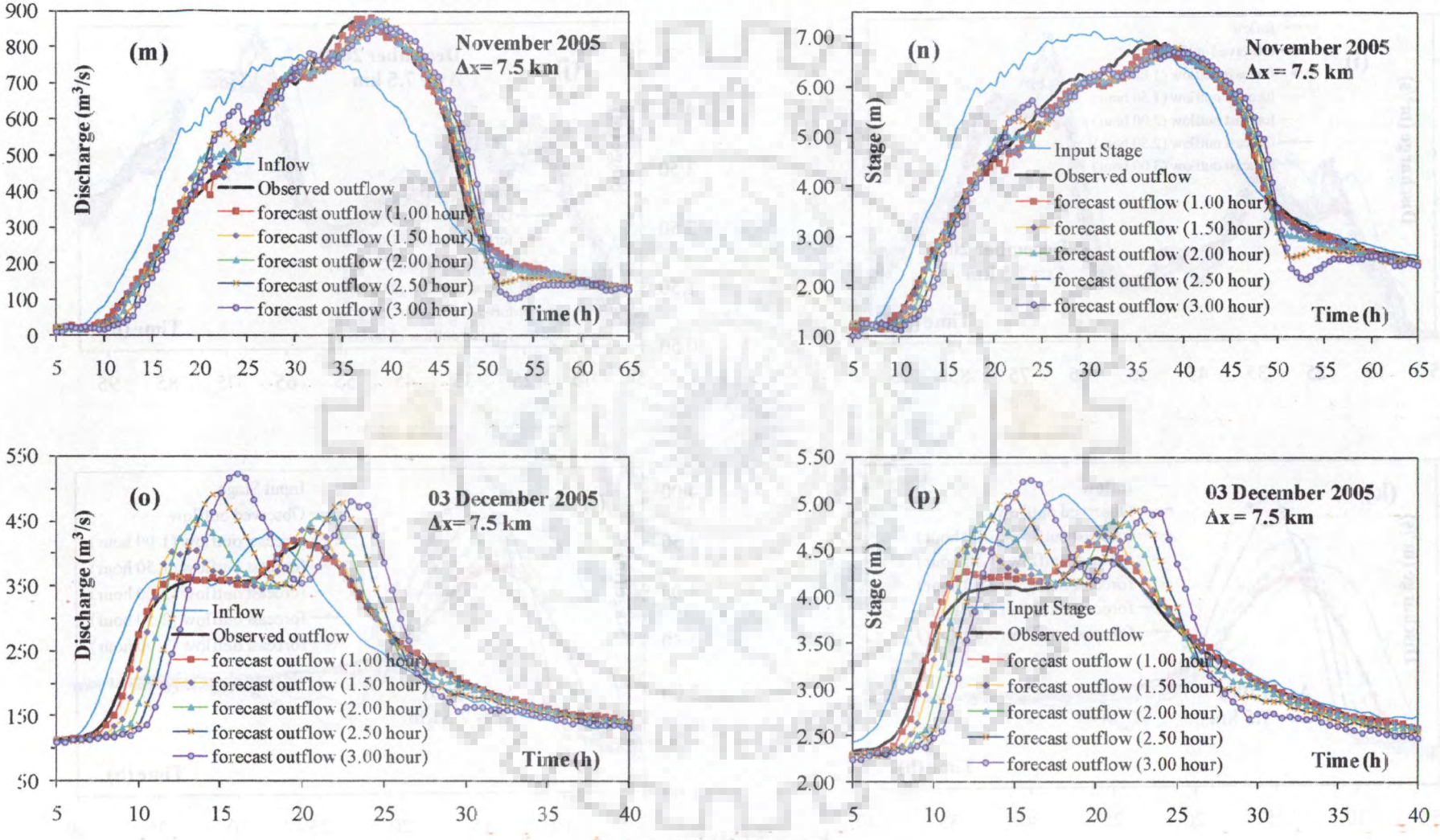
(m)
November 2005
Δx= 7.5 km
Discharge (m³/s)
Time (h)
Inflow
Observed outflow
forecast outflow (1.00 hour)
forecast outflow (1.50 hour)
forecast outflow (2.00 hour)
forecast outflow (2.50 hour)
forecast outflow (3.00 hour)
(n)
November 2005
Δx = 7.5 km
Stage (m)
Time (h)
Input Stage
Observed outflow
forecast outflow (1.00 hour)
forecast outflow (1.50 hour)
forecast outflow (2.00 hour)
forecast outflow (2.50 hour)
forecast outflow (3.00 hour)
(o)
03 December 2005
Δx= 7.5 km
Discharge (m³/s)
Time (h)
Inflow
Observed outflow
forecast outflow (1.00 hour)
forecast outflow (1.50 hour)
forecast outflow (2.00 hour)
forecast outflow (2.50 hour)
forecast outflow (3.00 hour)
(p)
03 December 2005
Δx = 7.5 km
Stage (m)
Time (h)
Input Stage
Observed outflow
forecast outflow (1.00 hour)
forecast outflow (1.50 hour)
forecast outflow (2.00 hour)
forecast outflow (2.50 hour)
forecast outflow (3.00 hour)

Fig 5.5 (iv)

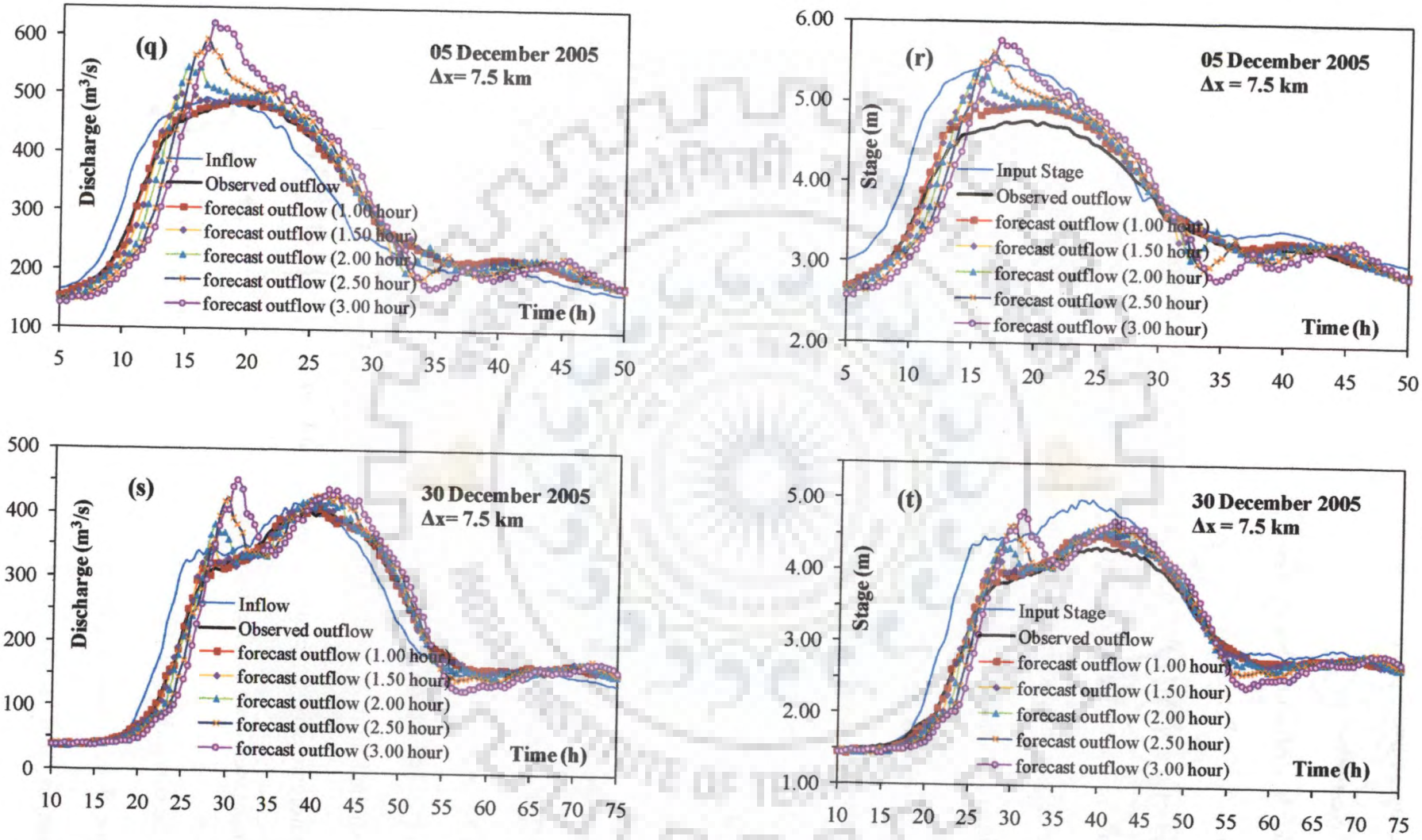

Figure 5.5 : Discharge and the computed stage forecast hydrographs by the VPMMDRF method at the Ponte Felcino station of the Pierantonio-Ponte Felcino reach for different flood events arrived at using two sub-reaches routing (Δx= 7.5 km).

5.6 SUMMARY AND CONCLUDING REMARKS

The discharge hydrograph forecasting and the corresponding stage hydrograph forecasting estimated at the Ponte Felcino station based on the study of ten different flood events and for different forecast lead-time intervals of up to 3.00 h over the 15 km long Pierantonio-Ponte Felcino reach of the Tiber River in Central Italy demonstrate the usefulness of the VPMMDRF method for forecasting at the Ponte Felcino station. This forecasting method developed based on the use of rating curves and cross-section details available only at the end-sections of the routing reach demonstrates that the hydrometric forecasting of floods could be done efficiently with limited data.

The results obtained for a single reach routing consideration (Δx= 15 km) and for two sub-reaches routing consideration (Δx= 7.15 km) reveal that, in general, the single reach routing based forecasts are better than the forecast based on two sub-reaches routing consideration, as the forecast error of the latter case accumulates at each node point which ultimately leads to high oscillations in the forecasted hydrographs.

The discharge forecasting and the corresponding stage forecasting capability of the VPMMDRF method is good for lower values of forecast lead-times, whereas it is not so for higher values of forecasting lead-times. However, the VPMMDRF method is performing well up to 3.00 h lead-time for single reach consideration for many of the events studied. Further, as the forecasting errors are efficiently minimized by the second order autoregressive forecast error estimation model, the VPMMDRF method is equally performing well even for the flood events having significant lateral flows.

It may be concluded that the VPMMDRF method can be used for hydrometric data-based real-time flood forecasting at a river gauging station in order to forecast the discharge hydrographs and simultaneously to forecast the corresponding estimated stage

hydrographs for lead-times up to approximately corresponding to the average travel time of the flood wave.

6 CONCLUSIONS

6.1 GENERAL

The main objective of the thesis has been to develop a routing procedure, based on a simplified hydraulic routing method, suitable for field applications under data deficient conditions, but at the same time its results are accurate enough to serve the practical purposes. With this consideration, the Variable Parameter McCarthy-Muskingum Discharge-routing (VPMMD) method advocated by *Price and Perumal* [2011] for routing in prismatic main channels was suitably amended for its applications under morphometric data deficient conditions. The amendment has been made for developing a routing procedure based on the reach-averaged rating curve and cross-section information obtained using the cross-sections and the rating curves information available only at the end-sections of the reach.

6.2 CONCLUSIONS

On the basis of the study carried out in this thesis, the following conclusions can be drawn:

1. The routing procedure developed in this study using the VPMMD method based on the reach-averaged normal rating curves of the end-sections of the routing reach and the associated channel cross-section information at these two sections enables the discharge hydrograph routing in channels with main and flood plain sections. The estimation of the corresponding stage hydrograph at the required river gauging station can also be obtained. The study reveals that this routing procedure is able to reproduce almost all the benchmark solutions of the synthetic

hydrograph routings very closely with the overall reproductions of the benchmark solutions >99% and with near zero mass conservation errors for all the hypothetical simulation studies.

2. In addition to the verification of the method using hypothetical studies, its field applications were also demonstrated by routing four-synthetic floods in longer (50km) and ten real flood events in shorter (15 km) length natural reaches of the Upper Tiber River in Central Italy. These routed results reveal that the routing procedure developed using the VPMMD method is capable of accurately routing the discharge hydrographs, and computing stage hydrographs at the required downstream gauging stations.

3. An investigation was also carried out to arrive at the applicability limits of the VPMMD method for discharge hydrograph routing and for simultaneously computing the stage hydrographs in prismatic rectangular and trapezoidal channel cross-sectional reaches without floodplains. The appropriateness of the use of scaled longitudinal water surface gradient $(1/S_o)(\partial y/\partial x)$ of the input stage hydrograph as the applicability criteria for determining the applicability limits of the VPMMD method is brought out. The appropriateness of using this criterion was verified through a number of numerical experiments covering a wide range of combinations of channel characteristics (i.e., channel bed slope and Manning's roughness coefficients) and upstream flow characteristics (i.e., peak, time to peak, and shape factor). On the basis of this study, it is inferred that the applicability of the VPMMD method to be assessed at the inlet of the reach for routing a given hydrograph require to satisfy the following criteria:

For discharge routing with ≤ 5% error in reproducing the pertinent characteristics of the corresponding benchmark solutions $(1/S_o)(\partial y/\partial x)_{max} \leq 0.57$

For stage computation with ≤ 5% error in reproducing the pertinent characteristics of the corresponding benchmark solutions $(1/S_o)(\partial y/\partial x)_{max} \leq 0.61$

Therefore, the VPMMD method can be conveniently used for routing floods within its applicability limits for many of the real-world flood routing problems.

4. The VPMMD method is also used for real-time flood forecasting applications over a selected river reach. A Variable Parameter McCarthy-Muskingum Discharge Real-Time Flood Forecasting (VPMMDRF) method is proposed using the VPMMD routing method as the basic model, in association with the second-order linear autoregressive model as the forecast error updating model. The study reveals that the proposed VPMMDRF method is amenable for real-time discharge hydrograph forecasting and its corresponding computed stage hydrograph forecasting up to a lead-time of 3 hours in a 15 km length of the river reach between Pierantonio and Ponte Felcino of the Tiber River in Central Italy.

6.3 FUTURE PROSPECTIVES

1. The limitations of the proposed study include the assumption of no lateral flow in the study reach. However, this simplified variable parameter method can account for the point lateral flow in the form of flows from river tributaries, and not as the distributed lateral flow. Accounting the distributed lateral flow contributions along the river reach may improve the accuracy of the real-time flood forecasted estimates. Hence the extension of this method to accommodate the distributed lateral flow contribution along the river reach forms the possible future work.

2. The capability of the proposed simplified variable parameter method needs to be investigated to establish the rating curves at the ungauged river stations.

ANNEXURE I

EQUATIONS EMPLOYED FOR PRICE'S [*PRICE*, 2009] SYNTHETIC RIVER CHANNEL STUDY

For the main channel:

$$A_c = \left[2B_b + s\left(y_{fl} + y\right)\right]\left(y_{fl} + y\right) \tag{I-1}$$

$$B_c = 2\left[B_b + s\left(y_{fl} + y\right)\right] \tag{I-2}$$

$$P_c = 2\left[B_b + \sqrt{1+s^2}\left(y_{fl} + y\right)\right] \tag{I-3}$$

$$\frac{dP_c}{dy} = 2\sqrt{1+s^2} \tag{I-4}$$

For the floodplains:

$$A_f = \left[B_{fl} - \frac{\left(B_t - B_{fl}\right)}{\tanh\left(-ky_{fl}\right)} - 2\left(B_b + sy_{fl}\right) - s\left(y - y_x\right)\right]\left(y_x + y\right) - \frac{\left(B_t - B_{fl}\right)}{k\tanh\left(-ky_{fl}\right)} \ln\left[\frac{1-\tanh\left(ky_x\right)}{1-\tanh\left(-ky\right)}\right] \tag{I-5}$$

$$B_f = B_{fl} + \frac{\left(B_b - B_{fl}\right)\tan h(ky)}{\tanh\left(-ky_{fl}\right)} - B_c \tag{I-6}$$

$$P_f^{(i+1)} = P_f^i + \Delta y\sqrt{1+\left(\frac{dB_f}{dy}\right)^2} \tag{I-7}$$

$$\frac{dB_f}{dy} = \frac{\left(B_b - B_{fl}\right)k\left[1-\tanh^2\left(ky\right)\right]}{\tanh\left(-ky_{fl}\right)} \tag{I-8}$$

$$\frac{dP_f}{dy} = \sqrt{1+\left(\frac{dB_f}{dy}\right)^2} \tag{I-9}$$

$$Q_c = A_c\left(\frac{A_c}{P_c}\right)^{2/3}\frac{s_o^{1/2}}{n_c} \tag{I-10}$$

$$Q_f = A_f\left(\frac{A_f}{P_f}\right)^{2/3}\frac{s_o^{1/2}}{n_f} \tag{I-11}$$

$$Q = Q_c + 2Q_f \tag{I-12}$$

$$A = A_c + 2A_f \tag{I-13}$$

$$B = B_c + 2B_f \tag{I-14}$$

$$c_o(Q) = \frac{Q_c}{3B}\left(\frac{5B_c}{A_c} - \frac{2dP_c/dy}{P_c}\right) + \frac{2Q_f}{3B}\left(\frac{5B_f}{A_f} - \frac{2dP_f/dy}{P_f}\right) \tag{I-15}$$

$$a_o(Q) = \frac{Q}{2S_oB}\left\{1 - \frac{B}{gA}\left(c_o(Q) - \frac{Q}{A}\right)^2\right\} \tag{I-16}$$

```
      DIMENSION VNR(30000), ak(30000),theta(30000)
      dimension y_equivalent(30000),y_actual(30000)
      character*25 fyle,fylea
c           supply summary table file name
      open(unit=1,file='summarytable_vpmmdfp.txt',
     1 status='unknown')
      write(1,108)
c           reading total number of input files and their file names
      write(*,*)'Enter number of input files'
      read*,l
      do 999 l=1,l
c           reading input file name from the text file
      open(unit=20,file='inputfilenames.txt')
      read(20,215)fyle
215   format(a)
      open(unit=2,file=fyle,status='unknown')
c           reading output file name from the text file
      open(unit=30,file='outputfilenames.txt')
      read(30,215)fylea
      open(unit=4,file=fylea,status='unknown')
c           reading dydxmax file name from the text file
      open(unit=40,file='dydxfilenames.txt')
      read(40,215)fyle
      open(unit=3,file=fyle,status='unknown')
C ***************************************************************
C     DESCRIPTION OF INPUT DATA
C     N      - TOTAL NUMBER OF INFLOW AND OUTFLOW VARIABLES
C     DT     - ROUTING TIME INTERVAL
C     SO     - CHANNEL BED SLOPE
C     TTL    - TOTAL LENGTH OF THE REACH
C     ANREACH- NUMBER OF SUBREACHES USED IN THE GIVEN ROUTING
C              REACH
c     JUMP   - NUMBER OF ROUTING INTERVALS TO BE SKIPPED FOR
C              INCRIMENTING THE ROUTING INTERVAL
C     REQLEN- DESIRED LENGTH OF REACH AT WHICH ROUTING
C     RESULTS ARE TO BE OBTAINED
C     QO     - INITIAL DISCHARGE
C     YO     - INITIAL FLOW DEPTH
C     CO     - INITIAL CELERITY
C     BO     - INITIAL SURFACE WIDTH
C     YNR    - NORMAL FLOW DEPTH
C     QNR    - NORMAL DISCHARGE
C     CNR    - NORMAL CELERITY
C     BNR    - NORMAL SURFACE WIDTH
c     VNR    - NORMAL VELOCITY
C K- NUMBER OF ORDINATES IN EACH COLUMN OF THE LOOK-UP TABLES
```

```
C       L       - NUMBER OF INPUT FILES
C*****************************************************************
        READ(2,*)N,DT,YO,SO,TTL,ANREACH,JUMP,REQLEN
        WRITE(4,99)N,DT,YO,SO,TTL,ANREACH,JUMP
99      FORMAT(20X,'NO.OF ORDINATES=',I6/20X,'ROUTING TIME INTERVAL
        (IN SEC.
       1 )=',F8.2/20X,'INITIAL DEPTH(IN MTS)=',F8.3/20X,'BED SLOPE
       2 (IN MTS./MTS.)=',F8.5/20X,'TOTAL LENGTH OF THE REACH(IN MTS.)
       3 =',F10.0/20X,'NUMBER OF SUB-REACHES=',F12.4/20X,'JUMP=',I5)
        WRITE(4,98)REQLEN
98      FORMAT(20X,'REQUIRED ROUTING REACH LENGTH=',F12.0)
        READ(2,*)AI(1),YOBS(1),QOBS(1),SIN(1)
        READ(2,*)K
        READ(2,*)(AI(I),I=2,(N+1)),(QOBS(I),I=2,(N+1))
        READ(2,*)(YOBS(I),I=2,(N+1)),(SIN(I),I=2,(N+1))
c               reading the data from the normal tables
        READ(2,*)(YNR(I),QNR(I),CNR(I),BNR(I),VNR(I),I=1,K)
C               OPERATION FOR SKIPPING THE READING OF INPUT DATA
C               AS PER THE VALUE OF JUMP
        N=N-1
        N=N/JUMP+1
        DO 2 J=2,N
        AI(J)=AI((J-1)*JUMP+2)
        QOBS(J)=QOBS((J-1)*JUMP+2)
        YOBS(J)=YOBS((J-1)*JUMP+2)
2       SIN(J)=SIN((J-1)*JUMP+2)
C               STORING OF ORIGINAL AI VALUES IN AIN1 ARRAY
        DO 6 I=1,N
6       AIN1(I)=AI(I)
C       ASSIGNMENT OF BENCHMARK STAGE VALUES AT THE INLET
C       SECTION AND COMPUTATION OF THE NON-DIMENSIONALIZED
C       WATER SURFACE GRADIENT AT THE INLET OF THE REACH
C       DYDXUP      - WATER SURFACE GRADIENT
C       QONR - NORMAL DISCHARGE
        do 120 i=1,n
        X5=sin(i)
        CALL GRADQO (YNR,QNR,X5,QOUP,K)
        QONR=QOUP
        DYDXUP(i)=1.-(AI(i)/QONR)**2
120     continue
C       WRITING INFLOW AND NON-DIMENSIONALIZED WATER SURFACE
C       SLOPE
        WRITE(3,333)(i,AIN1(i),DYDXUP(i),i=1,N)
333     FORMAT(2X,I5,3X,F12.3,3X,F10.6)
C       COMPUTATION OF DYBYDXMAX VALUE AND ITS TIME ORDINATE
        DYBYDXMAX=DYDXUP(i)
```

```
      DO 200 i=1,N
      IF(DYDXUP(i).GT.DYBYDXMAX)THEN
      DYBYDXMAX=DYDXUP(i)
      TPDYBYDXMAX=i
      END IF
200   CONTINUE
C           WRITING DYDXMAX VALUES
      WRITE(3,444)TPDYBYDXMAX,DYBYDXMAX
444   FORMAT(5x,'tpdydxmax=',F4.0,/5x,'dydxmax=',F9.6)
C           START OF SPACE STEP
C     DX  - LENGTH OF EQUAL SUB-REACH
      DX=TTL/ANREACH
      DX1=0.
C     DX1 - LENGTH OF CUMULATIVE ROUTED REACH
7     DX1=DX1+DX
      IF(DX1.GT.TTL)DX=TTL-(DX1-DX)
      WRITE(4,95)DX
95    FORMAT(25X,'REACH LENGTH=',F12.2)
      QO=AI(1)
      QIN=QO
      YIN=YO
C           COMPUTATION OF INITIAL SURFACE WIDTH
      X1=YIN
      CALL BINTL (YNR,BNR,X1,BINR,K)
      BMin=BINR
C           COMPUTATION OF INITIAL VELOCITY
      CALL VINTL (YNR,VNR,X1,VINR,K)
      VMoin=VINR
C           COMPUTATION OF INITIAL CELERITY
      CALL CINTL (YNR,CNR,X1,CINR,K)
      CELMoin=CINR
C           COMPUTATION OF UNREFINED AK & THETA
      AK(1)=DX/VMoin
      THETA(1)=0.5-qin/(2.*so*BMin*CELMoin*dx)
c           INITIAL ASSIGNMENTS
      QCOM(1)=QIN
      YCOM(1)=YIN
C           START OF TIME STEP
      J=1
5     J=J+1
      ak(j)=ak(j-1)
      theta(j)=theta(j-1)
C       C1,C2 AND C3 ARE THE COEFFICIENTS OF THE MUSKINGUM
C       ROUTING EQUATION
      CDIN=AK(j)*(1.-THETA(j))+DT/2.
      C1=(-AK(j)*THETA(j)+DT/2.)/CDIN
```

```
      C2=(AK(j-1)*THETA(j-1)+DT/2.)/CDIN
      C3=(AK(j-1)*(1.-THETA(j-1))-DT/2.)/CDIN
C             COMPUTATION OF UNREFINED OUTFLOW
      QCOM(J)=C1*AI(J)+C2*AI(J-1)+C3*QCOM(J-1)
C             COMPUTATION OF THE WEIGHTED FLOW
      Q3=Qcom(J)+THETA(J)*(AI(J)-Qcom(J))
C             COMPUTATION OF FLOW DEPTH AT MID SECTION
      X2=Q3
      CALL YMIDQ3 (QNR,YNR,X2,YMDNR,K)
      YMID=YMDNR
C             COMPUTATION OF REFINED AK & THETA
      X3=YMID
c             computation of velocity
      CALL VMONR (YNR,VNR,X3,VMNR,K)
      VMo=VMNR
c             computation of travel time
      ak(j)=dx/VMo
C             computation of wave celerity
      CALL CLmn (YNR,CNR,X3,CLM,K)
      CELMo=CLM
C             COMPUTATION OF SURFACE WIDTH
C             Bm     - SURFACE WIDTH
      CALL BWMNR (YNR,BNR,X3,BMNR,K)
      Bm=BMNR
      theta(j)=0.5-Q3/(2.*so*Bm*CELMo*dx)
C     C1,C2 AND C3 ARE THE COEFFICIENTS OF THE MUSKINGUM
C     ROUTING EQUATION
      CDIN=AK(j)*(1.-THETA(j))+DT/2.
      C1=(-AK(j)*THETA(j)+DT/2.)/CDIN
      C2=(AK(j-1)*THETA(j-1)+DT/2.)/CDIN
      C3=(AK(j-1)*(1.-THETA(j-1))-DT/2.)/CDIN
C             COMPUTATION OF REFINED OUTFLOW
      Qcom(j)=C1*AI(j)+C2*AI(j-1)+C3*Qcom(j-1)
C             COMPUTATION OF DISCHARGE AT MIDSECTION
      QMID=(AI(J)+Qcom(J))/2.
c             weighted discharge calculations
      Q3=Qcom(J)+THETA(J)*(AI(J)-Qcom(J))
      x7=Q3
c             computation of flow depth at mid section using refind values
      CALL YMIDQ3F (QNR,YNR,X7,YMDNRF,K)
      YMID=YMDNRF
C             COMPUTATION OF CELERITY AT MIDSECTION
      X6=YMID
      CALL CELYMID (YNR,CNR,X6,CELM,K)
      CELMID=CELM
C             COMPUTATION OF SURFACE WIDTH AT MIDSECTION
```

```
C           BMID - SURFACE WIDTH AT MID SECTION
      CALL BMYMID (YNR,BNR,X6,BMDNR,K)
      BMID=BMDNR
C           COMPUTATION OF STAGE AT THE OUTFLOW SECTION
      YCOM(J)=YMID+(QCOM(J)-QMID)/(CELMID*BMID)
      y_equivalent(j)=ycom(j)
c           computation of equivalent flow depth from the corresponding
c           routed discharge value
      x8=Qcom(j)
!     call ycomqcom (qnr,ynr,x8,ycomr,k)
!     y_equivalent(j)=ycomr
C     CONVERSION OF THE COMPUTED DOWNSTREAM STAGE
C     HYDROGRAPH OF THE EQUAVALENT CHANNEL SECTION TO THE
C     ACTUAL END SECTION
C           ESTIMATED STAGE HYDROGRAPH
C           */Applications for the Pirentanio-Ponte Felcino Reach of the
c           Upper Tiber River in Central Italy /*
      y_actual(j)=0.927*y_equivalent(j)+0.062
c           writing the actual flow depth values as the estimated
c           flow depth at the outlet section
      ycom(j)=y_actual(j)
      IF(J.LT.N)GO TO 5          ! end of time step loop
C     OUTFLOW OF THE SUB-REACH BECOMES INFLOW TO THE
C     NEXT SUB-REACH
      DO 28 I=1,N
28    AI(I)=QCOM(I)
C     CHECKING FOR THE COMPLETION OF THE ROUTING FOR THE LAST
C     SUB-REACH
      IF(DX1.LT.TTL) GO TO 7                    ! end of space step loop
C     WRITING THE INFLOW,DISCHARGE OBSERVED, DISCHARGE
C     COMPUTED, STAGE INFLOW,STAGE OBSERVED AND STAGE
C     COMPUTED ORDINATES
      WRITE(4,111)
111   FORMAT(1x,'Ord.no',2x,'Time(h)',2x,'Inflow',4x,'Qobs',6x,'Qcom'
     1 5x,'Yinf',5x,'Yobs',5x,'Ycom')
      WRITE(4,101)((J-1),(J-1)*DT/3600,AIN1(J),QOBS(J),QCOM(J),SIN(J),
     1 YOBS(J),YCOM(J),J=1,N)
101   FORMAT(I4,4F10.3,2x,F6.2,2X,F6.2,2X,F6.2)
C           COMPUTATION OF SUM OF INFLOW,OBSERVED, & COMPUTED
C           OUTFLOWS
C     NASH-SUTCLIFFE CRITERION ERROR IN VOLUME AND EFFICIENCY
      SUMAI1=0.
      SUMQC=0.
      SUMQO=0.
      TOTVAR=0.
      RESVAR=0.
```

```
      SUMYIN=0.
      SUMYC=0.
      SUMYO=0.
      TOTVARY=0.
      RESVARY=0.
      DO 22 J=1,N
      SUMAI1=SUMAI1+AIN1(J)
      SUMQC=SUMQC+QCOM(J)
      SUMQO=SUMQO+QOBS(J)
      SUMYIN=SUMYIN+SIN(J)
      SUMYC=SUMYC+YCOM(J)
22    SUMYO=SUMYO+YOBS(J)
      AVEAI=SUMAI1/N
      AVEQC=SUMQC/N
      AVEQO=SUMQO/N
      AVEYIN=SUMYIN/N
      AVEYC=SUMYC/N
      AVEYO=SUMYO/N
      DO 32 J=1,N
      TOTVAR=TOTVAR+(QOBS(J)-AVEQO)*(QOBS(J)-AVEQO)
      RESVAR=RESVAR+(QOBS(J)-QCOM(J))*(QOBS(J)-QCOM(J))
      TOTVARY=TOTVARY+(YOBS(J)-AVEYO)*(YOBS(J)-AVEYO)
32    RESVARY=RESVARY+(YOBS(J)-YCOM(J))*(YOBS(J)-YCOM(J))
      QVAREXP=(TOTVAR-RESVAR)/TOTVAR*100
      EVOL=(SUMQC-SUMAI1)/SUMAI1*100
      YVAREXP=(TOTVARY-RESVARY)/TOTVARY*100
      WRITE(4,102)SUMAI1,SUMQC,SUMQO,SUMYIN,SUMYC,SUMYO
      WRITE(4,104)QVAREXP,EVOL,YVAREXP
104   FORMAT(5X,'QVAREXP=',F8.2,4X,'EVOL=',F10.6,7X,'YVAREXP=',F8.2)
102   FORMAT(5X,'SUMAI=',F10.2,4X,'SUMQC=',F10.2,6X,'SUMQO=',F10.2,/
     1 5X,'SUMYIN=',F10.2,3X,'SUMYC=',F10.2,6X,'SUMYO=',F10.2)
C     REPRODUCTION OF PERTINENT CHARACTERISTICS OF ROUTED
C     DISCHARGE AND COMPUTED STAGE HYDROGRAPHS
      QPCOM=QCOM(J-1)
      QPOBS=QOBS(J-1)
      YPCOM=YCOM(J-1)
      YPOBS=YOBS(J-1)
      QPAIN1=AIN1(J-1)
      YPY1=SIN(J-1)
      DO 103 J=1,N
      IF(QCOM(J).GT.QPCOM)THEN
      QPCOM=QCOM(J)
      TPQCOMORD=J-1
      END IF
      IF(QOBS(J).GT.QPOBS)THEN
      QPOBS=QOBS(J)
```

```
      TPQOBSORD=J-1
      END IF
      IF(YCOM(J).GT.YPCOM)THEN
      YPCOM=YCOM(J)
      TPYCOMORD=J-1
      END IF
      IF(YOBS(J).GT.YPOBS)THEN
      YPOBS=YOBS(J)
      TPYOBSORD=J-1
      END IF
      IF(AIN1(J).GT.QPAIN1)THEN
      QPAIN1=AIN1(J)
      TPAIN1ORD=J-1
      END IF
      IF(SIN(J).GT.YPY1)THEN
      YPY1=SIN(J)
      TPY1ORD=J-1
      END IF
      TPQCOM=TPQCOMORD*DT/3600.
      TPQOBS=TPQOBSORD*DT/3600.
      TPYCOM=TPYCOMORD*DT/3600.
      TPYOBS=TPYOBSORD*DT/3600.
      TPAIN1=TPAIN1ORD*DT/3600.
      TPY1=TPY1ORD*DT/3600.
      QPER=(QPCOM-QPOBS)/QPOBS*100
      TPQER=(TPQCOM-TPQOBS)
      YPER=(YPCOM-YPOBS)/YPOBS*100
      TPYER=(TPYCOM-TPYOBS)
      ATTENQ=(QPAIN1-QPOBS)/QPAIN1*100
      ATTENY=(YPY1-YPOBS)/YPY1*100
103   CONTINUE
      WRITE(1,107)fylea,l,SO,QPOBS,QPCOM,TPQOBS,TPQCOM,
      1YPOBS,YPCOM,TPYOBS,TPYCOM,QPER,YPER,TPQER,TPYER,
      2DYBYDXMAX,
      2 EVOL,QVAREXP,YVAREXP,ATTENQ,ATTENY,
      3ANREACH,dx,dt
107   FORMAT(a,2x,i3,2X,f6.4,2x,F8.3,8X,F8.3,
      1 7X,F7.3,7X,F7.3,4X,F7.3,3X,F7.3,6X,F7.3,6X,F7.3,4X,F7.3,
      2  4X,F7.3,3X,F7.3,3X,F7.3,3X,F8.6,2X,F10.6,2X,F7.3,2X,F7.3,
      3  2X,F7.3,4X,F7.3,4x,f4.0,4x,f6.0,3x,f5.0)
999   continue        !end of input file loop & and go to the new input file
108   FORMAT('Testcode',19x,'setno',2x,'Slope',3x,'Qpobs(m3/s)',4x,
      1 'Qpcom(m3/s)',3x,'Tpqobs(h)',5x,'Tpqcom(h)',3x,'Ypobs(m)',2x
      2 'Ypcom(m)',4x,'Tpyobs(h)',4x,
      3 'Tpycom(h)',4x,'Qper(%)',4x,'Yper(%)',3x,'Tpqer(h)',2x,
      4 'Tpyer(h)',1x,'dydxmax',3x,'Evol(%)',5x,'Qvar(%)',2x,
```

```
     4 'Yvar(%)',2x,'AttenQ(%)',2x,'AttenY(%)',1x,'anreach',2x,
     5 'dx(m)',3x,'dt(sec)')
      STOP
      END
C                    // subroutines //
C*********************************************************************
c     */ The Look-up table consists of normal flow depth discharge relationships,
C     water surface width,wave celerity and velocity variables developed at
c     closer intervals of flow depth /*
c     */ Interpolation is done using second order polinomial interpolation method.
C     Reference:FORTRAN HYDRO- A computer program documentation
c     Prude University, U.S.A.,1971. /*
C     SUBROUTINE FOR INTERPOLATING Y1 WITH YNR & QNR TO
C     COMPUTE QONR
      SUBROUTINE GRADQO (YNR,QNR,X5,QOUP,K)
      DIMENSION YNR(30000),QNR(30000)
      DO 29 I=1,K
      IF(YNR(I)-X5)29,30,31
30    QOUP=QNR(I)
      GO TO 32
31    H9=YNR(I+1)-YNR(I)
      PQ9=(X5-YNR(I))/H9
      QOUP=QNR(I)+(PQ9/2.)*(QNR(I+1)-QNR(I-1))+(PQ9*PQ9/2.)
     1 *(QNR(I+1)-2.*QNR(I)+QNR(I-1))
      GO TO 32
29    CONTINUE
32    RETURN
      END
C     SUBROUTINE FOR INTERPOLATING YIN WITH YNR & BNR TO
C     COMPUTE BMin
      SUBROUTINE BINTL (YNR,BNR,X1,BINR,K)
      DIMENSION YNR(30000),BNR(30000)
      DO 490 I=1,K
      IF(YNR(I)-X1)490,400,410
400   BINR=BNR(I)
      GO TO 420
410   H1=YNR(I+1)-YNR(I)
      PQ1=(X1-YNR(I))/H1
      BINR=BNR(I)+(PQ1/2.)*(BNR(I+1)-BNR(I-1))+(PQ1*PQ1/2.)
     1 *(BNR(I+1)-2.*BNR(I)+BNR(I-1))
      GO TO 420
490   CONTINUE
420   RETURN
      END
C     SUBROUTINE FOR INTERPOLATING YIN WITH YNR & VNR TO
C     COMPUTE VMoin
```

```
      SUBROUTINE VINTL (YNR,VNR,X1,VINR,K)
      DIMENSION YNR(30000),VNR(30000)
      DO 52 I=1,K
      IF(YNR(I)-X1)52,62,72
62    VINR=VNR(I)
      GO TO 82
72    H2=YNR(I+1)-YNR(I)
      PQ2=(X1-YNR(I))/H2
      VINR=VNR(I)+(PQ2/2.)*(VNR(I+1)-VNR(I-1))+(PQ2*PQ2/2.)
     1 *(VNR(I+1)-2.*VNR(I)+VNR(I-1))
      GO TO 82
52    CONTINUE
82    RETURN
      END
C     SUBROUTINE FOR INTERPOLATING YIN WITH YNR & CNR TO
C     COMPUTE CELMoin
      SUBROUTINE CINTL (YNR,CNR,X1,CINR,K)
      DIMENSION YNR(30000),CNR(30000)
      DO 523 I=1,K
      IF(YNR(I)-X1)523,623,723
623   CINR=CNR(I)
      GO TO 823
723   H3=YNR(I+1)-YNR(I)
      PQ3=(X1-YNR(I))/H3
      CINR=CNR(I)+(PQ3/2.)*(CNR(I+1)-CNR(I-1))+(PQ3*PQ3/2.)
     1 *(CNR(I+1)-2.*CNR(I)+CNR(I-1))
      GO TO 823
523   CONTINUE
823   RETURN
      END
C     SUBROUTINE FOR INTERPOLATING Q3 WITH QNR & YNR TO
C     COMPUTE YMID
      SUBROUTINE YMIDQ3 (QNR,YNR,X2,YMDNR,K)
      DIMENSION QNR(30000),YNR(30000)
      DO 290 I=1,K
      IF(QNR(I)-X2)290,300,310
300   YMDNR=YNR(I)
      GO TO 320
310   H4=QNR(I+1)-QNR(I)
      PQ4=(X2-QNR(I))/H4
      YMDNR=YNR(I)+(PQ4/2.)*(YNR(I+1)-YNR(I-1))+(PQ4*PQ4/2.)
     1 *(YNR(I+1)-2.*YNR(I)+YNR(I-1))
      GO TO 320
290   CONTINUE
320   RETURN
      END
```

```
82      RETURN
        END
C       SUBROUTINE FOR INTERPOLATING YIN WITH YNR & CNR TO
C       COMPUTE CELMoin
        SUBROUTINE CINTL (YNR,CNR,X1,CINR,K)
        DIMENSION YNR(30000),CNR(30000)
        DO 523 I=1,K
        IF(YNR(I)-X1)523,623,723
623     CINR=CNR(I)
        GO TO 823
723     H3=YNR(I+1)-YNR(I)
        PQ3=(X1-YNR(I))/H3
        CINR=CNR(I)+(PQ3/2.)*(CNR(I+1)-CNR(I-1))+(PQ3*PQ3/2.)
       1 *(CNR(I+1)-2.*CNR(I)+CNR(I-1))
        GO TO 823
523     CONTINUE
823     RETURN
        END
C       SUBROUTINE FOR INTERPOLATING Q3 WITH QNR & YNR TO
C       COMPUTE YMID
        SUBROUTINE YMIDQ3 (QNR,YNR,X2,YMDNR,K)
        DIMENSION QNR(30000),YNR(30000)
        DO 290 I=1,K
        IF(QNR(I)-X2)290,300,310
300     YMDNR=YNR(I)
        GO TO 320
310     H4=QNR(I+1)-QNR(I)
        PQ4=(X2-QNR(I))/H4
        YMDNR=YNR(I)+(PQ4/2.)*(YNR(I+1)-YNR(I-1))+(PQ4*PQ4/2.)
       1 *(YNR(I+1)-2.*YNR(I)+YNR(I-1))
        GO TO 320
290     CONTINUE
320     RETURN
        END
C       SUBROUTINE FOR INTERPOLATING YMID WITH YNR & VNR
C       TO COMPUTE VMo
        SUBROUTINE VMONR (YNR,VNR,X3,VMNR,K)
        DIMENSION YNR(30000),VNR(30000)
        DO 398 I=1,K
        IF(YNR(I)-X3)398,308,318
308     VMNR=VNR(I)
        GO TO 328
318     H5=YNR(I+1)-YNR(I)
        PQ5=(X3-YNR(I))/H5
        VMNR=VNR(I)+(PQ5/2.)*(VNR(I+1)-VNR(I-1))+(PQ5*PQ5/2.)
       1 *(VNR(I+1)-2.*VNR(I)+VNR(I-1))
```

```
      GO TO 328
398   CONTINUE
328   RETURN
      END
C     SUBROUTINE FOR INTERPOLATING YMID WITH YNR & CNR TO
C     COMPUTE CELMo
      SUBROUTINE CLmn (YNR,CNR,X3,CLM,K)
      DIMENSION YNR(30000),CNR(30000)
      DO 152 I=1,K
      IF(YNR(I)-X3)152,162,172
162   CLM=CNR(I)
      GO TO 182
172   H6=YNR(I+1)-YNR(I)
      PQ6=(X3-YNR(I))/H6
      CLM=CNR(I)+(PQ6/2.)*(CNR(I+1)-CNR(I-1))+(PQ6*PQ6/2.)
     1 *(CNR(I+1)-2.*CNR(I)+CNR(I-1))
      GO TO 182
152   CONTINUE
182   RETURN
      END
C     SUBROUTINE FOR INTERPOLATING YMID WITH YNR & BNR TO
C     COMPUTE Bm
      SUBROUTINE BWMNR (YNR,BNR,X3,BMNR,K)
      DIMENSION YNR(30000),BNR(30000)
      DO 196 I=1,K
      IF(YNR(I)-X3)196,206,216
206   BMNR=BNR(I)
      GO TO 226
216   H7=YNR(I+1)-YNR(I)
      PQ7=(X3-YNR(I))/H7
      BMNR=BNR(I)+(PQ7/2.)*(BNR(I+1)-BNR(I-1))+(PQ7*PQ7/2.)
     1 *(BNR(I+1)-2.*BNR(I)+BNR(I-1))
      GO TO 226
196   CONTINUE
226   RETURN
      END
C     SUBROUTINE FOR INTERPOLATING YMID WITH YNR & CNR TO
C     COMPUTE CELMID
      SUBROUTINE CELYMID (YNR,CNR,X6,CELM,K)
      DIMENSION YNR(30000),CNR(30000)
      DO 351 I=1,K
      IF(YNR(I)-X6)351,361,371
361   CELM=CNR(I)
      GO TO 381
371H10=YNR(I+1)-YNR(I)
      PQ10=(X6-YNR(I))/H10
```

```
      CELM=CNR(I)+(PQ10/2.)*(CNR(I+1)-CNR(I-1))+(PQ10*PQ10/2.)
     1 *(CNR(I+1)-2.*CNR(I)+CNR(I-1))
      GO TO 381
  351 CONTINUE
  381 RETURN
      END
C     SUBROUTINE FOR INTERPOLATING YMID WITH YNR & BNR TO
C     COMPUTE BMID
      SUBROUTINE BMYMID (YNR,BNR,X6,BMDNR,K)
      DIMENSION YNR(30000),BNR(30000)
      DO 190 I=1,K
      IF(YNR(I)-X6)190,200,210
  200 BMDNR=BNR(I)
      GO TO 220
  210 H11=YNR(I+1)-YNR(I)
      PQ11=(X6-YNR(I))/H11
      BMDNR=BNR(I)+(PQ11/2.)*(BNR(I+1)-BNR(I-1))+(PQ11*PQ11/2.)
     1 *(BNR(I+1)-2.*BNR(I)+BNR(I-1))
      GO TO 220
  190 CONTINUE
  220 RETURN
      END
C     SUBROUTINE FOR INTERPOLATING REFINED Q3 WITH QNR&YNR TO
C     COMPUTE YMID
      SUBROUTINE YMIDQ3F (QNR,YNR,X7,YMDNRF,K)
      DIMENSION QNR(30000),YNR(30000)
      DO 990 I=1,K
      IF(QNR(I)-X7)990,900,910
  900 YMDNRF=YNR(I)
      GO TO 920
  910 H12=QNR(I+1)-QNR(I)
      PQ12=(X7-QNR(I))/H12
      YMDNRF=YNR(I)+(PQ12/2.)*(YNR(I+1)-YNR(I-1))+(PQ12*PQ12/2.)
     1 *(YNR(I+1)-2.*YNR(I)+YNR(I-1))
      GO TO 920
  990 CONTINUE
  920 RETURN
      END
C     SUBROUTINE FOR INTERPOLATING REFINED Qcom with QNR&YNR TO
C     COMPUTE Ycom
      subroutine ycomqcom (qnr,ynr,x8,ycomr,k)
      DIMENSION QNR(30000),YNR(30000)
      DO 991 I=1,K
      IF(QNR(I)-X8)991,901,911
  901 ycomr=YNR(I)
      GO TO 921
```

```
911     H14=QNR(I+1)-QNR(I)
        PQ14=(X8-QNR(I))/H14
        ycomr=YNR(I)+(PQ14/2.)*(YNR(I+1)-YNR(I-1))+(PQ14*PQ14/2.)
        1 *(YNR(I+1)-2.*YNR(I)+YNR(I-1))
        GO TO 921
991     CONTINUE
921     RETURN
        END
```

ANNEXURE III

FORTRAN 77 CODE FOR REAL-TIME FLOW FORECASTING AND CORRESPONDING STAGE FORECAST ESTIMATION BY THE VPMMD METHOD FOR NATURAL RIVER APPLICATION

```
C*****************************************************************
C  vpmmdrf.for
C*****************************************************************
C       */ Variable Parameter McCarthy-Muskingum Discharge-Routing (VPMMD)
C       method for real-time flood forecasting applications /*
C       */ AR(2) model  is used for estimating the forecast error.
C*****************************************************************
C       THIS PROGRAMME IS CODED BY CH.MADHUSUDANA RAO
C       RESEARCH SCHOLAR DEPT.OF HYDROLOGY,IIT-ROORKEE IN
C       FORTRAN 77(MSDEV) UNDER THE SUPERVISION OF Dr.M.PERUMAL
C       PROFESSOR.DEPT.OF HYDROLOGY,IIT ROORKEE
C*****************************************************************
C       */ Inertial terms are neglected in the Saint-Venant's equation /*
c       */ Stage forecast values are estimated simultaneously while doing the real-time
c         flood discharge forecasting /*
C       */ Back water effects are neglected /*
C       */ Performance evaluation is done using Nash-Sutcliffe and Persistence criterion
C       */ In the two dimensional array first dimension indicates the space step and the
C         second dimension indicates the time step /*
C       */ Warmup period is considered as 5 hours /*
C*****************************************************************
C       DESCRIPTION OF THE MAIN VARIABLES USED IN THE PROGRAMME

C       AI      - INFLOW HYDROGRAPH ORDINATE AT THE UPSTREAM
C                 BOUNDARY
C       Q       - DISCHARGE AT THE SPACE STEP
C       Y       - STAGE AT THE SPACE STEP
C       QOBS - OBSERVED OUTFLOW AT THE DOWNSTREAM BOUNDARY
C       YOBS - OBSERVED STAGE AT THE DOWNSTREAM BOUNDARY
C       YM      - COMPUTED STAGE AT THE MIDDLE OF THE SUB-REACH
C       SIN     - STAGE CORRESPONDING TO GIVEN INFLOW
C       TL      - FORECASTING LEAD TIME IN HOURS
c       K       - SPACE STEP
C*****************************************************************
        DIMENSION AI(1000),QOBS(1000),Q(1000,1000)
        DIMENSION QOBS1(1000,1000),YOBS1(1000,1000),Y(1000,1000)
        DIMENSION SIN1(1000,1000),YOBS(1000),SIN(1000)
        DIMENSION DQ(1000),V(1000,1000),F(1000,1000),DQEST(1000)
        DIMENSION QDACTUAL(1000,1000),VTF(1000,1000),VTV(1000,1000)
!
```

```
      DIMENSION YNR(1000),QNR(1000),CNR(1000),BNR(1000),VNR(1000)
      DIMENSION CELMID(1000),BMID(1000)
      DIMENSION YDACTUAL(1000,1000)
      DIMENSION AK(1000,1000),THETA(1000,1000),CELMo(1000),Bm(1000)
      DIMENSION YMID(1000),QMID(1000),Q3(1000)
!
      OPEN(UNIT=2,FILE='pi_pf_ff_dec1996.dat', STATUS='UNKNOWN')
      OPEN(UNIT=4,FILE='pi_pf_ff_dec1996.txt',STATUS='UNKNOWN')
      OPEN(UNIT=6,FILE='pi_pf_ff_dec1996_summary.txt',
      1 STATUS='UNKNOWN')
C*****************************************************************
C     DESCRIPTION OF INPUT DATA
C     N      - TOTAL NUMBER OF INFLOW AND OUTFLOW VARIABLES
C     DT     - ROUTING TIME INTERVAL
C     YIN    - INITIAL STAGE
C     SO     - CHANNEL BED SLOPE
C     TTL    - TOTAL LENGTH OF THE REACH
C     ANREACH- NUMBER OF SUBREACHES USED IN THE GIVEN
C     FORECASTING REACH
C     JUMP - NUMBER OF ROUTING INTERVALS TO BE SKIPPED FOR
C     INCRIMENTING THE ROUTING INTERVAL
C     QIN    - REFERENCE DISCHARGE (OR) INITIAL DISCHARGE
C     YIN    - REFERENCE FLOW DEPTH (OR)INITIAL FLOW DEPTH
C     YNR    - NORMAL FLOW DEPTH
C     QNR    - NORMAL DISCHARGE
C     CNR    - NORMAL CELERITY
C     BNR    - NORMAL SURFACE WIDTH
C     VNR    - NORMAL VELOCITY
C     NNR    - NUMBER OF ORDINATES IN EACH COLUMN OF A LOOK-UP
C     TABLE
C*****************************************************************
      READ(2,*)N,DT,YIN,SO,TTL,ANREACH,JUMP
      WRITE(4,99) N,DT,YIN,SO,TTL,ANREACH,JUMP
99    FORMAT(20X,'NO.OF ORDINATES=',I6/20X,'ROUTING TIME INTERVAL
      (IN SEC.
      1 )=',F8.2/20X,'INITIAL DEPTH(IN MTS)=',F8.3/20X,'BED SLOPE (IN MTS.
      2 /MTS.)=',F8.5/20X,'TOTAL LENGTH OF THE REACH(IN MTS.)
      3 =',F10.0/20X,'NUMBER OF SUB-REACHES=',F12.4/20X,'JUMP=',I5)
      READ(2,*)AI(1),YOBS(1),QOBS(1),SIN(1)
      READ(2,*)NNR
      READ(2,*)(AI(I),I=2,(N+1)),(QOBS(I),I=2,(N+1))
      READ(2,*)(YOBS(I),I=2,(N+1)),(SIN(I),I=2,(N+1))
C           reading the data from the normal tables
      READ(2,*)(YNR(I),QNR(I),CNR(I),BNR(I),VNR(I),I=1,NNR)
C           OPERATION FOR SKIPPING THE READING OF INPUT DATA
C           AS PER THE VALUE OF JUMP
```

```
      N=N-1
      N=N/JUMP+1
      DO 2 J=2,N
      AI(J)=AI((J-1)*JUMP+2)
      QOBS(J)=QOBS((J-1)*JUMP+2)
      YOBS(J)=YOBS((J-1)*JUMP+2)
2     SIN(J)=SIN((J-1)*JUMP+2)
C       DX  - LENGTH OF EQUAL SUB-REACH
C             NM     - NUMBER OF SPACE STEPS (OR)NODE POINTS
      DX=TTL/ANREACH
      NM=ANREACH+1
      QIN=AI(1)
C             WRITING COLUMN TITLES FOR RESULT TABLE
      WRITE(4,112)
C             WRITING COLUMN TITLE OF THE SUMMARY TABLE
      WRITE(6,114)
      X1=YIN
C             COMPUTATION OF INITIAL SURFACE WIDTH
c             Bmin   - initial surface width
      CALL Bmyin (YNR,BNR,X1,BYINR,NNR)
      Bmin=BYINR
C             COMPUTATION OF INITIAL CELERITY
c             CELMoin  - initial wave celerity
      CALL CELyin (YNR,CNR,X1,CLINR,NNR)
      CELMoin=CLINR
C             COMPUTATION OF INITIAL VELOCITY
c             VMoin- initial velocity
      CALL VMOyin (YNR,VNR,X1,VMOINR,NNR)
      VMoin=VMOINR
C             COMPUTATION OF UNREFINED AK & THETA
c             AK    - Travel time
c             THETA - Weighting parameter
      AK(1,1)=DX/VMoin
      THETA(1,1)=0.5-QIN/(2.*SO*Bmin*CELMoin*DX)
C             SPECIFYING THE INITIAL STEADY STATE CONDITIONS IN THE
C             COMPUTATIONAL STATE SPACE GRID
      DO 3 I=1,NM
      DO 4 J=1,N
      Q(I,J)=QIN
      Y(I,J)=YIN
      AK(I,J)=AK(1,1)
      THETA(I,J)=THETA(1,1)
4     CONTINUE
3     CONTINUE
C             ASSIGNMENT OF INFLOW ORDINATES AT THE UPSTREAM
C             BOUNDARY AND THE OBSERVED ORDINATES AT THE
```

```
C           DOWNSTREAM BOUNDARY
      DO 12 I=1,N
      Q(1,I)=AI(I)
      QOBS1(NM,I)=QOBS(I)
      YOBS1(NM,I)=YOBS(I)
12    SIN1(1,I)=SIN(I)
C           START OF TIME STEP
      J=1
C     TL    - FORECASTING LEAD TIME (SUPPLIED IN TERMS OF HOURS)
C     KCOUNT      - WARMUP PERIOD (SUPPLIED INTERMS OF NO.OF
C                   ORDINATES)
C     EQUAVALENT NUMBER OF TIME ORDINATES(OR)TIME STEPS FOR A
C     GIVEN LEAD TIME IF THE ROUTING TIME INTERVAL
C     DT=30 MINUTES
C           TL=1.0 HOUR=2 TIME ORDINATES
C           TL=1.5 HOUR=3 TIME ORDINATES
C           TL=2.0 HOUR=4 TIME ORDINATES
C           TL=2.5 HOUR=5 TIME ORDINATES
C           TL=3.0 HOUR=6 TIME ORDINATES
      WRITE(*,*)'Enter the lead time in hours'
      READ(*,*)DTLEAD
      WRITE(*,*)'Enter the warmup period (No.of Ordinates= 9)'
C     kcount=9
      READ(*,*)KCOUNT
      TL=INT(DTLEAD/0.5)
      WRITE(*,*)'nskip =',TL
      WRITE(*,*)'kcount=',kcount
      J=TL
5     J=J+1
C           START OF SPACE STEP
      DO 7 K=1,ANREACH
      IF(J.EQ.TL+1)Q(K+1,J-1)=Q(K+1,J-TL)
      CDIN=AK(K,J)*(1.-THETA(K,J))+DT/2.
C     C1,C2 AND C3 ARE THE COEFFICIENTS OF THE MUSKINGUM
C     ROUTING EQUATION
      C1=(-AK(K,J)*THETA(K,J)+DT/2.)/CDIN
      C2=(AK(K,J-1)*THETA(K,J-1)+DT/2.)/CDIN
      C3=(AK(K,J-1)*(1.-THETA(K,J-1))-DT/2.)/CDIN
C           COMPUTATION OF UNREFINED FORECAST FLOW
      Q(K+1,J)=C1*Q(K,J-TL)+C2*Q(K,J-TL)+C3*Q(K+1,J-1)
C           COMPUTATION OF THE DISCHARGE AT WEIGHTED SECTION
      Q3(J)=Q(K+1,J)+THETA(K,J)*(Q(K,J-TL)-Q(K+1,J))
C           COMPUTATION OF FLOW DEPTH AT MIDSECTION
      X2=Q3(J)
      CALL YMIDQ3 (QNR,YNR,X2,YMDNR,NNR)
      YMID(J)=YMDNR
```

```
      X3=YMID(J)
C           COMPUTATION OF VELOCITY
      CALL VELMO (YNR,VNR,X3,VELM,NNR)
      VMo=VELM
C           COMPUTATION OF WAVE CELERITY
      CALL CELMYMID (YNR,CNR,X3,CELM,NNR)
      CELMo(J)=CELM
C           COMPUTATION OF SURFACE WIDTH
      CALL BMND (YNR,BNR,X3,BMNR,NNR)
      Bm(J)=BMNR
      AK(K,J)=DX/VMo
      THETA(K,J)=0.5-Q3(J)/(2.*SO*Bm(J)*CELMo(J)*DX)
      CDIN=AK(K,J)*(1.-THETA(K,J))+DT/2.
C     C1,C2 AND C3 ARE THE COEFFICIENTS OF THE MUSKINGUM
C     ROUTING EQUATION
      C1=(-AK(K,J)*THETA(K,J)+DT/2.)/CDIN
      C2=(AK(K,J-1)*THETA(K,J-1)+DT/2.)/CDIN
      C3=(AK(K,J-1)*(1.-THETA(K,J-1))-DT/2.)/CDIN
C           COMPUTATION OF REFINED FORECAST FLOW
      Q(K+1,J)=C1*Q(K,J-TL)+C2*Q(K,J-TL)+C3*Q(K+1,J-1)
C           COMPUTATION OF THE DISCHARGE AT WEIGHTED SECTION
      Q3(J)=Q(K+1,J)+THETA(K,J)*(Q(K,J-TL)-Q(K+1,J))
      X4=Q3(J)
C           COMPUTE STAGE AT THE MID SECTION
      CALL YMQ3 (QNR,YNR,X4,YMNR,NNR)
      YMID(J)=YMNR
      X5=YMID(J)
C           COMPUTATION OF WAVE CELERITY AT MID SECTION
      CALL CELMYM (YNR,CNR,X5,CLM,NNR)
      CELMID(J)=CLM
C           BMID - SURFACE WIDTH AT MID SECTION
      CALL BWMID (YNR,BNR,X5,BMD,NNR)
      BMID(J)=BMD
C           COMPUTATION OF DISCHARGE AT MIDSECTION
      QMID(J)=(Q(K,J-TL)+Q(K+1,J))/2.
C           COMPUTATION OF STAGE
      Y(K+1,J)=YMID(J)+(Q(K+1,J)-QMID(J))/(CELMID(J)*BMID(J))
C           COMPUTATION OF FORECAST FLOW ERROR AT THE
C           FORECASTING SITE USING TWO-PARAMETER LINEAR AUTO
C           REGRESSIVE MODEL WITH ITS PARAMETERS A1 & A2
C           UPDATED AT EVERY ROUTING TIME INTERVAL
      IF(K+1.EQ.NM)DQ(J)=QOBS1(NM,J)-Q(K+1,J)
C           DQ     - ERROR IN FLOW FORECAST
      IF(K+1.EQ.NM.AND.J.GE.11)THEN
C           ASSIGNMENT OF DQ VALUES TO AN ARRAY DURING
C           WARMUP PERIOD
```

```
      DO 123 I=1,KCOUNT
      V(I,1)=DQ(J-I)
      V(I,2)=DQ(J-I-1)
      F(I,1)=DQ(J-I+1)
123   CONTINUE
      CALL TSUB(V,KCOUNT,2,VT)
      CALL MSUB(VT,V,2,KCOUNT,KCOUNT,2,VTV)
      CALL MSUB(VT,F,2,KCOUNT,KCOUNT,1,VTF)
      CALL INVSUB(VTV,2,VTF,1,A)
      A1=VTF(1,1)
      A2=VTF(2,1)
      print *,j,a1,a2
C           COMPUTATION OF UPDATED FORECAST ERROR
      DQEST(J)=A1*DQ(J-TL)+A2*DQ(J-(TL+1))
C     COMPUTATION OF CORRECTED(OR)ACTUAL FORECAST FLOW
C           (updated forecast error is added to the computed forecast flow)
      QDACTUAL(NM,J)=Q(K+1,J)+DQEST(J)
C           COMPUTATION OF THE DISCHARGE AT WEIGHTED SECTION
      Q3(J)=QDACTUAL(NM,J)+THETA(K,J)*(Q(K,J-TL)-QDACTUAL(NM,J))
      X4=Q3(J)
C           COMPUTE STAGE AT THE MID SECTION
      CALL YMQ3 (QNR,YNR,X4,YMNR,NNR)
      YMID(J)=YMNR
      X5=YMID(J)
C           COMPUTATION OF WAVE CELERITY AT MID SECTION
      CALL CELMYM (YNR,CNR,X5,CLM,NNR)
      CELMID(J)=CLM
C           BMID - SURFACE WIDTH AT MID SECTION
      CALL BWMID (YNR,BNR,X5,BMD,NNR)
      BMID(J)=BMD
C           COMPUTATION OF DISCHARGE AT MIDSECTION
      QMID(J)=(Q(K,J-TL)+QDACTUAL(NM,J))/2.
C           COMPUTATION OF STAGE
      Y(K+1,J)=YMID(J)+(QDACTUAL(NM,J)-QMID(J))/(CELMID(J)*BMID(J))
C           */ for Pierantanio-Ponte Felcino reach of the Tiber River Applications /*
C           conversion of the computed d/s stage hydrograph of the equivalent
C           section to the actual end section estimated stage hydrograph
      YDACTUAL(K+1,J)=0.927*Y(K+1,J)+0.062
      ENDIF
C           RETURNING TO SPACE STEP
7     CONTINUE
C           RETURNING TO TIME STEP
      IF(J.LT.N)GO TO 5
C           WRITING THE RESULTS CORRESPONDING TO THE
C           FORECASTING SITE
      WRITE(4,101)(DTLEAD,NM,J-1,(J-1)*DT/3600,Q(1,J),QDACTUAL(NM,J),
```

```
     1 QOBS1(NM,J),SIN1(1,J),YDACTUAL(NM,J),YOBS1(NM,J), J=11,N)
101  FORMAT(3X,F5.2,4X,I5,2X,I5,7F10.3)
C    COMPUTATION OF THE SUM OF INFLOW,OBSERVED
C    OUTFLOW,COMPUTED OUTFLOW,NASH-SUTCLIFFE CRITERION
C    ERROR IN VOLUME  AND EFFICIENCY
     SUMAI1=0.
     SUMQC=0.
     SUMQO=0.
     TOTVAR=0.
     RESVAR=0.
     SUMYIN=0.
     SUMYC=0.
     SUMYO=0.
     TOTVARY=0.
     RESVARY=0.
     DO 22 J=11,N
     SUMAI1=SUMAI1+Q(1,J)
     SUMQC=SUMQC+QDACTUAL(NM,J)
     SUMQO=SUMQO+QOBS1(NM,J)
     SUMYIN=SUMYIN+SIN1(1,J)
     SUMYC=SUMYC+YDACTUAL(NM,J)
22   SUMYO=SUMYO+YOBS1(NM,J)
     AVEAI=SUMAI1/N
     AVEQC=SUMQC/N
     AVEQO=SUMQO/N
     AVEYIN=SUMYIN/N
     AVEYC=SUMYC/N
     AVEYO=SUMYO/N
     DO 32 J=11,N
     TOTVAR=TOTVAR+(QOBS1(NM,J)-AVEQO)*(QOBS1(NM,J)-AVEQO)
     RESVAR=RESVAR+(QOBS1(NM,J)-QDACTUAL(NM,J))*(QOBS1(NM,J)-
     1 QDACTUAL(NM,J))
     TOTVARY=TOTVARY+(YOBS1(NM,J)-AVEYO)*(YOBS1(NM,J)-AVEYO)
32   RESVARY=RESVARY+(YOBS1(NM,J)-YDACTUAL(NM,J))*(YOBS1
     (NM,J)-
     1 YDACTUAL(NM,J))
     QVAREXP=(TOTVAR-RESVAR)/TOTVAR*100
     EVOL=(SUMQC-SUMAI1)/SUMAI1*100
     YVAREXP=(TOTVARY-RESVARY)/TOTVARY*100
C            COMPUTATION OF PERSISTENCE
     TOTVAR1=0.
     UP1=0.0
     BELOW1=0.0
     DO 35 J=11,N
     UP1=UP1+(QOBS1(NM,J)-QDACTUAL(NM,J))**2
35   BELOW1=BELOW1+(QOBS1(NM,J)-QOBS1(NM,J-TL))**2
```

```
      TOTVAR1=UP1/BELOW1
      PC=(1-TOTVAR1)*100.
      WRITE(4,102)SUMAI1,SUMQC,SUMQO,SUMYIN,SUMYC,SUMYO
      WRITE(4,104)QVAREXP,EVOL,YVAREXP
      WRITE(4,103)PC
104   FORMAT(5X,'QVAREXP=',F9.4,7X,'EVOL=',F12.5,5X,'YVAREXP=',F10.4)
102   FORMAT(5X,'SUMAI=',2X,F12.5,4X,'SUMQC=',2X,F12.5,2X,'SUMQO=',
     1 2X,F12.5,/
     2 5X,'SUMYIN=',F12.5,5X,'SUMYC=',1X,F12.5,3X,'SUMYO=',1X,F12.5)
103   FORMAT(5X,'PERSISTENCE=',F9.4)
C           CALCULATION OF PEAK VALUES AND PREPARATION OF
C           SUMMARY TABLE
      QPCOM=QDACTUAL(NM,J-1)
      YPCOM=YDACTUAL(NM,J-1)
      QPOBS=QOBS1(NM,J-1)
      YPOBS=YOBS1(NM,J-1)
      QPATT=Q(1,J-1)
      YPATT=SIN1(1,J-1)
      DO 300 J=11,N
      IF(QDACTUAL(NM,J).GT.QPCOM)THEN
      QPCOM=QDACTUAL(NM,J)
      TPQORD=J-1
      ENDIF
      IF(QOBS1(NM,J).GT.QPOBS)THEN
      QPOBS=QOBS1(NM,J)
      TPQOBSORD=J-1
      ENDIF
      IF(YDACTUAL(NM,J).GT.YPCOM)THEN
      YPCOM=YDACTUAL(NM,J)
      TPYORD=J-1
      ENDIF
      IF(YOBS1(NM,J).GT.YPOBS)THEN
      YPOBS=YOBS1(NM,J)
      TPYOBSORD=J-1
      ENDIF
      IF(Q(1,J).GT.QPATT)THEN
      QPATT=Q(1,J)
      TPATTORD=J-1
      END IF
      IF(SIN1(1,J).GT.YPATT)THEN
      YPATT=SIN1(1,J)
      TPATTORD=J-1
      ENDIF
      TPQ=TPQORD*DT/3600.
      TPQOBS=TPQOBSORD*DT/3600.
      TPY=TPYORD*DT/3600.
```

```
      TPYOBS=TPYOBSORD*DT/3600.
      QPER=(QPCOM-QPOBS)/QPOBS*100
      TPQER=TPQ-TPQOBS
      YPER=(YPCOM-YPOBS)/YPOBS*100
      TPYER=TPY-TPYOBS
      ATTENQ=(QPATT-QPOBS)/QPATT*100
      ATTENY=(YPATT-YPOBS)/YPATT*100
300   CONTINUE
      WRITE(6,8)DTLEAD,TPQOBS,TPQ,QPOBS,QPCOM,TPYOBS,TPY,
      1YPOBS,YPCOM,TPQER,QPER,TPYER,YPER,EVOL,QVAREXP,
      2YVAREXP,PC
8     FORMAT((4X,17F12.4))
C           WRITING COLUMN TITLES OF THE RESULT TABLE
112   FORMAT(3x,'Leadtime(h)',1x,'nm',2x,'ord.no.',1x,'Time(h)',4x,
      1 'Qinf',6x,'Qcom',6x,'Qobs',7x,'Yinf',6x,'Ycom',6x,'Yobs')
C           WRITING COLUMN TITLES OF THE SUMMARY TABLE
114   FORMAT(6x,'Leadtime(h)',4x,'tpqobs(h)',3x,'tpq(h)',5x,'qpobs',7x,
      1 'qpcom',7x,'tpyobs(h)',4x,'tpy(h)',7x,'ypobs',7x,'ypcom',7x,
      2 'tpqer(h)',4x,'qper(%)',5x,'tpyer(h)',4x,'yper(%)',4x,
      3 'evol(%)',5x,'qvar(%)',5x,'yvar(%)'5x,'pc(%)')
      STOP
      END
C ***************************************************************************
C                          / subroutines /
C***************************************************************************
C           SUBROUTINE FOR INTERPOLATING YIN WITH YNR & BNR TO
C           COMPUTE Bmin
      SUBROUTINE Bmyin (YNR,BNR,X1,BYINR,NNR)
      DIMENSION YNR(30000),BNR(30000)
      DO 491 I=1,NNR
      IF(YNR(I)-X1)491,401,411
401   BYINR=BNR(I)
      GO TO 421
411   H1=YNR(I+1)-YNR(I)
      PQ1=(X1-YNR(I))/H1
      BYINR=BNR(I)+(PQ1/2.)*(BNR(I+1)-BNR(I-1))+(PQ1*PQ1/2.)
      1 *(BNR(I+1)-2.*BNR(I)+BNR(I-1))
      GO TO 421
491   CONTINUE
421   RETURN
      END
C           SUBROUTINE FOR INTERPOLATING YIN WITH YNR & CNR TO
C           COMPUTE CELMoin
      SUBROUTINE CELyin (YNR,CNR,X1,CLINR,NNR)
      DIMENSION YNR(30000),CNR(30000)
      DO 52 I=1,NNR
```

```
      IF(YNR(I)-X1)52,62,72
62    CLINR=CNR(I)
      GO TO 82
72    H2=YNR(I+1)-YNR(I)
      PQ2=(X1-YNR(I))/H2
      CLINR=CNR(I)+(PQ2/2.)*(CNR(I+1)-CNR(I-1))+(PQ2*PQ2/2.)
      1 *(CNR(I+1)-2.*CNR(I)+CNR(I-1))
      GO TO 82
52    CONTINUE
82    RETURN
      END
C           SUBROUTINE FOR INTERPOLATING YIN WITH YNR & VNR TO
C           COMPUTE VMoin
      SUBROUTINE VMOyin (YNR,VNR,X1,VMOINR,NNR)
      DIMENSION YNR(30000),VNR(30000)
      DO 898 I=1,NNR
      IF(YNR(I)-X1)898,808,818
808   VMOINR=VNR(I)
      GO TO 828
818   H3=YNR(I+1)-YNR(I)
      PQ3=(X1-YNR(I))/H3
      VMOINR=VNR(I)+(PQ3/2.)*(VNR(I+1)-VNR(I-1))+(PQ3*PQ3/2.)
      1 *(VNR(I+1)-2.*VNR(I)+VNR(I-1))
      GO TO 828
898   CONTINUE
828   RETURN
      END
C           SUBROUTINE FOR INTERPOLATING Q3 WITH QNR & YNR TO
C           COMPUTE YMID
      SUBROUTINE YMIDQ3 (QNR,YNR,X2,YMDNR,NNR)
      DIMENSION QNR(30000),YNR(30000)
      DO 290 I=1,NNR
      IF(QNR(I)-X2)290,300,310
300   YMDNR=YNR(I)
      GO TO 320
310   H4=QNR(I+1)-QNR(I)
      PQ4=(X2-QNR(I))/H4
      YMDNR=YNR(I)+(PQ4/2.)*(YNR(I+1)-YNR(I-1))+(PQ4*PQ4/2.)
      1 *(YNR(I+1)-2.*YNR(I)+YNR(I-1))
      GO TO 320
290   CONTINUE
320   RETURN
      END
C     SUBROUTINE FOR INTERPOLATING YMID WITH YNR & VNR TO
C     COMPUTE VMo
      SUBROUTINE VELMO (YNR,VNR,X3,VELM,NNR)
```

```
      DIMENSION YNR(30000),VNR(30000)
      DO 398 I=1,NNR
      IF(YNR(I)-X3)398,308,318
308   VELM=VNR(I)
      GO TO 328
318   H5=YNR(I+1)-YNR(I)
      PQ5=(X3-YNR(I))/H5
      VELM=VNR(I)+(PQ5/2.)*(VNR(I+1)-VNR(I-1))+(PQ5*PQ5/2.)
     1 *(VNR(I+1)-2.*VNR(I)+VNR(I-1))
      GO TO 328
398   CONTINUE
328   RETURN
      END
C     SUBROUTINE FOR INTERPOLATING YMID WITH YNR & CNR TO
C     COMPUTE CELMo
      SUBROUTINE CELMYMID (YNR,CNR,X3,CELM,NNR)
      DIMENSION YNR(30000),CNR(30000)
      DO 151 I=1,NNR
      IF(YNR(I)-X3)151,161,171
161   CELM=CNR(I)
      GO TO 181
171   H6=YNR(I+1)-YNR(I)
      PQ6=(X3-YNR(I))/H6
      CELM=CNR(I)+(PQ6/2.)*(CNR(I+1)-CNR(I-1))+(PQ6*PQ6/2.)
     1 *(CNR(I+1)-2.*CNR(I)+CNR(I-1))
      GO TO 181
151   CONTINUE
181   RETURN
      END
C     SUBROUTINE FOR INTERPOLATING YMID WITH YNR & BNR TO
C     COMPUTE Bm
      SUBROUTINE BMND (YNR,BNR,X3,BMNR,NNR)
      DIMENSION YNR(30000),BNR(30000)
      DO 190 I=1,NNR
      IF(YNR(I)-X3)190,200,210
200   BMNR=BNR(I)
      GO TO 220
210   H7=YNR(I+1)-YNR(I)
      PQ7=(X3-YNR(I))/H7
      BMNR=BNR(I)+(PQ7/2.)*(BNR(I+1)-BNR(I-1))+(PQ7*PQ7/2.)
     1 *(BNR(I+1)-2.*BNR(I)+BNR(I-1))
      GO TO 220
190   CONTINUE
220   RETURN
      END
C     SUBROUTINE FOR INTERPOLATING Q3 WITH QNR & YNR TO
```

```
C       COMPUTE YMID
        SUBROUTINE YMQ3 (QNR,YNR,X4,YMNR,NNR)
        DIMENSION QNR(30000),YNR(30000)
        DO 690 I=1,NNR
        IF(QNR(I)-X4)690,600,610
600     YMNR=YNR(I)
        GO TO 620
610     H12=QNR(I+1)-QNR(I)
        PQ12=(X4-QNR(I))/H12
        YMNR=YNR(I)+(PQ12/2.)*(YNR(I+1)-YNR(I-1))+(PQ12*PQ12/2.)
        1 *(YNR(I+1)-2.*YNR(I)+YNR(I-1))
        GO TO 620
690     CONTINUE
620     RETURN
        END
C       SUBROUTINE FOR INTERPOLATING YMID WITH YNR & CNR TO
C       COMPUTE CELMID
        SUBROUTINE CELMYM (YNR,CNR,X5,CLM,NNR)
        DIMENSION YNR(30000),CNR(30000)
        DO 152 I=1,NNR
        IF(YNR(I)-X5)152,162,172
162     CLM=CNR(I)
        GO TO 182
172     H9=YNR(I+1)-YNR(I)
        PQ9=(X5-YNR(I))/H9
        CLM=CNR(I)+(PQ9/2.)*(CNR(I+1)-CNR(I-1))+(PQ9*PQ9/2.)
        1 *(CNR(I+1)-2.*CNR(I)+CNR(I-1))
        GO TO 182
152     CONTINUE
182     RETURN
        END
C       SUBROUTINE FOR INTERPOLATING YMID WITH YNR & BNR TO
C       COMPUTE BMID
        SUBROUTINE BWMID (YNR,BNR,X5,BMD,NNR)
        DIMENSION YNR(30000),BNR(30000)
        DO 990 I=1,NNR
        IF(YNR(I)-X5)990,900,910
900     BMD=BNR(I)
        GO TO 920
910     H10=YNR(I+1)-YNR(I)
        PQ10=(X5-YNR(I))/H10
        BMD=BNR(I)+(PQ10/2.)*(BNR(I+1)-BNR(I-1))+(PQ10*PQ10/2.)
        1 *(BNR(I+1)-2.*BNR(I)+BNR(I-1))
        GO TO 920
990     CONTINUE
920     RETURN
```

```
CLM=CNR(I)+(PQ9/2.)*(CNR(I+1)-CNR(I-1))+(PQ9*PQ9/2.)
     1 *(CNR(I+1)-2.*CNR(I)+CNR(I-1))
      GO TO 182
152   CONTINUE
182   RETURN
      END
C     SUBROUTINE FOR INTERPOLATING YMID WITH YNR & BNR TO
C     COMPUTE BMID
      SUBROUTINE BWMID (YNR,BNR,X5,BMD,NNR)
      DIMENSION YNR(30000),BNR(30000)
      DO 990 I=1,NNR
      IF(YNR(I)-X5)990,900,910
900   BMD=BNR(I)
      GO TO 920
910   H10=YNR(I+1)-YNR(I)
      PQ10=(X5-YNR(I))/H10
      BMD=BNR(I)+(PQ10/2.)*(BNR(I+1)-BNR(I-1))+(PQ10*PQ10/2.)
     1 *(BNR(I+1)-2.*BNR(I)+BNR(I-1))
      GO TO 920
990   CONTINUE
920   RETURN
      END
**********************************************************************
!                          / AR(2) model subroutine /
**********************************************************************

      SUBROUTINE TSUB(A,NR,NC,B)
      DIMENSION A(1000,1000),B(1000,1000)
      DO 1 I=1,NR
      DO 1 J=1,NC
1     B(J,I)=A(I,J)
      RETURN
      END
C
      SUBROUTINE MSUB(A,B,NRA,NCA,NRB,NCB,C)
      DIMENSION A(1000,1000),B(1000,1000),C(1000,1000)
      DO 60 I=1,NRA
      DO 80 K=1,NCB
      SUM=0.
      DO 70 J=1,NCA
70    SUM=SUM+A(I,J)*B(J,K)
80    C(I,K)=SUM
60    CONTINUE
      RETURN
      END
C
```

```
      SUBROUTINE INVSUB(X,N,Y,M,C)
      DIMENSION X(1000,1000),Y(1000,1000),IPIVOT(1000),
      1 INDEX(1000,1000)
      1 ,C(1000,1000)
       DOUBLE PRECISION A(1000,1000),B(1000,1000),AMAX,T,SWAP
      1 ,PIVOT(1000)
      EQUIVALENCE (IROW,JROW),(ICOLUM,JCOLUM),(AMAX,T,SWAP)
      DO 1 I=1,N
      DO 2 J=1,N
2     A(I,J)=X(I,J)
1     B(I,1)=Y(I,1)
c     initialisation
15    DO 20 J=1,N
20    IPIVOT(J)=0
30    DO 550 I=1,N
c     search for pivot element
40    AMAX=0.0
45    DO 105 J=1,N
50    IF(IPIVOT(J)-1)60,105,60
60    DO 100 K=1,N
70    IF(IPIVOT(K)-1)80,100,740
80    IF(DABS(AMAX)-DABS(A(J,K)))85,100,100
85    IROW=J
90    ICOLUM=K
95    AMAX=A(J,K)
100   CONTINUE
105   CONTINUE
110   IPIVOT(ICOLUM)=IPIVOT(ICOLUM)+1
c     interchange rows tonput pivot element on diagnol
130   IF(IROW-ICOLUM)140,260,140
140   CONTINUE
150   DO 200 l=1,N
160   SWAP=A(IROW,L)
170   A(IROW,L)=A(ICOLUM,L)
200   A(ICOLUM,L)=SWAP
205   IF(M)260,260,210
210   do 250 l=1,M
220   SWAP=B(IROW,L)
230   B(IROW,L)=B(ICOLUM,L)
250   B(ICOLUM,L)=SWAP
c       write(*,*)a(icolum,l),b(icolum,l)
c       pause 111
260   INDEX(I,1)=IROW
270   INDEX(I,2)=ICOLUM
310   PIVOT(I)=A(ICOLUM,ICOLUM)
c     divide pivot row by pivot element
```

```
330   A(ICOLUM,ICOLUM)=1.0
340   DO 350 L=1,N
350   A(ICOLUM,L)=A(ICOLUM,L)/PIVOT(I)
355   IF(M) 380,380,360
360   do 370 L=1,M
370   B(ICOLUM,L)=B(ICOLUM,L)/PIVOT(I)
c     reduce non pivot rows
380   DO 550 L1=1,n
390   IF(L1-ICOLUM)400,550,400
400   T=A(L1,ICOLUM)
420   A(L1,ICOLUM)=0.0
430   DO 450 L=1,N
450   A(L1,L)=A(L1,L)-A(ICOLUM,L)*T
455   IF(M)550,550,460
460   DO 500 L=1,M
500   B(L1,L)=B(L1,L)-B(ICOLUM,L)*T
550   CONTINUE
c     interchange columns
600   DO 710 I=1,N
610   L=N+1-I
620   IF(INDEX(L,1)-INDEX(L,2))630,710,630
630   JROW=INDEX(L,1)
640   JCOLUM=INDEX(L,2)
650   DO 705 K=1,N
660   SWAP=A(K,JROW)
670   A(K,JROW)=A(K,JCOLUM)
705   CONTINUE
700   A(K,JCOLUM)=SWAP
710   CONTINUE
      DO 3 I=1,N
3     Y(I,1)=B(I,1)
      DO 1100 I=1,N
      DO 1100 J=1,N
1100  C(I,J)=A(I,J)
740   RETURN
      END
```

REFERENCES

1. Abbott, M. B., and Refsgaard, J. C. (eds.). (1996). *Distributed hydrologic modeling.* Kluwer Academic Publishers, Boston, Mass.

2. Ackers, P. (1993), Stage discharge functions for two-stage channels: the impact of a new reach, *Journal of the Institution of Water and Environmental Management, 7*(1), 52-61.

3. Ahsan, M. and O'Conner, K.M. (1994), A reappraisal of the Kalman filtering technique, as applied in river flow forecasting, *J. Hydrol., 161*(1-4), 197-226, doi: 10.1016/0022-1694(94)90129-5.

4. Akan, A. O., and B. C. Yen (1977), A nonlinear diffusion-wave model for unsteady open-channel flow, *Proc. Cong. Int. Assoc. Hydraul. Res., 17th*, Baden-Baden, Germany, 2, 181–190.

5. Apollov, B. A., G. P. Kalinin, and V. D. Komarov (1964), Hydrological forecasting, translated from Russian, Israel Program for Scientific Translations, Jerusalem.

6. ASCE Task Committee on Application of Artificial Neural Networks in Hydrology, Artificial neural networks in hydrology, I: Preliminary concepts, *J. Hydrol. Eng., 5*(2), 115– 123, 2000a.

7. ASCE Task Committee on Application of Artificial Neural Networks in Hydrology, Artificial neural networks in hydrology. II: Hydrologic applications, *J. Hydrol. Eng., 5*(2), 124– 137, 2000b.

8. ASCE Task Committee on Definition of Criteria for Evaluation of Watershed Models of the Watershed Management Committee, Irrigation and Drainage Division (1993), Criteria for evaluation of watershed models, *J. Irrig. Drain. Eng., ASCE, 119*(3), 429–442.

9. Barbetta, S., Moramarco, T., Franchini, M., Melone, F., Brocca, L., and Singh V. P. (2011), Case Study: Improving real-time stage forecasting Muskingum model by incorporating the rating curve model, *J. Hydrol. Engg., ASCE, 16*(6), ISSN 1084-0699/2011/6-540-557, doi: 10.1061/(ASCE)HE.1943-5584.0000345.

10. Barré de Saint-Venant, A. J. C. (1871a), Théorie du Mouvement Non Permanent des Eaux, avec Application aux Crues de Rivières et à l'Introduction des Marées dans leur

Lit, *Comptes Rendus des séances de l'Académie des Sciences, Paris, France, 73*(4), 237-240 (in French).

11. Barré de Saint-Venant, A. J. C. (1871b), Théorie et Equations Générales du Mouvement Non Permanent des Eaux Courantes, *Comptes Rendus des séances de l'Académie des Sciences, Paris, France, Séance, 73*(17 July), 147–154 (in French).
12. Barth, A., and Rosso, R. (1993), Adaptive Calibration of a conceptual model for flash flood forecasting, *Water Resour.Res., 29*(8), 2561-2572.
13. Barth, A., Montanari, A., and Toth , E. (1999), Stochastic techniques for improving real-time flood predictions, *IAHR congress proceedings, Graz*, 22-27, August 1999 in Graz, Austria.
14. Becker, A. (1976), Simulation of nonlinear flow systems by combining linear models. *IAHS Publication No. 116*, 135-142.
15. Becker, A., and Kundzewicz, Z. W. (1987), Nonlinear flood routing with multilinear models, *Water Resour. Res., 23*(6), 1043-1048.
16. Bergman, M.J., and Delleur, J.W. (1985a), Kalman filter estimation and prediction of daily stream flows, 1. Review, algorithm, and simulation experiments, *Wat. Resour. Bull, 21*, 815-825.
17. Bergman, M.J., and Delleur, J.W. (1985b), 2, Application to the Potomac river, *Wat. Resour. Bull, 21*,827-832.
18. Bertoni, J.C., Tucci, C. E., and Clarke. R.T. (1992), Rainfall-based real-time flood forecasting, *J. Hydrol., 131* (1), 313-339.
19. Beven, K. J. (2001), *Rainfall-Runoff Modeling*: The Primer, John Wiley, Hoboken, N. J.
20. Birkhead, A. L., and C. S. James (1998), Synthesis of rating curves from local stages and remote discharge monitoring using nonlinear Muskingum routing, *J. Hydrol., 205*(1–2), 52–65.
21. Box, G. E. P., Jenkins, G. M. (1970), Time-series analysis, forecasting and control. San Francisco: Holden-Day.
22. Bras, R. L., and I. Rodriguez-Iturbe (1985), *Random Functions and Hydrology*, Addison-Wesley, Boston, Mass.

23. Burn, D.H., and McBean, E.A. (1985), River flow forecasting model for Sturgeon river, *J.Hydraul. Engng, 111*, 316-333.

24. Camacho L. and Lees, M. (2000), Multilinear discrete lag cascade model for channel routing, *J. Hydrol., 266*, 30-47.

25. Campolo, M., Andreussi, P. and Soldati, A. (1999) River flood forecasting with a neural network model. *Water Resour. Res., 35*, 1191-1197.

26. Chang, F. J., Chiang, Y.-M., and Chang, L.-C. (2007), Multi-step-ahead neural networks for flood forecasting, *Hydrol. Sci. J., 52*(1), 114–130.

27. Chaudhry, M. H. (1993), *Open Channel Flow*, Prentice-Hall, Upper Saddle River, N.J.

28. *Chiu,* C.L. (Ed.), (1985), Applications of Kalman filter to Hydrology, Hydraulics, and water resources, Proceedings of AGU, *Chapman Conference*, 1st edn. University of Pittsburgh.

29. Chow, V. T., D. R. Maidment, and L. W. Mays (1988), *Applied Hydrology*, McGraw-Hill, New York.

30. Chow, V.T. (1959), *Open Channel Hydraulics*, McGraw Hill, New York, USA.

31. Chowdhury, M. R. (2000), An assessment of flood forecasting in Bangladesh: The experience of the 1998 flood, *Natural Hazards 22*, 139–163.

32. Cluckie, I. D. (1993), Real-time flood forecasting using weather radar, in *Concise Encyclopedia of Environmental Systems*, edited by P. C. Young, pp. 291– 298, Elsevier, New York.

33. Cluckie, I. D., and R. Harpin (1980), A real time simulator of the rainfall runoff process, *Math. Comput. Simul., 24*, 119– 139.

34. Crago, R. D., and S. M. Richards (2000), Nonkinematic effects in storm hydrograph routing, *J. Hydrol. Eng., ASCE, 5*(3), 323–326.

35. Cunge, J. A. (1969), On the subject of a flood propagation method (Muskingum Method), *J. Hydraul. Res., IAHR, 7*(2), 205–230.

36. Danish Hydraulic Institute (DHI) (1999) User's manual and technical references for MIKE 11, Hørsholm, Denmark.

37. Danish Hydraulic Institute (DHI) (2008) User's manual and technical reference for MIKE 11 (version 2008), Hørsholm, Denmark.

38. Danish Hydraulic Institute (DHI) (2011) User's manual and technical reference for MIKE 11 (version 2011), Hørsholm, Denmark.

39. Danish Hydraulic Institute (DHI) (2011) User's manual and technical reference for MIKE SHE (version 2011), Horsholm, Denmark.

40. Dawson, C. W. & Wilby, R. (1998), An artificial neural network approach to rainfall-runoff modelling. *Hydrol. Sci. J. 43*, 47–66.

41. Dooge, J .C. I., W. G. Strupczewski, and J. J. Napiorkowski (1982), Hydrodynamic derivation of storage parameters of the Muskingum model, *J. Hydrol., 54*(4), 371–387.

42. Dooge, J. C. I. (1973), Linear theory of hydrologic systems, *USDA, Agric. Res. Serv., Tech. Bull., No.1468.*

43. Dooge, J. C. I. (1980), Flood routing in channels, Post Graduate Lecture Notes, Department of Civil Engineering, University College Dublin, Dublin, Ireland.

44. Dooge, J. C. I., and B. M. Harley (1967), Linear routing in uniform open channel, in *Proc. Int. Hydrol. Symp.*(6–8 September, 1967), Fort Collins, Colorado, USA, Vol. 1, 57–63.

45. Dooge, J. C. I., and J. J. Napiorkowski (1987), Applicability of diffusion analogy in flood routing, *Acta Geophysica Polonica, 35*(1), 66–75.

46. Ferrick, M. G. (1985), Analysis of river wave types, *Water Resour. Res., 21*(2), 209–220.

47. Ferrick, M. G., and Goodman (1998), N. J., Analysis of linear and monoclinal river wave solutions, *J. Hydrol. Eng., ASCE. 124*(7), 728–741.

48. Fread, D. L. (1985), Applicability criteria for kinematic and diffusion routing models, Laboratory of Hydrology, National Weather Service, NOAA, U.S. Dept. of Commerce, Silver Spring, Md.

49. French, R. H. (1986), *Open Channel Hydraulics,* McGraw-Hill, New York.

50. Garbrecht and Brunner, (1991), Hydrologic channel-flow routing for compound sections, *J. Hydraul. Eng., ASCE, 117*(5), 629-642.

51. Ge, S. X. (2001), Modern Flood Forecast Techniques (in Chinese), *Water Publ.*, Beijing.

52. Graham, D.N. and M. B. Butts (2005) Flexible, integrated watershed modelling with MIKE SHE, In Watershed Models, Eds. V.P. Singh & D.K. Frevert Pages 245-272, CRC Press. ISBN: 0849336090.

53. Hayami, S. (1951), On the propagation of flood waves, *Bull. Disaster Prevention Research Institute*, Kyoto Univ., Japan, 1(1), 1–16.

54. Heatherman, W. J. [2004], Muskingum-Cunge revisited, *World Water and Environmental Resources Congress 2004*, ASCE, Edited by G. Sehlke, D. F. Hayes, and D. K. Stevens (June 2-July 1, 2004), Salt Lake City, Utah, USA.

55. Henderson, F. M. (1966), *Open Channel Flow*, The Macmillan Co., New York.

56. Hill, T., Marquez, L., Connor, M. O., and Remus, W. (1994), Artificial neural networks for forecasting and decision making, *Int. J. Forecasting, 10*, 5–15.

57. Huang, W. -C. (1999), Kalman filter effective to hydrologic routing? *J. Marine Sci. Tech., 7*(1), 65-71.

58. Husain, T. (1985), Kalman filter estimation model in flood forecasting, *Adv. Wat. Resour., 8*, 15-21.

59. Imrie, C. E., Lekkas, D. F. & Lees M. J. (2000b), Comparison of non-linear transfer function and artificial network for flow routing. *Proceedings of the British Hydrological Society 7th National Hydrology Symposium*, Newcastle upon Tyne, UK, British Hydrological Society. pp. 5.15–5.16.

60. Imrie, C.E. and Durucan, S., (1999). River flow prediction using the cascade-correlation neural network learning architecture. In: *Proceedings of the Water 99 Joint Congress*. Brisbane, Australia, pp. 94-99.

61. Jain, A., and Srinivasulu, S. (2004), Development of effective and efficient rainfall-runoff models using integration of deterministic, real-coded genetic algorithms and artificial neural network techniques. *Water Resour. Res., 40*(4), W04302.

62. Jolly, J. P., and V. Yevjevich (1971), Amplification criterion of gradually varied, single peaked waves, *Hydrol. Pap. No. 51, Colorado State University*, Fort Collins, USA.

63. Jønch-Clausen, T., and Refsgaard , J.C. (1984), A mathematical modelling system for flood forecasting, Danish Hydraulic Institute, Hørsholm, Denmark.

64. Kalinin, G. P., and P. I. Milyukov (1958), Priblizhennyi raschet neutstanovivshegosya dvizheniya vodnykh mass (Approximate computation of unsteady flow of water masses), *Trudy TSIP, 66*.

65. Katapodes, N. D. (1982), On zero-inertia and kinematic waves, *J. Hydraul. Div. ASCE, 108*(11), 1380–1387.

66. Keefer, T. N., and R. S. McQuivey (1974), Multiple linearization flow routing model, *J. Hydraul. Div., ASCE, 100*(HY7), 1031-1046.

67. Kisi, O. (2004), River flow modeling using artificial neural networks, *J. Hydrol. Eng., ASCE*, 9(1), 60-63.

68. Kisi, O. (2007), Stream flow forecasting using different artificial neural network algorithm, *J. Hydrol. Eng., 12*(5), 532-539.

69. Kisi, O. (2008), River flow forecasting and estimation using different artificial neural network techniques, *J. Hydrol. Res., 39*(1), 27-40.

70. Koussis, A. D. (1976) An approximate dynamic flood routing method, *Proc. Int. Symp. On unsteady Flow in Open Channels, Paper L1*, Newcastle-Upon Tyne, U.K.

71. Koussis, A. D. (1980), Comparison of Muskingum method difference schemes, *J. Hydraul. Div., ASCE, 106*, (HY5), 925–929.

72. Kuchment, L. S. (1972), *Mathematical Modeling of Streamflow* (in Russian). Hydrometeorological Publishing House, Leningrad.

73. Kulandaiswamy, V.C. (1964), A basic study of the rainfall excess-surface runoff relationship in a basin system, Ph. D. Thesis, University of Illinois, Urbana, Illinois, USA.

74. Kundzewicz, Z. W. (1982) Parametric analysis of flood routing models (in German), *Report No. 23*, Mitteilungen, Inst. Wasserbau, III, University of Karlsruhe, Germany.

75. Kundzewicz, Z. W. (1984), Multilinear flood routing, *Acta Geophys. Pol., 32*(4), 419-445.

76. Kundzewicz, Z. W. (1986), Physically based hydrologic flood routing method, *Hydrol. Sci. J., IAHS, 31*(2), 237-261.

77. Laio, F., A. Porporato, R. Revelli, and L. Ridolfi, (2003), A comparison of nonlinear flood forecasting methods, *Water Resour. Res.*, *39*(5), 1129, doi: 10.1029/2002WR001551.

78. Laurenson, E. M. (1962), Hydrograph synthesis by runoff routing, *Water Research Laboratory, University of New South Wales Report No. 66.*

79. Laurenson, E. M. (1964), A basin storage model for runoff routing, *J. Hydrol., 2*, 141–163.

80. Lee Y. H. and Singh V. P. (1998), Application of the Kalman filter to the Nash model, *Hydrol. Process, 12*, 755-767.

81. Lees, M. J. (2000a), Data-based mechanistic modelling and forecasting of hydrological systems. *J. Hydro informatics 2*(1), 15–34.

82. Lees, M. J. (2000b), Advances in transfer function based flood forecasting. In *Flood Issues in Contemporary Water Management (ed. J. Marsalek), pp. 421–428. NATO Science Series 2*/71. Kluwer, Dordrecht.

83. Lekkas, D. F., C. Onof, M. J. Lee, and E. A. Baltas (2005), Application of artificial neural network for flood forecasting, *Global Nest: the int. J., 6*(3), 205-211.

84. Lekkas, D.F., Imrie, C.E. and Lees, M.J., (2001), Improved non-linear transfer function and neural network methods of flow routing for real-time forecasting, *Journal of Hydro Informatics, 3*, 153-164.

85. Lekkas, F. Demetris (2002), Development and comparison of data-based forecasting methods, Ph.D. Thesis, University of London.

86. Li, J. Z. (1988), Analysis and application of the dynamic characteristics of flood wave models, Int. *J. Hydroelectric Energy, 6*(1), 28-40 (in Chinese).

87. Lighthill, M. J., and G. B. Whitham (1955), On kinematic waves: 1. Flood movement in long rivers, *Proc. Roy. Soc. of London, A229*, 281–316.

88. Markar, M. S., Clark, S. Q., Yaowu, Min, and Zheng, Jing. (2004), Evaluation of hydrologic and hydraulic models for real-time flood forecasting use in the Yangtze River catchment, *Aust. Water Resour., 10*(1), 93–102.

89. Marsalek, J., C. Maksimovic, E. Zeman, and R. K. Price (Eds.) (1996), *Hydroinformatics Tools for Planning, Design, Operation, and Rehabilitation of Sewer Systems*, *NATO ASI Series*, *Ser. 2*, vol. 44, Springer, New York.

90. McCarthy, G. T. (1938), The unit hydrograph and flood routing, *Conf. North Atlantic Division*, U.S. Army Corps of Engineers, New London, Conn.

91. Mein, R. G., E. M. Laurenson, and T. A. McMahon (1974), Simple nonlinear method for flood estimation, *J. Hydraul. Div., ASCE, 100*(HY11), 1507–1518.

92. Miller, W. A., and Cunge, J. A. (1975), Simplified equations of unsteady flow, in: *Unsteady Flow in Open Channels*, Vol. I, K. Mahmood and V. Yevjevich (Eds.), Water Resour. Publ., Highlands Ranch, Colo., 183-249.

93. Moll, J. R. (1983), Real-time flood forecasting on river Rhine, *IAHS Publ.,* 147, 265-272.

94. Moramarco, T., Barbetta, S., Melone, F., and Singh, V. P. (2006), A real-time stage Muskingum forecasting model for a site without rating curve, *Hydrol. Sci. J., IAHS, 51*(1), 66-82.

95. More, R. J., and Bell, V. A. (2001), Comparison of rainfall-runoff models for flood forecasting, Part I, *R&D Technical Report* W241, Institute of Hydrology, Environment Agency, Rio House, Waterside Drive, Aztec West, Almondsbury, BRISTOL, BS32 4UD.

96. Moussa, R., and C. Bocquillon (1996), Criteria for the choice of flood-routing methods in natural channels, *J. Hydrol., 186*(1), 1–30.

97. Mukerji, A., Chandranath Chatterjee, and Narendra Singh Raghuwanshi (2009), Flood forecasting using ANN, Neuro-Fuzzy, and Neuro-GA models, *J.Hydrolo.Eng.,* Vol. 14, No. 6, ASCE, ISSN 1084-0699/2009/6-647–652, doi: 10.1061(ASCE)HE.1943-5584.0000040.

98. Nash, J. E. (1957), The form of instantaneous unit hydrograph, Int. *Assoc. Sci. Hydrol. Publ., 45*(3– 4), 114– 121.

99. Nash, J. E. (1959), Systematic determination of unit hydrograph parameters, *J. Geophys. Res., 64*(1), 111-115.

100. Nash, J. E. (1960), A unit hydrograph study with particular reference to British catchments, *Proc. Inst. Civ. Eng., 17*, 249–282.

101. Nash, J. E. (1980), News, The Oxford Symposium on Hydrological Forecasting, *Hydrol. Sci. bulletin-des Sci. Hydrologiques, 25*, 4, 366-368.

102. Nash, J. E., and J. V. Sutcliffe (1970), River flow forecasting through conceptual models, Part-1: A discussion of principles, *J. Hydrol., 10*(3), 282-290.

103. Natural Environment Research Council (NERC) (1975), Flood Routing Studies, in *Flood Studies Report*, Vol. III, Institute of Hydrology, Wallingford, UK.

104. Nayak, P. C., Sudheer, K. P., and Ramasastri, K. S. (2005a), Fuzzy computing based rainfall-runoff model for real time flood forecasting, *Hydrolog. Process. 19*(4), 955–968.

105. Nayak, P. C., Sudheer, K. P., Rangan, D. M., and Ramasastri, K. S. (2004), A Neuro-Fuzzy computing technique for modeling hydrological time series, *J. Hydrol., 291*(1–2), 52–66.

106. Neal, J.C., Atkinson, P.M. and Hutton C.W. (2007), Flood inundation model updating using an ensemble Kalman filter and spatially distributed measurements. *J. Hydrol., 336*(3-4), 401-415.

107. Nemec, J. (1985), Flood forecasting, John Wiley & Sons, New Yark.

108. O'Connell, P. E., and R. T. Clarke (1981), Adaptive hydrological forecasting—A review, *Bull. Int. Assoc. Sci. Hydrol., 26*, 179–205.

109. Parthajit Roy, P.S. Choudhary, Manabendra Saharia, (2010), Dynamic ANN modelling for flood forecasting in a river network, CP1298, *International conference on modeling, optimization, and computing, (ICMOC 2010), American Institute of Physics*, 978-0-7354-0854-8/10.

110. Patro, S., Chatterjee, C., Mohanty, S., Singh, R., and Raghuwanshi, N. S. (2009), Flood inundation modeling using MIKE FLOOD and remote sensing data, *J. Indian Soc. Remote Sens., 37*, 107–118.

111. Paudyal, N. G., (2002), Forecasting and warning of water-related disasters in a complex hydraulic setting-The case of Bangladesh, *Hydrol. Sci. J., 47*, S5–S18.

112. Perumal, M. (1992a), Discussion on the kinematic wave controversy, *J. Hydraul. Eng., ASCE, 118*(9), 1335-1337.

113. Perumal, M. (1992b), Multilinear Muskingum flood routing method, *J. Hydrol., 133*(3–4), 259–272.

114. Perumal, M. (1992c), The cause of negative initial outflow with the Muskingum method, *Hydrological Sci. J., 37*(4), 391-4401.

126. Perumal, M., Moramarco, T., Sahoo, B., and Barbetta, S. (2010), On the practical applicability of the VPMS routing method for rating curve development at ungauged river sites, *Water. Resour. Res., 46*, W03522, doi: 10.1029/2009WR008103, 1-9.

127. Perumal, M., P. E. O'Connell, and K. G. Ranga Raju (2001), Field applications of a variable-parameter Muskingum method, *J. Hydrol. Eng., 6*(3), 196–207.

128. Ponce, V. M. (1983), Accuracy of physically based coefficient method of flood routing, *Tech. Report SDSU Civil Engineering Series* No. 83150, San Diego State Univ., San Diego, California, USA.

129. Ponce, V. M. (1989), *Engineering Hydrology*, Principles and Practices, Prentice-Hall,

130. Ponce, V. M., and P. V. Chaganti (1994), Variable parameter Muskingum–Cunge method revisited, *J. Hydrol., 162*(3–4), 433–439.

131. Ponce, V. M., and V. Yevjevich (1978), Muskingum-Cunge method with variable parameters, *J. Hydraul. Div., ASCE, 104*(HY12), 1663–1667.

132. Ponce, V. M., R. N. Li, and D. B. Simons (1978), Applicability of kinematic and diffusion models, *J. Hydraul.Div., Am. Soc. Civ. Eng., 104*(3), 353-360.

133. Ponce, V.M. (1991), Kinematic wave controversy, *J. Hydraul. Eng., ASCE, 117*(4), 511-525.

134. Price, R. K. (1973), Flood routing methods for British rivers, *Proc. Inst. Civ. Eng., 55*, 913-930.

135. Price, R. K. (1978), River catchment flood control model, *Proc. Inst. Civ. Engrs., Part2, 65*, Sept, 655-668.

136. Price, R. K. (1985), Flood routing, in *Developments in Hydraulic Engineering*, P. Novak (Ed.), chapter 4, *Elsevier Applied Science Publishers*, London., 129–173

137. Price, R. K. (2009), An optimized routing model for flood forecasting, *Water Resour. Res., 45*, W02426, doi: 10.1029/2008WR007103.

138. Price, R. K. (2009), Volume conservative, non-linear flood routing, *J. Hydraul. Engr., (ASCE)HY*.1943-7900.0000088,1-30

139. Price, R. K. and M. Perumal (2011), Variable parameter McCarthy-Muskingum discharge routing method, (manuscript under preparation for a refereed journal).

140. Ranga Raju, K. G., G. L. Asawa, P. D. Porey, M. Perumal, and U. C. Kothyari (1993), Dam-break study for Jamrani dam, U. P., Report of Hydraulic Engineering Section, Department of Civil Engineering, University of Roorkee (currently Indian Institute of Technology Roorkee), Roorkee, India.

141. Reed, D. W. (1984), A review of British flood forecasting practice. Institute of *Hydrology Report* No. 90.

142. Refsgaard, J.C. (1997), Validation and intercomparison of different updating procedures for real-time forecasting, *Nordic Hydrology*, 28, 65-84.

143. Rockwood, D. M. (1958), Columbia basin streamflow routing by computer, J. Waterways and Harbors Division, ASCE, Vol. 84, Part 1, *Paper* No. 1874(December), (Also published in ASCE Transactions, 1961, Paper No. 3119).

144. Sahoo, B. (2007), Variable parameter flood routing methods for hydrological analysis of ungauged basins, Ph. D Thesis, Department of Hydrology, I.I.T. Roorkee.

145. Sajikumar, N., and Thandaveswara, B.S. (1999), A non-linear rainfall-runoff model using an artificial neural network, *J. Hydrol., 216*, 32-55.

146. Singh, S. R. (2007), A robust method of forecasting based on fuzzy time series, *Appl. Math. Comput., 188*(1), 472–484.

147. Singh, V. P. (1988). *Hydrologic systems: Rainfall-runoff modeling*, Vol. 1, Prentice-Hall, Inc., Englewood Cliffs, New Jersy.

148. Singh, V. P. (1989). *Hydrologic Systems: Watershed modeling*, Vol. 2, Prentice-Hall, Inc., Englewood Cliffs, New Jersy.

149. Singh, V. P. (1996), *Kinematic Wave Modeling in Water Resources: Surface-Water Hydrology,* John Wiley and Sons, Inc., New York.

150. Singh, V. P., Li, J. Z., and Wang, G.-T. (1998), Flood peak attenuation and forecast, *J. of Hydrol. Eng.*, Vol. 3, No.1, ASCE, ISSN 1084-0699/98/0001-0020-0025/ 12518.

151. Strupczewski, W. G., and Z. W. Kundzewicz (1980), Muskingum method revisited, *J. Hydrol., 48*, 327-342.

152. Sudheer, K. P. (2005), Knowledge extraction from trained neural network river flow models, *J. Hydrol. Eng., 10*(4), 264–269.

153. Sudheer, K. P., Gosain, A. K., and Ramasastri, K. S. (2002), A data driven algorithm for constructing artificial neural network rainfall-runoff models. *Hydrolog. Process., 16*(6), 1325–1330.

154. Szilagyi, J. (2003), State-space discretization of the KMN-cascade in a sample-data system framework for stream flow forecasting. *J. Hydrologic Eng., 8*(6), 339–347.

155. Szilagyi, J. (2006), Discrete state-space approximation of the continuous Kalilin-Milyukov-Nash cascade of non-integer storage elements, *J. Hydrol. 328*(1), 132-140.

156. Szollosi-Nagy. A (1982), The discretization of the continuous linear cascade by means of state space analysis". *J.Hydrol, 58*,223-236.

157. Szollosi-Nagy. A. (1976), An adaptive identification and prediction algorithm for the real- time forecasting of hydrological time series, *Hydrol. Sci. bulletin-des Sci. Hydrologiques, XXI, 1*(3), 163-176.

158. Tang, X. -N., D. W. Knight, and P. G. Samuels (1999a), Volume conservation in variable parameter Muskingum–Cunge method, *J. Hydraul. Engrg., ASCE, 125*(6), 610–620.

159. Tang, X. -N., D. W. Knight, and P. G. Samuels (1999b), Variable parameter Muskingum-Cunge method for flood routing in a compound channel, *J. Hydraul. Res., IAHR, 37*(5), 591–614.

160. Thirumalaiah, K, and M. C. Deo. (2000), Hydrological forecasting using neural networks, *J. of Hydrol. Eng. ASCE*, Vol. 5, No. 2, ISSN 1084-0699/00/0002-0180–0189/16187.

161. Thirumalaiah, K., and M. C. Deo (1998b), River stage forecasting using artificial neural networks, *J. Hydrol. Eng., ASCE, 3*(1), 26−32.

162. Thirumalaiah. K., and M. C. Deo (1998a), Real-time flood forecasting using neural networks, *J. Computer- Aided Civil and Infrastructure Engg.*, Blackwell Publishers, Oxford, UK, 13, 101-111.

163. Thomas, I. E., and P. R. Wormleaton (1970), Flood routing using a convective diffusion model, *Civil Eng. and Public Works Review*, 65, 257–259.

164. Thomas, I. E., and P. R. Wormleaton (1971), Finite difference solution of the flood diffusion equation, *J. Hydrol., 12*, 211–221.

165. Todini, E. (1978), Mutually interactive state-parameter (MISP) estimation, in Applications of Kalman Filter to Hydrology, Hydraulics, and Water Resources, edited by C.-L. Chu, *Stochastic Hydraul. Prog. Dep. Civ. Eng.*, Univ. of Pittsburgh, Pittsburgh, Pa.

166. Todini, E. (2007), A mass conservative and water storage consistent variable parameter Muskingum-Cunge approach, *Hydrol. Earth Syst. Sci., 11*, 1645-1659.

167. Tsai, C. W. -S. (2003), Applicability of kinematic, noninertia, and quasi-steady dynamic wave models to unsteady flow routing, *J. Hydraul. Engg., 129*(8), 613–627.

168. U.S. Army Corps of Engineers (USACE) (2010), HEC-HMS hydrologic Modeling System user's manual (version 3.5), Hydrol. Eng., Cent., Davis, Calif.

169. U.S. Army Corps of Engineers (USACE) (2010), HEC-RAS river analysis system user's manual (version 4.0 beta), *Rep. CPD-68*, Hydrol. Eng., Cent., Davis, Calif.

170. Viessman, W., Jr., and G. L. Lewis (1996), *Introduction to Hydrology*, 4th ed., Harper Collins, New York.

171. Weinmann, P. E., and E. M. Laurenson (1979), Approximate flood routing methods: a review, *J. Hydraul. Div., ASCE, 105*(12), 1521–1526.

172. WMO (1992), Simulated real-time inter comparison of hydrological models, In: *WMO operational hydrology report*, no 38, WMO no 779, World Meteorological Organization, Geneva.

173. Wong, T. H. F. (1984), Improved parameters and procedures for flood routing in rivers, Ph. D. Thesis, Monash University, Victoria , Australia.

174. Wong, T. H. F., and E. M. Laurenson (1983), Wave speed-discharge relation in natural channels, *Water Resour. Res., 19*(3), 701–706.

175. Wong, T. H. F., and E. M. Laurenson (1984), A model of flood wave speed-discharge characteristics of rivers, *Water Resour. Res., 20*(12), 1883–1890.

176. Woolhiser, D. A., and J. A. Liggett (1967), Unsteady one-dimensional flow over a plane: the rising hydrograph, *Water Resour. Res., 3*(3), 753–771.

177. Xiao-Ling Wu, Xiao-Hua Xiang, Chuan-Hai Wang, Xi Chen, Chong-Yu Xu, and Zhongbo Yu (2011), A coupled hydraulic and Kalman filter model for real time correction of flood forecast in the Three Gorges Inter zone of Yangtze River, China, *J.Hydrol. Eng.*, doi: 10.1061/ (ASCE) HE.1943-5584.0000473.

178. Yang, Z., and Han, D., (2006), Derivation of unit hydrograph using a transfer function approach, *Water Resour. Res.* 42, W01501, doi: 10.1029/2005WR004227.

179. Zoppou, C., and I. C. O'Neill (1982), Criteria for the choice of flood routing methods in natural channels, in *Proc. Hydrology and Water Resources Symposium, Melbourne*, Inst. of Eng., Barton, A.C.T., 75–81.